GEOCHEMISTRY OF INTERTIDAL SEDIMENTS WITHIN ESTUARIES ALONG CENTRAL WEST COAST OF INDIA

A THESIS SUBMITTED TO GOA UNIVERSITY FOR THE AWARD OF THE DEGREE OF

DOCTOR OF PHILOSOPHY

IN

MARINE SCIENCE

BY

MAHESHWAR R. NASNODKAR

M.Sc

UNDER THE GUIDANCE OF

PROF. G. N. NAYAK

Department of Marine Sciences,

Goa University,

Taleigao, Goa - 403206

FEBRUARY 2016

DEDICATED

TO MY

PARENTS AND FAMILY

STATEMENT

As required under the University ordinance OB.9.9 (iv), I state that the present thesis entitled "**GEOCHEMISTRY OF INTERTIDAL SEDIMENTS WITHIN ESTUARIES ALONG CENTRAL WEST COAST OF INDIA**" is my original contribution and the same has not been submitted on any other previous occasion. To the best of my knowledge, the present study is the first comprehensive work of its kind from the area mentioned.

The literature related to the problem investigated has been cited. Due acknowledgements have been made wherever facilities and suggestions have been availed of.

Place: Goa University

Date: 25-2-2016

Mr. Maheshwar R. Nasnodkar

CERTIFICATE

This is to certify that the thesis entitled, "**GEOCHEMISTRY OF INTERTIDAL SEDIMENTS WITHIN ESTUARIES ALONG CENTRAL WEST COAST OF INDIA**", submitted by Mr. Maheshwar R. Nasnodkar for the award of the Degree of Doctor of Philosophy in Marine Science is based on his original studies carried out by him under my supervision. The thesis or any part thereof has not been previously submitted for any other degree or diploma in any universities or institutions.

Place: Goa University

Date: 25-2-2016

Prof. G. N. Nayak

(Research Guide)
Department of Marine Sciences
Goa University,
Goa - India

Acknowledgements

There are a number of people without whom this thesis would not have been in the present form. I am able to complete this thesis with their support and encouragement. I am greatly indebted to all of them.

Foremost, I wish to express my deepest gratitude to my research guide, Prof. G. N. Nayak, Department of Marine Sciences, Goa University, Goa, for his constant guidance, motivation, patience and support throughout my Ph.D programme. I truly appreciate him for being an open person to ideas and for encouraging me to carry out research work of my interest. His suggestions and comments throughout the course of my degree are valuable to me. This work would not have been possible without his guidance and encouragement and he will always continue to be a source of inspiration for me to do quality research work in future.

I am thankful to Dr. S. R. Shetye, Vice Chancellor, Goa University and Prof. M. K. Janarthanam, Dean of the Faculty for their support and encouragement. I would also like to thank Prof. Dileep Deobagkar, former Vice Chancellor, Goa University, Prof. P. V. Desai, Prof. G. N. Nayak and Prof. S. N. Bhosle, former Deans of the faculty for their encouragement.

I thank Prof. V. P. Kamat, Registrar, Goa University and his subordinates for their kind administrative help and support.

I wish to place my special thanks to members of FRC committee, Prof. S.N. Bhosle, former Professor and Head, Department of Microbiology, Goa University, Goa for her constructive criticism, valuable suggestions and encouragement throughout the course of work.

My special thanks goes to the Department of Science and Technology (DST) for granting fellowship under “Innovation in Science Pursuit for Inspired Research” (INSPIRE) programme to carry out my research work.

I sincerely thank members of assessment committee, Dr. P. C. Rao, Scientist G, National Institute of Oceanography, Dona Paula, Goa and Prof. V. M. Matta, Department of Marine

Sciences, Goa University, Goa for assessment of two years research work and up-gradation from junior research fellow to senior research fellow.

I am greatly indebted to Dr. S. W. A. Naqvi, Director, NIO, Goa, India and Dr. S. R. Shetye, former Director, NIO, Goa, India for kindly allowing me to utilize the required facilities at the Institute.

I would also like to express profound gratitude to Dr. P. C. Rao for his kind help in getting done the X-ray diffractograms and for his help in computing the results. I am also thankful to technical officer Mr. Girish Prabhu, NIO, Goa for his co-operation and support during the analysis.

My sincere thanks to former Heads and present Head, Prof. C. U. Rivonkar, Department of Marine Sciences, Goa University and other faculty members viz. Prof. H. B. Menon, Prof. V. M. Matta, Dr. S. Upadhyay and Dr. Aftab Can for their encouragement and support.

I am also thankful to the non-teaching staffs of the Department of Marine Sciences viz. Mr. Yashwant, Mr. Samrat, Mr. Ashok, Mr. Shatrugan, Mr. Rosario, Mr. Ratnakar, Mr. Narayan, Mr. Atchut, Mrs. Sanjana, Mrs. Mangal, Mrs. Conceicao and Ms. Reena for their support. I also thank Mr. Serrao, Mr. Martin and Mr. Ulhas for their kind help.

I wish to place my special thanks to Mr. Dinesh T. Velip for his kind help and support during field work and sampling.

My sincere thanks goes to my research colleagues, Leena, Ratnaprabha, Anant, Samida, Sunil, Cheryl, Poornima, Shabnam, Maria, Janvi, Tanu, Shilpa, Shrivardhan, Vinay, Sweety, Mahabaleshwar, Ganesh, Veloisa, Satyam, Vinit, Vijaylaxmi, Samiksha, Sahita, Mithila, Cynthia, Kalpana, Arjun, Neha, Nupur, Atiba and other research students of the department for their help and co-operation.

I owe a lot to my parents who have always been a source of encouragement and inspiration to me throughout my life. Very special thanks to my brothers and other family members for their love, care, constant support and encouragement.

Above all I thank almighty God for granting me health, strength and wisdom to undertake and complete this research work successfully.

Mr. Maheshwar R. Nasnodkar

Table of contents

	Title	Page No.
	Contents	i
	List of Tables	iii
	List of Figures	vi
	Preface	x
Chapter 1	**INTRODUCTION**	**1-21**
1.1	Introduction	2
1.2	Literature Review	8
1.3	Objectives	18
1.4	Study area	19
Chapter 2	**METHODOLOGY**	**22-38**
2.1	Introduction	23
2.2	Field survey: sampling and sub-sampling	27
2.3	Laboratory analysis	27
2.3.1	Sediment component analysis (sand:silt:clay)	28
2.3.2	Clay mineral analysis	29
2.3.3	Clay fraction chemical analysis	30
2.3.4	Organic carbon estimation	30
2.3.5	Sediment digestion for bulk metal analysis	31
2.3.6	Chemical speciation of metals	31
2.3.7	Atomic Absorption Spectrophotometer (AAS) analysis	34
2.4	Data processing	35
Chapter 3	**RESULTS AND DISCUSSION**	**39-213**
	Section I: Lower estuarine region	**40-121**
3.1.1	Sediment components	40
3.1.2	pH	48
3.1.3	Organic carbon	50
3.1.4	Bulk sediment chemistry	53
3.1.5	Clay mineralogy	80
3.1.6	Clay chemistry	85
3.1.7	Speciation of elements	106
3.1.8	Screening quick reference table (SQUIRT)	120
3.1.9	Risk assessment code (RAC)	121
	Section II: Middle estuarine region	**122-209**
3.2.1	Sediment components	122
3.2.2	pH	129
3.2.3	Organic carbon	131
3.2.4	Bulk sediment chemistry	134
3.2.5	Clay mineralogy	160
3.2.6	Clay chemistry	165
3.2.7	Speciation of elements	184
3.2.8	Screening quick reference table (SQUIRT)	206
3.2.9	Risk assessment code (RAC)	208

	Section III: Comparison of lower and middle estuarine regions	**209-213**
3.3.1	Sediment components, pH, organic carbon and metals in bulk sediments	209
3.3.2	Clay minerals and metals in the clay fraction	211
3.3.3	Speciation of elements	213
Chapter 4	**SUMMARY AND CONCLUSION**	**214-223**
	REFERENCES	**224-247**

List of Tables

	Title	Page No.
Table 1.1	Literature survey of the studies carried out in the recent past in India and other parts of the world	8
Table 2.1	Details of sediment cores and sampling locations	28
Table 2.2	Time schedule to be used for pipette analysis	29
Table 2.3.a	Screening quick reference table (SQUIRT) for metals in marine sediments (Buchman 1999)	37
Table 2.3.b	Sediment guidelines and terms used in SQUIRT	37
Table 3.1.1a	Range and average concentration of sediment components, pH and organic carbon in cores VS-1, VG-1, MD-1, S-1 and GP-1	41
Table 3.1.1b	Section wise range and average concentration of sediment components, pH and organic carbon in cores VS-1, VG-1, MD-1, S-1 and GP-1, where L=Lower, M=Middle and U=Upper sections	42
Table 3.1.2a	Range and average concentration of major metals in cores VS-1, VG-1, MD-1, S-1 and GP-1	54
Table 3.1.2b	Section wise range and average concentration of major metals in cores VS-1, VG-1, MD-1, S-1 and GP-1 where L=Lower, M=Middle and U=Upper sections	54
Table 3.1.2c	Range and average concentration of trace metals in cores VS-1, VG-1, MD-1, S-1 and GP-1	55
Table 3.1.2d	Section wise range and average concentration of trace metals in cores VS-1, VG-1, MD-1, S-1 and GP-1 where L=Lower, M=Middle and U=Upper sections	56
Table 3.1.3a	Correlation between sediment components, pH, organic carbon and metals in bulk sediments in core VS-1	72
Table 3.1.3b	Correlation between sediment components, pH, organic carbon and metals in bulk sediments in core VG-1	73
Table 3.1.3c	Correlation between sediment components, pH, organic carbon and metals in bulk sediments in core MD-1	74
Table 3.1.3d	Correlation between sediment components, pH, organic carbon and metals in bulk sediments in core S-1	76
Table 3.1.3e	Correlation between sediment components, pH, organic carbon and metals in bulk sediments in core GP-1	77
Table 3.1.4a	Range and average concentration of clay minerals in cores VS-1, VG-1, S-1 and GP-1.	81
Table 3.1.4b	Range and average concentration of major metals in clay fraction in cores VS-1, VG-1, MD-1, S-1 and GP-1	87
Table 3.1.4c	Range and average concentration of trace metals in clay fraction in cores VS-1, VG-1, MD-1, S-1 and GP-1	87
Table 3.1.5a	Correlation between clay minerals and metals in clay fraction in core VS-1	98
Table 3.1.5b	Correlation between clay minerals and metals in clay fraction in core VG-1	99
Table 3.1.5c	Correlation between metals in clay fraction in core MD-1	99

Table 3.1.5d	Correlation between clay minerals and metals in clay fraction in core S-1	100
Table 3.1.5e	Correlation between clay minerals and metals in clay fraction in core GP-1	101
Table 3.1.6	Average concentration of metals in the bulk sediments for the samples considered for the clay fraction in sediment cores VS-1, VG-1, MD-1, S-1 and GP-1	104
Table 3.1.7	Range and average concentration of Fe, Mn, Ni, Co, Cu, Zn and Cr in different fractions of cores VS-1, VG-1, S-1, MD-1 and GP-1	107
Table 3.1.8	Average concentration of total metals and bioavailable fractions in selected sub-samples in cores VS-1, VG-1, MD-1, S-1 and GP-1	120
Table 3.2.1a	Range and average concentration of sediment components, pH and organic carbon in cores VS-2, VG-2, MD-2, S-2 and GP-2	123
Table 3.2.1b	Section wise range and average concentration of sediment components, pH and organic carbon in cores VS-2, VG-2, MD-2, S-2 and GP-2, where L=Lower, M=Middle and U=Upper sections	124
Table 3.2.2a	Range and average concentration of major metals in cores VS-2, VG-2, MD-2, S-2 and GP-2	135
Table 3.2.2b	Section wise range and average concentration of major metals in cores VS-2, VG-2, MD-2, S-2 and GP-2 where L=Lower, M=Middle and U=Upper sections	135
Table 3.2.2c	Range and average concentration of trace metals in cores VS-2, VG-2, MD-2, S-2 and GP-2	136
Table 3.2.2d	Section wise range and average concentration of trace metals in cores VS-2, VG-2, MD-2, S-2 and GP-2 where L=Lower, M=Middle and U=Upper sections	137
Table 3.2.3a	Correlation between sediment components, pH, organic carbon and metals in bulk sediments in core VS-2	153
Table 3.2.3b	Correlation between sediment components, pH, organic carbon and metals in bulk sediments in core VG-2	154
Table 3.2.3c	Correlation between sediment components, pH, organic carbon and metals in bulk sediments in core MD-2	155
Table 3.2.3d	Correlation between sediment components, pH, organic carbon and metals in bulk sediments in core S-2	156
Table 3.2.3e	Correlation between sediment components, pH, organic carbon and metals in bulk sediments in core GP-2	156
Table 3.2.4a	Range and average concentration of clay minerals in cores VS-2, VG-2, S-2 and GP-2	161
Table 3.2.4b	Range and average concentration of major metals in clay fraction in cores VS-2, VG-2, MD-2, S-2 and GP-2	166
Table 3.2.4c	Range and average concentration of trace metals in clay fraction in cores VS-2, VG-2, MD-2, S-2 and GP-2	166
Table 3.2.5a	Correlation between clay minerals and metals in clay fraction in core VS-2	177
Table 3.2.5b	Correlation between clay minerals and metals in clay fraction in core VG-2	178

Table 3.2.5c	Correlation between metals in clay fraction in core MD-2	178
Table 3.2.5d	Correlation between clay minerals and metals in clay fraction in core S-2	179
Table 3.2.5e	Correlation between clay minerals and metals in clay fraction in core GP-2	180
Table 3.2.6	Average concentration of metals in the bulk sediments for the samples considered for the clay fraction in sediment cores VS-2, VG-2, MD-2, S-2 and GP-2	183
Table 3.2.7	Range and average concentration of Fe, Mn, Ni, Co, Cu, Zn and Cr in different fractions of cores VS-2, VG-2, S-2, MD-2 and GP-2	185
Table 3.2.8	Average concentration of total metals and bioavailable fractions in selected sub-samples in cores VS-2, VG-2, MD-2, S-2 and GP-2	207

List of Figures

	Title	Page No.
Fig. 2.1	Flow chart of the steps followed in sediment core sampling and analysis	23
Fig. 2.2	Map showing location of studied estuaries along central west coast of India	24
Fig. 2.3a	Map showing locations of the sediment cores collected from the Vashishti estuary	25
Fig. 2.3b	Map showing locations of the sediment cores collected from the Vaghotan estuary	25
Fig. 2.3c	Map showing locations of the sediment cores collected from the Mandovi estuary	26
Fig. 2.3d	Map showing locations of the sediment cores collected from the Sharavathi estuary	26
Fig. 2.3e	Map showing locations of the sediment cores collected from the Gurupur estuary	27
Fig. 2.4	Ternary diagram proposed by Pejrup (1988)	35
Fig. 3.1.1	Variation of sediment components with average line in sediment cores VS-1, VG-1, MD-1, S-1 and GP-1	43
Fig. 3.1.2	Ternary plots for cores VS-1, VG-1, MD-1, S-1 and GP-1	44
Fig. 3.1.3	Variation of pH with average line in sediment cores VS-1, VG-1, MD-1, S-1 and GP-1	49
Fig. 3.1.4	Variation of organic carbon with average line in sediment cores VS-1, VG-1, MD-1, S-1 and GP-1	51
Fig. 3.1.5a	Variation of Al, Fe, Mn, Ni, Co, Cu, Zn and Cr with average line in bulk sediments in the core VS-1	57
Fig. 3.1.5b	Variation of Al, Fe, Mn, Ni, Co, Cu, Zn and Cr with average line in bulk sediments in the core VG-1	58
Fig. 3.1.5c	Variation of Al, Fe, Mn, Ni, Co, Cu, Zn and Cr with average line in bulk sediments in the core MD-1	59
Fig. 3.1.5d	Variation of Al, Fe, Mn, Ni, Co, Cu, Zn and Cr with average line in bulk sediments in the core S-1	60
Fig. 3.1.5e	Variation of Al, Fe, Mn, Ni, Co, Cu, Zn and Cr with average line in bulk sediments in the core GP-1	61
Fig. 3.1.6a	Distribution of sediment components along the study area	66
Fig. 3.1.6b	Distribution of pH along the study area.	68
Fig. 3.1.6c	Distribution of organic carbon along the study area.	69
Fig. 3.1.6d	Distribution of major metals in the bulk sediments along the study area.	70
Fig. 3.1.6e	Distribution of trace metals in the bulk sediments along the study area.	71
Fig. 3.1.7	Isocon plots for sediment components, pH, organic carbon and metals in the bulk sediments	79
Fig. 3.1.8a	Variation of clay minerals with average line in sediment core VS-1	82

Fig. 3.1.8b	Variation of clay minerals with average line in sediment core VG-1	83
Fig. 3.1.8c	Variation of clay minerals with average line in sediment core S-1	84
Fig. 3.1.8d	Variation of clay minerals with average line in sediment core GP-1	85
Fig. 3.1.9a	Variation of metals in clay fraction with average line in sediment core VS-1	86
Fig. 3.1.9b	Variation of metals in clay fraction with average line in sediment core VG-1	88
Fig. 3.1.9c	Variation of metals in clay fraction with average line in sediment core MD-1	89
Fig. 3.1.9d	Variation of metals in clay fraction with average line in sediment core S-1	90
Fig. 3.1.9e	Variation of metals in clay fraction with average line in sediment core GP-1	91
Fig. 3.1.10	Distribution of clay minerals along the study area	94
Fig. 3.1.11a	Distribution of major metals in the clay fraction along the study area	96
Fig. 3.1.11b	Distribution of trace metals in the clay fraction along the study area	97
Fig. 3.1.12	Isocon plots for clay minerals and metals in the clay fraction	102
Fig. 3.1.13	Isocon plots for metals in cores VS-1, VG-1, MD-1, S-1 and GP-1	105
Fig. 3.1.14a	Variation of Fe associated with different fractions in core VS-1	106
Fig. 3.1.14b	Variation of Mn associated with different fractions in core VS-1	108
Fig. 3.1.14c	Variation of Ni associated with different fractions in core VS-1	108
Fig. 3.1.14d	Variation of Co associated with different fractions in core VS-1	109
Fig. 3.1.14e	Variation of Cu associated with different fractions in core VS-1	109
Fig. 3.1.14f	Variation of Zn associated with different fractions in core VS-1	110
Fig. 3.1.14g	Variation of Cr associated with different fractions in core VS-1	110
Fig. 3.1.14h	Variation of Fe associated with different fractions in core VG-1	111
Fig. 3.1.14i	Variation of Mn associated with different fractions in core VG-1	112
Fig. 3.1.14j	Variation of Ni associated with different fractions in core VG-1	112
Fig. 3.1.14k	Variation of Co associated with different fractions in core VG-1	113
Fig. 3.1.14l	Variation of Cu associated with different fractions in core VG-1	113
Fig. 3.1.14m	Variation of Zn associated with different fractions in core VG-1	114
Fig. 3.1.14n	Variation of Cr associated with different fractions in core VG-1	114
Fig. 3.1.14o	Variation of Zn associated with different fractions in core MD-1	115
Fig. 3.1.14p	Variation of Zn associated with different fractions in core S-1	116
Fig. 3.1.14q	Variation of Zn associated with different fractions in core GP-1	117
Fig. 3.2.1	Variation of sediment components with average line in sediment cores VS-2, VG-2, MD-2, S-2 and GP-2	125
Fig. 3.2.2	Ternary plots for cores VS-2, VG-2, MD-2, S-2 and GP-2	126
Fig. 3.2.3	Variation of pH with average line in sediment cores VS-2, VG-	130

	2, MD-2, S-2 and GP-2	
Fig. 3.2.4	Variation of organic carbon with average line in sediment cores VS-2, VG-2, MD-2, S-2 and GP-2	132
Fig. 3.2.5a	Variation of Al, Fe, Mn, Ni, Co, Cu, Zn and Cr with average line in bulk sediments in the core VS-2	138
Fig. 3.2.5b	Variation of Al, Fe, Mn, Ni, Co, Cu, Zn and Cr with average line in bulk sediments in the core VG-2	139
Fig. 3.2.5c	Variation of Al, Fe, Mn, Ni, Co, Cu, Zn and Cr with average line in bulk sediments in the core MD-2	140
Fig. 3.2.5d	Variation of Al, Fe, Mn, Ni, Co, Cu, Zn and Cr with average line in bulk sediments in the core S-2	141
Fig. 3.2.5e	Variation of Al, Fe, Mn, Ni, Co, Cu, Zn and Cr with average line in bulk sediments in the core GP-2	142
Fig. 3.2.6a	Distribution of sediment components along the study area	148
Fig. 3.2.6b	Distribution of pH along the study area.	149
Fig. 3.2.6c	Distribution of organic carbon along the study area.	150
Fig. 3.2.6d	Distribution of major metals in the bulk sediments along the study area.	151
Fig. 3.2.6e	Distribution of trace metals in the bulk sediments along the study area.	152
Fig. 3.2.7	Isocon plots for sediment components, pH, organic carbon and metals in the bulk sediments	159
Fig. 3.2.8a	Variation of clay minerals with average line in sediment core VS-2	162
Fig. 3.2.8b	Variation of clay minerals with average line in sediment core VG-2	163
Fig. 3.2.8c	Variation of clay minerals with average line in sediment core S-2	164
Fig. 3.2.8d	Variation of clay minerals with average line in sediment core GP-2	165
Fig. 3.2.9a	Variation of metals in clay fraction with average line in sediment core VS-2	167
Fig. 3.2.9b	Variation of metals in clay fraction with average line in sediment core VG-2	168
Fig. 3.2.9c	Variation of metals in clay fraction with average line in sediment core MD-2	169
Fig. 3.2.9d	Variation of metals in clay fraction with average line in sediment core S-2	170
Fig. 3.2.9e	Variation of metals in clay fraction with average line in sediment core GP-2	171
Fig. 3.2.10	Distribution of clay minerals along the study area	174
Fig. 3.2.11a	Distribution of major metals in the clay fraction along the study area	175
Fig. 3.2.11b	Distribution of trace metals in the clay fraction along the study area	176

Fig. 3.2.12	Isocon plots for clay minerals and metals in the clay fraction	181
Fig. 3.2.13	Isocon plots for metals in cores VS-2, VG-2, MD-2, S-2 and GP-2	183
Fig. 3.2.14a	Variation of Fe associated with different fractions in core VS-2	187
Fig. 3.2.14b	Variation of Mn associated with different fractions in core VS-2	187
Fig. 3.2.14c	Variation of Ni associated with different fractions in core VS-2	188
Fig. 3.2.14d	Variation of Co associated with different fractions in core VS-2	188
Fig. 3.2.14e	Variation of Cu associated with different fractions in core VS-2	189
Fig. 3.2.14f	Variation of Zn associated with different fractions in core VS-2	189
Fig. 3.2.14g	Variation of Cr associated with different fractions in core VS-2	190
Fig. 3.2.14h	Variation of Fe associated with different fractions in core VG-2	191
Fig. 3.2.14i	Variation of Ni associated with different fractions in core VG-2	191
Fig. 3.2.14j	Variation of Co associated with different fractions in core VG-2	192
Fig. 3.2.14k	Variation of Cu associated with different fractions in core VG-2	192
Fig. 3.2.14l	Variation of Cr associated with different fractions in core VG-2	193
Fig. 3.2.14m	Variation of Fe associated with different fractions in core MD-2	194
Fig. 3.2.14n	Variation of Mn associated with different fractions in core MD-2	195
Fig. 3.2.14o	Variation of Ni associated with different fractions in core MD-2	195
Fig. 3.2.14p	Variation of Co associated with different fractions in core MD-2	196
Fig. 3.2.14q	Variation of Zn associated with different fractions in core MD-2	196
Fig. 3.2.14r	Variation of Cr associated with different fractions in core MD-2	197
Fig. 3.2.14s	Variation of Fe associated with different fractions in core S-2	198
Fig. 3.2.14t	Variation of Mn associated with different fractions in core S-2	199
Fig. 3.2.14u	Variation of Ni associated with different fractions in core S-2	199
Fig. 3.2.14v	Variation of Co associated with different fractions in core S-2	200
Fig. 3.2.14w	Variation of Cu associated with different fractions in core S-2	200
Fig. 3.2.14x	Variation of Cr associated with different fractions in core S-2	201
Fig. 3.2.14y	Variation of Fe associated with different fractions in core GP-2	202
Fig. 3.2.14z	Variation of Ni associated with different fractions in core GP-2	202
Fig. 3.2.14aa	Variation of Co associated with different fractions in core GP-2	203
Fig. 3.2.14ab	Variation of Zn associated with different fractions in core GP-2	203
Fig. 3.2.14ac	Variation of Cr associated with different fractions in core GP-2	204
Fig. 3.3.1	Isocon plots for comparing sediment components, pH, organic carbon and metals in the bulk sediments in Vashishti (VS-1 v/s VS-2), Vaghotan (VG-1 v/s VG-2), Mandovi (MD-1 v/s MD-2) Sharavathi (S-1 v/s S-2) and Gurupur estuaries (GP-1 v/s GP-2)	210
Fig. 3.3.2	Isocon plots for comparing clay minerals and metals in the clay fraction in Vashishti (VS-1 v/s VS-2), Vaghotan (VG-1 v/s VG-2), Mandovi (MD-1 v/s MD-2) Sharavathi (S-1 v/s S-2) and Gurupur estuaries (GP-1 v/s GP-2)	212

Preface

Mudflat, one of the important sub-environments in estuaries, is known for deposition of material entering into an estuary through natural as well as anthropogenic pathways. Prior to deposition within mudflats, the material tend to get modified with change in physico-chemical parameters viz., salinity, pH, Eh and dissolved oxygen within estuaries. The variation in these physico-chemical parameters is most common in lower and middle estuarine regions in comparison to upper estuarine region. However, change in energy conditions and associated mixing processes results in varying depositional environment among lower and middle estuarine regions. Further, mudflats are known to preserve undisturbed signature of environmental changes and therefore, study of estuarine mudflat core sediments from lower and middle regions will facilitate reconstruction of the depositional environment within estuaries with time. Metal is common non-biodegradable contaminant which enters the estuarine environment and causes concern to sediment associated biota due to its bioaccumulation and toxicity characteristics. It has been reported that with change in physico-chemical parameters metals can be mobilized and released from sediments to water column resulting in their availability to biota. Hence, it is necessary to study various forms of metals along with total metal concentration to understand the impact of metals on the estuarine environment.

The Vashishti, Vaghotan, Mandovi, Sharavathi and Gurupur estuaries are smaller rivers/estuaries with length of less than 200 km, along central west coast of India. These estuaries experience tropical climate. The rivers have highest water flow rate during monsoon period. The tidal range, rock types in the catchment area, amount of rainfall and associated runoff differ among these estuaries. Further, there is enhanced supply of metals and other pollutants in estuaries along central west coast of India as a result of rapid industrialization and urbanization in the recent years. Moreover, construction of dams on rivers and its tributaries, and agricultural and dredging activities in and around the catchment area have changed the deposition pattern of estuarine sediments as well as metals. With this background, in the present study an attempt has been made to understand the depositional environment within lower and middle regions of estuaries along central west coast of India.

The first chapter includes introduction, wherein detailed information on estuaries is provided. It comprises of definition of an estuary and its classification based on geomorphology, circulation pattern and tidal range. Further, information regarding estuarine sub-environments is also provided with major emphasis on the mudflat sedimentary environment. Details regarding the material entering the estuarine environment through natural as well as human induced activities, undergoing modification with respect to physical, chemical and biological parameters, and deposition in quiet estuarine sub-environment-mudflats are presented. Also, factors regulating distribution and abundance of sediment components, organic matter and metals in lower as well as middle estuarine regions are emphasized. Recent literature on depositional environment of lower and middle estuarine regions is presented in this chapter. The description of the study area and objectives of the present study are detailed at the end of this chapter. The study area consists of five estuaries namely, Vashishti, Vaghotan, Mandovi, Sharavathi and Gurupur estuaries, along central west coast of India. The second chapter includes detailed information on material and methods adopted in order to fulfill the objectives of the present study. Details of core sediment sampling, sub-sampling, storage and standard analytical procedure adopted are given in this chapter.

The third chapter describes results of the various sedimentological and geochemical analysis carried out on sediment sub-samples and presents discussion and inferences drawn. It is divided into three sections. Section I involves study of sediment components, pH, organic carbon content, bulk element chemistry, clay mineralogy, clay chemistry and speciation of elements in the lower estuarine regions along central west coast of India. The study of sediment components, pH, organic carbon content, bulk element chemistry, clay mineralogy, clay chemistry and speciation of elements in the middle estuarine regions along central west coast of India is presented in the section II. While, comparison of sediment components, pH, organic carbon content, bulk element chemistry, clay mineralogy, clay chemistry and speciation of elements in the lower estuarine region with that of middle estuarine region is presented in the section III. Summary of the results and discussions is given in fourth chapter. The references cited are listed at the end of the thesis.

Chapter 1

INTRODUCTION

1.1 Introduction

An estuary is a partially enclosed body of water along the coast where freshwater from rivers and streams meets and mixes with salt water from the sea. Estuary has been defined in numerous ways by authors based on its physico-chemical, geological and biological characteristics. According to Pritchard (1967) an estuary is a semi-enclosed body of water, which has a free connection with the open sea, and within which sea water is measurably diluted with fresh water derived from the land drainage. Estuary is also defined as an inlet of the sea reaching into a river valley as far as the upper limit of the tidal rise by Fairbridge (1980). Estuary is divided into three regions a) a marine or lower estuary, which has free connections with the open sea; b) a middle estuary subjected to strong salt and fresh water mixing; and c) fluvial or upper estuary, characterized by freshwater but subjected to strong tidal action. The boundaries distinguishing these regions shift according to tidal and riverine influences.

On the basis of geology/geomorphology an estuary is divided into five types by Pritchard (1967). (a) Drowned river valleys (coastal plain estuaries) which are formed as a result of sub-aerial weathering and/or sea level rise. Such kinds of estuaries are usually shallow, V-shaped and exhibit meandering characteristics. Depth and width of such estuaries increase uniformly towards the mouth. (b) Rias are special type of drowned river valley estuaries with dissected mouth. (c) Estuaries formed due to the erosion by glacier, are commonly known as Fjords. Fjords are long and deep and generally occur at higher latitudes. They are also characterised by shallow sill seen at the fjord mouth and fjord intersections. (d) Bar-Built estuary is one in which sedimentation has kept pace with inundation and a characteristic bar is seen at the mouth. (e) Estuaries formed due to tectonic processes which are created as a result of subsidence or land movement associated with faulting, folding, volcanoes, landslides and other diastrophic movements.

Estuaries can also be divided into different types based on their salinity stratification (Pritchard 1955). (a) Salt wedge estuaries are dominated by river water and are generally seen where tidal range is small. The sharp changes in the salinity and large quantity of suspended load are characteristics of such estuaries. (b) In partially mixed estuaries, the vigorous rise and fall of the tide generates strong turbulence and causes partial mixing between the fresh water and the salt water. On the other hand, (c) well mixed or fully mixed estuaries have

strong tidal mixing and lower rate of river flow that mixes the sea water throughout the shallow estuary. In such kind of estuaries, salinity does not show much variation with depth. The rotation of the earth influences well mixed estuaries.

Tidal range varies from one estuary to another based on its geomorphological conditions and location of an estuary. Using this characteristic, estuary is classified as microtidal, mesotidal and macrotidal estuary. Estuaries with tidal range of less than 2 m are named as microtidal estuaries. They are dominated by river water and can form salt wedge type of estuary. Estuaries whose tidal range varies between 2 to 4 m are termed as mesotidal estuaries. They exhibit meandering characteristics and formation of two deltas namely, ebb tide delta and flood tide delta (Boothroyd 1978) due to time velocity asymmetry. The region having tidal range of more than 4 m leads to the formation of macrotidal estuaries. The tidal influence is very strong in such estuaries.

Further, as stated earlier, estuary can be divided into lower, middle and upper regions on the basis of river-sea water mixing. The mixing of fresh and saline water brings change in the physico-chemical parameters which in turn alter material within an estuary transported through natural and anthropogenic activities. In comparison to upper estuarine region, lower and middle regions of an estuary are therefore of considerable importance with respect to the biogeochemical processes as waves and tides are forcing factors for mixing (Xin et al. 2010).

Intertidal mudflats and mangroves are prominent sub-environments found on the fringe of estuaries (O'Brien et al. 2000). Mudflats are formed by the deposition of mud by tides or rivers. It generally consists of silt and clay with high organic matter. They are exposed and submerged during low and high tides, respectively (Wang et al. 2008). According to Dyer et al. (2000), mudflats can be divided into three categories, namely: the lower tidal flats that lie between mean low water neap and mean low water spring tides and are often subjected to strong tidal currents; the middle flats which are located between mean low water and mean high water neaps; the upper tidal flats that lie between mean high water neap and mean high water springs. The occurrence and extend of mudflats in an estuary is determined by tidal range, duration, limit of tidal water penetration as well as nature of substratum in estuaries (Pethick 1984).

Mudflats are developed in lower as well as middle regions of an estuary. However, processes and factors influencing their formation differ within these regions. Grain size distribution in an estuary is influenced by the physical processes concerned with the transportation and deposition of sediments (Raj et al. 2013). Tidal flats contain higher percentage of coarser sediments near the mouth of an estuary (Kenjale 1993). This is directly influenced by the tidal action. The higher hydrodynamic condition near the mouth of an estuary favours the deposition of coarser sediments (Siraswar and Nayak 2011). On the other hand, wave and tidal energy carrying finer sediments from the lower estuarine region decreases as they approaches the middle estuarine region and deposits the same facilitating development of finer sediment rich mudflats. In general, systematic sediment size sorting is observed within mudflats from lower to middle estuary. Further, mudflats are proved to be accumulation sites of sediments and contaminants (Madkour 2013). Among the pollutants, metals have received significant attention in the recent years due to their long-term effects on the environment. Trace metals are introduced into the estuarine environment through run-off, atmospheric and marine sources as a result of natural processes as well as from human induced activities. Metals in the dissolved phase get adsorbed onto suspended matter, which gradually sink to the bottom and later incorporate into cohesive sediments of mudflats within estuaries. Over a period of time, layers of sediments are deposited within mudflats. The surface sediments represent the recent input, whereas the layers below are older deposits reflecting changes in environmental conditions from past to present in a sequence (Volvoikar 2014). Mudflats preserve undisturbed record of environmental changes (Singh and Nayak 2009) and therefore, study of estuarine mudflat core sediments from lower and middle regions will help to reconstruct the depositional environment within estuaries with time.

The behaviour of suspended matter, which initiates the adsorption of metals onto sediments, varies between lower and middle estuarine regions. Tidal and seasonal variations in salinity and water temperature within an estuary regulate biological and chemical processes that consequently affect suspended matter by flocculating or deflocculating it. The degree of flocculation is highly dependent upon a number of parameters such as mineralogy (Winterwerp and van Kesteren 2004), electrolytic levels which tend to be altered through salinity in an estuary (Krone 1963), which can in turn affect the zeta-potential of clay particles (Chassagne et al. 2009), suspended sediment concentration (SSC; Burban et al. 1989), organic content (Kranck 1984), and turbulent mixing (Winterwerp 1998; Manning 2004a). The flocculation of mineral particles containing organic matter greatly enhances the

settling velocity of the aggregates (Kranck 1984). This process is predominant in the middle estuarine region which favours deposition of finer sediments associated with organic matter, than that of the lower estuarine region. Further, as the suspended sediment concentration increases, flocculation potential and the resultant settling velocity also increases, while the turbulence creates inter-particle collisions and stimulates flocculation (Mehta 1989; McAnally and Mehta 2001). However, too much turbulence can break flocs apart. The suspended sediment concentration and the turbulence show peak values in the middle estuary.

Estuarine mudflats are complex mixing zones of organic matter derived from diverse sources such as terrigenous, marine, atmospheric and anthropogenic. Terrestrial sources of organic matter, such as soil and vascular plants from the upper reach are the dominant contributor in estuaries (Wu et al. 2000). Heavy rainfall leads to increased addition of terrestrial organic matter along with higher freshwater discharge to estuarine environment (Zong et al. 2006). However, activities like construction of dam for the diversion of fresh water for drinking and irrigational purposes in the recent times have resulted in changes in the natural flow of fresh water and sedimentation patterns (Rodriguez et al. 2001). This led to increase in tidal surge thereby increasing organic matter of marine origin into the estuary. In addition, phytoplankton produced in riverine and coastal waters, marsh plants, and benthic organisms act as major sources of organic matter (Mudge and Norris 1997; Shi et al. 2001). In the recent years, more and more river-estuary systems are influenced by anthropogenic inputs as a result of intense shipping activities, oil spills, and atmospheric deposition as well as changes in land-use patterns, deforestation, and discharge of industrial and municipal waste contributing to additional input of organic matter (Rabouille et al. 2001). Organic matter readily gets adsorbed onto finer sediments due to its larger surface area (Binning and Baird 2001). Therefore, concentration of organic matter is generally higher in the middle estuarine region, favouring deposition of finer sediments, as compared to the lower estuarine region.

The metal concentration within estuarine mudflat sediments often contains a substantial natural contribution from the earth's upper continental crust (Achyuthan et al. 2002) as a result of weathering. In addition, with time there is change in the life style of human's and to meet their needs, more and more industries were set up in the last few years. In general, there is revolution in industrialization and urbanization in the last few decades. This has transformed estuaries as sink for pollutants, which eventually settles down in mudflat sediments. The concentration of metals found in the recent times is considerably higher when

compared to mudflat sediments that were deposited before pre-industrial time (Trefry and Presley 1976). The concentration of metals in sediments varies within an estuary. As stated earlier, in comparison to lower estuarine region, the mixing of fresh and saline waters is higher in the middle estuarine region which facilitates suspension of finer sediments (Billen et al. 1991) for a longer period of time and therefore retains more metals. In addition, middle estuarine region generally receives higher metal and other pollutant input from industries located in its proximity. Willams et al. (1994) stated that the distribution of metals in sediments depends upon factors such as the grain size, mineralogy, distance of element sources to estuary, hydrodynamics, the chemical characteristics (e.g. sorption-adsorption capacity of trace metals, flocculation, etc.), and the chemical and biochemical condition of sedimentary environment. These factors generally favour higher deposition of metals in the middle estuarine region than the lower estuarine region. Earlier studies on estuarine mudflat sediments have reported higher concentration of metals in the middle portion of the estuary than the lower region (Siraswar and Nayak 2011; Pande and Nayak 2013) along west coast of India.

The content of metals in river sediments, chiefly in the clay fraction, is a very good indicator of environmental pollution (Helios-Rybicka and Kyziol 1990). In the finest fraction of sediments (clay), due to the active surface of their components there takes place a continuous enrichment of metals (Nobi et al. 2010). The physico-chemical properties of clays, mainly cation exchange capacity and specific surface area determine the interaction of metals in an estuary (Sondi and Pravdic 1998). The weathering of rocks releases metals, which are held in the lattice structure of alumino-silicate minerals in clays (Volvoikar and Nayak 2013a). Also, clay minerals, due to their large specific surfaces, possess the ability to adsorb cations (Bradl 2002). The presence of humic substances further enhances sorption of metals onto clay minerals through surface-metal-ligand complexation (Hizal and Apak 2006). However, distribution of clay minerals is not uniform within an estuary. The changes in salinity, in addition to temperature and geology of the area govern the percentage of clay minerals in an estuary (Weaver 1989; Chamley 1989). If the rock present in the catchment area is basic rock like basalt, weathering of the rock will release more smectite and weathering of acidic rock like granite, will release more kaolinite. Further, the higher smectite indicates the presence of littoral plains with poorly-drained vertisols formed under seasonal climatic factors, while kaolinite points to altitude-controlled, well-drained source areas with intense hydrolysis under warm and humid climate (Bican-Brisan and Hosu 2006). Illite and especially chlorite

suggest relatively high altitude source areas controlled by an intense mechanical alteration and a fast transport of the terrigenous supply into the sedimentation basin. In addition, smectite generally flocculates faster in highly saline conditions, whereas flocculation of kaolinite is higher in the slight saline conditions. Further, as smectite being finer in size (0.1 - 0.9 μm) than illite, chlorite and kaolinite it tend to adsorb more metals. Therefore, mixing of fresh and saline water determines flocculation of clay minerals and in turn regulates sorption of metals onto clay minerals within an estuary.

Metals have great ecological significance in the estuarine environment due to their persistence, bioaccumulation and toxicity characteristics (Klavin et al. 2000; Tam and Wong 2000). Metals are essential for aquatic organisms, however can become toxic if present above a certain threshold concentration (Depledge et al. 1994). The total metal concentration and distribution of metals in sediments provide the information about spatial extent as well as magnitude of change of the environment (Martin et al. 2012). In estuaries, where fresh water interacts with saline waters, changes in pH, Eh and turbidity are most common (Wotter et al. 2011). The variation in these physico-chemical parameters can cause remobilization of metals from sediments, thereby affecting concentration of chemical speciation of metals and can even pose an environmental risk (Calmano et al. 1993). Additionally, mobility and bioavailability of metals in sediments strongly depend on the mineralogical and chemical forms in which they occur (Baeyens et al. 2003) and each chemical form of a particular metal have considerable impact on the ecosystem (Tessier et al. 1979). Therefore, it is necessary to study different forms of metal in addition to the total metal content to understand bioavailability of metals, their origin, transport and mobilization (Larumbe and Casado 1989; Perin et al. 1997). The sequential extraction procedure has been widely used to separate out metals associated with five different fractions. The mobility of metals is highest in the first two fractions, i.e. exchangeable and carbonate (Lasheen and Ammar 2009). Metals tend to mobilize from Fe-Mn oxide and organic/sulphide bound fractions, however, mobility of metals is less when compared to the first two fractions namely exchangeable and carbonate phases. In residual fraction, metals remain stable and are unaffected by changes in physico-chemical parameters.

1.2 Literature review

Table 1.1 Literature survey of the studies carried out in the recent past in India and other parts of the world.

Authors	Parameters analyzed	Observations
Fernandes and Nayak (2015)	Sediment components, organic carbon, total metal concentration and metals in different size fractions.	The study involved sand, silt, clay, organic carbon and bulk metal concentration (Al, Fe, Mn, Ni, Co, Cu, Zn and Cr) in mudflat and mangrove core sediments representing middle Sharavathi estuary. In addition, metal concentrations in different sediment size fractions (sand (<4Ø), medium silt (6Ø) and clay (8Ø)) was also studied by authors. Finer sediments, organic carbon and bulk metals concentration was higher in the mudflat environment, while mangrove sediments were higher in coarser material. The degradation of organic matter and complexation of metals with organic carbon helped in their adsorption onto finer sediments. Further, enrichment factor for Zn was higher in silt and clay fractions, while it was higher in sand and silt fractions for Co in the mangrove core than the mudflat core. Copper was higher in silt and clay fractions of mudflat core. Chromium was enriched in sand, silt as well as clay fractions of both the cores.
Anand and Kala (2015)	Total metal concentration	This study was carried out to determine the distribution of heavy metals (Cd, Cu, Pb, Cr, Ni, and Zn) in the coastal waters and sediments of Mandapam, Thoothukudi, Arumuganeri and Kanyakumari coasts. Water and sediment samples were enriched in heavy metal concentration which was attributed by the authors to input from anthropogenic activities in the catchment area.
Nasnodkar and	Grain size,	The distribution of grain size, organic carbon and metals

Nayak (2015)	organic carbon and total metals concentration	in mudflat core sediments collected from lower regions of three tropical estuaries, viz. Mandovi, Sharavathi and Gurupur was studied. The similar distribution pattern of metals to that of finer sediments and organic carbon in three estuaries indicated role of finer sediments and organic carbon in distribution of metals. In addition, correlation, factor and cluster analyses suggested role of Fe and/or Mn oxides in adsorption of metals onto sediments. However, the factors regulating distribution of metals varied among the three estuaries. In addition, metals showed difference in their associations with Fe and/or Mn oxide within cores collected from Mandovi and Sharavathi estuaries. The difference in metals behaviour was attributed by authors to variation in rock types in basins, in addition to changes in response to natural forces and human activities, with time, as well as variation in tidal range.
Lak et al. (2015)	Grain size and total metal concentration	The study involved in understanding distribution of heavy metals (Fe, Al, Mn, Cu, Zn, Cr, Pb, Ni and Cd) in Shafaroud River-South West of Caspian Sea sediments of various size (<38 μm, 38-63 μm, 63-125 μm, 125-250 μm, 250-500 μm, 500 μm-1 mm). It indicated higher concentration of metals viz. Cu, Mn and Zn in < 38 μm (clay and silt) size particles. Metals viz. Al and Cd were higher in 63-125 μm size particles, while Fe and Pb were higher in 125-250 μm and 38-63 μm size particles respectively. The concentration of Cr and Ni was higher in 250-500 μm size particles.
Guo and Yang (2015)	Grain size and Total metal concentration	The distribution of heavy metals (Cu, Zn, Cr and Pb) in three sediment cores collected from the lower basin of the Changjiang (Yangtze River) and the inner shelf mud of the East China Sea were analysed by authors. Their study suggested enrichment in concentrations of Pb and

		Zn since 1950s. Further, after removing the grain size effect on elemental concentrations, they inferred that the sources of heavy metals predominantly came from natural weathering detritus, while human contamination had increased over the last half century.
Cao et al. (2015)	Total metal concentration	The elements (Al, Fe, Mn, Cr, Co, Ni, Cu, Zn, As, Pb and Ca) in the bottom sediment of the Changjiang Estuary and its adjacent continental shelf of the East China Sea were studied to map their spatial distribution and to assess their potential risk to the associated biota. Except Ca, rest all the metals were higher in the inner shelf and north-eastern part, and were found to decrease from the coast to the offshore of the Changjiang Estuary. Ca was most abundant in the outer shelf sediments and decreased in inner shelf. Authors reported that the sediments appeared to be contaminated with arsenic (As) due to economic development from 1980s in the inner shelf. However, the potential ecological risk from the metals was low in the coastal sea off the Changjiang.
Abdullah et al. (2015)	Clay minerals	The clay mineral composition of the surface estuarine sediments from the selected estuaries (Terengganu River, Kemaman River, Dungun River and Besut River) of Terengganu was investigated by the authors in order to know the types of clay minerals, source of sediments and their distribution. Results indicated that the clay minerals found from the Holocene sediments were dominated with kaolinite and illite/muscovite and few amounts of chlorite and smectite. The abundance of kaolinite and illite was attributed to the weathering products of granite or igneous rocks along the East Coast of Peninsular Malaysia containing feldspar and mica. They further suggested that warm and humid

		climate lead to excessive weathering of rocks and transformation of minerals.
Chakraborty et al. (2015)	Organic carbon and speciation of metals	The chemical speciation of lead (Pb) and cadmium (Cd) in the coastal and estuarine sediments along the central east coast of India was studied. The results of this study suggested that concentrations of non-residual and dynamic complexes (which are good indicators of bioavailability) of these toxic metals gradually increased with increasing total metal loading in sediments. Their study indicated role of total metal loading and trace metal competitions in distribution and speciation of metals. Also, total organic carbon (TOC) to a certain extent played important role in regulating speciation of Pb and Cd in sediments.
Osakwe et al. (2014)	Speciation of elements	The sequential extraction procedure was employed to investigate the potential environmental risk of metals (Cd, Cu, Zn, Ni, Pb and Fe) in sediments from the upper reaches of Imo River system in South-eastern Nigeria. Chemical speciation of metals revealed that Cd in sediment prevailed mostly in exchangeable fraction, while Cu, Pb and Fe were more in the residual fraction. Metals viz. Zn and Ni were found more in carbonate, organic and residual fractions. Further, mobility factor indices for metals in sediments revealed a high environmental contamination risk for Ni and Cd, which suggested an environmental threat to the river ecosystem.
Zhuang and Gao (2014)	Total metal concentration	Surface sediments in the Xiaoqinghe estuary, South-western coastal Laizhou Bay, were examined to assess the bio-toxic risk of heavy metals (Cd, Cu, Ni, Pb and Zn) with the effects range-low and effects range median guidelines (ERL-ERMs) and the concentration ratio of simultaneously extractable metals to acid volatile

		sulfides ([SEM]/[AVS]). Based on the ERL-ERM guidelines, bio-toxic effect caused by Cu, Ni, Pb and Zn could be expected in the riverine surface sediments of the Xiaoqinghe estuary; and Ni indicated bio-toxic effects in the surface sediments in the marine area. Further, AVS–SEM guidelines revealed that no bio-toxic effect could be caused by any of the studied metals in both riverine and marine sediments, since there were excess sulfides in surface sediments which could form water-insoluble substances with free metal ions and reduce the bioavailability of heavy metals.
Oyedotun et al. (2013)	Grain size	Grain size distribution in 44 short sediment cores (length < 15 cm) collected from the Camel estuary was studied. In the lower estuarine region, mixture of fine-medium and coarser sand suggested marine sediment source, and higher energy processes. In the middle estuary, mixture of finer sediments (silt and clay) with fine-medium sand suggested fluvially-sourced material, while concentration of fine sand, silt and clay was higher in the upper estuary. The absence of fine-medium sand in the upper estuary suggested that marine-derived sediments were not supplied to the far inner estuary.
Singh et al. (2013)	Sediment components, organic carbon and total metal concentration	Three mudflat sediment cores collected from intertidal regions of the Zuari estuary and Cumbarjua canal were analysed for sediment components, organic carbon, trace (Co, Cr, Zn, Cu, and Pb) and major metals (Al, Mn, Fe, Ca, Mg, and K). The cores collected from the upper middle estuarine environment showed higher percentage of finer sediments, organic carbon and most of the metals than core which was sampled from the lower estuarine environment. Further, enrichment factor computed in all the cores was found to be above 2 for

		all the studied metals except Zn, which suggested a high degree of metal contamination.
Volvoikar and Nayak (2013a)	Grain size, organic carbon, total metals, metals in clay-sized fraction and metal speciation	The distributions of sediment components, organic carbon, metals (Fe, Mn, Al, Co, Zn, Cu, Ni and Pb) in bulk sediments and clay sized fraction was investigated in sediment cores collected from intertidal mudflats of Vaitarna estuary. The study of depositional environment of mudflat sediments suggested sorting of grain size under varying hydrodynamic energy conditions. Metals viz. Fe, Mn, Al, Co, Cu and Ni suggested their anthropogenic origin in addition to their lithogenic source in the Vaitarna estuary. On the other hand, Pb and Zn indicated their lithogenic origin.
Pande and Nayak (2013)	Sediment components, organic carbon and total metals concentration	The study involved spatial and depth-wise distribution of sediment components, organic carbon and selected metals (Fe, Mn, Al, Ni, Cr, Co, Zn and Pb) across upper and middle tidal flats from lower and middle estuarine regions of Kundalika Estuary, central west coast of India. Deposition of sediments indicated change in hydrodynamic conditions with time in lower and middle estuarine regions. Clay, organic carbon and Fe-Mn oxides played important role in distribution of metals. Further, Ni, Cr and Co indicated anthropogenic source in the middle flats of the lower estuary.
Ganesh et al. (2013)	Grain size and clay minerals	The textural and clay mineralogical study of Gosthani estuarine sediments was carried out. The textural study indicated sediments of medium grain size, moderately sorted, positively skewed and were deposited under moderate to low energy conditions with dominant rolling and suspension mechanisms. The clay mineralogy of these sediments indicated dominance of illite, while kaolinite, montmorillonite and chlorite were present in minor amounts in sediments. The hinterland

		lithology composed of khondalites with associated acidic and basic rocks was the major source for clay minerals.
Feng et al. 2012	Total metal concentration and ^{210}Pb sediment dating	The distribution of heavy metals (Pb, Zn, Cd and As) in surface and core sediments of the Pearl River Estuary was investigated. The spatial distribution of heavy metals displayed a decreasing pattern from the turbidity maxima to both upstream and downstream of the estuary, which suggested that suspended sediments played an important role in the trace metal distribution in the Pearl River Estuary. In the sediment cores, fluxes of heavy metals were consistent with a predominant anthropogenic input in the period 1970-1990. Further, from the mid-1990s to the 2000s, they reported significant decrease in heavy metal pollution which was attributed to pollution control in the Pearl River Delta.
Banerjee et al. (2012)	^{210}Pb geochronology and total metal concentration	^{210}Pb geochronology and trace metal distribution in four sediment cores collected from selected locations of Sundarbans mangroves and Hooghly estuary, North-East coast of India were determined. The mass accumulation rates ranged from 0.41 g cm^{-2} year^{-1} (estuarine region) to 0.66 g cm^{-2} year^{-1} (mangrove region). In mangroves as well as estuarine systems, Fe-Mn oxy-hydroxides were observed to be a major factor for trace metal accumulation when compared to organic matter. Core collected from the Hooghly estuary showed less contamination in comparison to the mangrove region due to high energy conditions.
Lan et al. (2012)	Clay minerals	The surface sediments off the Yangtze River estuary were studied in order to understand the assemblages and the distributions of clay minerals. Their results showed dominance of illite in sediments. Illite-smectite-kaolinite-chlorite-assemblage was the main type of the

		clay minerals assemblage in the area. Further, their study suggested rocks in the basin of the Yellow River and the Yangtze River as the source for clay minerals.
Liu et al. (2011)	Grain size, pH, total organic carbon, cation exchange capacity, total metals and speciation of metals	In this study a sediment core collected from coastal zone near the Qiao Island in the Pearl River Estuary was analyzed for total metal concentrations (Cu, Pb, Cr, Zn), chemical partitioning, and physico-chemical properties. The sediment pH influenced Cr, Cu, and Zn associated with Fe/Mn oxides, organic/sulfide and residual fractions. The influence of total organic carbon content and cation exchange capacity on the total concentrations and fractions of almost all the metals was not seen. Residual and Fe/Mn oxides fractions were dominant binding phases for Cu, Pb, Cr, and Zn.
Siraswar and Nayak (2011)	Sand, silt, clay, organic carbon and total metal concentration	The sediment cores representing lower, lower middle and upper middle regions of the Mandovi estuary were analysed for sediment components, organic carbon and bulk metal concentration. Coarser sediments were higher in the lower estuarine region, while finer sediments and organic carbon were higher in lower middle and upper middle estuarine regions. The distribution of metals in sediments was influenced by finer sediments, organic carbon and Fe-Mn oxides.
Zakir and Shikazona (2011)	Speciation of elements	The geochemical partitioning of Fe, Mn, Co, Ni and Mo were examined in sediments collected from the whole old Nakagawa river (NR), Tokyo, Japan. Metals viz. Co, Ni and Mo were highest in amorphous Fe oxy-hydroxide phase, whereas Fe and Mn were highest in silicates and residual phase. The normalization of metals using Al suggested that most of the sampling stations of NR were enriched with Ni, Mo and Mn. Further, risk assessment code (RAC) indicated medium degree risk to sediment associated biota from Ni, Mo,

		Co and Mn.
Delgado et al. (2011)	Clay minerals and speciation of metals.	Clay minerals and speciation of metals analyses were carried out in sediments of the Guadiana Estuary. Mineralogical analysis showed presence of quartz, albite, and clay minerals (illite, smectite, kaolinite, and vermiculite) along with several small, reactive compounds (including soluble sulphated salts, Fe-Mn oxy-hydroxides, organic matter, and pyrite) in sediments capable of retaining metals, which can be subsequently released, causing environmental degradation. BCR (Community Bureau of Reference) sequential extraction suggested higher As, Cd, Cu, Mn, Pb and Zn in the mobile fractions. The environmental risk indices demonstrated moderate to considerable ecological risk for almost the entire estuary, associated mainly with acid mine drainage from the nearby Iberian Pyrite Belt.
Fernandes and Nayak (2010)	Sediment components, pH, organic carbon, phosphorus, nitrogen and total metal concentration	A 60 cm mudflat sediment core collected from the Ulhas estuary was studied for sediment components, pH, TOC, TP, TN, and metals such as Fe, Mn, Cu, Pb, Co, Ni, Zn, Cr, V and A1. On the basis of distribution pattern of sediment components, core was divided into three sections, namely lower, middle and upper sections. Finer sediments were higher in lower and upper sections, while the middle section was dominated with coarser sediments. The variation in grain size along the length of the core indicated difference in sedimentation rate and associated processes with time.
Chunyan et al. (2010)	Clay minerals	The authors studied clay minerals in the surficial sediments of major coastal estuaries, i.e., from North to South, the Yellow, abandoned Yellow, Yangtze, Qiantang, Ou, Min, Han, and Pearl River estuaries. The results showed the change of diagnostic clay minerals

		from smectite to kaolinite from the Yellow to the Pearl River estuary. The ratio of S/Ch decreased Southward, while K/I moved reversely, implying change in climate setting from cool/dry to humid/hot with intensified weathering processes. Further, indicated role of climate, parent-rock, and sediment transport along the coast in the distribution of clay minerals.
Sharmin et al. (2010)	Clay minerals and speciation of elements	The geochemical partitioning and mobility pattern of Fe, Mn, Cd, Cu, Cr and Ni in sediment samples collected from Nomi River, Tokyo, Japan was studied. The highest concentration of Cd was reported in adsorbed, exchangeable and carbonate (AEC) fractions, while, Fe, Mn, Cr and Ni were higher in the residual phase. The maximum association of Cu was recorded with amorphous Fe oxy-hydroxide phase. The risk assessment code applied suggested medium risk from Cu, Ni and Cr to sediment associated biota, whereas Cd indicated high degree of risk.
Okuku et al. (2010)	Speciation of elements	The sediment samples collected from eight sites along the Eastern African Coast were analysed for speciation of metals (Al, Cd, Co, Cr, Cu, Fe, Mn, Ni, and Zn) using three-step BCR sequential extraction procedure. Cd, Mn and Co was more concentrated in labile fractions compared to other elements and therefore, suggested their availability for biological uptake.
Fernandes and Nayak (2009)	Sediment components, organic carbon, total phosphorus, and total metals concentration	The distribution of sediment components, organic carbon, total phosphorus, and selected elements (Fe, Mn and Cr) was studied in mudflat sediment cores from lower and middle Mandovi estuary. The study revealed that the sediment components, organic carbon, and phosphorus played an important role in distribution of Fe, Mn and Cr. It also indicated that hydrodynamic energy conditions resulting in deposition of sediments

		varied among lower and middle estuarine regions. Further, remobilization of elements, early diagenetic processes operating and importance of the oxic-anoxic layer in the distribution and concentration of trace metals was discussed.
Patchineelam and Neto (2007)	Sediment components, organic matter and clay minerals	Grain size, organic matter and clay mineral analyses were carried out in bottom sediments of Guanabara Bay. The inner section of the bay was enriched with finer sediments and organic matter. Among the clay minerals, kaolinite was higher than illite and smectite. The clay minerals identified showed detrital characteristics which indicated an absence of recent authigenic processes within the surface sediments of the bay. Further, smectite was low (0.15 %) for the station having average salinity of 14 $^{o}/_{oo}$ in the inner region, whereas, it was higher (17 %) for the station with average salinity of 32 $^{o}/_{oo}$ in more saline region of the bay. An inverse relationship between kaolinite and smectite in relative abundance was observed along the bay.

1.3 Objectives

The central west coast of India is known for smaller rivers/estuaries having length of less than 200 km. This region experiences tropical climate and water flow rate in rivers along this region is highest during monsoon period. However, there is difference in estuaries with respect to amount of rainfall and associated runoff they receive. In addition, rock types in the catchment area and tidal range varies among the estuaries along this region. Further, rapid industrialization and urbanization has enhanced release of metals and pollutants. In addition, other human induced activities like construction of dams, agricultural practices, dredging activities etc. have altered the deposition pattern of estuarine sediments and metals. With this background, in the present study an attempt has been made to understand the depositional environment within lower and middle regions of estuaries along central west coast of India with the following objectives.

- To study the distribution (spatial and temporal) and abundance of sediment components from selected locations within estuaries along central west coast of India.

- To understand the source and the factors influencing the distribution of sediment components along central west coast of India.

1.4 Study area

The west coast of India extends from Gujarat to Kanyakumari in Tamil Nadu. It is bounded in the west by the Arabian Sea. Maharashtra, Goa and Karnataka together comprise the central portion of the west coast of India. This region is highly diverse with respect to coastal environmental features such as estuaries, creeks, lagoons, bays etc. Among these, an estuary is a highly dynamic environment due to variations in pH, salinity, temperature, dissolved oxygen, redox potential, and amount and composition of sediment particles (Chapman and Wang 2001). The variation in these physico-chemical parameters brings about modification in dissolved and particulate matter entering the estuarine environment through natural weathering of rocks as well as from pollutants released by human activities (Jordao et al. 2002). Such biogeochemical processes within estuaries are of importance as they affect the net fluxes of the pollutants (Boldt et al. 2013), which can cause concern to associated biota.

A large number of rivers originate in the Western Ghats and drain into the Arabian Sea. They are fast flowing and are mostly perennial rivers. This characteristic of the rivers leads to the formation of estuaries rather than deltas. Mudflat is one of the important sub-environments found in estuaries. Estuaries receive material from multiple sources such as natural weathering of rocks, domestic and industrial sewage outfalls, effluents from mines, and agricultural runoff which eventually gets deposited within mudflat sediments. The growing population and associated rapid industrialization in and around central west coast of India has increased anthropogenic inputs. Therefore, estuarine mudflats are under increasing stress from the human activities as well as by sea level change. The geochemical study of estuarine mudflat sediments was hence felt essential to understand the depositional environment of sediments with time along with abundance of metals.

For the present study five estuaries namely, Vashishi, Vaghotan, Mandovi, Sharavathi and Gurupur were selected from North to South within central west coast of India.

Vashishti River originates in the Western Ghats and drain into the Arabian Sea. The river forms a wider channel with sweeping meanders from Chiplun city and has a long stretch of 40 km comprising mudflats and mangroves. Shoals and sand bars are present at the mouth of the Vashishti River and they show a seasonal shift. The highest tide near the mouth is 3.1 m during spring and reduces to 0.7 m during neap tide. Estuary is dominated by semi-diurnal tides (Panchang 2014). The river has number of tributaries, the most important of which are Jagbudi and Tambi. The catchment area of the Vashishti river consists of Deccan trap basalts (Zingde et al. 1995) having tholeiitic composition (Wensink 1973). The southwest monsoon with an average precipitation of 2500 mm rainfall and strong winds (Ingole et al. 2002) brings material from catchment area to the estuary. The middle estuarine region of the Vashishti is in close proximity of Lote Parshuram industrial zone that accommodates various chemical industries which discharge their untreated wastes into the Vashishti river and this discharge was estimated to reach a mark of 45,000 m^3/day by 2010 (Nair et al. 1998). In addition to industrial hazards, the estuary is also subjected to other anthropogenic activities such as domestic and agricultural wastes discharge and sand mining (Dandekar 2010).

The Vaghotan River with a total length of 68 km flowing from the east to west direction rises in the Kajirda region of the Western Ghats (Sahyadris), in Maharashtra and flows for a distance of 24 km where it becomes tidal. The river further rapidly widens to join the sea in a wide estuary that is protected from the South by the rocky height of the Vijayadurg fort. The river is free from sand bars and is therefore navigable for vessels of medium size up to 32 km inland. The River Vaghotan reflects a dominant tectonic control with steep graded profiles and deep V-shaped valleys. Its basin area consists of extensive cover of laterite (Tripati et al. 1998) over the Deccan trap basalts. It receives an annual average rainfall of 3,028 mm, most of which occurs during the monsoon period. The Vaghotan River debouches water and sediments into the Vijaydurg bay. The sediment in the bay is composed of sand and silty clay with variable proportions of quartz, feldspar, calcareous minerals and heavy minerals. The rate of deposition at the South of Vijaydurg coast is reported to be around 1.27 cm/year based on ^{210}Pb geochronology (Gujar 1996; Gujar et al. 2005).

The Mandovi River forms an important estuarine system on the central west coast of India. It has a tidal range of 2.3 and 1.5 m during spring and neap tide, respectively (Rao et al. 2011). The river is 70 km long and has a catchment area of 1150 km^2 (Pathak et al. 1988). The catchment area of the Mandovi estuary comprises of Western Dharwar Craton (WDC)

containing meta-volcanic and meta-sedimentary rocks (Naqvi 2005). The river drains through the Western Ghats. The river receives an annual average rainfall of 2932 mm. During monsoon, a salt wedge is formed at the mouth region due to strong tidal action and large riverine flow. There are about 27 active large mines in the basin area of Mandovi that generate 1500-6000 tons of rejects per day per mine, a substantial portion of which is expected to ultimately end up in the river (Fernandes and Nayak 2009). The estuarine channel of the Mandovi River is widely used for the transport of iron and ferro-manganese ores to the Marmugao harbour throughout the year.

The Sharavathi River originates near Ambuthirtha and joins the Arabian Sea at Honnavar. It has a total length of 130 km and a catchment area of 3600 km^2 (Ramachandra et al. 2004). Sharavathi has a tidal range of 1.41 and 0.66 m during spring and neap tide respectively (Kumar et al. 2011). The basin area of the Sharavathi River consists of two groups of rocks, namely Dharwar system and peninsular gneiss containing metamorphic and crystalline rocks which are made up of granites and granitic-gneisses. The annual average rainfall near Honnavar is 3521 mm (Avinash et al. 2008). In 1964, a dam was constructed near Linganamakki on Sharavathi which is used for generation of hydroelectric power. There were well established open cast mining activities in the catchment area of this river, however, they have been halted since last few years. The extensive urbanisation, especially near Honnavar has exposed estuary to increasing stress from domestic wastes in addition to activities like agriculture and sand mining.

The Gurupur River is also known as Phalguni/Kulur River. It has a total length of 87 km and a catchment area of 540.62 km^2. The highest tide is 1.54 m near Mangalore and decreases to 0.25 m during neap tide (Radheshyam et al. 2010). The rock types in the catchment area of the Gurupur River consists of gneisses and continental type of sedimentary deposits with dolerite and norite dikes (Radhakrishna and Vaidyanadhan 1994). The Gurupur estuary receives an annual average rainfall of 3900 mm (Kumar et al. 2010). Kudremukh mine of Karnataka is one of the largest iron ore mine within the catchment area of Gurupur. The iron ore concentrate from Kudremukh mine was transported to Kudremukh Iron Ore Company Limited (KIOCL) located at Mangalore through pipelines; the ore was pelletised and then exported to different countries. The mine has not been in working conditions for the past few years. The Baikampady industrial zone accommodates various chemical and pharmaceutical industries, is located on the bank of the Gurupur River.

Chapter 2

METHODOLOGY

2.1 Introduction

According to Leedy and Ormrod (2001), "research is a viable approach to a problem only when there are data to support it". A scientific study involves a process of collecting representative sample data from an area and processing it, to infer attributes of that area. The sample should essentially represent the given environment to fulfil the objectives of the study. It is vital to avoid or minimize sample contamination during sampling, subsequent sub-sampling, storage and analytical procedure. Each step mentioned in the analytical protocol has to be strictly adhered for ensuring a reliable analytical result.

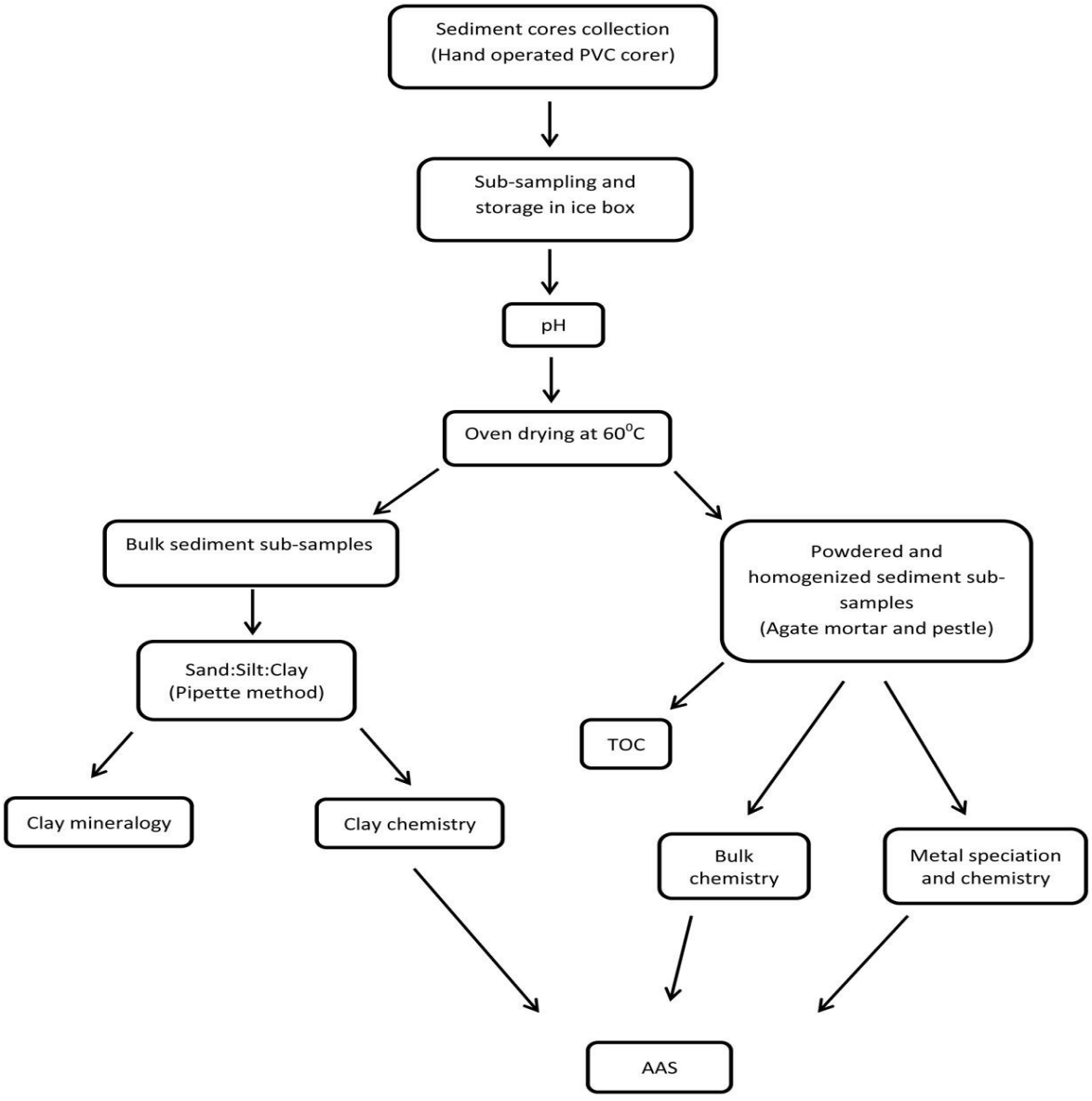

Fig. 2.1 Flow chart of the steps followed in sediment core sampling and analysis

In the present study, sediment cores were collected from the mudflats, sub-environment of the estuaries, representing lower and middle estuarine regions. During sampling, care was taken to avoid metallic interference as the present study involved metal analysis. Microbial activities are known to alter the chemical composition of sediments; hence, in order to avoid such alterations, sediment sub-samples were stored in ice. The apparatus were acid washed, rinsed with distilled water and later dried in the oven prior to analysis. Analytical reagents of suprapure grade were used throughout the study. Each and every step mentioned in the standard protocol was strictly followed.

The detailed information regarding method of sampling, sub-sampling, storage, analytical procedures used for obtaining reliable data are outlined in the form of a flow chart (Fig 2.1). Also, details of data processing are given in this chapter.

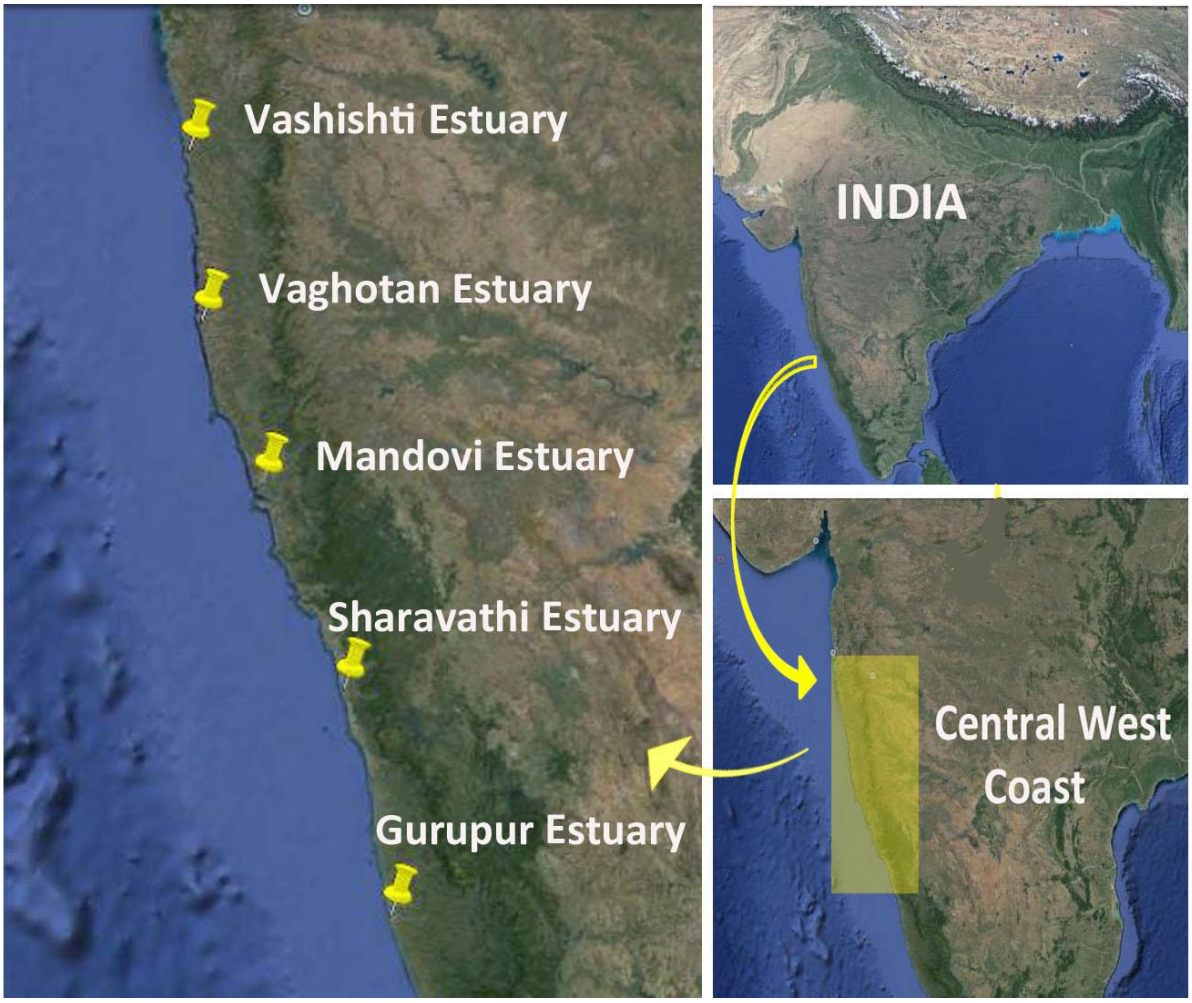

Fig. 2.2 Map showing location of studied estuaries along the central west coast of India

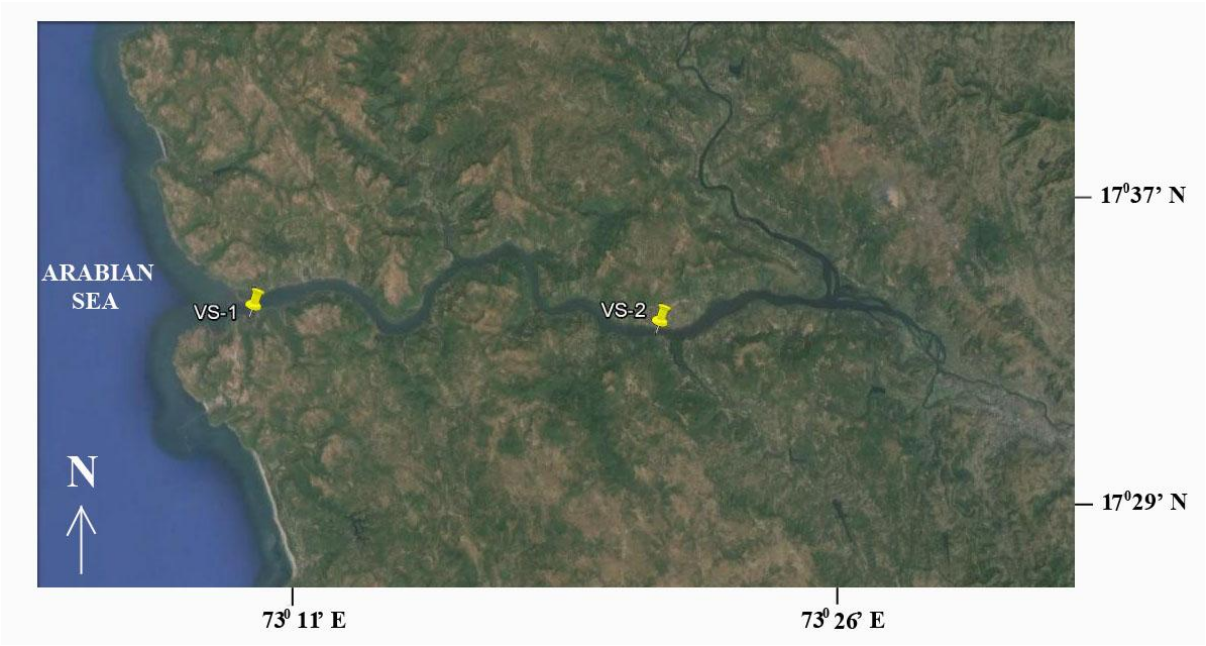

Fig. 2.3a Map showing locations of the sediment cores collected from the Vashishti estuary

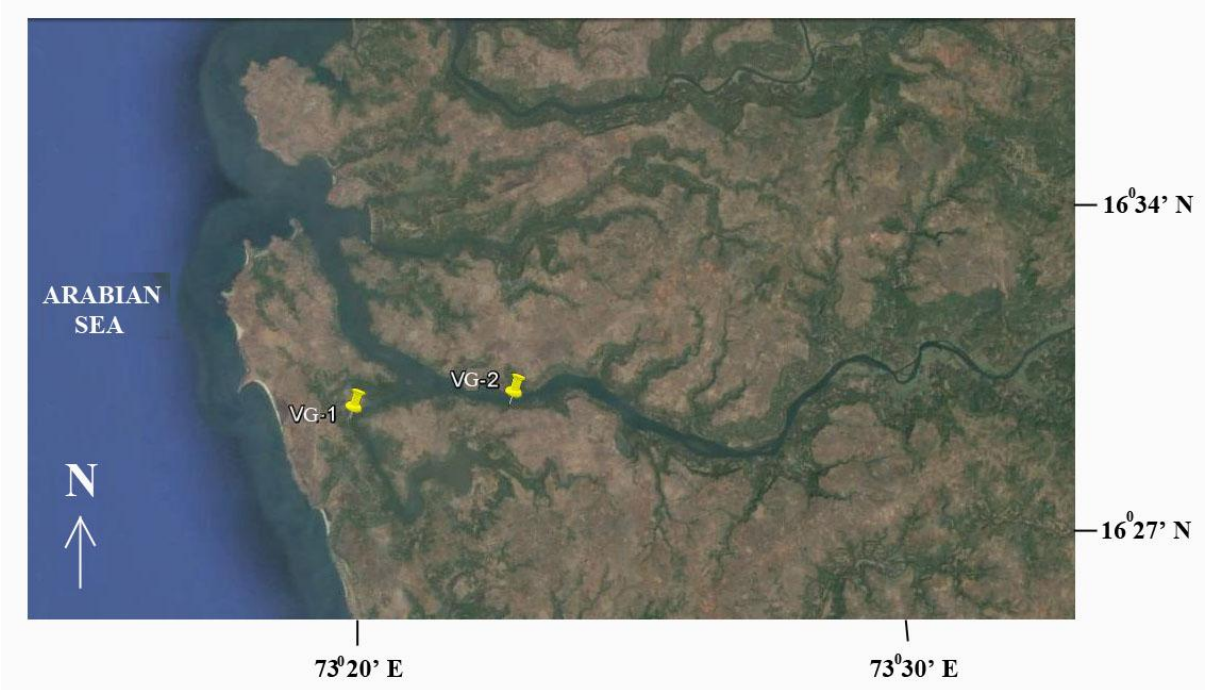

Fig. 2.3b Map showing locations of the sediment cores collected from the Vaghotan estuary

Fig. 2.3c Map showing locations of the sediment cores collected from the Mandovi estuary

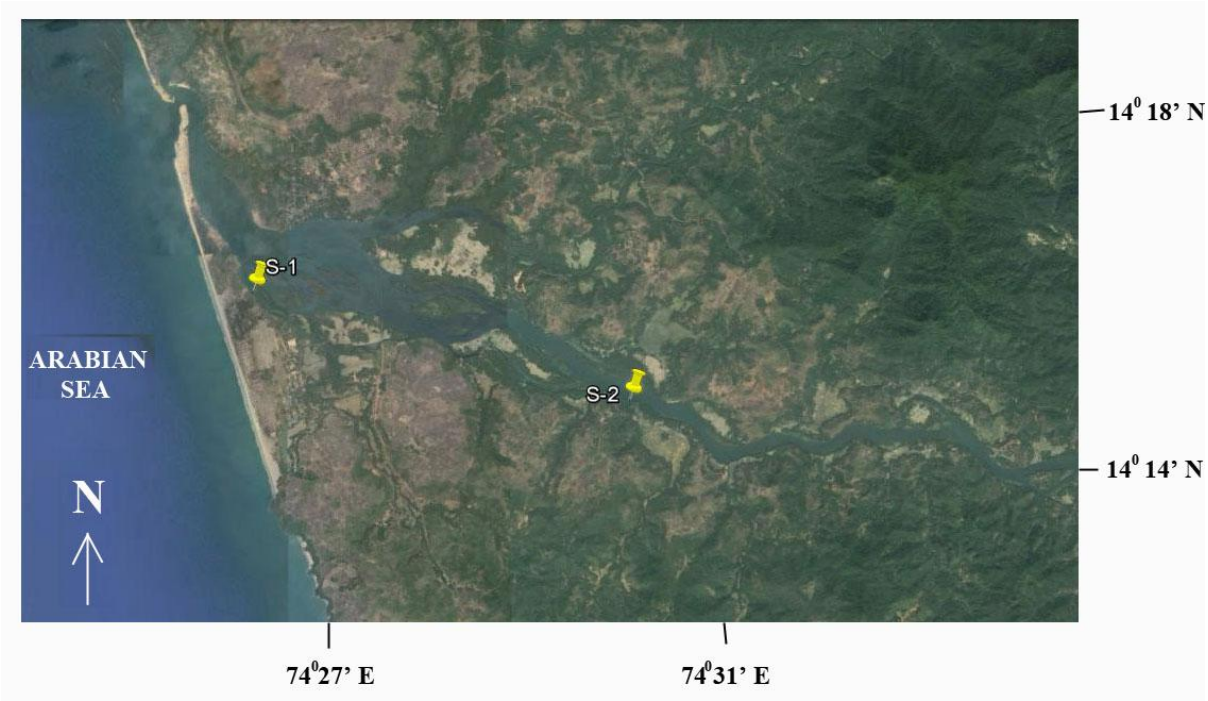

Fig. 2.3d Map showing locations of the sediment cores collected from the Sharavathi estuary

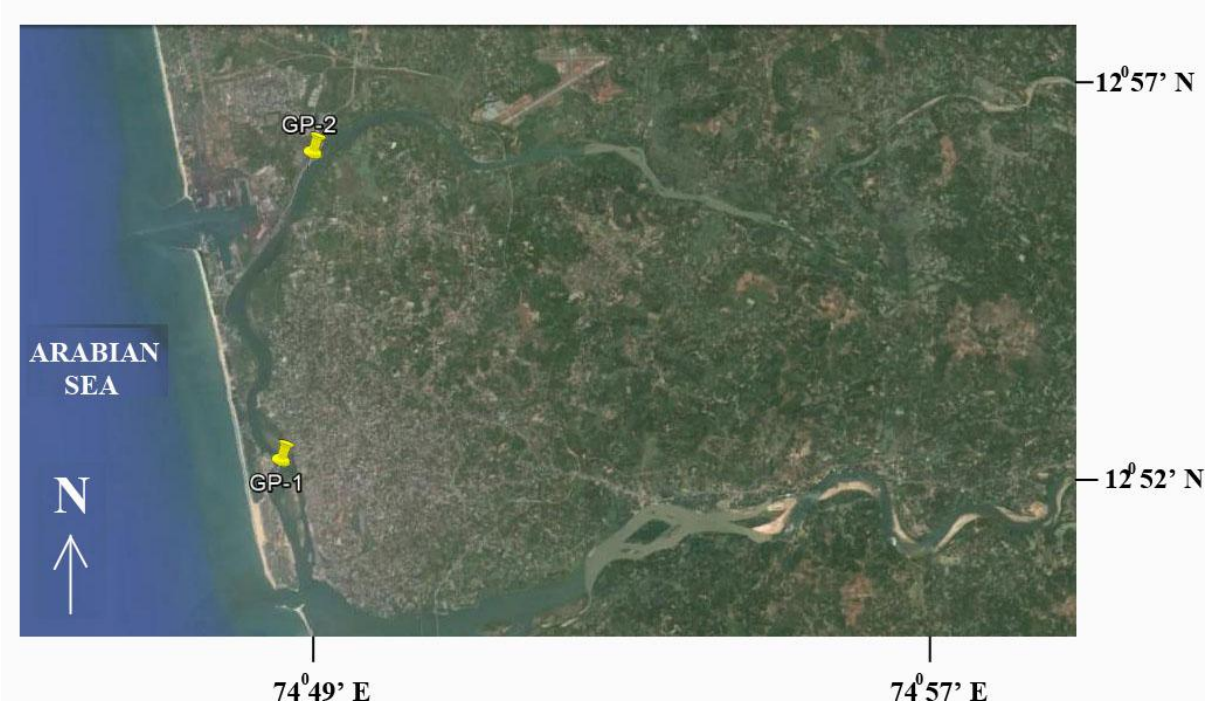

Fig. 2.3e Map showing locations of the sediment cores collected from the Gurupur estuary

2.2 Field survey: sampling and sub-sampling

Intertidal mudflat sediment cores were collected from the five tropical estuaries, along central west coast of India during the field survey conducted in May 2011. Total of 10 sediment cores (Fig. 2.2 and 2.3), two from each estuary, representing lower and middle estuarine regions were collected. Cores varied in their length from 48 cm to 82 cm. Detailed information regarding the cores is presented in the Table 2.1. Sediment cores were collected using a hand operated PVC corer and sampling stations were located using a global positioning system (GPS). Following the sediment core collection, core length was measured. Further, cores were sub-sampled at 2 cm interval using a plastic knife. Sub-samples were then sealed in clean plastic bags, labelled, stored in ice box and later transferred to the laboratory.

2.3 Laboratory analysis

Upon reaching to the laboratory, pH of the sub-samples was measured (Thermo Orion 420A + model) and the sub-samples were stored at 4^0C till further analysis. Later, the sub-samples were oven dried at 60^0C. Part of the dried sediments was used for the analysis of sediment components (sand:silt:clay), clay mineralogy and clay chemistry. Portion of the dried

sediments was finely powdered and homogenized using an agate mortar and pestle. The powdered and homogenized sediment samples were used for the estimation of total organic carbon, bulk metal chemistry and speciation of metal. The procedures followed for the determination of various sediment parameters are detailed below.

Table 2.1 Details of sediment cores and sampling locations

Name of the Estuary	Portion of the Estuary	Station location	Length of the core (cm)
Vashishti	Lower (VS-1)	17^0 34’ 31.20”N; 73^0 10’ 22.79”E	48
	Middle (VS-2)	17^0 34’ 02.47”N; 73^0 21’ 55.26”E	70
Vaghotan	Lower (VG-1)	16° 30' 17.81"N; 73° 20' 55.60"E	60
	Middle (VG-2)	16° 30' 31.25"N; 73° 23' 46.06"E	54
Mandovi	Lower (MD-1)	15°30' 23.81"N; 73° 49' 25.60"E	58
	Middle (MD-2)	15° 31' 11. 37"N; 73° 55' 29.43"E	82
Sharavathi	Lower (S-1)	14^0 15’ 51.40”N; 74^0 26’ 18.90”E	68
	Middle (S-2)	14^0 14’ 39.46”N; 74^0 30’ 35.90”E	60
Gurupur	Lower (GP-1)	12^0 52’ 19.10”N; 74^0 49’ 27.90”E	60
	Middle (GP-2)	12^0 56’ 18.26”N; 74^0 49’ 53.88”E	72

2.3.1 Sediment component analysis (sand:silt:clay)

To determine the sand:silt:clay ratio, pipette analysis was carried out following the method given by Folk (1974). The analysis is based on Stoke’s settling velocity principle. Distilled water was added to a 1000 ml glass beaker containing 10 g of oven dried sediment sample and stirred with the help of a glass rod. After allowing the sediment to settle for overnight, the water from the beaker was decanted using a decanting pipe without disturbing the sediment in the beaker. This step was repeated for 4 to 5 times in order to remove the salinity of the sediment. Following decantation, 10 ml of 10 % sodium hexametaphosphate was added to dissociate clay particles. On the next day, 5 ml of 30 % hydrogen peroxide solution was added to oxidize organic matter completely. Contents of the beaker were poured over 63 micron (230 mesh size) sieve and the filtrate was then collected in a 1000 ml cylinder. The beaker as well as the material collected over the sieve was washed thoroughly until the solution became clear. The solution from the cylinder was made up to 1000 ml mark using distilled water and homogenized for about 2 minutes with the help of a stirrer. The stirring time was noted down and the solution was allowed to settle. The room temperature was

determined using a thermometer and by following the Table 2.2, pipetting time was calculated for size 8 ϕ.

Table 2.2 Time schedule to be used for pipette analysis

Size Ø	Depth at which pipette is to be inserted (cm)	Time at which water is to be pipetted out Hours: Minutes: Seconds				
		28^0C	29^0C	30^0C	31^0C	32^0C
4	20	0:00:48	0:00:46	0:00:46	0:00:44	0:00:44
5	10	0:01:36	0:01:34	0:01:32	0:01:29	0:01:28
6	10	0:06:25	0:06:15	0:06:06	0:06:57	0:05:52
7	10	0:25:40	0:25:02	0:24:25	0:24:49	0:23:27
8	10	1:42:45	1:40:13	1:37:42	1:37:15	1:33:51
9	10	6:30:00	6:40:40	6:32:50	6:32:10	6:11:30
10	10	27:06:00	26:30:00	-	-	-

The sand remained on the sieve was transferred to a pre-weighed labelled 100 ml beaker and kept for drying at 60^0C. At calculated time, 25 ml of the solution from the cylinder representing the clay fraction was pipetted out by inserting the pipette up to 10 cm depth. The pipetted solution was then transferred into a clean pre-weighed 100 ml beaker. The beaker was then kept for drying at 60^0C. After drying the samples, the beakers containing sand and clay were weighed. The percentage of sand, silt and clay was calculated using following formulae.

% Sand = (Weight of sand / Total weight of sediments) ×100

X = (Weight of clay × 1000/25) – 1

% Clay = (X / Total weight of sediment) ×100

% Silt = 100 - (% of Sand + % of Clay)

2.3.2 Clay mineral analysis

Clay mineral analysis of selected sub-samples was carried out. It involves same procedure as followed for pipette analysis up to stirring the sample in a 1000 ml cylinder. However, the pipetting time for the clay mineral analysis was calculated for size 9 ϕ. The decanting pipe was inserted up to 10 cm depth and the sample was transferred to a clean 500 ml beaker. 5 ml

of acetic acid and 10 ml of hydrogen peroxide were added to the beaker and stirred well in order to remove carbonates and organic matter, respectively. The contents from the beaker were then allowed to settle for overnight. The clear liquid at the top of the beaker was decanted using a decanting pipe. Later, distilled water was added to the beaker and the contents were allowed to settle overnight. This step was repeated for 4 to 5 times to free clay from excess reagents. Using the pipette, 1 ml of the clay was then pipetted and spread uniformly over a pre-numbered clean glass slide. The slide was air dried completely to obtain uniformly distributed thin layer of clay. The prepared slide was exposed to ethylene glycol vapours at 100^0C for 1 hour. The slide was then scanned from 3^0 to 15^0 2Ɵ at 1.2^0 2Ɵ/min on the X-ray diffractometer (PW 1840 model), using nickel-filtered Cu Kα radiation. Further, slide was scanned again in the range of 24^0 to 26^0 2Ɵ at 0.5^0 2Ɵ/min in order to distinguish between kaolinite and illite peaks. The percentage of clay minerals was calculated by weighting the integrated peak area of basal reflection in the glycolated X-ray diffractograms by following the semi-quantitative method given by Biscaye (1965).

2.3.3 Clay fraction chemical analysis

The clay fraction of the selected sub-samples for the study of clay chemistry was obtained by following the procedure of pipette method up to the step of decanting. In this study, the contents of the beaker were directly dried in the oven in order to evaporate the water. The dried clay fraction was then acid digested for metal analysis following the procedure given by Jarvis and Jarvis (1985).

2.3.4 Organic carbon estimation

The total organic carbon in sediment sub-samples was estimated by following the method given by Gaudette et al. (1974). It utilizes exothermic heating and oxidation with potassium dichromate ($K_2Cr_2O_7$) and concentrated sulphuric acid (H_2SO_4). Details of the procedure are as follows.

An amount of 0.5 g of the homogenised sediment sample was treated with 10 ml of 1N standard dichromate solution and 20 ml of concentrated H_2SO_4 with silver sulphate in a clean 500 ml conical flask. The flask was gently rotated for a minute and allowed to stand for 30 minutes. After 30 minutes, 200 ml of the milliQ water, 10 ml of 85 % phosphoric acid

(H_3PO_4) and 0.2 g sodium fluoride were added to this mixture. Excess dichromate solution was then back titrated with 0.5 N ferrous ammonium sulphate ($Fe(NH_4)_2SO_46H_2O$) solution using diphenylamine as an indicator to a one-drop end point i.e. brilliant green. In this method, silver sulphate was used to prevent oxidation of chloride ions. Standardization blank without the sample was run following the same procedure. Total organic carbon percentage was calculated as follows.

% of Total organic carbon = 10 (1-T/S) × F

Where,

S = Standardization blank titration, ml of ferrous solution

T = Sample titration, ml of ferrous solution

F = Factor which is derived as follow

F = (1.0 N) × 12/4000 × 100/Sample weight

= 0.6, when sample weight is exactly 0.5 g

Where,

12/4000 = m. eq. wt. carbon

2.3.5 Sediment digestion for bulk metal analysis

Total digestion of sediment sample was carried out following the method proposed by Jarvis and Jarvis (1985). 0.2 g of finely powdered sediment sample was placed in a Teflon beaker. 10 ml of acid mixture of HF, HNO_3, $HClO_4$ was added slowly to the sediment sample in the ratio of 7:3:1. Proper care was taken to avoid excessive frothing and the mixture was completely dried on a hot plate at 150^0C. After drying, 5 ml of the above acid mixture was added to the beaker and dried for 1 hour. Later, 2 ml of the concentrated HCl was added and dried completely. Further, 10 ml of 1:1 HNO_3 was added to the final residue of the teflon beaker and warmed for few minutes. The contents of the teflon beaker were transferred to a 50 ml volumetric flask and the volume was made up to 50 ml with milliQ water. This solution was then transferred to the pre-cleaned plastic bottle. Also, separated clay fractions from the selected sub-samples were acid digested following the above mentioned procedure.

2.3.6 Chemical speciation of metals

Selected sub-samples were processed through modified sequential extraction procedure (Dessai and Nayak 2009) proposed by Tessier et al. (1979) to investigate different phases of

metals. Using this procedure, it is possible to identify metals associated with number of fractions: “exchangeable”, “carbonates”, “Fe/Mn oxides”, “organic/sulphidic” and “residual” (Tessier et al. 1984). The non-residual, including exchangeable, carbonate, reducible and oxidizable, is considered to be mobile or environmentally reactive fraction with respect to geological and chemical processes. In contrast, the residual also called lithogenous or detrital fraction is usually considered to be immobile or environmentally unreactive. Metals in this fraction remain fixed in sediments within matrix of silicates and other detrital minerals (Wang et al. 2012).

Fraction I: Adsorbed and exchangeable (F1)

The metals in this fraction are weakly adsorbed on sediments or on their essential components namely clays, Fe hydrated oxides and humic acids. The metals that can be released by ion-exchange processes are held in this fraction (Marin et al. 1997; Tokalioglu et al. 2000). Changes in ionic composition and pH could cause re-mobilisation of metals from this fraction. Metals in this fraction are easily available for biological uptake. Magnesium chloride is an effective reagent for desorbing sediment adsorbed metals (Tessier et al. 1979).

1 g of finely powdered sediment sample was taken in a 50 ml plastic centrifuge tube. To this, 8 ml of 1 M magnesium chloride ($MgCl_2$) solution was added at pH 7. The mixture was frequently agitated for 1 hour at room temperature on the orbital shaker (Model RC2100). Then this mixture was centrifuged (Remi cooling compufuge, CPR30) for 10 minutes at 8000 rpm. The supernatant was transferred to a 25 ml volumetric flask and the final volume was made up to 25 ml using milliQ water. Later, the solution was stored in a clean 25 ml plastic bottle for metal analysis. The residue was washed with deionised water.

Fraction 2: Carbonate bound (F2)

The metals associated with the carbonate fraction can be mobilized with changes in pH. Buffered acetic acid and sodium acetate are highly effective in leaching of metals from this fraction.

8 ml of 1 M sodium acetate solution (NaOAc, adjusted to pH 5 with acetic acid) was added to the residue from the first fraction (F1). The mixture was agitated for 5 hours on the orbital shaker at room temperature. The solution was then centrifuged for 10 minutes at 8000 rpm. The supernatant was transferred to a 25 ml volumetric flask and the final volume was made up to 25 ml using milliQ water. Later, the solution was stored in a clean 25 ml plastic bottle for metal analysis. The residue was washed with deionised water.

Fraction 3: Fe-Mn oxide bound fraction (F3)

Metals viz. Fe and Mn often exhibit similar behaviour in aquatic environment. They get reduced in anoxic conditions and are oxidized (present as oxides or oxy hydroxides) under oxic conditions (Lin et al. 2011). These oxides are present as coatings on the finer sediments and in oxic conditions, they can scavenge trace metals from the water column (Venkatramanan et al. 2014). Fe-Mn oxy hydroxides are sensitive to redox potential changes and in anaerobic conditions they are thermodynamically unstable. This property of Fe-Mn oxy hydroxides can cause mobilization of metals adsorbed on to their surfaces (Kumar et al. 2011). Hydroxylamine hydrochloride and acetic acid can reduce iron and manganese oxides to their ferrous and manganous form, respectively and are capable of retaining large amounts of liberated metals in solution.

The residue from the second fraction (F2) was extracted with 20 ml of 0.04 M hydroxylamine hydrochloride ($NH_2OH.HCl$) in 25 % (v/v) HOAc at 96 ± 3^0C with occasional agitation for 6 hours. The solution was then centrifuged for 10 minutes at 8000 rpm. The supernatant was transferred to a 25 ml volumetric flask and the final volume was made up to 25 ml using milliQ water. Later, the solution was stored in a clean 25 ml plastic bottle for metal analysis. The residue was washed with deionised water.

Fraction 4: Organic carbon and sulphide bound fraction (F4)

The metals in this fraction are associated with organic matter such as living organisms, detritus or organic coatings on inorganic mineral particles (Tessier et al. 1979). It also includes metals bound to the sulphide minerals. The metals bound to this fraction are temporarily inaccessible. The processes of aerobic or anaerobic decomposition of organic

matter can induce metal release to water or other fractions. Hydrogen peroxide in acidic medium is used to oxidize organic matter in sediments, while ammonium acetate is used to prevent adsorption of extracted metals on the oxidized sediments (Tessier et al. 1979).

3 ml of 0.02 M HNO_3 and 5 ml of 30 % H_2O_2 after adjusting to pH 2 with HNO_3 were added to the residue from the third fraction (F3). The mixture was agitated periodically to 85^0C for 2 hours. Then, 3 ml of 30 % H_2O_2 (adjusted to pH 2 with HNO_3) was added. The mixture was then again heated at 85^0C for 3 hours with intermittent agitation. The sample was allowed to cool at room temperature. After cooling, 5 ml of 3.2 M NH_4OAc in 20 % (v/v) HNO_3 was added and then diluted to 20 ml followed by continuous agitation for 30 minutes. After agitation, solution was centrifuged, decanted and stored. The residue was washed with deionised water.

Fraction 5: Residual fraction (F5)

This fraction includes mainly metals built in the crystal lattice of minerals. In natural conditions, they are practically inaccessible for living organisms and can be treated as permanently immobile.

The residue from the fourth fraction (F4) was transferred into a clean acid washed teflon beaker and digested completely with an acid mixture following the method given by Jarvis and Jarvis (1985).

2.3.7 Atomic Absorption Spectrophotometer (AAS) analysis

The digested solution obtained for bulk metal chemistry, clay chemistry as well as those attained during sequential extraction procedure was aspirated into the flame atomic absorption spectrophotometer (AAS, VarianAA240FS) for the analysis of metals viz. aluminium (Al), iron (Fe), manganese (Mn), nickel (Ni), cobalt (Co), cupper (Cu), zinc (Zn) and chromium (Cr). Reagents blank and certified reference standard 2702 obtained from the National Institute of Standards and Technology (NIST) were also treated following the same procedure and analysed along with the sample solutions. The accuracy of the analytical procedure was assessed using certified standard reference material 2702. The average

recoveries, ± standard deviations found for each metal were 96±12, 89±12, 91±15, 86±16, 74±12, 82±15, 84±16 and 79±14 for Al, Fe, Mn, Ni, Co, Cu, Zn and Cr, respectively. The AAS was standardized by calibrating curve method before analysing the samples. The calibration standards of different concentrations were prepared for all the metals from the stock solution (1000 mg/l). The instrument was also checked for its reproducibility by repeating the standard after every ten samples.

The recoveries for metals from the sequential extraction procedure were good and were calculated as follow.

Recovery = (Fraction 1 + Fraction 2 + Fraction 3 + Fraction 4 + Fraction 5) / Total metal concentration obtained after total acid digestion × 100.

2.4 Data processing

A triangular/ternary diagram proposed by Pejrup (1988) was used to understand the hydrodynamic conditions prevailed during deposition of sediments over a period of time. Ternary diagram (Fig 2.4) is divided into four sections (I to IV) which reflect increasing violent hydrodynamic conditions. Each section is further divided into four classes (A to D) with respect to their sand content. Thus, there are total 16 groups each having a different number and a letter providing the groups with unique characteristics.

Ternary diagram as well as vertical depth wise distribution of sand, silt, clay, organic carbon, pH and metals in the studied cores was plotted using the software Grapher 7.

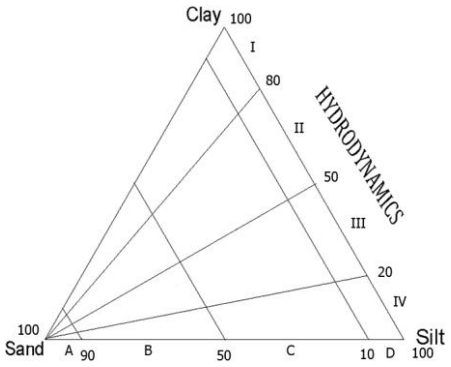

Fig. 2.4 Ternary diagram proposed by Pejrup (1988)

Statistical analysis

Pearson's correlation and paired sample t-test analyses were performed on sand, silt, clay, organic carbon, pH and metals of the studied cores using Statistica 7.

Global average shale values

The global average shale values proposed by Turekian and Wedepohl (1961) were used in the present study as a reference material for the assessment of contamination levels. The global average shale values are 8.8 %, 4.72 %, 850 ppm, 50 ppm, 19 ppm, 45 ppm, 95 ppm and 90 ppm for Al, Fe, Mn, Ni, Co, Cu, Zn and Cr, respectively.

Screening quick reference table

In order to understand the risk of studied metals to the sediment dwelling organisms, the data set of the metals in the bulk sediments and bioavailable fractions (sum of the first four fractions) were compared with sediment quality values (SQV) using the screening quick reference table (SQUIRT) (Table 2.3a). SQUIRT was developed by NOAA for screening purposes. The guideline values were categorized by Buchman (1999) into five classes (Table 2.3b) namely TEL, ERL, PEL, ERM and AET. The probability of toxicity of metals to sediment dwelling organisms is known to increase from TEL to AET. The SQV is applied to achieve information on the toxicity of metals to the biota and thus, to understand its impact on the environment.

Table 2.3.a Screening quick reference table (SQUIRT) for metals in marine sediments (Buchman 1999). Except Fe, all the values are in µg/g.

Elements	Threshold Effect Level (TEL)	Effect Range Low (ERL)	Probable Effect Level (PEL)	Effect Range Median (ERM)	Apparent Effect Threshold (AET)
Fe %	-	-	-	-	22 (Neanthes)
Mn	-	-	-	-	260 (Neanthes)
Ni	15.9	20.9	42.8	51.6	110 (Echinoderm Larvae)
Co	-	-	-	-	10 (Neanthes)
Cu	18.7	34	108	207	390 (Microtox and oyster larvae)
Zn	124	150	271	410	410 (Infaunal community)
Cr	52.3	81	160	370	62 (Neanthes)

Table 2.3.b Sediment guidelines and terms used in SQUIRT.

Sediment guidelines	
Threshold Effect Level (TEL)	Maximum concentration at which no toxic effects are observed
Effects Range Low (ERL)	10^{th} percentile values in effects or toxicity may begin to be observed in sensitive species
Probable Effects Level (PEL)	Lower limit of concentration at which toxic effects are observed
Effects Range Median (ERM)	50^{th} percentile value in effects
Apparent effects Threshold (AET)	Concentration above which adverse biological impacts are observed

Risk assessment code

The risk assessment code was also attempted to determine the risk of metals to the marine biota released from exchangeable and carbonate fractions using the following criteria, % of the total concentration <1: no risk, will be considered safe for the environment, 1-10: low risk, 11-30: medium risk, 31-50: high risk, > 50: very high risk, and can easily enter the food chain (Perin et al. 1985).

Chapter 3

RESULTS

AND

DISCUSSION

Introduction

The study area constitutes five estuaries viz. Vashishti, Vaghotan, Mandovi, Sharavathi and Gurupur from North to South, along central west coast of India. The mudflat sedimentary environments in these estuaries were investigated to understand deposition environment, metal enrichment, source and bioavailability of metals and their possible impact on associated biota. The sediment cores collected were divided into sections based on grain size variations to distinguish varying hydrodynamic and geochemical conditions with time.

Section I: Lower estuarine region

3.1.1 Sediment components

Vashishti estuary

The percentage of sand in the lower region of the Vashishti estuary (core VS-1) ranged from 0.14 % to 5.64 % (avg. 2.12 %), while silt and clay varied from 17.18 % to 48.09 % (avg. 38.61 %) and 49.64 % to 81.24 % (avg. 59.27 %) respectively (Table 3.1.1a). The core VS-1 was divided into two parts based on distribution of sediment components, lower 48 to 12 cm and upper section 12 cm to surface (Fig. 3.1.1a). In the lower section, sand varied from 0.14 % to 5.64 % (avg. 2.47 %), while silt and clay varied from 31.94 % to 48.09 % (avg. 41.04 %) and 49.64 % to 67.92 % (avg. 56.48 %) respectively (Table 3.1.1b). In the upper section, sand, silt and clay varied from 0.31% to 1.58 % (avg. 0.80 %), 17.18 % to 36.18 % (avg. 29.35 %) and 63.08 % to 81.24 % (avg. 69.85 %) respectively.

In core VS-1 (Fig. 3.1.1a), overall decrease in sand percentage was seen in the lower section with peak value at 43 cm and 18 cm, while silt and clay altered around an average line. However, silt percentage was slightly higher from 30 to 28 cm and also 22 to 14 cm depth. Further, in the upper section, percentage of sand and silt decreased towards the surface, while there was an increase in clay percentage towards the surface. Silt compensated clay all along the depth profile. The data plotted on the ternary diagram indicated deposition of sediments in relatively violent hydrodynamic energy conditions with high clay content (Fig. 3.1.2a).

Table 3.1.1a Range and average concentration of sediment components, pH and organic carbon in cores VS-1, VG-1, MD-1, S-1 and GP-1

Sediment core	Sand (%)			Silt (%)			Clay (%)			pH			Organic Carbon (%)		
	Range		Avg	Range		Avg	Range		Avg	Range		Avg	Range		Avg
	Min	Max		Min	Max		Min	Max		Min	Max		Min	Max	
VS-1	0.14	5.64	2.12	17.18	48.09	38.61	49.64	81.24	59.27	6.80	7.69	7.29	1.90	5.15	2.68
VG-1	2.47	16.51	10.23	30.85	49.19	37.81	38.40	62.60	51.96	5.73	6.88	6.52	2.14	3.30	2.60
MD-1	3.15	72.29	36.80	10.11	54.36	34.99	14.48	45.36	28.21	6.30	8.03	7.43	0.48	3.33	2.12
S-1	21.75	94.28	69.42	0.36	35.08	12.47	0.12	50.32	18.11	6.17	8.17	7.49	0.12	2.05	0.70
GP-1	27.17	93.49	62.85	1.80	52.67	22.05	1.00	33.52	15.10	6.36	7.26	6.86	0.09	1.87	0.95

Table 3.1.1b Section wise range and average concentration of sediment components, pH and organic carbon in cores VS-1, VG-1, MD-1, S-1 and GP-1, where L=Lower, M=Middle and U=Upper sections

Sediment core	Sand (%)			Silt (%)			Clay (%)			pH			Organic Carbon (%)		
	Range		Avg	Range		Avg	Range		Avg	Range		Avg	Range		Avg
	Min	Max		Min	Max		Min	Max		Min	Max		Min	Max	
VS-1 (L)	0.14	5.64	2.47	31.94	48.09	41.04	49.64	67.92	56.48	6.83	7.69	7.34	1.90	5.15	2.80
(U)	0.31	1.58	0.80	17.18	36.18	29.35	63.08	81.24	69.85	6.80	7.28	7.07	2.11	2.55	2.22
VG-1 (L)	8.46	15.58	10.92	30.85	41.15	34.29	48.12	58.32	54.79	6.76	6.88	6.81	2.31	2.78	2.53
(M)	2.47	13.39	5.82	32.53	47.39	38.49	47.88	62.60	55.69	6.10	6.81	6.59	2.43	3.07	2.68
(U)	8.59	16.51	12.36	33.34	49.19	39.43	38.40	55.32	48.21	5.73	6.82	6.31	2.14	3.31	2.59
MD-1 (L)	62.90	72.29	67.59	10.11	15.14	12.82	17.60	22.92	19.59	7.65	8.03	7.83	0.48	0.86	0.68
(U)	3.15	52.15	25.07	28.89	54.36	43.44	14.48	45.36	31.49	6.30	7.68	7.28	1.66	3.33	2.67
S-1 (L)	42.39	94.28	86.53	0.36	16.49	5.62	0.64	41.12	7.85	7.09	8.17	7.90	0.12	1.31	0.30
(U)	21.75	86.39	55.91	0.78	35.08	17.88	0.12	50.32	26.21	6.17	8.10	7.16	0.18	2.05	1.02
GP-1 (L)	27.17	93.49	53.66	1.8	52.67	26.07	2.64	33.52	20.27	6.75	7.26	6.99	0.09	1.87	1.20
(M)	73.25	91.55	82.93	5.29	21.49	12.77	1.00	10.64	4.30	6.36	7.08	6.71	0.20	1.00	0.44
(U)	37.82	62.14	49.46	24.02	34.18	29.16	13.84	28.00	21.38	6.47	6.84	6.68	0.67	1.67	1.21

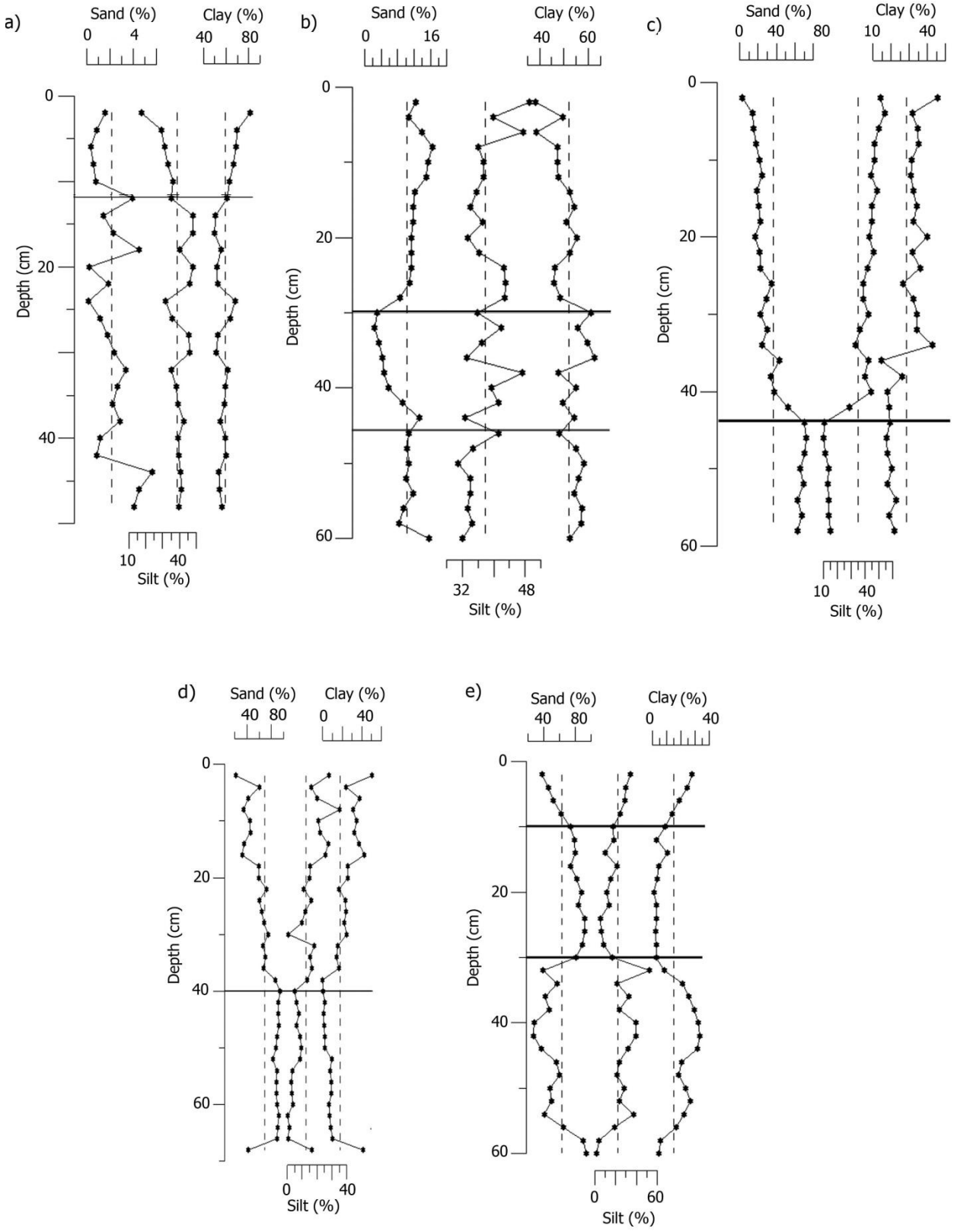

Fig. 3.1.1 Variation of sediment components with average line in sediment cores VS-1 (a), VG-1(b), MD-1 (c), S-1 (d) and GP-1 (e).

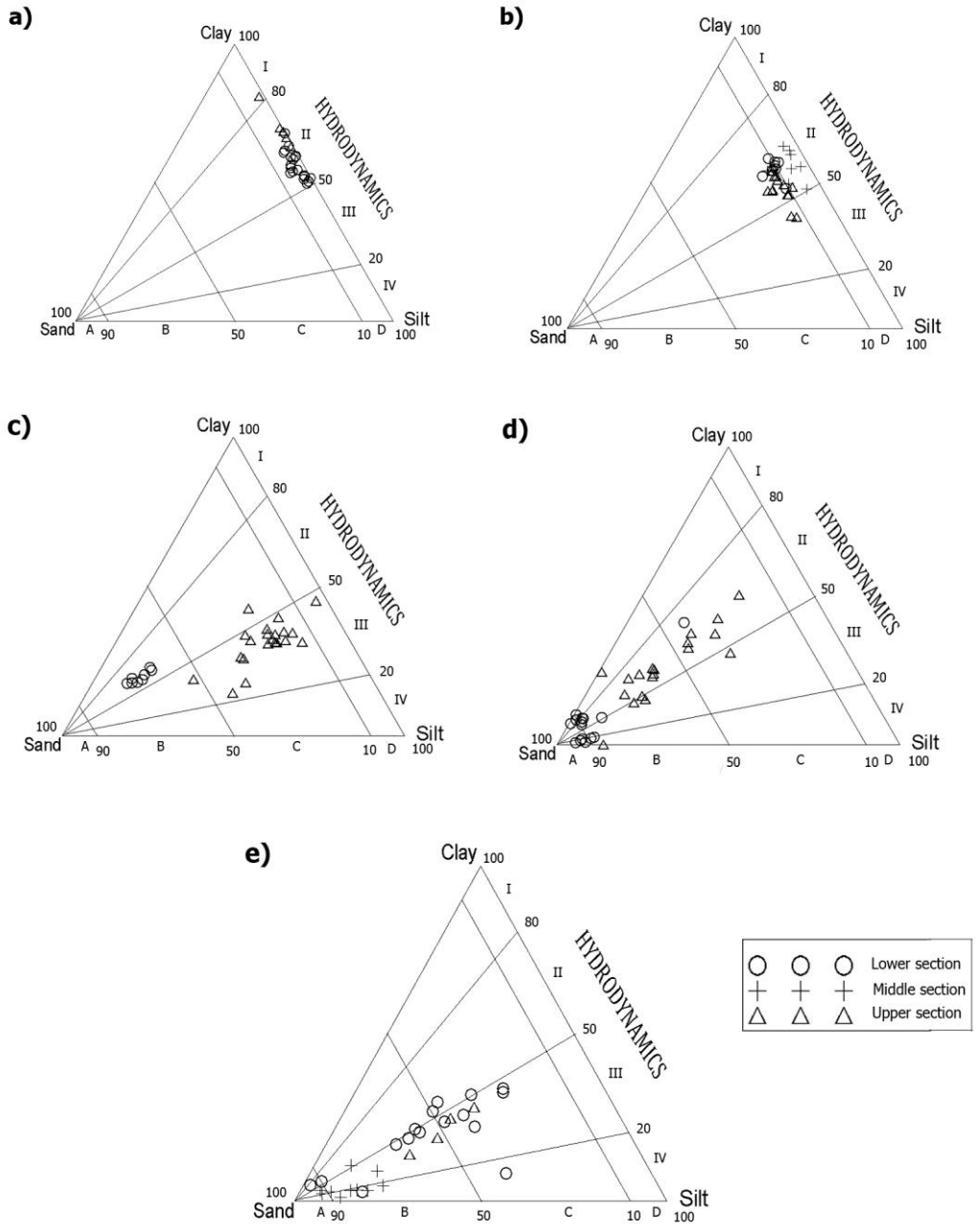

Fig. 3.1.2 Ternary plots for cores VS-1, VG-1, MD-1, S-1 and GP-1.

Vaghotan estuary

Sand in the Vaghotan estuary (core VG-1) ranged from 2.47 % to 16.51 % (avg. 10.23 %), while silt and clay varied from 30.85 % to 49.19 % (avg. 37.81 %) and 38.40 % to 62.60 % (avg. 51.96 %) respectively (Table 3.1.1a). On the basis of variations in distribution pattern of sediment components core VG-1 (Fig. 3.1.1b) was divided into three sections, the lower (60 to 46 cm), middle (46 to 30 cm) and upper (30 to surface) sections. In the lower section

(Table 3.1.1b), sand ranged from 8.46 % to 15.58 % (avg. 10.92 %), while silt and clay varied from 30.85 % to 41.15 % (avg. 34.29 %) and 48.12 % to 58.32 % (avg. 54.79 %) respectively. In the middle section, sand, silt and clay varied from 2.47 % to 13.39 % (avg. 5.82 %), 32.53 % to 47.39 % (avg. 38.49 %) and 47.88 % to 62.60 % (avg. 55.69 %) respectively. In the upper section, sand ranged from 8.59 % to 16.51 % (avg. 12.36 %), while silt and clay varied from 33.34 % to 49.19 % (avg. 39.43 %) and 38.40 % to 55.32 % (avg. 48.21 %) respectively.

The percentage of sand maintained along average line in the lower section, whereas it showed decreasing trend in the middle section which was followed by an increase up to 8 cm depth in the upper section (Fig. 3.1.1b). Thereafter, percentage of sand decreased towards the surface. Silt percentage was less than the average line in the lower section. It showed an increase from lower to middle sections. However, in the upper section, silt percentage decreased from 30 to 8 cm depth. Further, there was an increase in silt percentage towards the surface. Clay percentage was more than the average line in the lower section with not much variation. In the middle section, clay exhibited increasing distribution pattern which was followed by a decreasing trend towards the surface in the upper section. Sediments of lower and middle sections of the Vaghotan estuary seemed to be deposited under relatively violent energy conditions, whereas sediments of the upper section were deposited under relatively violent to violent energy conditions (Fig. 3.1.2b).

Mandovi estuary

In core MD-1, collected from the Mandovi estuary, sand ranged from 3.15 % to 72.29 % (avg. 36.80 %), while silt and clay varied from 10.11 % to 54.36 % (avg. 34.99 %) and 14.48 % to 45.36 % (avg. 28.21 %) respectively (Table 3.1.1a). On the basis of variations in distribution pattern of sediment components core MD-1 (Fig. 3.1.1c) was divided into two sections, the lower (58 to 44 cm) and the upper (44 to surface) sections. The percentage of sand in the lower section (Table 3.1.1b) of the core MD-1 ranged from 62.90 % to 72.29 % (avg. 67.59 %), while silt and clay varied from 10.11 % to 15.14 % (avg. 12.82 %) and 17.60 % to 22.92 % (avg. 19.59 %) respectively. On the other hand, in the upper section of the core MD-1, sand ranged from 3.15 % to 52.15 % (avg. 25.07 %), while silt and clay varied from 28.89 % to 54.36 % (avg. 43.44 %) and 14.48 % to 45.36 % (avg. 31.49 %) respectively.

In core MD-1 (Fig. 3.1.1c), sand percentage was more than the average line in the lower section and was less than the average line in the upper section. In the lower section of core MD-1, sand dominated over silt and clay with an average value of 67.59 %. The distribution pattern of coarser as well as finer sediments did not show much variation in this section. In the upper section, average sand percentage (25.07 %) reduced to less than half of the lower section and showed sudden decrease up to 40 cm depth. This was followed by a gradual decrease towards the surface. The decreasing trend of sand was well compensated by increasing trend of finer sediments. The data plotted on the ternary diagram showed (Fig. 3.1.2c) accumulation of coarser sediments in the lower section of the core MD-1 with sand percentage varying from 50 to 90 % fell within group BII. This indicated sediment deposition under less violent hydrodynamic energy conditions. However, sediments from the upper section suggested their deposition under relatively violent conditions. Thus, indicating change in the depositional environment with time.

Sharavathi estuary

In core S-1, sand ranged from 21.75 % to 94.28 % (avg. 69.42 %), while silt and clay varied from 0.36 % to 35.08 % (avg. 12.47 %) and 0.12 % to 50.32 % (avg. 18.11 %) respectively (Table 3.1.1a). The core was divided into two sections based on distribution of sediment components. The lower and upper sections are from 68 to 40 cm and 40 to surface of the core S-1 (Fig. 3.1.1d) respectively. The percentage of sand in the lower section of the core S-1 (Table 3.1.1b) ranged from 42.39 % to 94.28 % (avg. 86.53 %), while silt and clay varied from 0.36 % to 16.49 % (avg. 5.62 %) and 0.64 % to 41.12 % (avg. 7.85 %) respectively. On the other hand, in the upper section of the core S-1, sand ranged from 21.75 % to 86.39 % (avg. 55.91 %), while silt and clay varied from 0.78 % to 35.08 % (avg. 17.88 %) and 0.12 % to 50.32 % (avg. 26.21 %) respectively.

Similar to core MD-1, sand percentage in core S-1 (Fig. 3.1.1d) was more than the average line and less than the average line in lower and upper sections respectively. In the lower section of the core S-1, sand showed sharp increase from bottom to 66 cm depth and further remained nearly constant throughout the section. Silt showed a corresponding opposite distribution pattern to that of sand profile in this section. The clay percentage decreased sharply from bottom to 66 cm depth, from where gradual decrease was seen. In the upper section, decreasing pattern of sand was compensated by increasing pattern of silt and clay.

The data plotted on the ternary diagram indicated deposition of coarser sediments of the lower section under (Fig. 3.1.2d) varying, calm to extremely violent conditions. Sediments in the upper section, with comparatively finer sediments, indicated their deposition under less violent conditions.

Gurupur estuary

In core GP-1, sand, silt and clay varied from 27.17 % to 93.49 % (avg. 62.85 %), 1.80 % to 52.67 % (avg. 22.05 %) and 1.00 % to 33.52 % (avg. 15.10 %) respectively (Table 3.1.1a). The core GP-1 collected from the lower region of the Gurupur estuary was divided into three sections based on the distribution pattern of sediment components from bottom to surface (Fig. 3.1.1e). The lower, middle and upper sections were from 60 to 30 cm, 30 to 10 cm and 10 to surface of the core GP-1 respectively. The percentage of sand in the lower section of the core GP-1, ranged from 27.17 % to 93.49 % (avg. 53.66 %), while silt and clay varied from 1.80 % to 52.67 % (avg. 26.07 %) and 2.64 % to 33.52 % (avg. 20.27 %) respectively (Table 3.1.1b). On the other hand, in the middle section of the core GP-1, sand ranged from 73.25 % to 91.55 % (avg. 82.93 %), while silt and clay varied from 5.29 % to 21.49 % (avg. 12.77 %) and 1.00 % to 10.64 % (avg. 4.30 %) respectively. In the upper section, sand, silt and clay ranged from 37.82 % to 62.14 % (avg. 49.46 %), 24.02 % to 34.18 % (avg. 29.16 %) and 13.84 % to 28.00 % (avg. 21.38 %) respectively.

In the lower section of the core GP-1 (Fig. 3.1.1e), sand showed overall decreasing trend with its percentage largely within less than the average line. The distribution patterns of silt and clay were opposite to that of sand. In the middle section, percentage of sand was more than the average line and that of silt and clay was less than the average line. Further, in the upper section, sand percentage decreased, while silt and clay percentage increased towards the surface. The data plotted on the ternary diagram showed that (Fig. 3.1.2e) finer sediments were deposited under less violent to relatively violent conditions in the lower section. In the middle section, coarser sediments were deposited under relatively violent to extremely violent conditions, whereas in the upper section sediments were deposited under relatively violent conditions.

3.1.2 pH

Vashishti estuary

The value of pH in the core VS-1 (Table 3.1.1a) varied from 6.80 to 7.69 (avg. 7.29). In the lower section of the core VS-1, pH ranged from 6.83 to 7.69 (avg. 7.34), whereas it varied from 6.80 to 7.28 (avg. 7.07) in the upper section (Table 3.1.1b).

In the lower section (Fig. 3.1.3a), pH exhibited fluctuating distribution pattern and was largely more than the average line. Further, in the upper section, pH showed an overall increasing trend towards the surface of the core VS-1. However, pH value was less than the average line in this section.

Vaghotan estuary

In core VG-1 (Table 3.1.1a), pH varied from 5.73 to 6.88 (avg. 6.52). In this core, pH varied from 6.76 to 6.88 (avg. 6.81), 6.10 to 6.81 (avg. 6.59) and 5.73 to 6.82 (avg. 6.31) in lower, middle and upper sections respectively (Table 3.1.1b).

In the lower section (Fig. 3.1.3b), pH remained nearly constant and was more than the average line. Further, in the middle section, pH was more than the average line and maintained constant level up to 38 cm, followed by a drastic decrease at 36 cm. Thereafter, pH maintained along average line in the middle section. In the upper section, although pH value was less than the average line, it showed gradual increase towards the surface in the core VG-1.

Mandovi estuary

The value of pH in the core MD-1 (Table 3.1.1a) varied from 6.30 to 8.03 (avg. 7.43). In the lower section (Table 3.1.1b), it varied from 7.65 to 8.03 (avg. 7.83), whereas in the upper section it ranged from 6.30 to 7.68 (avg. 7.28).

A gradual decrease in pH was observed from bottom to surface of the core MD-1 (Fig. 3.1.3c).

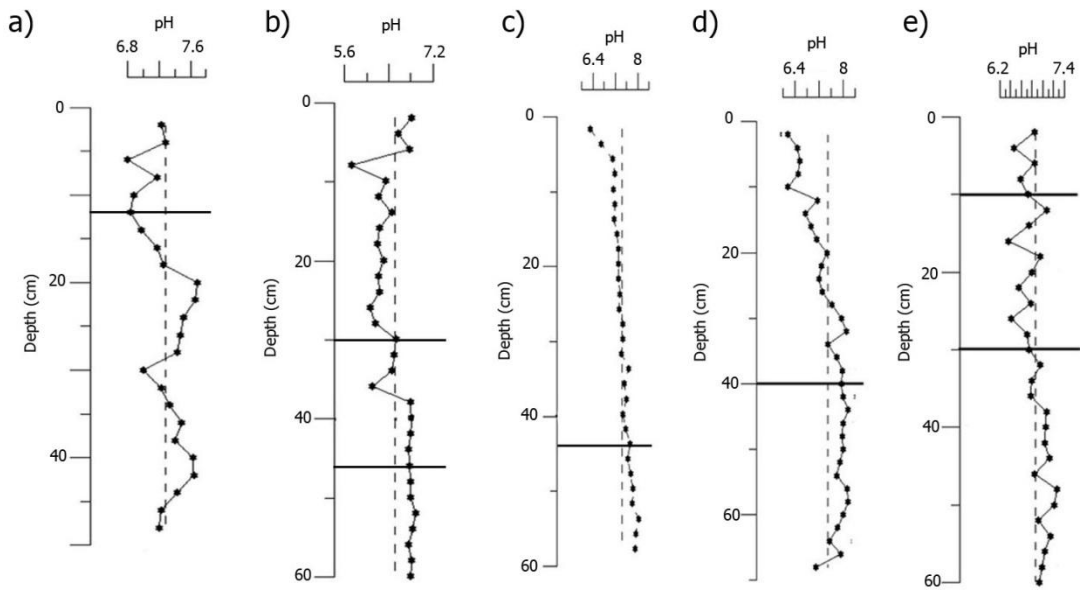

Fig. 3.1.3 Variation of pH with average line in sediment cores VS-1 (a), VG-1 (b), MD-1 (c), S-1 (d) and GP-1 (e).

Sharavathi estuary

In core S-1 (Table 3.1.1a), pH varied from 6.17 to 8.17 (avg. 7.49). It varied from 7.09 to 8.17 (avg. 7.90) and 6.17 to 8.10 (avg. 7.16) in lower and upper sections respectively (Table 3.1.1b).

In the lower section (Fig. 3.1.3d), pH was more than the average line, whereas it decreased from more than the average line to less than the average line towards the surface in the upper section.

Gurupur estuary

In core GP-1 (Table 3.1.1a), pH varied from 6.36 to 7.26 (avg. 6.86). In lower, middle and upper sections of the core GP-1, pH varied from 6.75 to 7.26 (avg. 6.99), 6.36 to 7.08 (avg. 6.71) and 6.47 to 6.84 (avg. 6.68) respectively (Table 3.1.1b).

The pH showed overall decrease from bottom to surface of the core GP-1 (Fig. 3.1.3e).

3.1.3 Organic carbon

Vashishti estuary

In core VS-1 (Table 3.1.1a), organic carbon percentage ranged from 1.90 % to 5.15 % (avg. 2.68 %). In lower and upper sections it varied from 1.90 % to 5.15 % (avg. 2.80 %) and 2.11 % to 2.55 % (avg. 2.22 %) respectively (Table 3.1.1b).

The organic carbon concentration remained nearly constant from bottom to surface of the core VS-1 (Fig. 3.1.4a), except from 22 to 14 cm depth where an increase in its concentration was seen.

Vaghotan estuary

The organic carbon percentage in the core VG-1 (Table 3.1.1a) ranged from 2.14 % to 3.30 % (avg. 2.60 %). It varied from 2.31 % to 2.78 % (avg. 2.53 %), 2.43 % to 3.07 % (avg. 2.68 %) and 2.14 % to 3.31 % (avg. 2.59 %) in lower, middle and upper sections respectively (Table 3.1.1b).

The concentration of organic carbon showed overall increase from lower to middle sections of the core VG-1 (Fig. 3.1.4b). The concentration drastically decreased from 34 to 28 cm. In the upper section, from 30 to 10 cm depth its concentration was less than the average line, while further above its concentration was more than the average line towards the surface. Overall an increasing distribution pattern of organic carbon was seen in the upper section of the core VG-1.

Mandovi estuary

In core MD-1 (Table 3.1.1a), organic carbon percentage ranged from 0.48 % to 3.33 % (avg. 2.12 %). In the lower section of the core MD-1 (Table 3.1.1b), organic carbon percentage ranged from 0.48 % to 0.86 % (avg. 0.68 %), whereas in the upper section it varied from 1.66 % to 3.33 % (avg. 2.67 %).

The average organic carbon percentage was higher in the upper section of the cores MD-1 (Fig. 3.1.4c). Organic carbon percentage remained less than the average line in the lower section, while in the upper section overall increasing trend was observed up to the surface of the core MD-1.

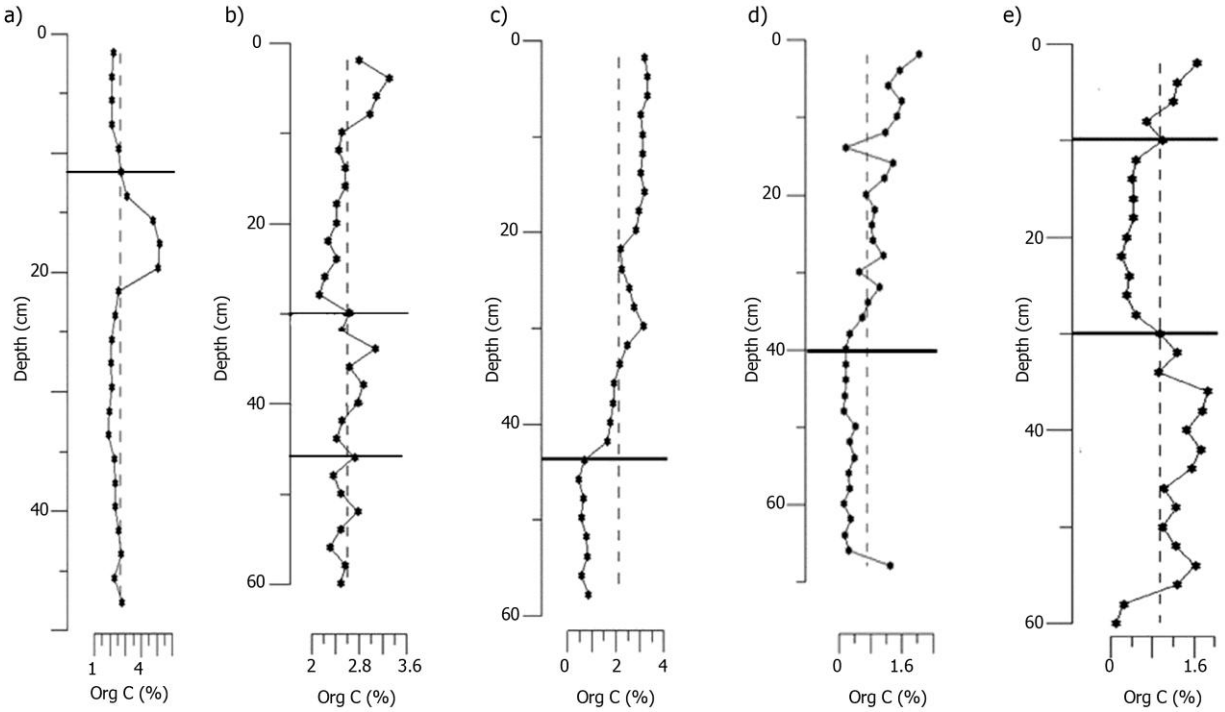

Fig. 3.1.4. Variation of organic carbon with average line in sediment cores VS-1 (a), VG-1 (b), MD-1 (c), S-1 (d) and GP-1 (e).

Sharavathi estuary

The organic carbon percentage in the core S-1 (Table 3.1.1a) ranged from 0.12 % to 2.05 % (avg. 0.70 %). It varied from 0.12 % to 1.31 % (avg. 0.30 %) and 0.18 % to 2.05 % (avg. 1.02 %) in lower and upper sections respectively (Table 3.1.1b).

Similar to the core MD-1, average organic carbon percentage showed higher value in the upper section of the core S-1 (Fig. 3.1.4d). In the lower section of the core S-1, organic carbon showed sudden decrease from bottom to 66 cm depth, from where its concentration remained nearly constant throughout the section. In the upper section, an increasing distribution pattern of organic carbon was observed up to the surface, with prominent decreasing peak seen at 14 cm depth.

Gurupur estuary

In core GP-1 (Table 3.1.1a), organic carbon percentage ranged from 0.09 % to 1.87 % (avg. 0.95 %). It varied from 0.09 % to 1.87 % (avg. 1.20 %), 0.20 % to 1.00 % (avg. 0.44 %) and 0.67 % to 1.67 % (avg. 1.21 %) in lower, middle and upper sections respectively (Table 3.1.1b).

In the lower section of the core GP-1 (Fig. 3.1.4e), the concentration of organic carbon increased with fluctuating trends from bottom to 36 cm depth which was followed by a decrease. In the middle section, organic carbon percentage was lower than the average line which was followed by an increasing trend up to the surface in the upper section.

When the average values of sediment components of five estuaries were considered (Table 3.1.1a), sand increased, while silt, clay and organic carbon decreased from cores VS-1 to S-1 i.e. from North to South. However, at core GP-1, slight decrease in sand and an increase in silt and organic carbon were noted. The pH along this coast, between cores VS-1 and GP-1 varied from 6.52 to 7.49.

When sediment components were compared among sections, average sand was higher in the lower section at cores VS-1, MD-1 and S-1 (Table 3.1.1b). In case of the core VG-1, lower and upper sections showed high sand compared to middle, while in the core GP-1, middle section showed higher sand. Silt showed higher value in the upper section in cores VG-1, MD-1, S-1 and GP-1. But, it maintained higher value in the lower section in the core VS-1. Clay was higher in the upper section in cores VS-1, MD-1, S-1 and GP-1. However, in the core VG-1, middle section maintained higher value of clay.

Using the average values of sand, silt and clay when different sections were compared, it was clear that sand decreased, while finer sediments increased from lower to upper sections in cores VS-1, MD-1 and S-1. This indicated decrease in sediment size over the years in these cores. In core VG-1, sand decreased and finer sediments increased from lower to middle sections. However, upper section showed higher sand and silt, and lower clay indicating coarse material input in the recent years. In core GP-1, higher sand percentage in the middle section suggested additional input of sand material.

The pH values indicated decrease from lower to upper sections in cores VS-1, MD-1, S-1 and also in VG-1 and GP-1. Higher values of the organic carbon were observed for the sections with higher finer sediments, except in core VS-1 where higher organic carbon value was obtained for the lower section.

In cores MD-1 and S-1, decrease in sand content was well represented in profiles (Fig. 3.1.1), which was compensated by an increase in silt and clay from bottom to surface of the cores. In case of the core VS-1, sand and silt showed decrease, whereas clay showed an increase. In these cores, pH decreased while organic carbon increased from bottom to surface. This indicated association of organic carbon with finer sediments. In case of the core VG-1, sand decreased and finer sediments increased from lower to middle section. However, in the upper section, sand and silt were increased, while clay was decreased. In this core, pH profile agreed with sand, and organic carbon with silt profile. In core GP-1, higher sand input in the middle section was responsible for diluting concentration of silt, clay and organic carbon and also, in decreasing the pH values.

3.1.4 Bulk sediment chemistry

Major metals (Al, Fe and Mn)

Vashishti estuary

Al, Fe and Mn varied from 7.52 % to 9.85 % (avg. 8.71 %), 9.20 % to 14.95 % (avg. 12.06 %) and 685 ppm to 1245 ppm (avg. 1045 ppm) respectively (Table 3.1.2a) in the core VS-1. In the lower section (Table 3.1.2b), concentration of Al, Fe and Mn varied from 7.52 % to 9.53 % (avg. 8.66 %), 9.20 % to 14.95 % (avg. 12.34 %) and 685 ppm to 1245 ppm (avg. 1037 ppm) respectively. On the other hand, in the upper section, concentration of Al, Fe and Mn ranged from 8.19 % to 9.85 % (avg. 8.89 %), 10.21 % to 11.90 % (avg. 10.98 %) and 957 ppm to 1155 ppm (avg. 1067 ppm) respectively.

Aluminium exhibited fluctuating distribution pattern in the lower section (Fig. 3.1.5a) with increasing trend from bottom up to 32 cm, followed by decreasing trend up to 16 cm and then showed increase. While in the upper section, a prominent increasing trend was seen towards the surface of the core VS-1. The distribution pattern of Fe also showed similar distribution

Table 3.1.2a Range and average concentration of major metals in cores VS-1, VG-1, MD-1, S-1 and GP-1

Sediment core	Al (%)			Fe (%)			Mn (ppm)		
	Range		Avg	Range		Avg	Range		Avg
	Min	Max		Min	Max		Min	Max	
VS-1	7.52	9.85	8.71	9.20	14.95	12.06	685	1245	1045
VG-1	7.97	11.50	10.33	11.18	14.38	13.26	882	2520	1375
MD-1	3.56	6.58	5.03	0.31	5.64	2.84	336	1366	650
S-1	2.11	9.48	4.77	0.31	6.02	2.23	16	192	115
GP-1	3.15	11.23	6.65	1.08	5.91	3.51	43	156	108

Table 3.1.2b Section wise range and average concentration of major metals in cores VS-1, VG-1, MD-1, S-1 and GP-1 where L=Lower, M=Middle and U=Upper sections

Sediment core	Al (%)			Fe (%)			Mn (ppm)		
	Range		Avg	Range		Avg	Range		Avg
	Min	Max		Min	Max		Min	Max	
VS-1 (L)	7.52	9.53	8.66	9.20	14.95	12.34	685	1245	1037
(U)	8.19	9.85	8.89	10.21	11.90	10.98	957	1155	1067
VG-1 (L)	9.36	11.12	10.37	11.18	13.98	13.04	1202	1541	1410
(M)	7.97	10.90	9.63	12.42	13.87	13.04	1188	2520	1586
(U)	9.81	11.50	10.70	11.86	14.38	13.51	882	1849	1234
MD-1 (L)	3.55	4.91	4.18	0.31	4.77	1.68	336	494	403
(U)	4.60	6.58	5.36	0.78	5.64	3.28	417	1366	744
S-1 (L)	2.11	6.75	3.40	0.31	6.02	2.79	16	192	115
(U)	2.66	9.48	5.86	0.37	3.57	1.80	36	181	115
GP-1 (L)	3.31	11.23	8.22	1.08	5.91	4.28	43	156	115
(M)	3.15	5.78	4.22	1.58	2.82	2.28	59	155	103
(U)	4.26	7.36	6.46	2.34	4.38	3.53	85	120	97

Table 3.1.2c Range and average concentration of trace metals in cores VS-1, VG-1, MD-1, S-1 and GP-1

Sediment core	Ni (ppm)			Co (ppm)			Cu (ppm)			Zn (ppm)			Cr (ppm)		
	Range		Avg	Range		Avg	Range		Avg	Range		Avg	Range		Avg
	Min	Max		Min	Max		Min	Max		Min	Max		Min	Max	
VS-1	45	96	68	22	66	51	237	325	281	339	387	363	127	176	149
VG-1	114	132	126	66	95	86	416	636	489	89	109	100	82	134	110
MD-1	27	58	42	8	23	15	10	31	21	35	1531	219	23	175	76
S-1	11	51	32	3	15	7	2	43	15	33	2293	730	5	96	41
GP-1	13	59	40	3	12	8	2	38	16	278	1919	644	16	127	81

Table 3.1.2d Section wise range and average concentration of trace metals in cores VS-1, VG-1, MD-1, S-1 and GP-1 where L=Lower, M=Middle and U=Upper sections

Sediment core	Ni (ppm)			Co (ppm)			Cu (ppm)			Zn (ppm)			Cr (ppm)		
	Range		Avg	Range		Avg	Range		Avg	Range		Avg	Range		Avg
	Min	Max		Min	Max		Min	Max		Min	Max		Min	Max	
VS-1 (L)	45	92	66	41	67	53	247	325	289	339	387	361	128	176	151
(U)	54	96	77	22	56	44	238	266	253	356	384	370	132	145	140
VG-1 (L)	119	132	127	77	91	85	459	553	486	90	101	97	97	125	112
(M)	124	131	128	66	89	82	417	591	482	93	98	96	105	117	111
(U)	114	130	124	79	95	88	424	636	495	96	109	104	83	134	107
MD-1 (L)	27	36	33	8	13	9	10	18	15	141	304	209	23	174	74
(U)	36	58	45	13	23	18	20	31	23	35	1531	223	53	121	77
S-1 (L)	11	39	23	3	11	5	2	14	7	33	2165	1026	5	96	39
(U)	26	51	39	3	15	9	5	43	21	85	2293	497	18	61	42
GP-1 (L)	13	59	44	3	12	9	2	38	20	278	463	397	16	127	85
(M)	16	49	33	4	8	6	3	22	10	359	1468	599	28	105	64
(U)	29	48	40	7	9	8	7	15	12	1467	1918	1739	71	124	107

with increase from bottom to 32 cm, followed by decrease up to 20 cm and then increase in the lower section. In the upper section, Fe exhibited decreasing trend except at the surface. The concentration of Mn decreased from bottom to 20 cm depth with fluctuations in the lower section which was followed by an increase up to the surface.

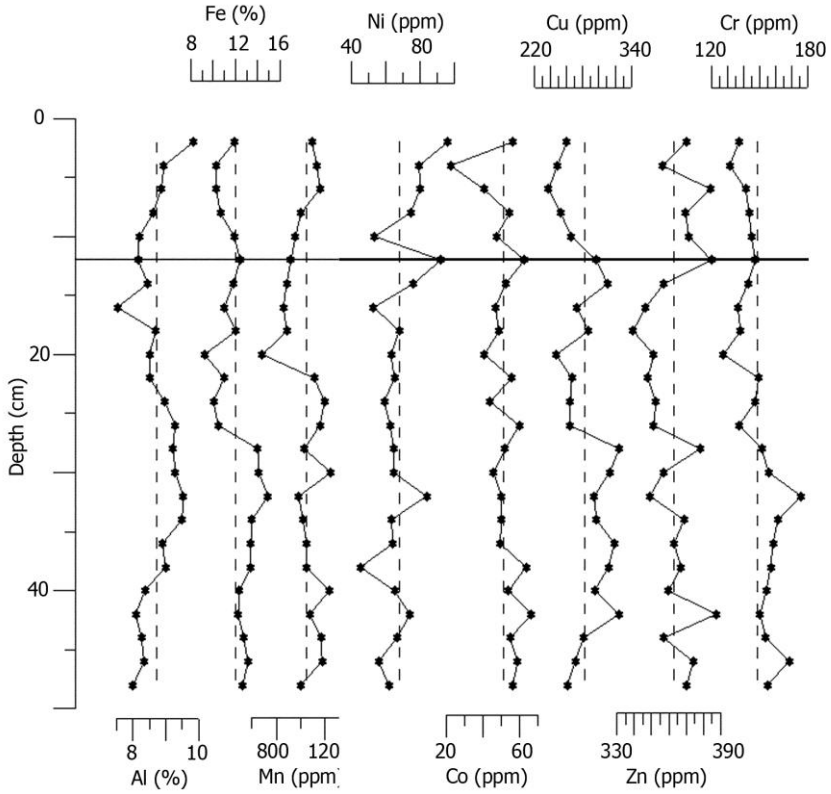

Fig. 3.1.5a Variation of Al, Fe, Mn, Ni, Co, Cu, Zn and Cr with average line in bulk sediments in the core VS-1.

Vaghotan estuary

In core VG-1, Al, Fe and Mn varied from 7.97 % to 11.50 % (avg. 10.33 %), 11.18 % to 14.38 % (avg. 13.26 %) and 882 ppm to 2520 ppm (avg. 1375 ppm) respectively (Table 3.1.2a). In the lower section (Table 3.1.2b), Al, Fe and Mn ranged from 9.36 % to 11.12 % (avg. 10.37 %), 11.18% to 13.98 % (avg. 13.04 %) and 1202 ppm to 1541 ppm (avg. 1410 ppm) respectively; while they varied from 7.97 % to 10.90 % (avg. 9.63 %), 12.42% to 13.87 % (avg. 13.04 %) and 1188 ppm to 2520 ppm (avg. 1586 ppm) respectively in the middle section. In the upper section, Al, Fe and Mn ranged from 9.81 % to 11.50 % (avg. 10.70 %), 11.86 % to 14.38 % (avg. 13.51 %) and 882 ppm to 1849 ppm (avg. 1234 ppm) respectively.

In the lower section (Fig. 3.1.5b), Al increased, Fe decreased and Mn was fluctuating around the average line. In the middle section, Al showed lower values with negative peak at 40 cm, whereas Fe and Mn showed higher fluctuations around the average. In the upper section, all the three elements fluctuated around the average except top 10 cm where they showed a decreasing trend.

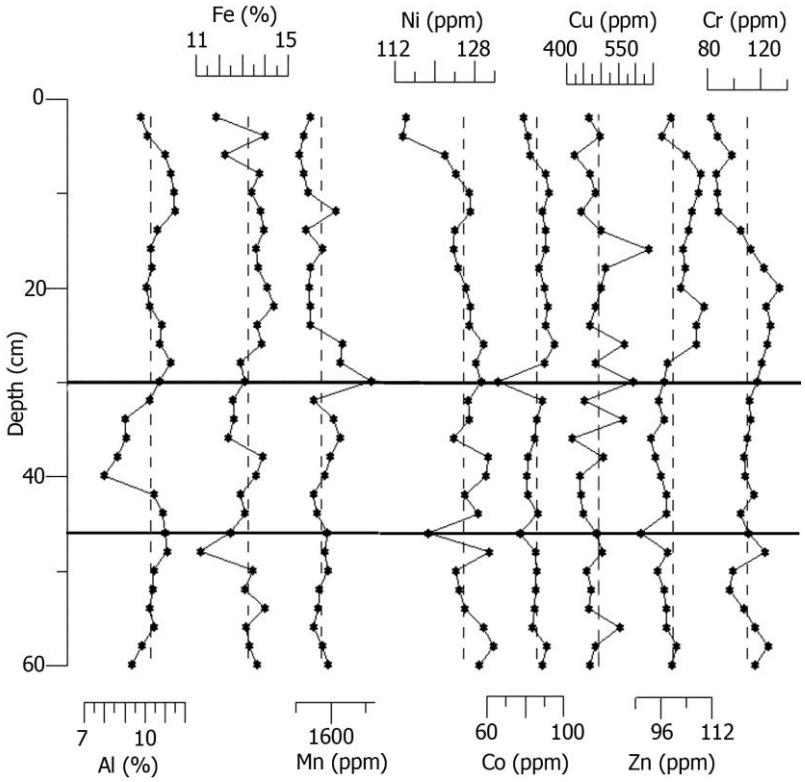

Fig. 3.1.5b Variation of Al, Fe, Mn, Ni, Co, Cu, Zn and Cr with average line in bulk sediments in the core VG-1.

Mandovi estuary

In core MD-1(Table 3.1.2a), Al, Fe and Mn varied from 3.56 % to 6.58 % (avg. 5.03 %), 0.31 % to 5.64 % (avg. 2.84 %) and 336 ppm to 1366 ppm (avg. 650 ppm) respectively. In the lower section of the core MD-1 (Table 3.1.2b), Al, Fe and Mn varied from 3.55 % to 4.91 % (avg. 4.18 %), 0.31 % to 4.77 % (avg. 1.68 %) and 336 ppm to 494 ppm (avg. 403 ppm) respectively; while, in the upper section of the core MD-1 Al, Fe and Mn ranged from 4.60 % to 6.58 % (avg. 5.36 %), 0.78 % to 5.64 % (avg. 3.28 %) and 417 ppm to 1366 ppm (avg. 744 ppm) respectively.

Aluminium concentration increased from bottom up to 26 cm (Fig. 3.1.5c). Further, it showed slight decrease towards surface. Iron concentration decreased in the lower section with sharp increasing peak at 54 cm depth. In the upper section, Fe showed overall an increasing distribution pattern up to the surface. Manganese exhibited gradual increasing trend from bottom to 20 cm depth and then maintained constant trend.

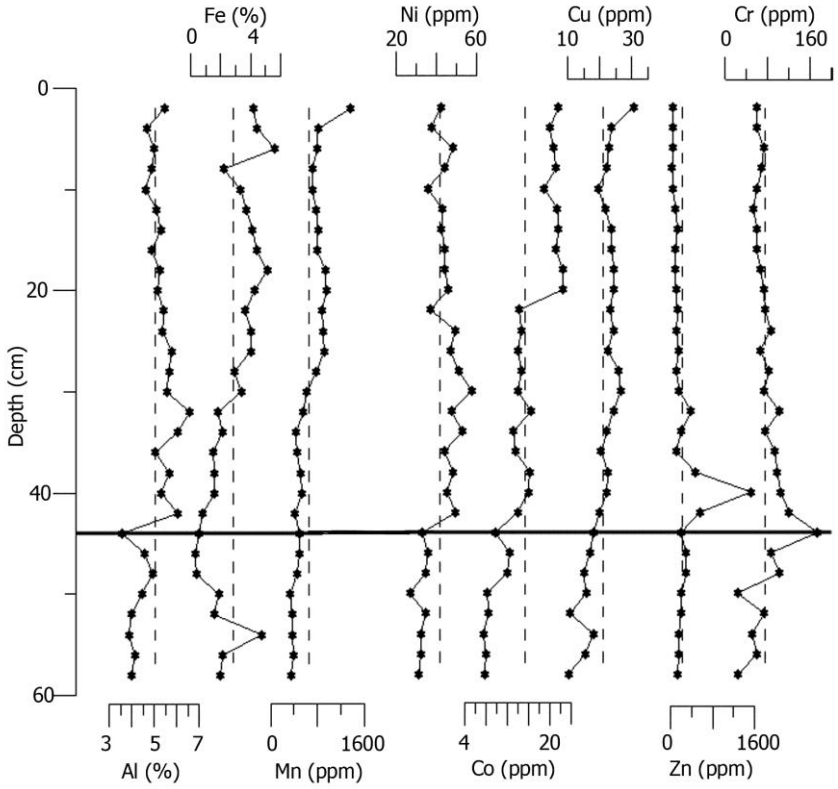

Fig. 3.1.5c Variation of Al, Fe, Mn, Ni, Co, Cu, Zn and Cr with average line in bulk sediments in the core MD-1.

Sharavathi estuary

In core S-1 (Table 3.1.2a), Al, Fe and Mn varied from 2.11 % to 9.48 % (avg. 4.77 %), 0.31 % to 6.02 % (avg. 2.23 %) and 16 ppm to 192 ppm (avg. 115 ppm) respectively. In the lower section of the core S-1 (Table 3.1.2b), Al, Fe and Mn varied from 2.11 % to 6.75 % (avg. 3.40 %), 0.31 % to 6.02 % (avg. 2.79 %), 16 ppm to 192 ppm (avg. 115 ppm) respectively; while, in the upper section of the core S-1 Al, Fe and Mn ranged from 2.66 % to 9.48 % (avg. 5.86 %), 0.37 % to 3.57 % (avg. 1.80 %) and 36 ppm to 181 ppm (avg. 115 ppm) respectively.

In the lower section (Fig. 3.1.5d), Al, Fe and Mn showed, fluctuating distribution with Al values less than the average line, and Fe and Mn on the average line. Further, Fe and Mn exhibited higher degree of fluctuations compared to Al. In the upper section, Al concentration increased towards the surface. Also, Mn showed an increasing distribution pattern with fluctuations. Iron maintained almost constant values from 40 to 10 cm depth, which was followed by an increase towards the surface.

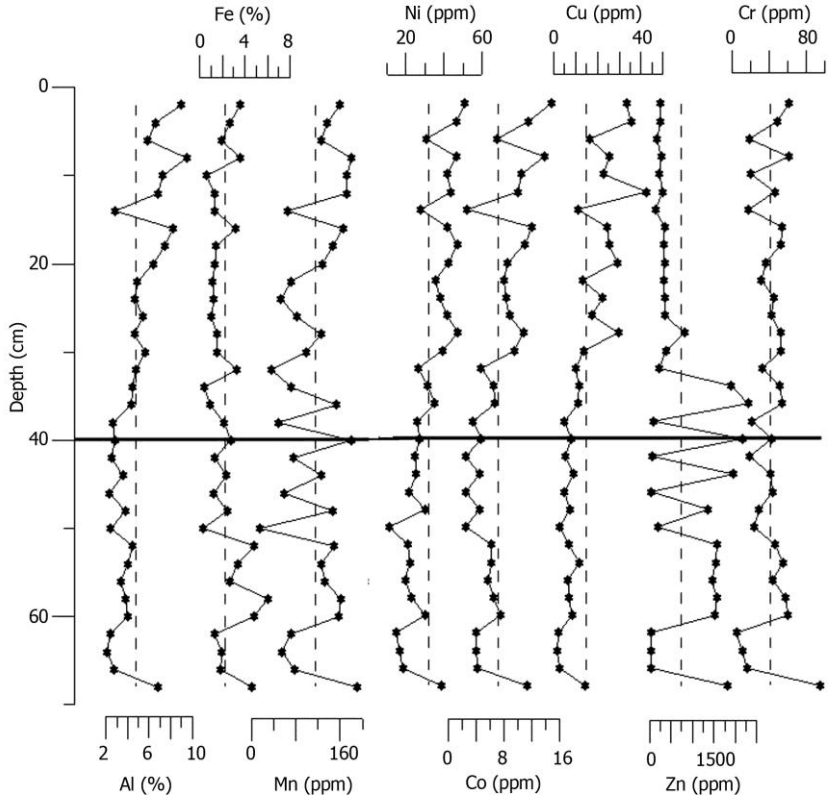

Fig. 3.1.5d Variation of Al, Fe, Mn, Ni, Co, Cu, Zn and Cr with average line in bulk sediments in the core S-1.

Gurupur estuary

In core GP-1 (Table 3.1.2a), Al, Fe and Mn varied from 3.15 % to 11.23 % (avg. 6.65 %), 1.08 % to 5.91 % (avg. 3.51 %) and 43 ppm to 156 ppm (avg. 108 ppm) respectively. In the lower section of the core GP-1 (Table 3.1.2b), Al, Fe and Mn ranged from 3.31 % to 11.23 % (avg. 8.22 %), 1.08 % to 5.91 % (avg. 4.28 %) and 43 ppm to 156 ppm (avg. 115 ppm) respectively; while, in the middle section Al, Fe and Mn varied from 3.15 % to 5.78 % (avg. 4.22 %), 1.58 % to 2.82 % (avg. 2.28 %) and 59 ppm to 155 ppm (avg. 103 ppm) respectively. In the upper section, Al, Fe and Mn varied from 4.26 % to 7.36 % (avg. 6.46 %), 2.34 % to 4.38 % (avg. 3.53 %) and 85 ppm to 120 ppm (avg. 97 ppm) respectively.

The concentration of Al, Fe and Mn showed more than the average line in the lower section and less than the average line in the middle section (Fig. 3.1.5e). Further, they showed an increasing distribution pattern towards the surface in the upper section. All the three elements showed large fluctuations in the lower section.

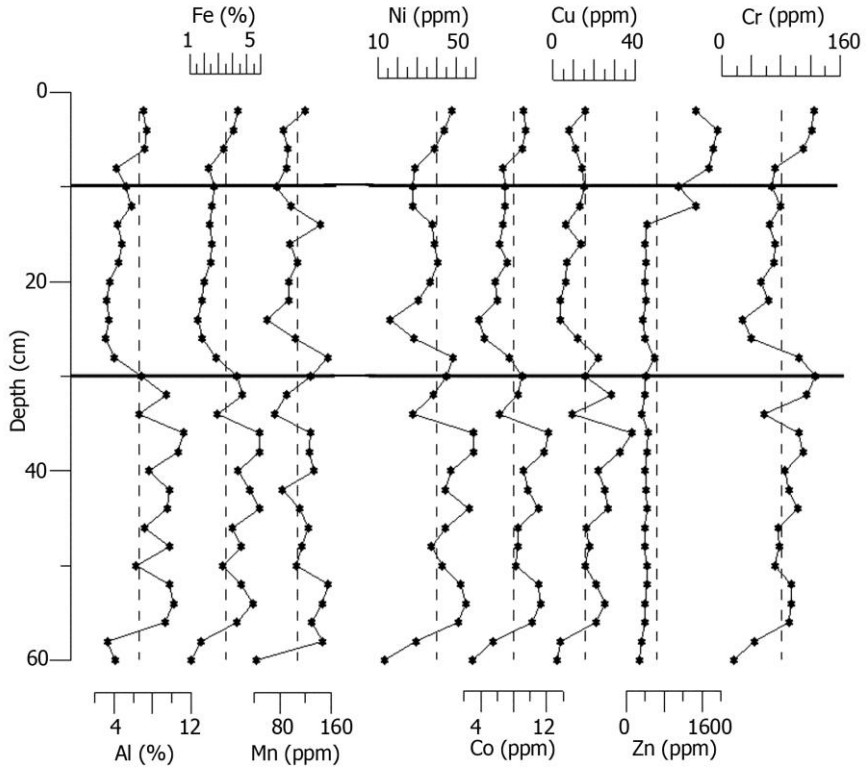

Fig. 3.1.5e Variation of Al, Fe, Mn, Ni, Co, Cu, Zn and Cr with average line in bulk sediments in the core GP-1.

Trace metals (Ni, Co, Cu, Zn and Cr)

Vashishti estuary

In core VS-1 (Table 3.1.2c), Ni, Co, Cu, Zn and Cr varied from 45 ppm to 96 ppm (avg. 68 ppm), 22 ppm to 66 ppm (avg. 51 ppm), 237 ppm to 325 ppm (avg. 281 ppm), 339 ppm to 387 ppm (avg. 363 ppm) and 127 ppm to 176 ppm (avg. 149 ppm) respectively. In the lower section (Table 3.1.2d), concentration of Ni, Co, Cu, Zn and Cr varied from 45 ppm to 92 ppm (avg. 66 ppm), 41 ppm to 67 ppm (avg. 53 ppm), 247 ppm to 325 ppm (avg. 289 ppm), 339 ppm to 387 ppm (avg. 361 ppm) and 128 ppm to 176 ppm (avg. 151 ppm) respectively. On the other hand, in the upper section, concentration of Ni, Co, Cu, Zn and Cr ranged from 54

ppm to 96 ppm (avg. 77 ppm), 22 ppm to 56 ppm (avg. 44 ppm), 238 ppm to 266 ppm (avg. 253 ppm), 356 ppm to 384 ppm (avg. 370 ppm) and 132 ppm to 145 ppm (avg. 140 ppm) respectively.

Nickel in the lower section showed an overall increase with fluctuations up to 32 cm and then maintained constant values around the average line (Fig. 3.1.5a). The distribution of Ni in the upper section showed a prominent increase which was similar to the distribution of clay. Metals viz. Cu and Cr showed similar distribution pattern to Fe with increase up to 32 cm from bottom followed by decrease up to 20 cm and then increased up to 12 cm. In the upper section, both the metals showed decreasing trend. Cobalt fluctuated around an average line from lower to upper sections, except at 4 cm depth where it exhibited sharp negative peak. Zinc showed decrease from bottom to 18 cm depth which was followed by an increase up to 12 cm depth. Further, in the upper section, although concentration of Zn decreased towards the surface, it maintained more than the average line.

Vaghotan estuary

In core VG-1 (Table 3.1.2c), Ni, Co, Cu, Zn and Cr ranged from 114 ppm to 132 ppm (avg. 125 ppm), 66 ppm to 95 ppm (avg. 86 ppm), 416 ppm to 636 ppm (avg. 489 ppm), 89 ppm to 109 ppm (avg. 100 ppm) and 82 ppm to 134 ppm (avg. 110 ppm) respectively. In the lower section (Table 3.1.2d), Ni, Co, Cu, Zn and Cr ranged from 119 ppm to 132 ppm (avg. 127 ppm), 77 ppm to 91 ppm (avg. 85 ppm), 459 ppm to 553 ppm (avg. 486 ppm), 90 ppm to 101 ppm (avg. 97 ppm) and 97 ppm to 125 ppm (avg. 112 ppm) respectively. In the middle section, Ni, Co, Cu, Zn and Cr varied from 124 ppm to 131 ppm (avg. 128 ppm), 66 ppm to 89 ppm (avg. 82 ppm), 417 ppm to 591 ppm (avg. 482 ppm), 93 ppm to 98 ppm (avg. 96 ppm) and 105 ppm to 117 ppm (avg. 111 ppm) respectively; while in the upper section, Ni, Co, Cu, Zn and Cr ranged from 114 ppm to 130 ppm (avg. 124 ppm), 79 ppm to 95 ppm (avg. 88 ppm), 424 ppm to 636 ppm (avg. 495 ppm), 96 ppm to 109 ppm (avg. 104 ppm) and 83 ppm to 134 ppm (avg. 107 ppm) respectively.

Metals viz. Ni, Co, Cu and Cr fluctuated around an average line in lower and middle sections and showed overall decrease towards the surface in the upper section (Fig 3.1.5b). The concentration of Zn however, decreased from lower to middle sections and was less than the

average line. In the upper section, concentration of Zn increased up to 8 cm depth and was more than the average line. Further, its concentration decreased towards the surface.

Mandovi estuary

In core MD-1 (Table 3.1.2c), Ni, Co, Cu, Zn and Cr ranged from 27 ppm to 58 ppm (avg. 42 ppm), 8 ppm to 23 ppm (avg. 15 ppm), 10 ppm to 31 ppm (avg. 21 ppm), 35 ppm to 1531 ppm (avg. 219 ppm) and 23 ppm to 175 ppm (avg. 76 ppm) respectively. In the lower section of the core MD-1 (Table 3.1.2d), Ni, Co, Cu, Zn and Cr varied from 27 ppm to 36 ppm (avg. 33 ppm), 8 ppm to 13 ppm (avg. 9 ppm), 10 ppm to 18 ppm (avg. 15 ppm), 141 ppm to 304 ppm (avg. 209 ppm) and 23 ppm to 174 ppm (avg. 74 ppm) respectively; while in the upper section of the core MD-1, Ni, Co, Cu, Zn and Cr ranged from 36 ppm to 58 ppm (avg. 45 ppm), 13 ppm to 23 ppm (avg. 18 ppm), 20 ppm to 31 ppm (avg. 23 ppm), 35 ppm to 1531 ppm (avg. 223 ppm) and 53 ppm to 121 ppm (avg. 77 ppm) respectively.

Metals viz. Ni, Co and Zn did not show much variation throughout the lower section, similar to Mn (Fig. 3.1.5c). Metals viz. Cu and Cr exhibited increasing distribution pattern in this section. In the upper section, Cu exhibited similar distribution pattern to that of Mn with increasing trend up to the surface. Metals viz. Zn and Cr showed gradual decrease up to the surface with sharp increasing peak observed in case of Zn at 40 cm depth. Nickel exhibited increasing pattern up to 30 cm depth, from where its concentration gradually decreased towards the surface. Cobalt showed gentle increase up to 22 cm depth, followed by sudden increase up to 20 cm depth. In the upper 20 cm of the core MD-1 Co was nearly constant.

Sharavathi estuary

In core S-1 (Table 3.1.2c), Ni, Co, Cu, Zn and Cr varied from 11 ppm to 51 ppm (avg. 32 ppm), 3 ppm to 15 ppm (avg. 7 ppm), 2 ppm to 43 ppm (avg. 15 ppm), 33 ppm to 2293 ppm (avg. 730 ppm) and 5 ppm to 96 ppm (avg. 41 ppm) respectively. In the lower section of the core S-1 (Table 3.1.2d), Ni, Co, Cu, Zn and Cr varied from 11 ppm to 39 ppm (avg. 23 ppm), 3 ppm to 11 ppm (avg. 5 ppm), 2 ppm to 14 ppm (avg. 7 ppm), 33 ppm to 2165 ppm (avg. 1026 ppm) and 5 ppm to 96 ppm (avg. 39 ppm) respectively; while, in the upper section of the core S-1, Ni, Co, Cu, Zn and Cr ranged from 26 ppm to 51 ppm (avg. 39 ppm), 3 ppm to

15 ppm (avg. 9 ppm), 5 ppm to 43 ppm (avg. 21 ppm), 85 ppm to 2293 ppm (avg. 497 ppm) and 18 ppm to 61 ppm (avg. 42 ppm) respectively.

In the lower section (Fig. 3.1.5d), Ni, Co and Cu showed fluctuating distribution pattern with concentration less than the average line. Chromium fluctuated around the average line in this section. Further, in the upper section, Ni, Co, Cu and Cr showed overall an increasing trend. Zinc exhibited large fluctuating distribution pattern from lower section to 32 cm of the upper section. Thereafter, its concentration remained nearly constant in the upper section.

Gurupur estuary

In core GP-1 (Table 3.1.2c), Ni, Co, Cu, Zn and Cr varied from 13 ppm to 59 ppm (avg. 40 ppm), 3 ppm to 12 ppm (avg. 8 ppm), 2 ppm to 38 ppm (avg. 16 ppm), 278 ppm to 1919 ppm (avg. 644 ppm) and 16 ppm to 127 ppm (avg. 81 ppm) respectively. In the lower section of the core GP-1 (Table 3.1.2d), Ni, Co, Cu, Zn and Cr varied from 13 ppm to 59 ppm (avg. 44 ppm), 3 ppm to 12 ppm (avg. 9 ppm), 2 ppm to 38 ppm (avg. 20 ppm), 278 ppm to 463 ppm (avg. 397 ppm) and 16 ppm to 127 ppm (avg. 85 ppm) respectively; while, in the middle section Ni, Co, Cu, Zn and Cr ranged from 16 ppm to 49 ppm (avg. 33 ppm), 4 ppm to 8 ppm (avg. 6 ppm), 3 ppm to 22 ppm (avg. 10 ppm), 359 ppm to 1468 ppm (avg. 599 ppm) and 28 ppm to 105 ppm (avg. 64 ppm) respectively. In the upper section, Ni, Co, Cu, Zn and Cr varied from 29 ppm to 48 ppm (avg. 40 ppm), 7 ppm to 9 ppm (avg. 8 ppm), 7 ppm to 15 ppm (avg. 12 ppm), 1467 ppm to 1918 ppm (avg. 1739 ppm) and 71 ppm to 124 ppm (avg. 107 ppm) respectively.

Metals viz. Ni, Co, Cu and Cr exhibited large fluctuations in the lower section similar to that of Al, Fe and Mn (Fig. 3.1.5e). Their concentration was more than the average line in the lower section and was less than the average line in the middle section. Also, these metals showed an increasing trend towards the surface in the upper section. Zinc exhibited nearly constant concentration from bottom to 14 cm depth which was followed by an increase towards the surface.

When the average values of major elements were considered, Al, Fe and Mn were highest in the core VG-1 and lowest in the core S-1 (Table 3.1.2a). However, values of these elements were also higher in the core VS-1.

When the average values were compared between sections (Table 3.1.2b), in core VS-1, Al and Mn were higher in the upper section, while Mn remained higher in the lower section. In core VG-1, Al and Fe, were higher in the upper section and Mn in the middle section. Iron values, however, varied in a small range from 13.04 to 13.51 %. In core MD-1, all the three elements viz. Al, Fe and Mn were higher in the upper section. In core S-1, Al was high in the upper section, Fe in the lower section, while Mn showed same concentration in both sections. In core GP-1, highest value for all the three elements was seen in the lower section. Lowest value for Al and Fe was in the middle section, while for Mn it was in the upper section.

In case of trace metals when five estuaries were compared, highest value was recorded in the core VG-1 for Ni, Co and Cu (Table 3.1.2c). Core VS-1 showed highest value for Cr and core S-1 for Zn. Lowest value for all the studied metals were obtained for core S-1, except for Zn. Core MD-1 showed lowest value of Zn.

When the average values of the sections were compared (Table 3.1.2d), in core VS-1, Ni and Zn were higher in the upper section and Co, Cu and Cr in the lower section. In core VG-1, Co, Cu and Zn were highest in the upper section, while Cr showed highest value in the lower section and Ni in the middle section. However, similar to Fe, variation in Ni values was in small range between 124 and 128 ppm. In core MD-1, all the studied metals showed higher concentration in the upper section. In core S-1, all the metals except Zn were highest in the upper section. In core GP-1, Zn and Cr showed highest value in the upper section, while Ni, Co and Cu showed highest value in the lower section.

When the sediment components of five estuaries were compared at lower estuarine regions, it was noted that sand varied from 2.12 % to 69.42 %, while silt and clay ranged from 12.47 % to 38.61 % and 15.10 % to 59.27 % respectively (Table 3.1.1a). It was evident from the contour diagram (Fig. 3.1.6a) that sand percentage increased and clay percentage decreased from North to South in the lower estuarine mudflats along central west coast of India. Silt percentage also exhibited overall decrease from Vashishti to Gurupur estuaries. The variation in grain size was attributed to the location of the core samples from which they were collected and processes influencing lower estuary. In addition, the rock types in catchment area of five estuaries seemed to have affected sediment grain size. The basin area of the Vashishti River is overlaid by the lateritic plateau that was either formed by in-situ from the laterisation of Deccan trap basalts or formed due to the lateritic material brought down from

the Sahyadrian hill ranges. The Deccan trap basalts have uniform tholeiitic composition and are dark green to black volcanic rocks with a wide variety of textural character (Wensink 1973). Similar to Vashishti, basin area of the Vaghotan River also has thick and extensive

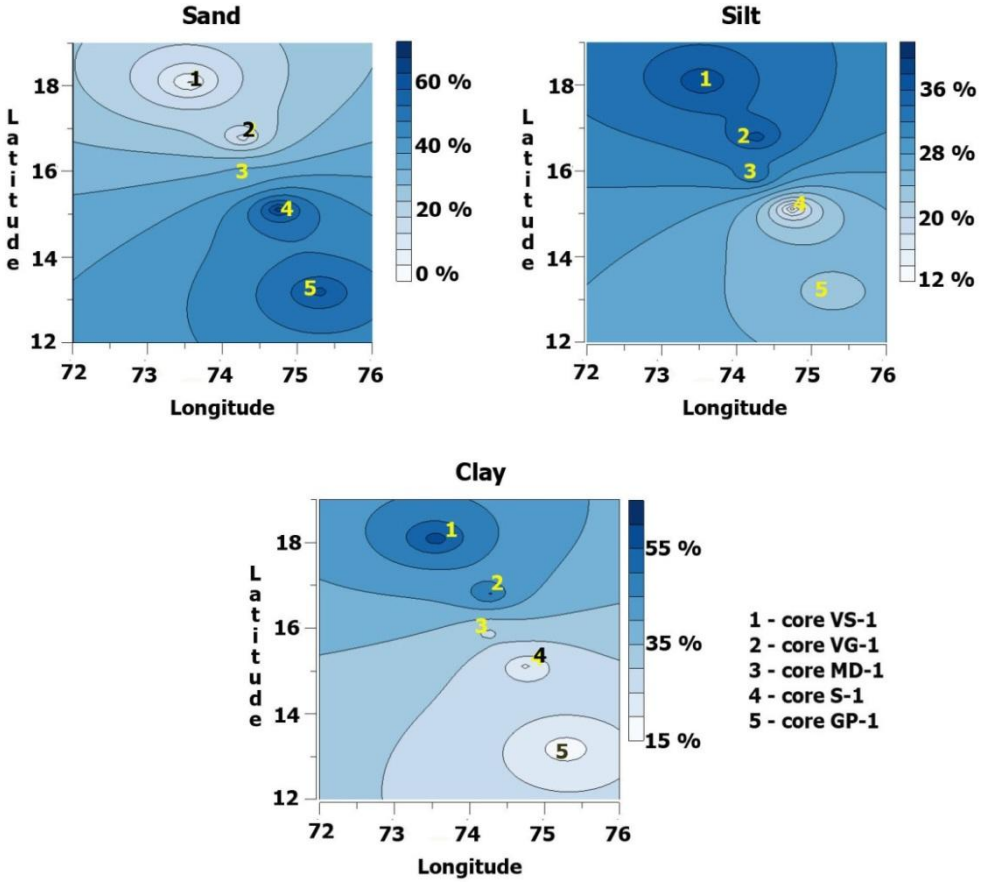

Fig. 3.1.6a Distribution of sediment components along the study area.

cover of laterite over the Deccan trap basalts (Tripati et al. 1998; Gujar et al. 2008). The geological formations within catchment area of Mandovi estuary include Western Dharwar Craton (WDC) of meso-archaean age. The WDC is characterized by high-Mg basalts and komatites with meta-volcanic and meta-sedimentary rocks (Naqvi 2005). The catchment area of the Sharavathi estuary consists of pre-Cambrian rocks. The Dharwar system and peninsular gneiss are the two major groups of rocks found in the Sharavathi river basin. The Dharwar system contains metamorphic rocks and is rich in iron and manganese. The peninsular gneisses are crystalline rocks and are made up of granite, granodiorite, granito-gneiss, migmatite etc. The basin area of the Gurupur River is overlaid by the Pliocene to Recent laterite capped plateaus and alluvium over the gneisses and continental type of sedimentary deposits with dolerite and norite dikes (Radhakrishna and Vaidyanadhan 1994) containing iron bearing minerals. Overall, the rock types vary from basalts to granite from

North to South along central west coast of India. The weathering of basalts releases finer sediments (Wilson 1978), whereas granite on the other hand, has a coarse grained texture which releases higher proportion of sand. Also, the amount of rainfall increases from North to South along central west coast of India, which might have helped in retaining only coarser sediments in the Southern portion of central west coast of India. In addition, tidal range is one of the important factors which affect the sediment grain size (Nasnodkar and Nayak 2015) and it varies from high to low along west coast of India from North to South, respectively (Mukhopadhyay and Karisiddaiah 2014). It is a known fact that mudflats are well developed with higher clay fraction in regions subjected to high tidal influence (Verney et al. 2006). On the other hand, higher rainfall and runoff will carry finer sediments in suspension retaining coarser sediments within the estuary.

In the lower section of all the cores (Fig. 3.1.1), except core GP-1, sand was higher. Sand percentage was more than the average in cores MD-1 and S-1, decreased from more than the average to less than the average in the core VS-1 and maintained along average line in the core VG-1 in this section. Further, in the upper section, sand percentage was less than the average in cores VS-1 and MD-1, decreased from along the average line to less than the average line in the core S-1. Also, sand percentage in the middle section of the core VG-1 was less than the average line. The higher sand in the lower section indicated presence of relatively higher hydrodynamic environment in the past along central west coast of India. The transition from relatively higher to lower energy environment must have led to decrease in sand in the upper section of cores VS-1, MD-1 and S-1, and in the middle section of the core VG-1. However, the increase in sand percentage in the upper section of the core VG-1 must be the result of increased human activities, such as sediment dredging in the recent times in the catchment area. In core GP-1, the decrease in sand percentage in the lower section and increase in the middle section was attributed to the change in morphology of the Gurupur estuary with time (Nasnodkar and Nayak 2015). Gurupur and adjacent Netravathi rivers join the Arabian Sea near Mangalore and gave rise to two spits, the Northern sand spit at the Gurupur River known as ‘Mangalore spit’ and the Southern spit 'Ullal' at the Netravati River. The supply of sediment for the growth of these spits was reported as from longshore drift and river discharge (Kunte and Wagle 1991). The estuarine mouths of Gurupur and Netravathi rivers have been reportedly migrating towards the North since long (Bannur et al. 1991;Gangadhar 1995), forcing the two spits to change the shape, size and orientation (Hegde and Raveendra 2000). The alignment of the shoal near the estuarine mouth of the Netravathi

River has altered the flow direction towards the Gurupur estuary (Hegde and Raveendra 2000). This might have resulted in the erosion of the Mangalore spit, directing coarser sediments into the Gurupur estuary. Raghavan et al. (2001), stated that Mangalore spit which consists of coarse to fine sand has reduced by 750 m from its distal end in length and its width has increased by 155 m from 1910 to 1993. Therefore, it may be construed that erosion of the Mangalore spit may have led to increase in coarser sediments observed in the middle section in the Gurupur estuary. Further, construction of breakwater to impede the erosion of the Mangalore spit in 1996 (Raghavan et al. 2001) must have led to decrease in sand observed in the upper section.

pH at lower estuarine regions in five estuaries varied from 6.52 to 7.49 (Table 3.1.1a). It showed fluctuating pattern from North to South along central west coast of India (Fig. 3.1.6b). In all the five estuaries there was change in pH towards more acidic nature from bottom to surface of a core.

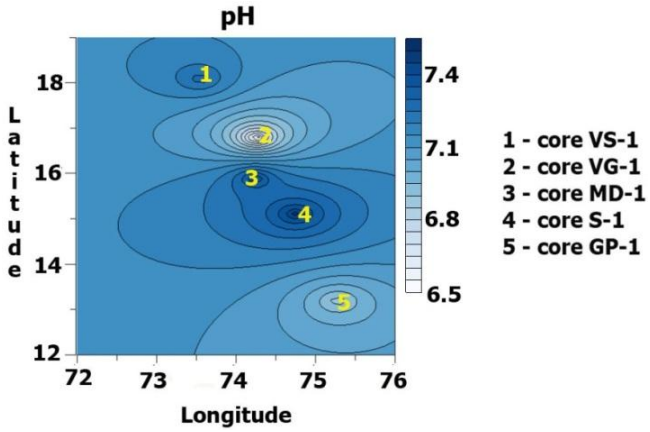

Fig. 3.1.6b Distribution of pH along the study area.

When organic carbon of five estuaries was compared at lower estuarine regions, it was noted that organic carbon varied from 0.70 % to 2.68 % (Table 3.1.1a). The percentage of organic carbon showed overall decrease from Vashishti to Gurupur estuaries (Fig. 3.1.6c).

The decrease in organic carbon from North to South along central west coast of India, similar to finer sediments suggested that grain size exerts a significant impact on the abundance of organic matter in sediments. Organic carbon has higher affinity towards finer sediments (Hedge et al. 1993) due to the higher surface area/volume ratio of finer sediment grain (Muzuka and Shaghude 2000).

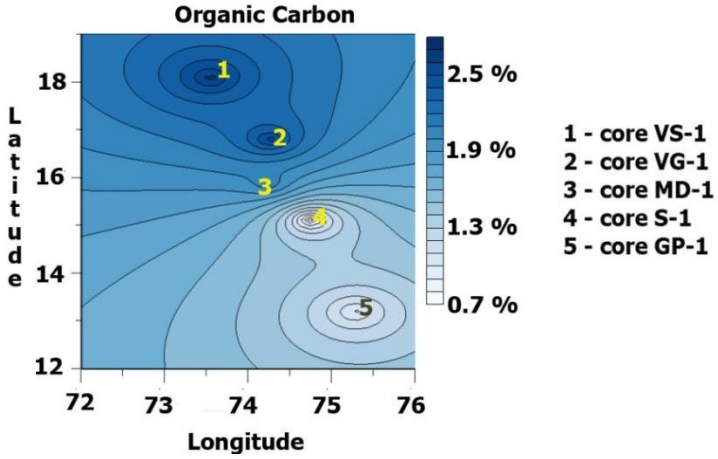

Fig. 3.1.6c Distribution of organic carbon along the study area.

The distribution pattern of organic carbon was similar to silt and clay in cores MD-1, S-1 and GP-1, and similar to silt in cores VS-1 and VG-1 suggesting its association with finer sediments. Organic carbon concentration was highest near the surface of the cores viz. VG-1, MD-1, S-1 and GP-1 and decreased with depth in the upper section of cores VG-1, MD-1 and S-1, and from upper to middle sections of the core GP-1. This suggested that in addition to grain size, degradation of organic matter by micro-organisms might have influenced organic carbon concentration in sediments. In core VS-1, relatively higher percentage of organic carbon, observed from 22 to 14 cm pointed towards higher deposition of organic matter in the recent past and/or partial decomposition and preservation of refractory organic matter in the sediments (Banerjee et al. 2012). Decomposition of organic matter associated with fresh water interaction with sea water must be responsible for change in pH.

In the study area, major metals in the bulk sediments varied with a range for Al from 4.77 % to 10.33 %, Fe from 2.23 % to 13.26 % and Mn from 108 ppm to 1375 ppm, while trace metals varied with a range for Ni from 32 ppm to 126 ppm, Co from 7 ppm to 86 ppm, Cu from 15 ppm to 489 ppm, Zn from 100 ppm to 730 ppm and Cr from 41 ppm to 149 ppm (Table 3.1.2a and c). Major as well as trace metals (except Zn) showed overall decrease from North to South along central west coast of India (Fig. 3.1.6d and e), similar to finer sediments and organic carbon. Hence, suggested that sediment grain size along with organic matter regulated the distribution of metals in the lower region of tropical estuaries. Finer-grained fractions and their associated sediment phases have a higher proportion of metals due to the larger surface area of smaller particles (Mikulic et al. 2008).

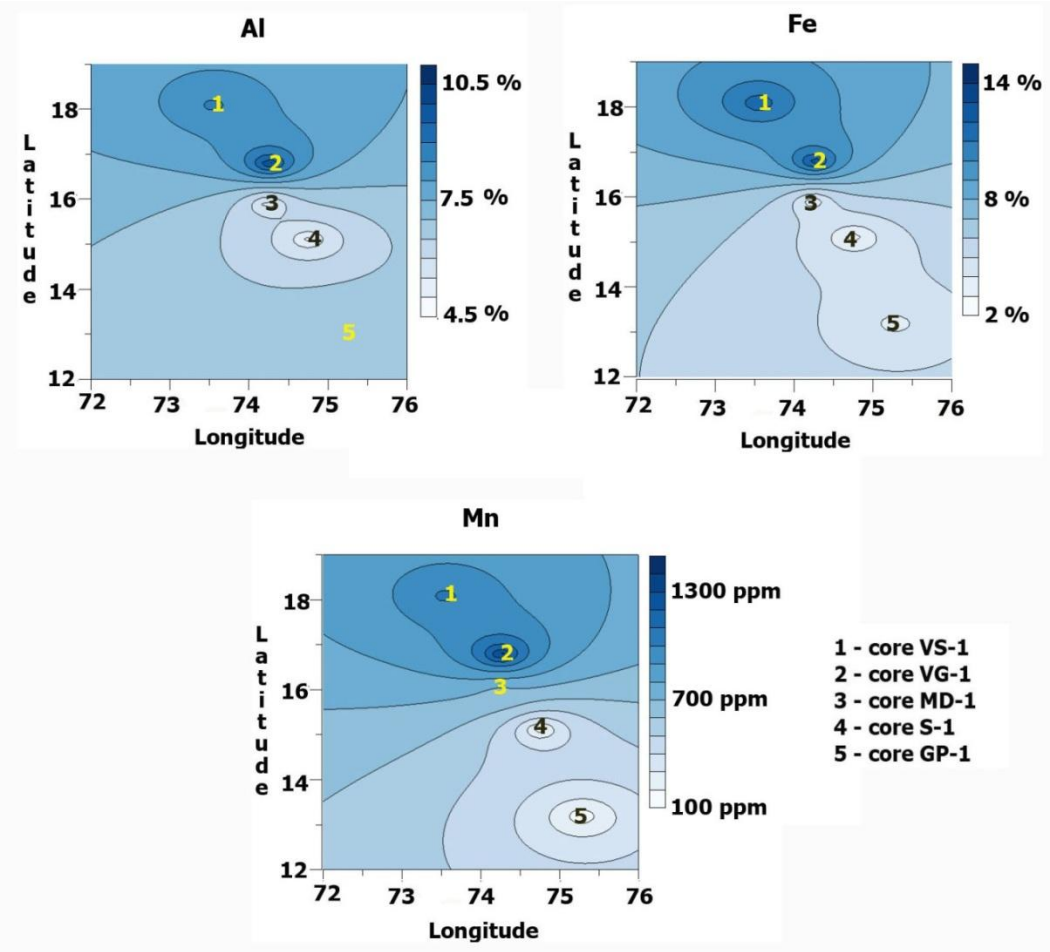

Fig. 3.1.6d Distribution of major metals in the bulk sediments along the study area.

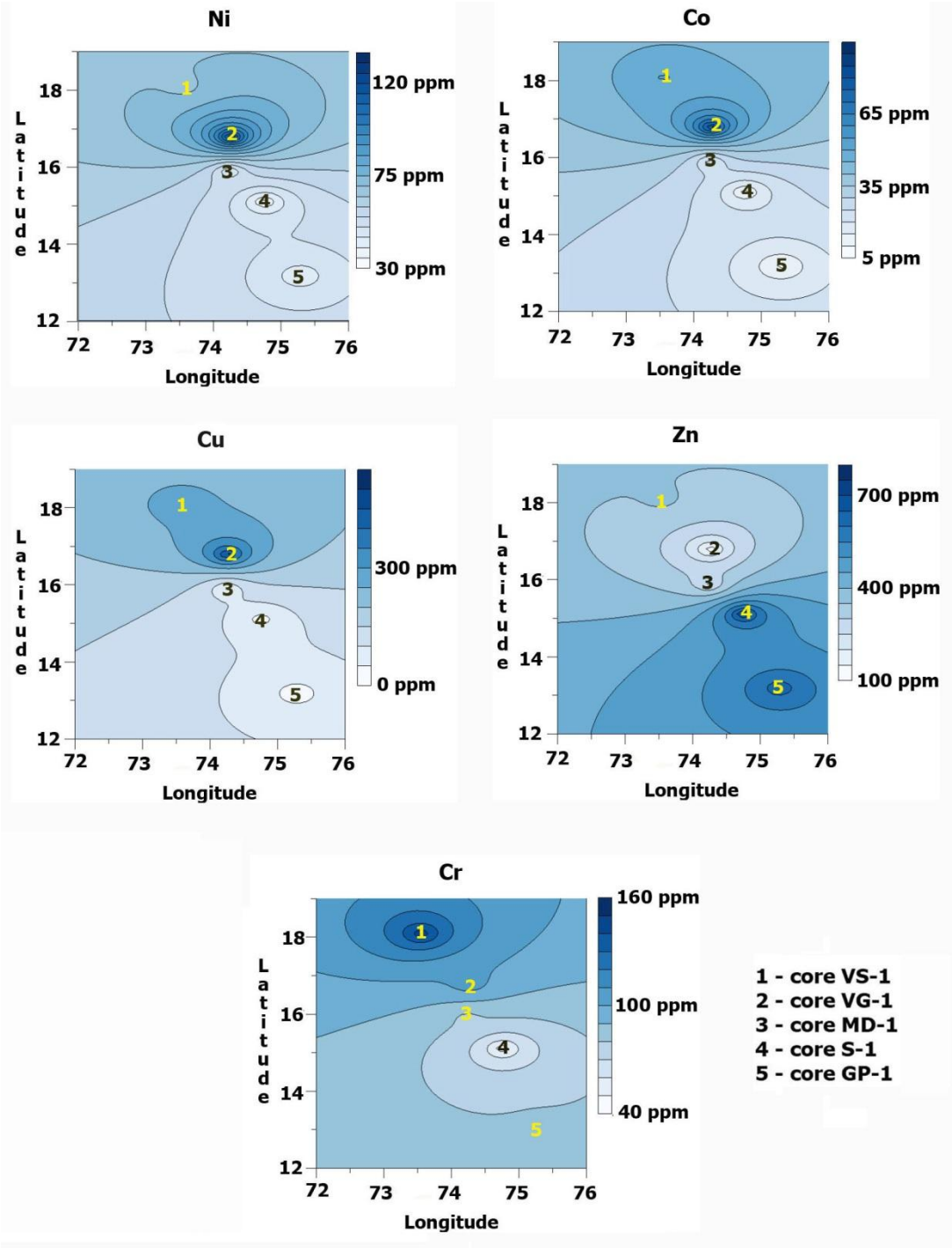

Fig. 3.1.6e Distribution of trace metals in the bulk sediments along the study area.

Similar to distribution of silt and clay, the average concentration of metals (Table 3.1.2b and d) was higher in the upper section than the lower section in cores MD-1 (all the metals) and S-1 (except Fe and Zn). In addition, Mn, Ni, Zn and Cr in the core VS-1, Co, Cu, and Zn in the core VG-1, Zn and Cr in the core GP-1 were higher in the upper section. The sectional variation in concentration of metals therefore, indicated role of grain size in the vertical

distribution of metals in Mandovi, Sharavathi and other estuaries. Among the studied tropical estuaries, Mandovi, Sharavathi and Gurupur estuaries host mining and associated activities in their catchment area. In addition, development activities in the catchment area has increased over the years with population expansion and bringing more land under agricultural activities. These activities must be responsible for releasing higher finer sediments with organic matter load. Hydrodynamic change from higher energy to relatively lower can also be due to increase in sea level (Rhein 2013), which brings in more saline water into the estuary and provides condition for deposition of more finer sediments

Pearson's correlation analysis of the core VS-1 (Table 3.1.3a), revealed significant correlation between sand and Fe as well as Cr; silt with organic carbon and Cu; and clay with Al and Ni. Further, Fe exhibited significant correlation with Cu and Cr. Also, Co with Cu; and Cu with Cr showed significant correlation.

Table 3.1.3a Correlation between sediment components, pH, organic carbon and metals in bulk sediments in core VS-1 (n=24). Values in bold indicates significant correlation at $p<0.05$

	Sand (%)	Silt (%)	Clay (%)	Org C (%)	pH	Al (%)	Fe (%)	Mn (ppm)	Ni (ppm)	Co (ppm)	Cu (ppm)	Zn (ppm)	Cr (ppm)
Sand (%)	1.00												
Silt (%)	0.19	1.00											
Clay (%)	-0.38	**-0.98**	1.00										
Org C (%)	0.12	**0.43**	**-0.43**	1.00									
pH	-0.13	0.20	-0.16	0.10	1.00								
Al (%)	-0.15	**-0.46**	**0.46**	**-0.48**	0.06	1.00							
Fe (%)	**0.59**	0.17	-0.28	-0.36	-0.12	0.25	1.00						
Mn (ppm)	0.02	-0.32	0.30	**-0.71**	0.10	0.30	0.18	1.00					
Ni (ppm)	-0.05	**-0.59**	**0.56**	-0.20	-0.30	0.30	-0.03	-0.02	1.00				
Co (ppm)	0.36	0.12	-0.19	-0.15	0.14	-0.15	0.38	0.05	-0.06	1.00			
Cu (ppm)	0.26	**0.42**	**-0.44**	-0.15	0.13	0.09	**0.74**	0.03	-0.10	**0.44**	1.00		
Zn (ppm)	-0.08	-0.27	0.27	**-0.48**	-0.31	-0.07	0.19	0.15	0.25	0.35	0.16	1.00	
Cr (ppm)	**0.50**	0.13	-0.22	**-0.51**	0.02	0.16	**0.82**	0.35	-0.15	0.39	**0.49**	0.18	1.00

The similar distribution pattern of Fe to that of sand in the core VS-1 indicated either its association with coarser sand particles (Aloupi and Angelidis 2002) or presence of Fe rich minerals in sand grade. The significant correlation between Fe and sand further supported association of Fe with coarser sediments. Also, similar distribution pattern of Cu, Co and Cr to that of Fe and significant correlation of Fe with Cu and Cr indicated that distribution of Cu and Cr was regulated by Fe as with change in redox conditions they are precipitated along with iron sulphides (Kumar and Edward, 2009) in deeper levels. Copper seemed to be associated with silt, while Al and Ni with clay. The increase in Mn and Zn concentration towards surface of the core VS-1 probably suggested anthropogenic input in the recent years.

It is important to mention here that the core VS-1 was collected in the vicinity of a fishing jetty and therefore the scrapings of paint from the fishing trawlers might have contributed towards higher Zn concentration in sediments in the recent years, while elevated concentration of Mn towards surface was possibly associated with increasing discharge of municipal and industrial waste water.

The results of correlation analysis of the core VG-1 showed significant correlation of sand with Al, Co and Zn; while clay with Mn, Ni and Cr (Table 3.1.3b). Among the metals, Zn showed significant correlation with Al and Fe; while Mn with Ni. Further, Zn exhibited significant association with Co, while Cr with Ni.

Table 3.1.3b Correlation between sediment components, pH, organic carbon and metals in bulk sedimentsin core VG-1 (n=30). Values in bold indicates significant correlation at $p<0.05$

	Sand (%)	Silt (%)	Clay (%)	Org C (%)	pH	Al (%)	Fe (%)	Mn (ppm)	Ni (ppm)	Co (ppm)	Cu (ppm)	Zn (ppm)	Cr (ppm)
Sand (%)	1.00												
Silt (%)	-0.12	1.00											
Clay (%)	**-0.55**	**-0.76**	1.00										
Org C (%)	-0.10	0.28	-0.17	1.00									
pH	-0.15	0.03	0.07	0.19	1.00								
Al (%)	**0.54**	-0.02	-0.33	-0.31	-0.29	1.00							
Fe (%)	0.24	-0.24	0.05	-0.12	-0.33	-0.09	1.00						
Mn (ppm)	**-0.51**	-0.12	**0.43**	-0.23	-0.04	-0.13	-0.12	1.00					
Ni (ppm)	-0.24	-0.30	**0.40**	**-0.54**	-0.01	-0.10	0.14	**0.39**	1.00				
Co (ppm)	**0.42**	-0.19	-0.11	**-0.40**	**-0.49**	0.20	0.36	**-0.36**	0.25	1.00			
Cu (ppm)	-0.19	-0.14	0.24	-0.09	-0.20	0.03	0.15	0.34	0.14	-0.05	1.00		
Zn (ppm)	**0.60**	0.03	**-0.41**	-0.23	**-0.59**	**0.42**	**0.43**	-0.36	0.13	**0.61**	0.11	1.00	
Cr (ppm)	-0.33	-0.18	**0.37**	**-0.58**	-0.10	-0.13	0.08	0.26	**0.56**	0.17	0.31	0.03	1.00

The distribution pattern of Al was somewhat similar to sand particularly in lower and upper sections in the core VG-1. Also, Co and Zn exhibited similar distribution as sand to a certain extent. In addition, distribution of Mn, Ni and Cr was similar to clay in this core. The vertical distribution of these metals as well as results of correlation analysis therefore, indicated adsorption of Al, Co and Zn onto sand and that of Mn, Ni and Cr onto clay size particles. The coarser sediments stay in place for a longer period of time (Tessier and Campbell 1982) and therefore sometimes develop oxide coatings and hence, adsorb trace metals. Moreover, all the trace metals might not be necessarily associated with the fine-grained alumino-silicates, but rather with the coarser silt fraction (Roussiez et al. 2006). This explains the adsorption of some of the metals onto sand. Further, in this core, all the metals exhibited overall decrease towards the surface which probably suggests their diffusion from sediments in the recent years. In the partly reduced sediment layers, dissolution of Fe-Mn oxyhydroxides takes place

producing Fe^{+2} and Mn^{+2} species (Volvoikar and Nayak 2013b). This process in turn releases trace metals adsorbed onto Fe-Mn oxyhydroxides. In addition, diversion of river water by canals for irrigation and drinking purpose in the recent years must have led to changes in natural flow of fresh water affecting sedimentation patterns (Rodriguez et al. 2001). Zhang et al. (2002) reported that in the intertidal flats, hydrological dynamics regulates the grain size distribution and grain size in turn regulates the distribution of the element concentration. The decrease in sand and clay and an increase in silt in the top 10 cm of the core VG-1 supported the change in sedimentation pattern in the recent years.

The results of correlation analysis of the core MD-1 revealed significant correlation of finer sediments with organic carbon; and Al, Fe, Mn, Ni, Co and Cu with finer sediments and organic carbon (Table 3.1.3c). Among the metals, Al showed significant correlation with Ni, Co and Cu; Fe with Mn, Co and Cu; while Mn with Co and Cu. Further, Ni with Co and Cu; Co with Cu; and Zn with Cr also showed, significant correlation.

Table 3.1.3c Correlation between sediment components, pH, organic carbon and metals in bulk sedimentsin core MD-1 (n=29). Values in bold indicates significant correlation at $p<0.05$

	Sand (%)	Silt (%)	Clay (%)	Org C (%)	pH	Al (%)	Fe (%)	Mn (ppm)	Ni (ppm)	Co (ppm)	Cu (ppm)	Zn (ppm)	Cr (ppm)
Sand (%)	1.00												
Silt (%)	**-0.96**	1.00											
Clay (%)	**-0.86**	**0.67**	1.00										
Org C (%)	**-0.96**	**0.94**	**0.78**	1.00									
pH	**0.82**	**-0.81**	**-0.66**	**-0.81**	1.00								
Al (%)	**-0.57**	**0.55**	**0.47**	**0.52**	-0.35	1.00							
Fe (%)	**-0.69**	**0.63**	**0.65**	**0.70**	**-0.54**	0.10	1.00						
Mn (ppm)	**-0.80**	**0.74**	**0.73**	**0.76**	**-0.86**	0.35	**0.68**	1.00					
Ni (ppm)	**-0.62**	**0.60**	**0.52**	**0.63**	-0.31	**0.80**	0.23	0.35	1.00				
Co (ppm)	**-0.85**	**0.85**	**0.67**	**0.88**	**-0.82**	**0.44**	**0.56**	**0.76**	**0.47**	1.00			
Cu (ppm)	**-0.86**	**0.82**	**0.74**	**0.81**	**-0.73**	**0.67**	**0.54**	**0.78**	**0.70**	**0.72**	1.00		
Zn (ppm)	0.21	-0.08	**-0.39**	-0.27	0.22	0.21	**-0.43**	-0.31	0.12	-0.14	-0.06	1.00	
Cr (ppm)	0.19	-0.13	-0.26	-0.18	0.12	0.15	**-0.50**	-0.15	0.24	-0.08	0.08	**0.38**	1.00

The increasing distribution pattern of metals (except Zn and Cr) from lower to upper sections, similar to silt, clay and organic carbon suggested their adsorption onto finer sediments and organic carbon in the core MD-1. The significant correlation of Al, Fe, Mn, Ni, Co and Cu with finer sediments and organic carbon further supported the same. Finer-grained sediments hold a higher proportion of trace elements due to the larger surface area of smaller particles (Mikulic et al. 2008). Also, the strong correlation between these trace metals and organic carbon underlines an association in the form of organometallic complexes (Zourarah et al. 2009). Moreover, gradual decrease in organic carbon, Al, Fe, Mn, Ni, Co and Cu with depth

indicated that these metals were significantly redistributed by the degradation of organic matter. During initial deposition, trace metals associated with organic matter (Salomons and Forstner 1984) tend to get redistributed upon early aerobic degradation of organic matter, resulting in a gradual decrease in metal concentration with depth (Valette-Silver 1993). Further, catchment area of the Mandovi estuary is known for Fe and Mn ore mining and its associated activities. It is most likely that Fe and Mn may play an important role in the distribution of metals. Iron and Manganese exhibit similar behaviour in the estuarine environment. Upon reaching sediments, Fe and Mn oxide are readily reduced into anoxic sediments either as electron acceptors in microbial mediated respiratory oxidation of organic carbon (Thamdrup 2000) or reduced chemically by hydrogen sulphide (Kappler and Straub 2005). Reduced Fe and Mn may remobilize and precipitate as carbonates, adsorb onto clay minerals, carbonates, and metal oxide (Kristiansen et al. 2002) in relatively oxic conditions. The enrichment of Fe and Mn in the upper section of the core MD-1 therefore indicated that they were precipitated as insoluble oxy-hydroxide in sediments when brought across a redox gradient into an oxidizing environment (Brown et al. 2000) while, their lower concentration in the lower section suggested their dissolution under reducing diagenetic conditions (Dulaiova et al. 2008; Ram et al. 2009). In this core, trace metals viz. Ni, Co and Cu showed significant correlation with Fe and/or Mn suggesting role of Fe and/or Mn oxide in distribution of these trace metals as they are known to scavenge trace metals from the water column (Venkatramanan et al. 2014). Among the metals, distribution pattern of Zn and Cr was different from rest of the metals indicating their different source in the estuary and the significant correlation among themselves suggested their close association.

The correlation analysis results of the core S-1 showed significant correlation of finer sediments with organic carbon; silt with Ni, Co and Cu; clay with Al, Mn, Ni, Co and Cu; organic carbon with Al, Mn, Ni, Co, Cu and Cr; and pH with Zn (Table 3.1.3d). Among the metals, Al exhibited significant correlation with Mn, Ni, Co, Cu and Cr; Fe with Mn, Zn and Cr; while Mn with all the trace metals. In addition, Ni showed significant correlation with Co, Cu and Cr; Co with Cu and Cr; while Cu and Zn with Cr.

Similar to Mandovi estuary, most of the metals (Al, Mn, Ni, Co, Cu and Cr) in the Sharavathi estuary showed overall increasing distribution pattern from lower to upper sections as that of finer sediments and organic carbon. Also, these metals exhibited significant correlation with silt and/or clay and/or organic carbon indicating their adsorption onto finer sediments and

Table 3.1.3d Correlation between sediment components, pH, organic carbon and metals in bulk sediments in core S-1 (n=34). Values in bold indicates significant correlation at p<0.05

	Sand (%)	Silt (%)	Clay (%)	Org C (%)	pH	Al (%)	Fe (%)	Mn (ppm)	Ni (ppm)	Co (ppm)	Cu (ppm)	Zn (ppm)	Cr (ppm)
Sand (%)	1.00												
Silt (%)	**-0.90**	1.00											
Clay (%)	**-0.96**	**0.76**	1.00										
Org C (%)	**-0.84**	**0.75**	**0.82**	1.00									
pH	**0.88**	**-0.78**	**-0.85**	**-0.82**	1.00								
Al (%)	**-0.83**	**0.73**	**0.82**	**0.90**	**-0.75**	1.00							
Fe (%)	0.02	-0.04	0.02	0.02	0.10	0.17	1.00						
Mn (ppm)	**-0.37**	0.27	**0.39**	**0.38**	-0.33	**0.59**	**0.51**	1.00					
Ni (ppm)	**-0.74**	**0.64**	**0.74**	**0.80**	**-0.68**	**0.85**	-0.04	**0.51**	1.00				
Co (ppm)	**-0.74**	**0.57**	**0.77**	**0.87**	**-0.69**	**0.94**	0.22	**0.63**	**0.88**	1.00			
Cu (ppm)	**-0.74**	**0.64**	**0.73**	**0.81**	**-0.69**	**0.81**	-0.07	**0.46**	**0.89**	**0.82**	1.00		
Zn (ppm)	0.28	-0.23	-0.28	-0.27	**0.37**	-0.13	**0.39**	**0.48**	-0.11	-0.05	-0.22	1.00	
Cr (ppm)	-0.31	0.22	0.34	**0.38**	-0.12	**0.52**	**0.52**	**0.60**	**0.51**	**0.62**	**0.38**	**0.53**	1.00

complexation with organic carbon (Chatterjee et al. 2007). In the lower section of the core S-1, most of the metals exhibited fluctuating distribution patterns which suggested their mobilization from the sediments. As seen from the triangular diagram, lower section of the core S-1 was enriched in coarser sediments (Fig. 3.2d) with sand percentage between 90 and 100 %. In coarser sediments, the porosity is much higher compared to finer sediments and there is enough opportunity for the metals to get mobilized from the coarser sediments (Clark 1992). The increasing concentration of Al, Mn, Ni, Co and Cu observed in finer sediments enriched upper section of the core S-1 compared to the lower section further supported their mobilization and re-precipitation under oxic conditions. The significant correlation of Mn with all the trace metals indicated role of Mn oxide in regulation of trace metals across the redox boundary (Kumar and Edward 2009). The Fe oxide too seemed to have certain role in distribution of Zn and Cr. According to Zabetoglou et al. (2002), Fe often correlates well with concentrations of trace metals in aquatic environments. However, nature, crystallinity, size of the crystals, surface charge of metal oxide and mixed metal oxide (e.g., Fe-Al oxide) also play an important role in the sorption selectivity of trace elements in cationic form (Violante et al. 2008). This might be the possible reason for difference in affinity of trace metals towards Fe and Mn. Further, like Mandovi estuary, Sharavathi estuary is also a reservoir of iron ore mining wastes. Therefore, input of Fe and Mn from mining related activities must be facilitating adsorption of trace metals onto sediments. Among the metals, the distribution pattern of Zn was different from rest of the trace metals particularly in the upper section and its poor correlation with most of the trace metals indicated different source, may be anthropogenic (scrapings of paint from barges used for transportation of iron ore and fishing trawlers as well as agricultural and domestic wastes).

The correlation analysis results of the core GP-1 revealed significant correlation of finer sediments with organic carbon; Al, Fe, Ni, Co, Cu and Cr with finer sediments and organic carbon (Table 3.1.3e). Also, pH showed significant correlation with Al, Fe and Co. Among the metals, Al exhibited significant correlation with Fe, Ni, Co, Cu and Cr, while Fe and Mn with all the trace metals (except Zn). In addition, Ni showed significant correlation with Co, Cu and Cr; Co with Cu and Cr; while Cu and Zn with Cr.

Table 3.1.3e Correlation between sediment components, pH, organic carbon and metals in bulk sediments in core GP-1 (n=30). Values in bold indicates significant correlation at $p<0.05$

	Sand (%)	Silt (%)	Clay (%)	Org C (%)	pH	Al (%)	Fe (%)	Mn (ppm)	Ni (ppm)	Co (ppm)	Cu (ppm)	Zn (ppm)	Cr (ppm)
Sand (%)	1.00												
Silt (%)	**-0.92**	1.00											
Clay (%)	**-0.91**	**0.68**	1.00										
Org C (%)	**-0.91**	**0.81**	**0.87**	1.00									
pH	**-0.40**	0.31	**0.42**	**0.42**	1.00								
Al (%)	**-0.82**	**0.74**	**0.77**	**0.92**	**0.53**	1.00							
Fe (%)	**-0.84**	**0.76**	**0.78**	**0.95**	**0.46**	**0.95**	1.00						
Mn (ppm)	-0.18	0.10	0.23	0.28	0.23	0.30	**0.42**	1.00					
Ni (ppm)	**-0.65**	**0.56**	**0.64**	**0.76**	0.30	**0.74**	**0.86**	**0.70**	1.00				
Co (ppm)	**-0.79**	**0.70**	**0.75**	**0.90**	**0.40**	**0.89**	**0.94**	**0.55**	**0.92**	1.00			
Cu (ppm)	**-0.69**	**0.67**	**0.59**	**0.81**	0.36	**0.83**	**0.87**	**0.42**	**0.77**	**0.82**	1.00		
Zn (ppm)	-0.16	0.19	0.11	0.12	-0.27	-0.06	-0.04	-0.20	-0.07	0.09	-0.13	1.00	
Cr (ppm)	**-0.64**	**0.68**	**0.49**	**0.73**	0.12	**0.66**	**0.77**	**0.43**	**0.77**	**0.82**	**0.63**	**0.36**	1.00

The decrease in metal concentration (except Zn) in the middle section than lower and upper sections of the core GP-1 was attributed to dilution of concentration by input of coarser sediments. German and Svensson (2002) reported that change in particle size distribution results in a variation in distribution pattern of metals in the sediments, with higher proportion of metals associated with finer fractions than coarser. In this core, except Zn, all the metals exhibited similar distribution pattern as that of finer sediments and organic carbon. Also, significant correlation of most of the metals (Al, Fe, Ni, Co, Cu and Cr) with finer sediments and organic carbon suggested that sediment grain size exerts a significant control on the vertical distribution of metals (Nasnodkar and Nayak 2015). In addition, significant correlation of trace metals with Fe and Mn indicated role of Fe-Mn oxide in distribution of metals in the lower region of the Gurupur estuary. The basin area of the Gurupur River, as discussed earlier, is rich in Fe bearing minerals, in addition to Mn. The natural weathering of basin rocks might be the source of Fe and Mn in the Gurupur river sediments. Additionally, as mentioned earlier, the Kudremukh iron ore mine is located in the catchment area of the Gurupur River and the heavy rainfall in this region must be bringing large amount of Fe rich material, in addition to Mn from the catchment area into the river which might have favoured

the adsorption of trace metals. Further, similar to Sharavathi estuary, distribution pattern of Zn in the Gurupur estuary was different in comparison to other metals and its enrichment in the top 14 cm of the core GP-1 indicated different source, probably originating from the anthropogenic activities like scrapings of paint from fishing trawlers as well as agricultural and domestic wastes. The poor correlation of Zn with most of the trace metals further supported its different source.

Further, in order to understand difference in sediment components, pH, organic carbon, metals concentration in the bulk sediments among the cores, the data was plotted on the isocon diagram (Fig.3.1.7). On comparison of core VS-1 with core VG-1, clay, pH, Cr and Zn were higher in the core VS-1, while sand, Al, Co, Ni, Cu and Mn were higher in the core VG-1. Organic carbon and silt were slightly higher in the core VS-1, while Fe in the core VG-1. The comparison of cores VS-1 and MD-1 indicated higher clay, silt, Al, Fe, Mn, Ni, Co, Cu, Zn and Cr in the core VS-1, while sand was higher in the core MD-1. Organic carbon was slightly higher in the core VS-1, while pH in the core MD-1. Between cores VS-1 and S-1, clay, silt organic carbon, Al, Fe, Mn, Ni, Co, Cu and Cr were higher in the core VS-1, whereas sand and Zn in the core S-1. pH was slightly higher in the core S-1. Further, between cores VS-1 and GP-1, clay, silt, organic carbon, Al, Fe, Mn, Ni, Co, Cu and Cr were higher in the core VS-1, while sand and Zn in the core GP-1. pH was slightly higher in the core VS-1. On comparison of cores VG-1 and MD-1, clay, Al, Fe, Mn, Ni, Co, Cu and Cr were higher in the core VG-1, while sand and Zn in the core MD-1. The concentration of organic carbon and silt was slightly higher in the core VG-1, while pH in the core MD-1. Among cores VG-1 and S-1, clay, silt, organic carbon, Al, Fe, Mn, Ni, Co, Cu and Cr were higher in the core VG-1, while sand, pH and Zn in the core S-1. Between cores VG-1 and GP-1, clay, silt, organic carbon, Al, Fe, Mn, Ni, Co, Cu and Cr were higher in the core VG-1, whereas sand and Zn in the core GP-1. pH was slightly higher in the core GP-1. Further, on comparison of cores MD-1 and S-1, clay, silt, organic carbon, Fe, Mn, Ni, Co, Cu and Cr were higher in the core MD-1 while sand and Zn in the core S-1. Aluminium was slightly higher in the core MD-1, whereas pH in the core S-1. Among cores MD-1 and GP-1, silt, clay, organic carbon, pH, Co, Cu and Mn were higher in the core MD-1 while, sand, Fe, Al and Zn in the core GP-1. Nickel was slightly higher in the core MD-1, while Cr in the core GP-1. Further, between cores S-1 and GP-1, Zn was higher in the core S-1, whereas silt, Cr, Fe, Ni, Al and Co in the core GP-1. Sand, clay, pH and Mn were slightly higher in the core S-1, while organic carbon and Cu in the core GP-1.

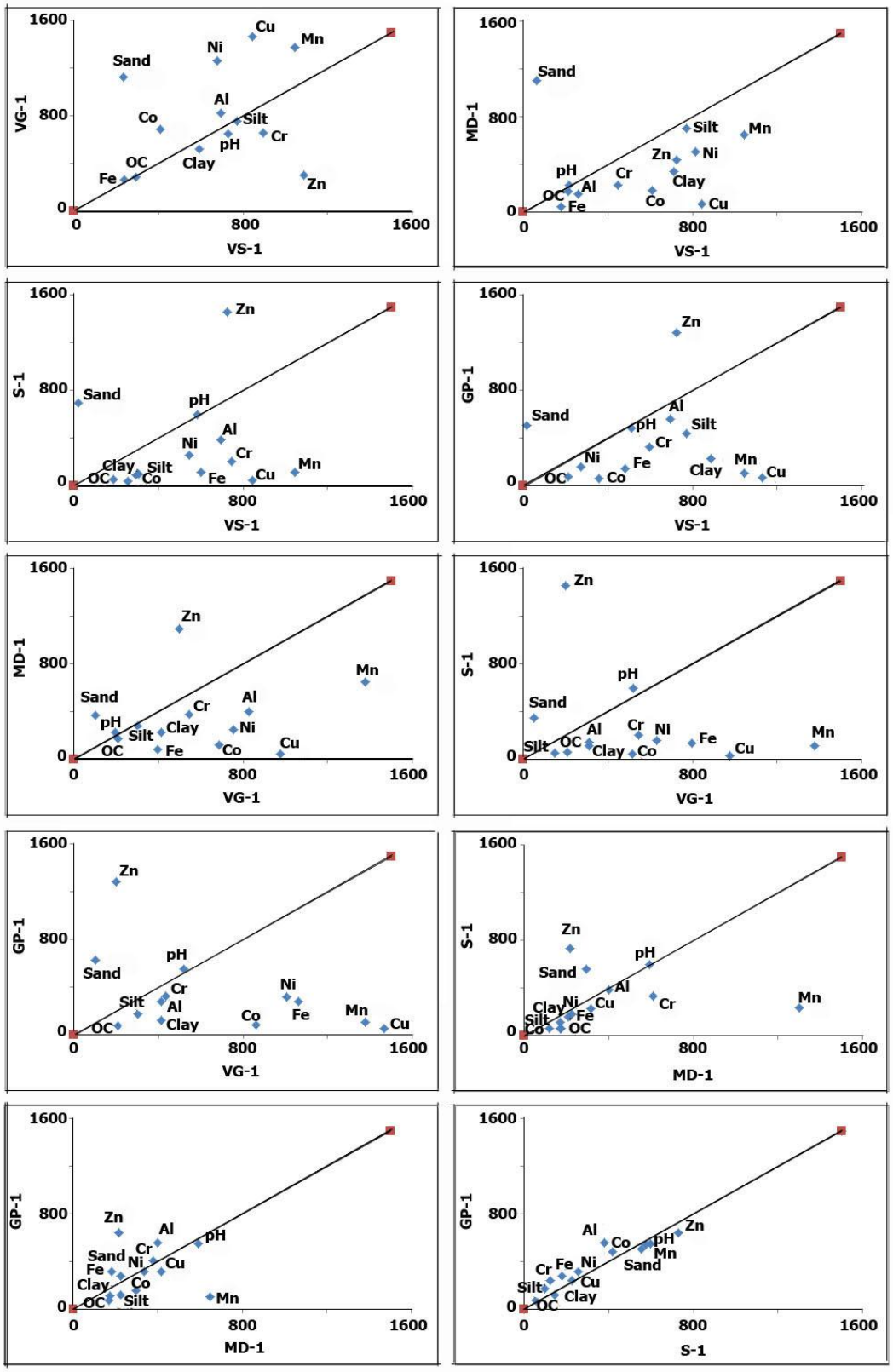

Fig. 3.1.7 Isocon plots for sediment components, pH, organic carbon and metals in the bulk sediments

As discussed earlier, change in the catchment area geology has led to variation in grain size from North to South along the study area. The basalt in the North might have led to higher finer sediments in the Vashishti estuary. However, most of the metals were present in higher concentration in the Vaghotan estuary than the Vashishti. Further, on comparison of Mandovi, Sharavathi and Gurupur estuaries with either Vashishti or Vaghotan estuary a systematic pattern was observed with respect to sediment components, organic carbon and metals. It was sand that seemed to be higher in Mandovi, Sharavathi and Gurupur estuaries than Vashishti and Vaghotan estuaries, in which finer sediments, organic carbon and most of the metals were in higher concentration. The granite and granitic gneisses towards the South of the study area must be responsible for higher sand percentage. However, higher concentration of Zn in Mandovi, Sharavathi and Gurupur estuaries in comparison to Vashishti and Vaghotan estuaries (except in core MD-1 v/s core VS-1) indicated anthropogenic input.

3.1.5 Clay mineralogy

Vashishti estuary

In core VS-1, the abundance of clay minerals was in the order of smectite > kaolinite > illite > chlorite (Table 3.1.4a). The percentage of smectite, illite, kaolinite and chlorite ranged from 27.84 % to 76.10 % (avg. 53.00 %), 6.93 % to 37.94 % (avg. 14.50 %), 19.26 % to 38.01 % (avg. 25.63 %) and 3.16 % to 10.10 % (avg. 6.87 %) respectively.

Distribution of clay minerals in the core VS-1 is presented in the figure 3.1.8a. The distribution pattern of all the clay minerals showed slight fluctuating trend from bottom to 22 cm depth followed by drastic change up to 18 cm. This change has resulted in positive peak at 18 cm for kaolinite and illite, and negative peak for smectite. From 14 cm to surface, percentage of smectite increased, whereas kaolinite and illite showed fluctuations around the average line. Chlorite showed fluctuating distribution pattern from 22 cm and surface.

Table 3.1.4a Range and average concentration of clay minerals in cores VS-1, VG-1, S-1 and GP-1.

Sediment core	Smectite (%)			Illite (%)			Kaolinite (%)			Chlorite (%)		
	Range		Avg	Range		Avg	Range		Avg	Range		Avg
	Min	Max		Min	Max		Min	Max		Min	Max	
VS-1	27.84	76.10	53.00	6.93	37.94	14.50	19.26	38.01	25.63	3.16	10.10	6.87
VG-1	11.86	38.40	25.30	11.49	25.40	18.74	33.76	56.50	46.47	4.32	16.95	9.49
*Lower Mandovi estuary			22.06			19.23			37.58			21.13
S-1	2.42	11.11	5.02	6.65	23.71	12.15	59.68	79.75	74.01	4.51	14.58	8.82
GP-1	2.59	6.70	4.67	9.39	21.93	14.51	61.97	76.98	69.93	6.72	15.91	10.90

*Average concentration of clay minerals in the lower Mandovi estuary was referred from Singh (2008)

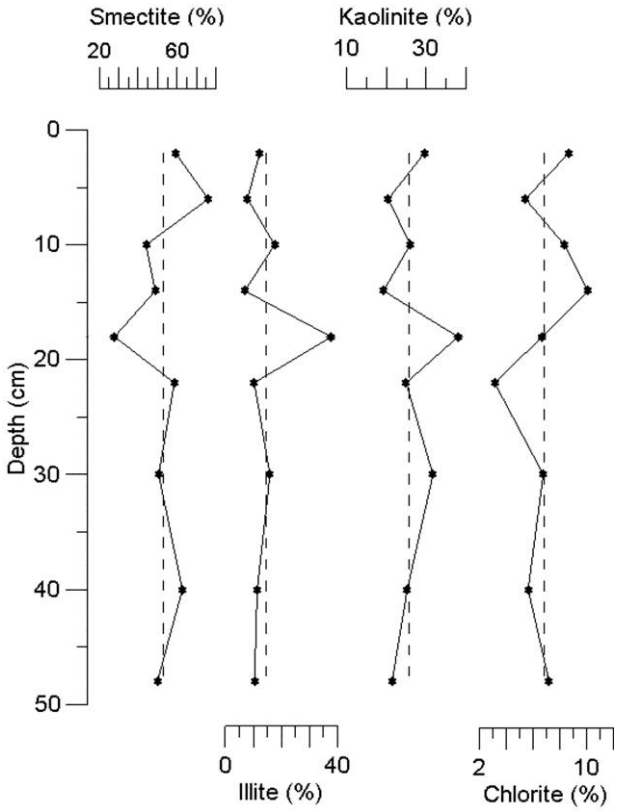

Fig. 3.1.8a Variation of clay minerals with average line in sediment core VS-1

Vaghotan estuary

In the lower estuarine region of the Vaghotan estuary (core VG-1) the abundance of clay minerals was in the order of kaolinite > smectite > illite > chlorite (Table 3.1.4a). The percentage of smectite ranged from 11.86 % to 38.40 % (avg. 25.30 %), while illite varied from 11.49 % to 25.40 % (avg. 18.74 %). The percentage of kaolinite and chlorite ranged from 33.76 % to 56.50 % (avg. 46.47 %) and 4.32 % to 16.95 % (avg. 9.49 %) respectively.

Distribution of clay minerals in the core VG-1 is presented in the figure 3.1.8b. The smectite and kaolinite values remained constant from bottom to 30 cm, followed by a fluctuating trend towards the surface. Illite and chlorite showed fluctuation around the average line opposite to each other from bottom to 30 cm of the core VG-1, from where chlorite decreased with fluctuations and illite maintained almost constant trend. The distribution pattern of kaolinite was largely opposite to that of smectite in this core.

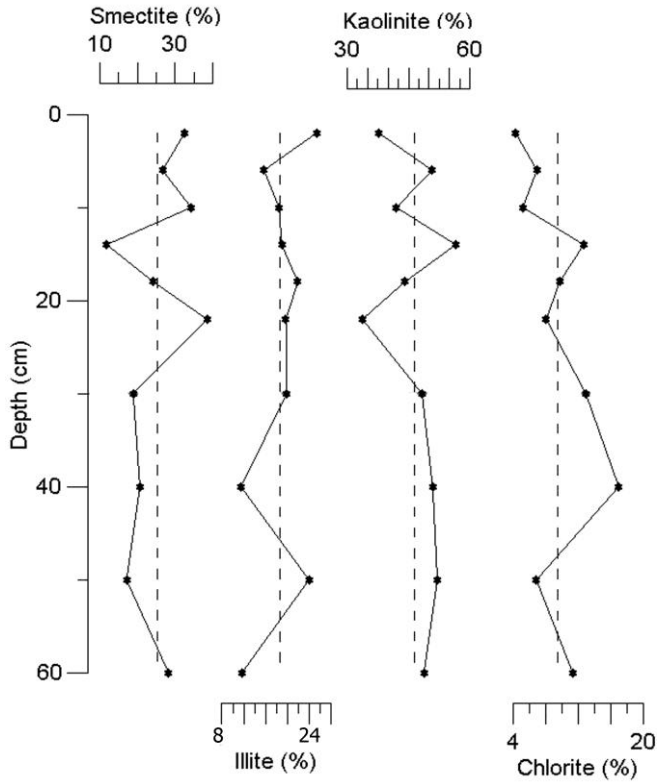

Fig. 3.1.8b Variation of clay minerals with average line in sediment core VG-1

Mandovi estuary

Clay mineral analysis carried out by Singh et al. (2014) in the sediment core collected from the lower region of the Mandovi estuary has been used in the present study. They reported abundance of kaolinite in the lower estuarine core. The average percentage of smectite, illite, kaolinite and chlorite reported by Singh et al. (2014) is 22.06 %, 19.23 %, 37.58 % and 21.13 % respectively.

Sharavathi estuary

In core S-1, kaolinite was abundant in comparison to other clay minerals. Clay minerals assemblage was in the decreasing order of abundance i.e. kaolinite > illite > chlorite > smectite (Table 3.1.4a). The percentage of smectite, illite, kaolinite and chlorite varied from 2.42 % to 11.11 % (avg. 5.02 %), 6.65 % to 23.71 % (avg. 12.15 %), 59.68 % to 79.75 % (avg. 74.01 %) and 4.51 % to 14.58 % (avg. 8.82 %) respectively.

Distribution of clay minerals in the core S-1 is presented in the figure 3.1.8c. From bottom to 30 cm, all the minerals showed large fluctuations. Between 30 cm and surface, distribution pattern of smectite and illite showed decreasing trend, whereas kaolinite and chlorite showed an increase towards the surface of the core S-1, with chlorite showing positive peak at 16 cm. Kaolinite exhibited opposite trend to that of smectite from bottom to surface. Similarly, chlorite exhibited increasing trend whereas illite decreasing trend when the whole profile was considered.

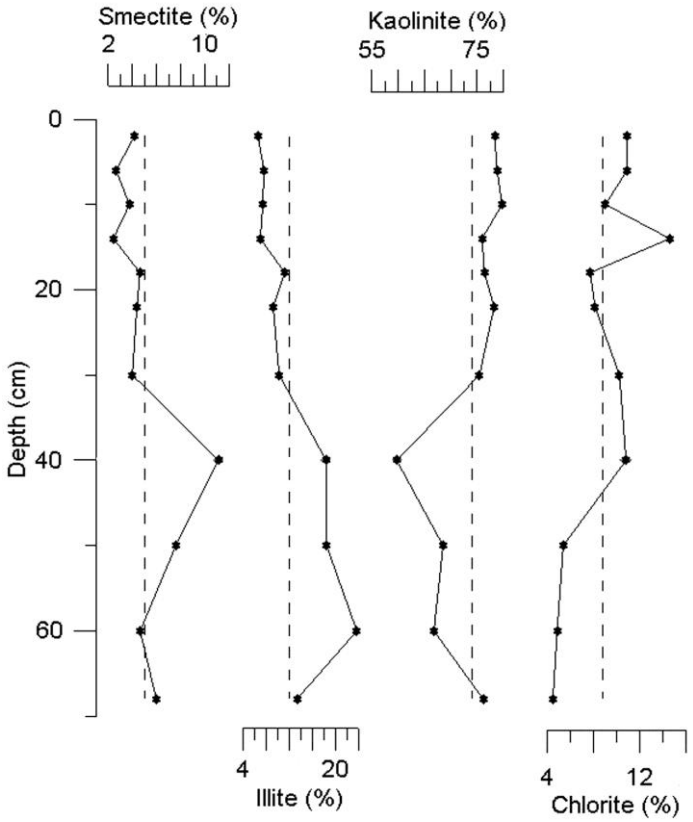

Fig. 3.1.8c Variation of clay minerals with average line in sediment core S-1

Gurupur estuary

Similar to core S-1, core GP-1 collected from the lower region of the Gurupur estuary also indicated kaolinite as the dominant clay mineral. Clay mineral assemblage was in the order of abundance i.e. kaolinite > illite > chlorite > smectite (Table 3.1.4a). Smectite in this core varied 2.59 % to 6.70 % (avg. 4.67 %) and illite ranged from 9.39 % to 21.93 % (avg. 14.51 %); while, kaolinite and chlorite ranged from 61.97 % to 76.98 % (avg. 69.93 %) and 6.72 % to 15.91 % (avg. 10.90 %) respectively.

Distribution of clay minerals in the core GP-1 is presented in the figure 3.1.8d. The smectite and illite showed overall increase from bottom to 18 cm, while, kaolinite and chlorite exhibited increase from bottom to 40 cm followed by decrease up to 10 cm with fluctuations. In top 10 cm, all the clay minerals exhibited an increasing trend towards the surface.

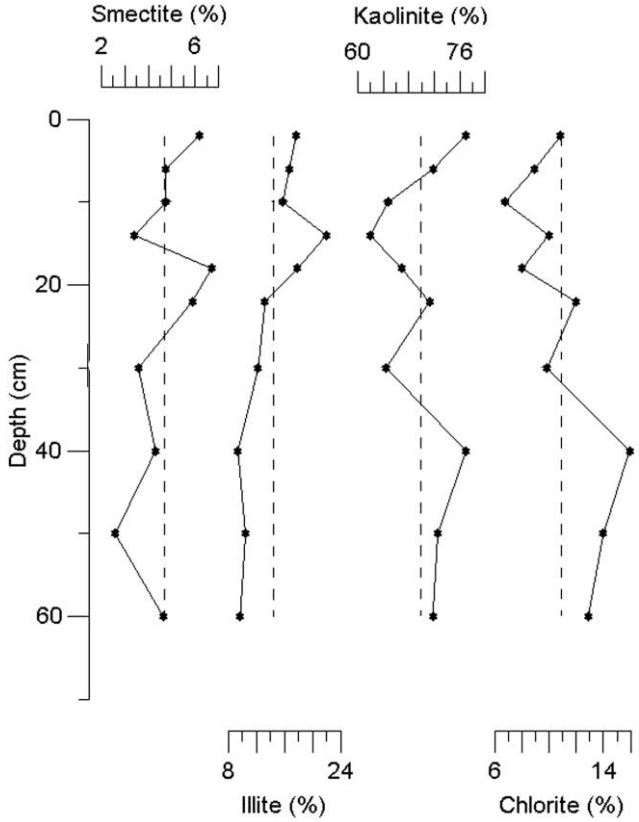

Fig. 3.1.8d Variation of clay minerals with average line in sediment core GP-1

When average values of clay minerals of five estuaries were considered, smectite decreased from VS-1 to GP-1 i.e. from North to South. Kaolinite showed overall increase towards South with exceptions, namely Mandovi and Gurupur, wherein it was present in slightly lower concentration. Illite along this coast, between VS-1 and GP-1 varied from 12.15 to 19.23 %, while chlorite from 6.87 to 21.13 %.

3.1: 6 Clay chemistry

Major metals (Al, Fe and Mn)

Vashishti estuary

The concentration of Al, Fe and Mn in the clay fraction of the core VS-1 varied from 8.06 % to 9.90 % (avg. 8.77 %), 9.37 % to 12.27 % (avg. 10.54 %) and 605 ppm to 1160 ppm (avg. 856 ppm) respectively (Table 3.1.4b).

Element distribution profile in the clay component of the core VS-1 is presented in the figure 3.1.9a. Metals viz. Fe and Mn exhibited overall increasing trend from bottom to around 22 cm, while Al showed increase from bottom to 30 cm, followed by a decreasing trend up to 22 cm. Further, Al and Mn showed increase towards the surface, while Fe showed decrease. However, Mn in the upper 2 cm showed decrease.

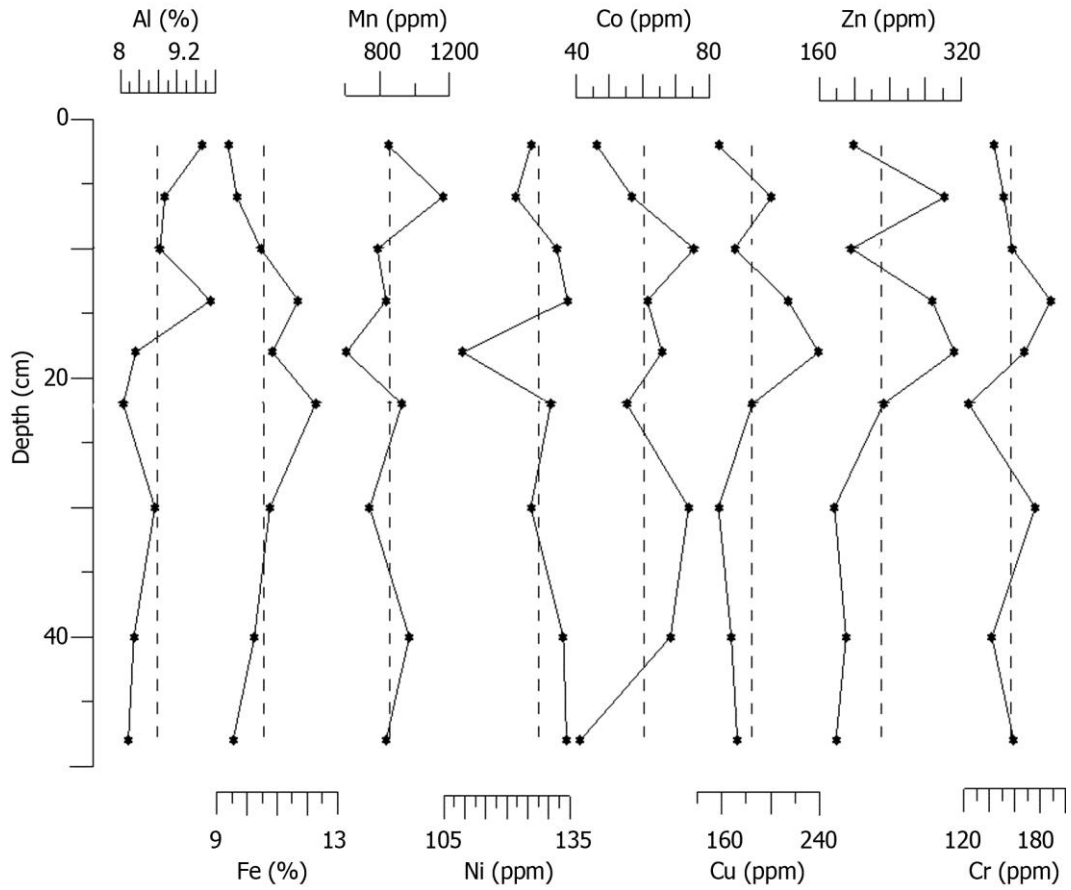

Fig. 3.1.9a Variation of metals in clay fraction with average line in sediment core VS-1

Vaghotan estuary

The concentration of Al, Fe and Mn in the clay fraction of the core VG-1 ranged from 8.03 % to 14.34 % (avg. 11.37 %), 3.91 % to 5.33 % (avg. 4.75 %) and 501 ppm to 1320 ppm (avg. 842 ppm) respectively (Table 3.1.4b).

Table 3.1.4b Range and average concentration of major metals in clay fraction in cores VS-1, VG-1, MD-1, S-1 and GP-1

Sediment core	Al (%)			Fe (%)			Mn (ppm)		
	Range		Avg	Range		Avg	Range		Avg
	Min	Max		Min	Max		Min	Max	
VS-1	8.06	9.90	8.77	9.37	12.27	10.54	605	1160	856
VG-1	8.03	14.34	11.37	3.91	5.33	4.75	501	1320	842
MD-1	6.14	9.95	7.94	3.02	6.17	4.37	344	2915	1368
S-1	6.24	9.67	8.06	2.55	4.94	4.01	219	393	263
GP-1	3.38	11.94	7.34	1.13	3.07	2.12	52	148	104

Table 3.1.4c Range and average concentration of trace metals in clay fraction in cores VS-1, VG-1, MD-1, S-1 and GP-1

Sediment core	Ni (ppm)			Co (ppm)			Cu (ppm)			Zn (ppm)			Cr (ppm)		
	Range		Avg	Range		Avg	Range		Avg	Range		Avg	Range		Avg
	Min	Max		Min	Max		Min	Max		Min	Max		Min	Max	
VS-1	110	135	128	41	75	60	157	240	185	178	313	231	124	188	157
VG-1	48	70	60	30	43	38	172	259	215	159	466	264	134	178	158
MD-1	55	95	67	20	39	27	146	263	208	222	374	294	178	278	207
S-1	53	94	70	21	40	28	140	511	212	190	1338	264	119	286	226
GP-1	26	64	46	10	22	18	120	367	239	193	372	281	73	319	191

Element distribution profile in the clay component of the core VG-1 is presented in the figure 3.1.9b. From bottom to around 30 cm, Al and Fe exhibited an overall increase, while Mn showed an increase from bottom to 50 cm which was followed by a gradual decrease up to 30 cm. Further, Al showed overall decreasing trend from 30 cm to the surface. Iron exhibited overall an increase from 30 to 6 cm which was followed by a decrease towards the surface, while Mn showed overall decrease from 30 to 22 cm and then increased towards the surface.

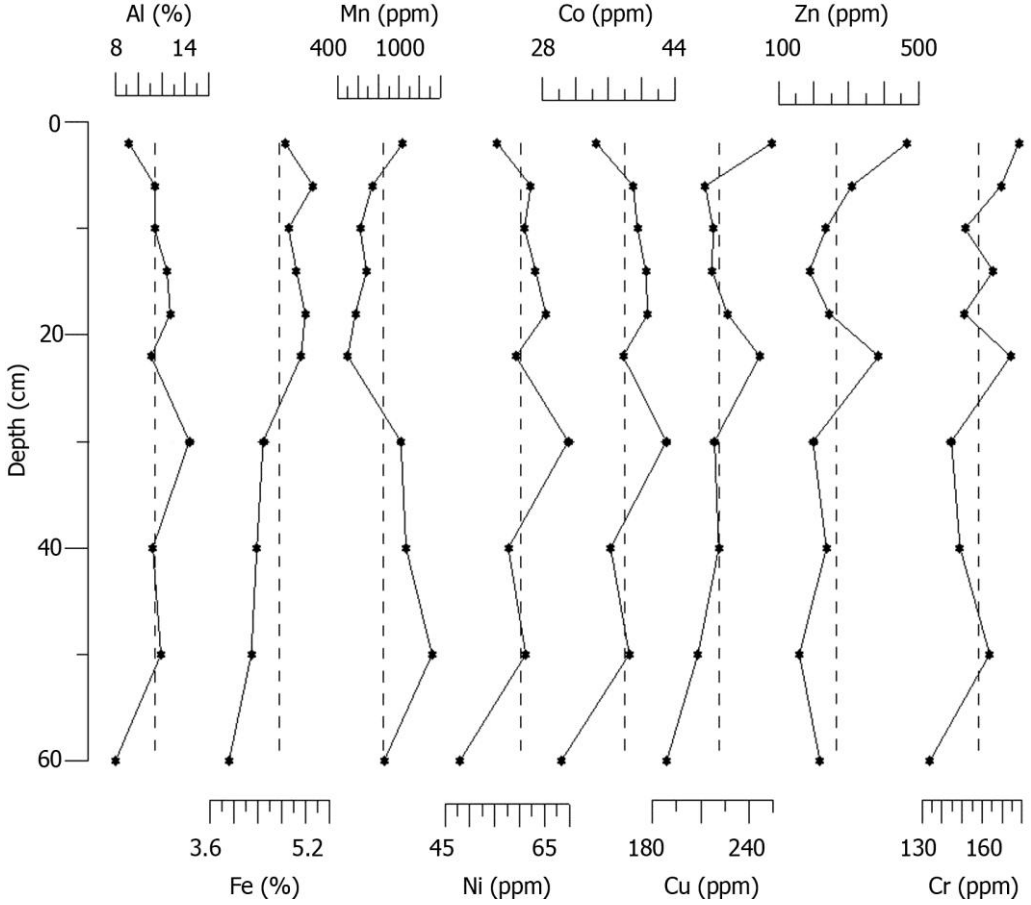

Fig. 3.1.9b Variation of metals in clay fraction with average line in sediment core VG-1

Mandovi estuary

In core MD-1, the concentration of Al, Fe and Mn in the clay fraction ranged from 6.14 % to 9.95 % (avg. 7.94 %), 3.02 % to 6.17 % (avg. 4.37 %) and 344 ppm to 2915 ppm (avg. 1368 ppm) respectively (Table 3.1.4b).

Element distribution profile in the clay component of the core MD-1 is presented in the figure 3.1.9c. From bottom to 40 cm, Al showed overall an increasing trend, while Fe exhibited decreasing trend. The concentration of Mn remained nearly constant from bottom to 40 cm.

Further, Al and Fe showed increasing peak at 30 cm between 40 and 22 cm. Manganese exhibited overall an increase from 40 to 22 cm. The concentration of Al and Fe decreased from 22 to 18 cm which was followed by nearly constant trend up to 6 cm. Further, they showed an increase towards the surface. Manganese showed decrease from 22 to 6 cm and further, increased towards the surface.

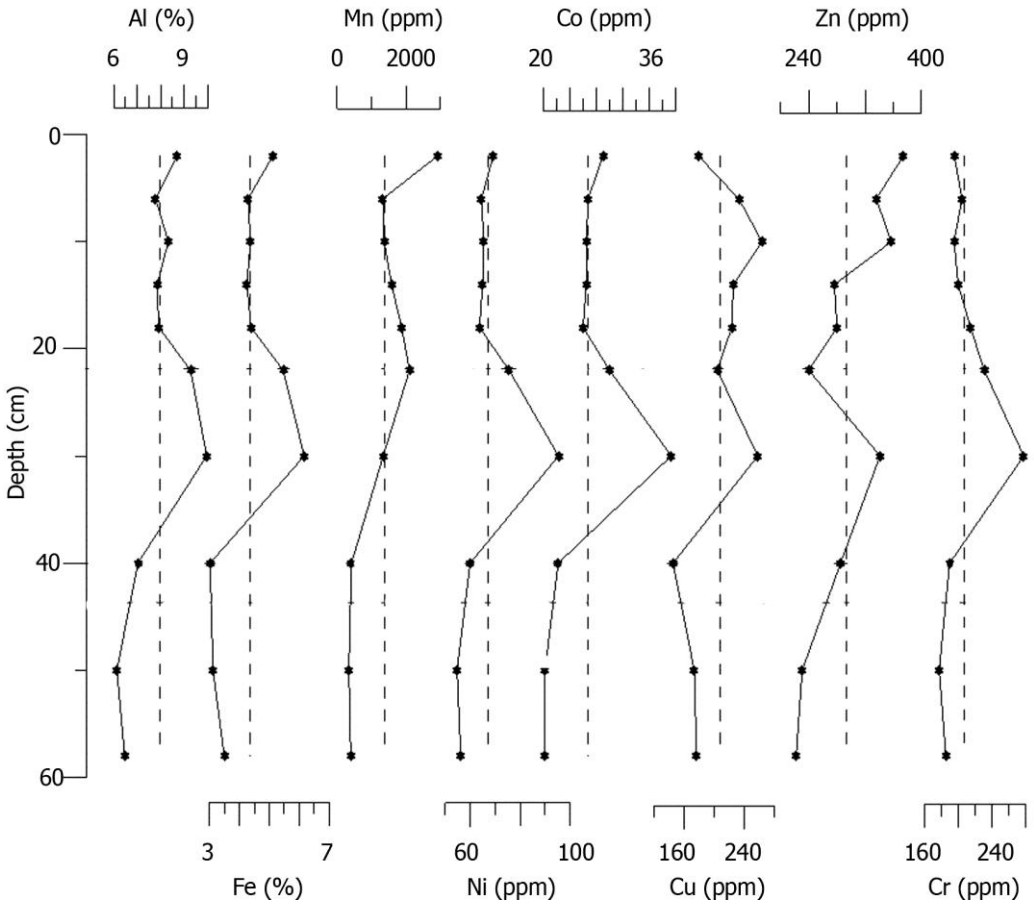

Fig. 3.1.9c Variation of metals in clay fraction with average line in sediment core MD-1

Sharavathi estuary

In this estuary (core S-1), concentration of Al, Fe and Mn in the clay fraction ranged from 6.24 % to 9.67 % (avg. 8.06 %), 2.55 % to 4.94 % (avg. 4.01 %) and 219 ppm to 393 ppm (avg. 263 ppm) respectively (Table 3.1.4b).

Distribution of metals in the clay component of the core S-1 is presented in the figure 3.1.9d. Metals viz. Al and Fe showed decreasing peak at 60 cm, while Mn exhibited overall an increase. Further, Al, Fe and Mn showed overall decrease from 50 to 30 cm. The concentration of Al and Fe showed overall increasing trend from 30 cm to surface of the core

S-1, while Mn exhibited fluctuating trend with overall decreasing trend towards the surface. At 18 cm, all the three metals showed negative peak and at 22 cm positive peak.

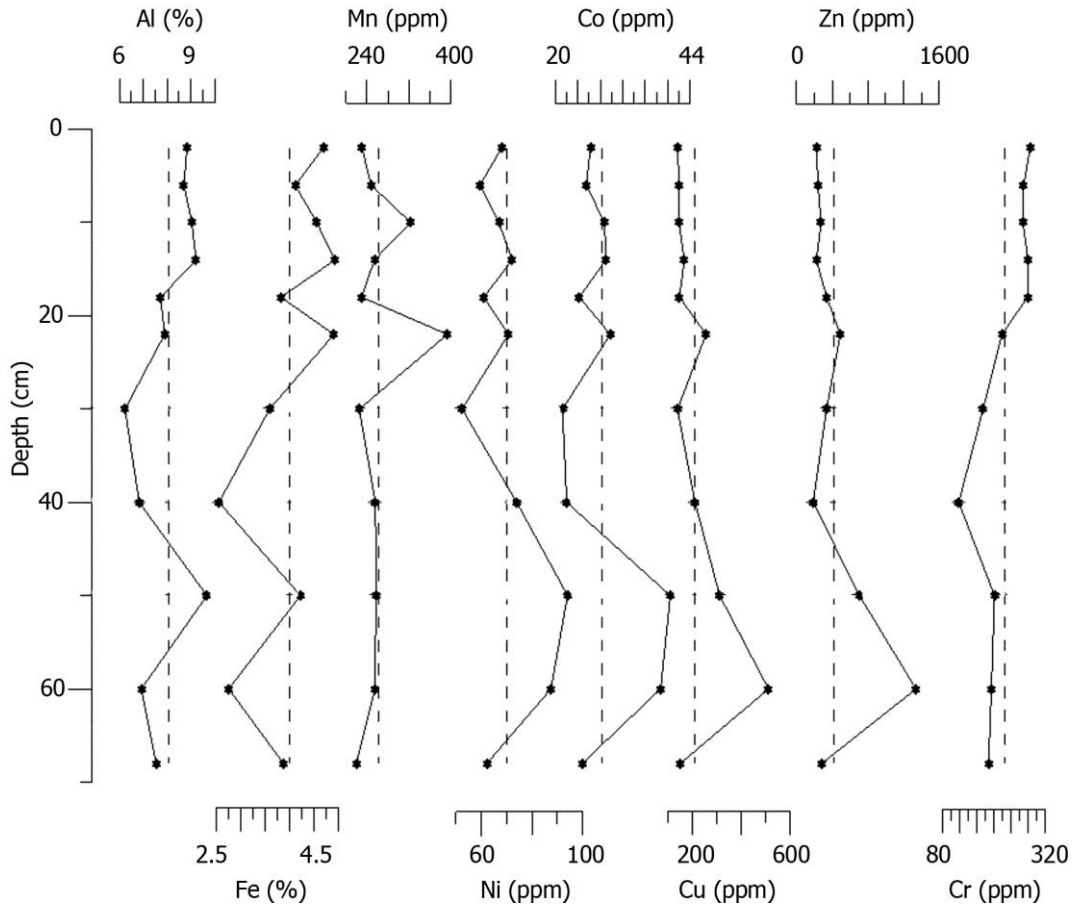

Fig. 3.1.9d Variation of metals in clay fraction with average line in sediment core S-1

Gurupur estuary

Metals viz. Al, Fe and Mn in clay fraction in the core GP-1 varied from 3.38 % to 11.94 % (avg. 7.34 %), 1.13 % to 3.07 % (avg. 2.12 %) and 52 ppm to 148 ppm (avg. 104 ppm) respectively (Table 3.1.4b).

Element distribution profile of clay component in the core GP-1 is presented in the figure 3.1.9e. Metals viz. Al and Fe showed overall increasing trend from bottom to 40 cm, while Mn, exhibited overall decreasing trend. From 40 to 22 cm, Al and Fe exhibited decreasing distribution pattern, whereas Mn showed increasing distribution pattern. Further, Al, Fe and Mn showed decrease from 22 to 18 cm. Thereafter, concentration of these metals increased towards the surface.

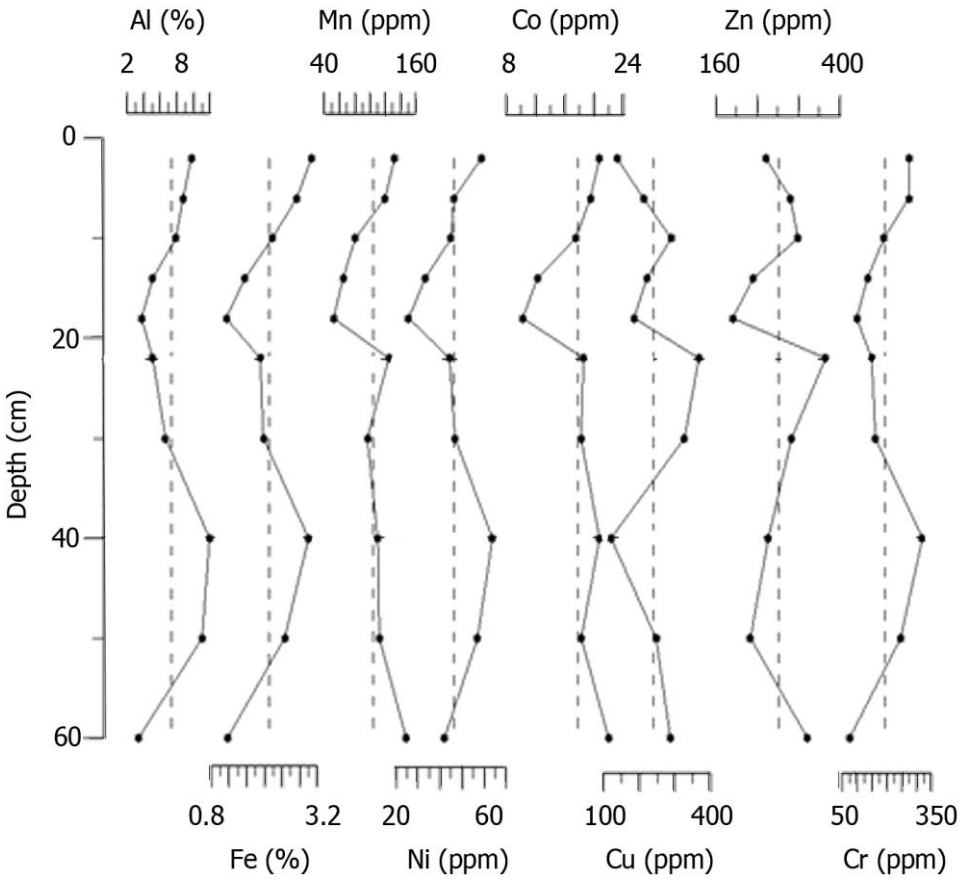

Fig. 3.1.9e Variation of metals in clay fraction with average line in core GP-1

Trace metals (Ni, Co, Cu, Zn and Cr)

Vashishti estuary

The concentration of Ni, Co, Cu, Zn and Cr in the clay fraction of the core VS-1 varied from 110 ppm to 135 ppm (avg. 128 ppm), 41 ppm to 75 ppm (avg. 60 ppm), 157 ppm to 240 ppm (avg. 185 ppm), 178 ppm to 313 ppm (avg. 231 ppm) and 124 ppm to 188 ppm (avg. 157 ppm) respectively (Table 3.1.4c).

Nickel showed decreasing trend from bottom to 30 cm which was followed by an increase up to 22 cm (Fig 3.1.9a). Metals viz. Cu and Zn exhibited overall increasing trend from bottom to around 22 cm, while Co and Cr showed similar distribution to that of Al. Nickel showed decreasing peak from 22 to 16 cm whereas other metals namely Cu, Co, Zn and Cr exhibited increasing peak in this part. Further, all the trace metals showed overall decrease towards the surface with Cu and Zn showing a positive peak at 6 cm depth, similar to Mn.

Vaghotan estuary

The concentration of Ni, Co, Cu, Zn and Cr in the clay fraction of the core VG-1 ranged from 48 ppm to 70 ppm (avg. 60 ppm), 30 ppm to 43 ppm (avg. 38 ppm), 172 ppm to 259 ppm (avg. 215 ppm), 159 ppm to 466 ppm (avg. 264 ppm) and 134 ppm to 178 ppm (avg. 158 ppm) respectively (Table 3.1.4c).

The distribution pattern of Ni and Co was largely similar to Al throughout the core VG-1 (Fig 3.1.9b). From bottom to around 30 cm, Cu exhibited overall an increase, while Zn showed slight fluctuations. Chromium showed an increase from bottom to 50 cm which was followed by a gradual decrease up to 30 cm, similar to Mn. Further, Cu, Zn and Cr showed sharp increase from 30 to 22 cm. From 22 to 6 cm, these trace metals showed increase with initial decrease. Increase towards surface was similar to that of Mn.

Mandovi estuary

In core MD-1, the concentration of Ni, Co, Cu, Zn and Cr in the clay fraction ranged from 55 ppm to 95 ppm (avg. 67 ppm), 20 ppm to 39 ppm (avg. 27 ppm), 146 ppm to 263 ppm (avg. 208 ppm), 222 ppm to 374 ppm (avg. 294 ppm) and 178 ppm to 278 ppm (avg. 207 ppm) respectively (Table 3.1.4c).

The concentration of Ni, Co and Cr remained nearly constant from bottom to 40 cm (Fig 3.1.9c). Copper exhibited decreasing trend, while Zn showed an overall increasing trend from bottom to 40 cm. All the trace metals showed increasing peak at 30 cm between 40 and 22 cm. The distribution of Ni and Co was similar to Al and Fe from 22 cm to surface. Zinc exhibited overall an increase from 22 cm to surface, whereas Cr showed decrease from 22 to 10 cm and maintained along average line up to 6 cm. Further, it showed a decreasing trend towards the surface. The concentration of Cu increased from 22 to 10 cm which was followed by a decreasing trend towards the surface.

Sharavathi estuary

In this estuary (core S-1), concentration of Ni, Co, Cu, Zn and Cr in the clay fraction ranged from 53 ppm to 94 ppm (avg. 70 ppm), 21 ppm to 40 ppm (avg. 28 ppm), 140 ppm to 511

ppm (avg. 212 ppm), 190 ppm to 1338 ppm (avg. 264 ppm) and 119 ppm to 286 ppm (avg. 226 ppm) respectively (Table 3.1.4c).

Metals viz. Ni, Co, Cu and Zn exhibited increasing peak at 60 cm, whereas concentration of Cr remained nearly constant (Fig 3.1.9d). Further, all the trace metals showed overall decrease from 50 to 30 cm. Metals viz. Ni, Co, Cu and Zn showed overall decrease from 30 cm to surface similar to Mn, while Cr exhibited overall increasing trend, similar to Al and Fe.

Gurupur estuary

Metals viz. Ni, Co, Cu, Zn and Cr in the clay fraction of the core GP-1 varied from 26 ppm to 64 ppm (avg. 46 ppm), 10 ppm to 22 ppm (avg. 18 ppm), 120 ppm to 367 ppm (avg. 239 ppm), 193 ppm to 372 ppm (avg. 281 ppm) and 73 ppm to 319 ppm (avg. 191 ppm) respectively (Table 3.1.4c).

Metals viz. Ni and Cr showed overall increasing trend from bottom to 40 cm, while Co, Cu and Zn exhibited overall decreasing trend (Fig 3.1.9e). From 40 to 22 cm, Ni, Co and Cr exhibited decreasing distribution pattern, whereas Cu and Zn showed increasing distribution pattern. Further, trace metals showed decrease from 22 to 18 cm. Thereafter, concentration of Ni, Co and Cr increased towards the surface, while Cu and Zn showed an increase from 18 to 10 cm which was followed by a decreasing trend towards the surface.

When the average values of major elements in the clay fraction of five estuaries were considered, Al was highest in the core VG-1, Fe in the core VS-1 and Mn in the core MD-1. All three elements were present in lowest concentration in the core GP-1.

With respect to trace metals in the clay fraction when five estuaries were compared highest value was recorded in the core VS-1 for Ni and Co. Core GP-1 showed highest value for Cu, while core MD-1 for Zn. Chromium was highest in the core S-1. Metals viz. Ni and Co exhibited lowest value in the core GP-1, while Cu, Zn and Cr in the core VS-1.

In the study area, clay minerals varied with a range for smectite from 4.67 % to 53.00 %, illite from 12.15% to 19.23 %, kaolinite from 25.63 % to 74.01 % and chlorite from 6.87 % to 21.13 % (Table 3.1.4a). When the data of clay minerals for five estuaries was compared it

revealed decrease in percentage of smectite from Vashishti to Gurupur estuary, while, there was overall increase in percentage of kaolinite from North towards the South in the study area (Fig 3.1.10). The systematic variation in percentage of these clay minerals can be attributed to change in source rocks from North to South in the catchment area of rivers studied, (as discussed earlier). Chauhan and Vogelsang (2006) stated that the difference in clay mineral assemblages within sediments of the estuaries indicates change in hinterland geology, drainage and climate, and source. The weathering of Deccan trap basalts (Parthasarathy, 2003) in arid to semi-arid climate must have led to the release of smectite in

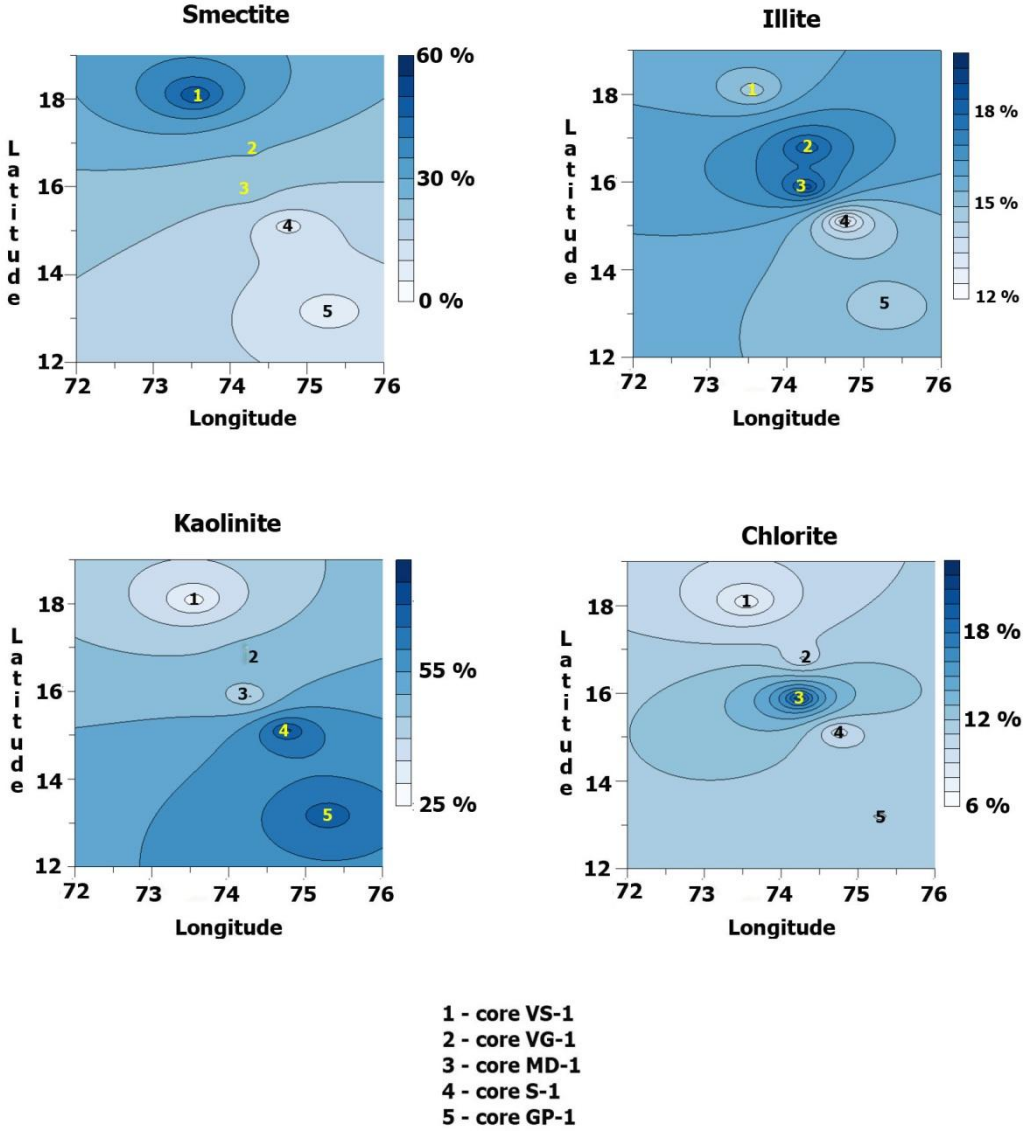

Fig 3.1.10 Distribution of clay minerals along the study area

sediments of the Vashisthi and Vaghotan estuaries. Rao and Rao (1995) have earlier reported presence of high smectite in the inner continental shelf off Ratnagiri-Goa along continental margins of India which they concluded of basaltic source. Further South, rock types vary

from meta-volcanic and meta-sedimentary rocks to granites and granite gneisses, as discussed earlier. The weathering of granites might have released more kaolinite. The present study also indicated presence of considerable amount of illite in estuaries along central west coast of India. Illite is generally transformed from smectite during the process of transportation. According to Eberl (1984) Al^{3+} ions substitute for Si^{4+} in the smectite tetrahedral sheets, thereby increasing the negative charge on smectite interlayers. Upon achieving critical layer charge, the interlayer potassium dehydrates expands smectite interlayers into non expanding illite interlayers. In addition, illite could also be formed by the weathering of non-layer silicate, such as feldspar from granites under moderate hydrolysis conditions, and by the degradation of micas (Fagel et al. 2003). The weathering of igneous and metamorphic rocks might have released chlorite as it is commonly found in igneous rocks as an alteration product of mafic minerals such as pyroxene, amphibole and biotite, and also associate with metamorphic rocks.

The processes such as size sorting during transport (Reddy et al. 1992), differential flocculation (Singer 1984), dispersal of clay minerals due to prevalence of regional and local currents, supply of sediment from multiple sources and organo-mineral interactions (Naidu et al. 1985) tend to affect distribution of clay minerals. These factors might have led to variations in concentration of clay minerals in cores VS-1, VG-1, S-1 and GP-1 with time.

Within the study area, major metals in the clay component varied with a range for Al from 7.34 % to 11.37 %, Fe from 2.12 % to 10.54 % and Mn from 104 ppm to 1368 ppm, while trace metals varied with a range for Ni from 46 ppm to 128 ppm, Co from 18 ppm to 60 ppm, Cu from 185 ppm to 239 ppm, Zn from 231 ppm to 294 ppm and Cr from 157 ppm to 226 ppm (Table 3.1.4b and c). Among these metals, only Fe, Ni and Co showed overall decrease from North to South along central west coast of India (Fig. 3.1.11a and b), similar to clay, while rest of the metals exhibited fluctuating distribution pattern.

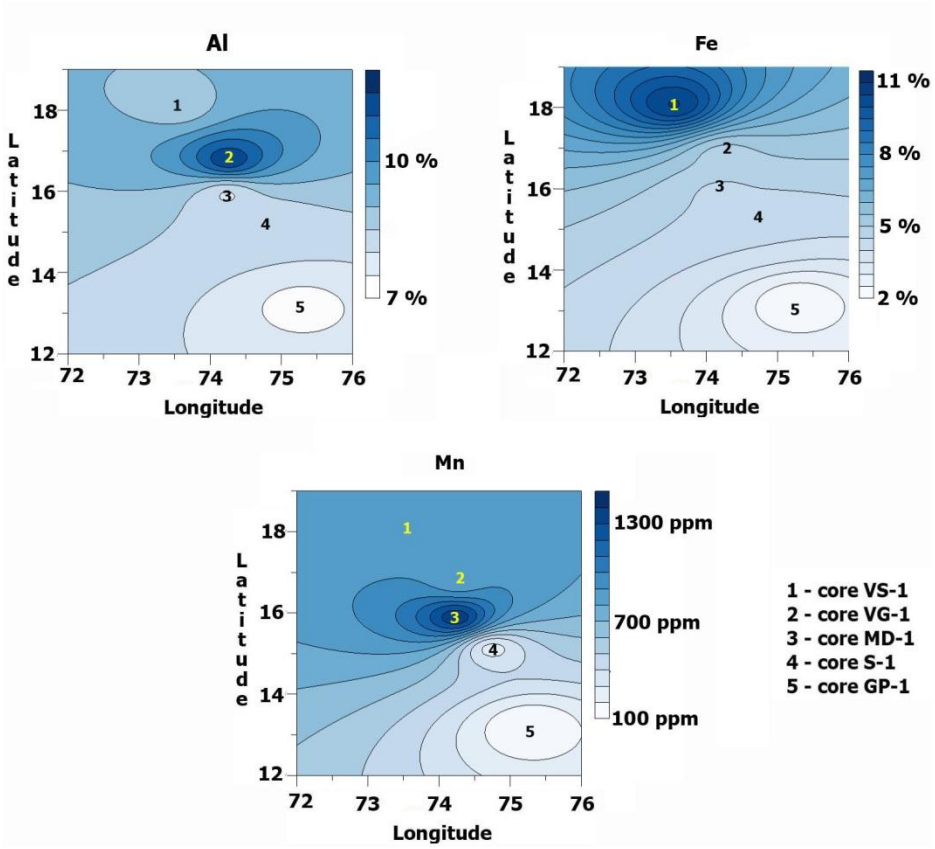

Fig 3.1.11a Distribution of major metals in the clay fraction along the study area

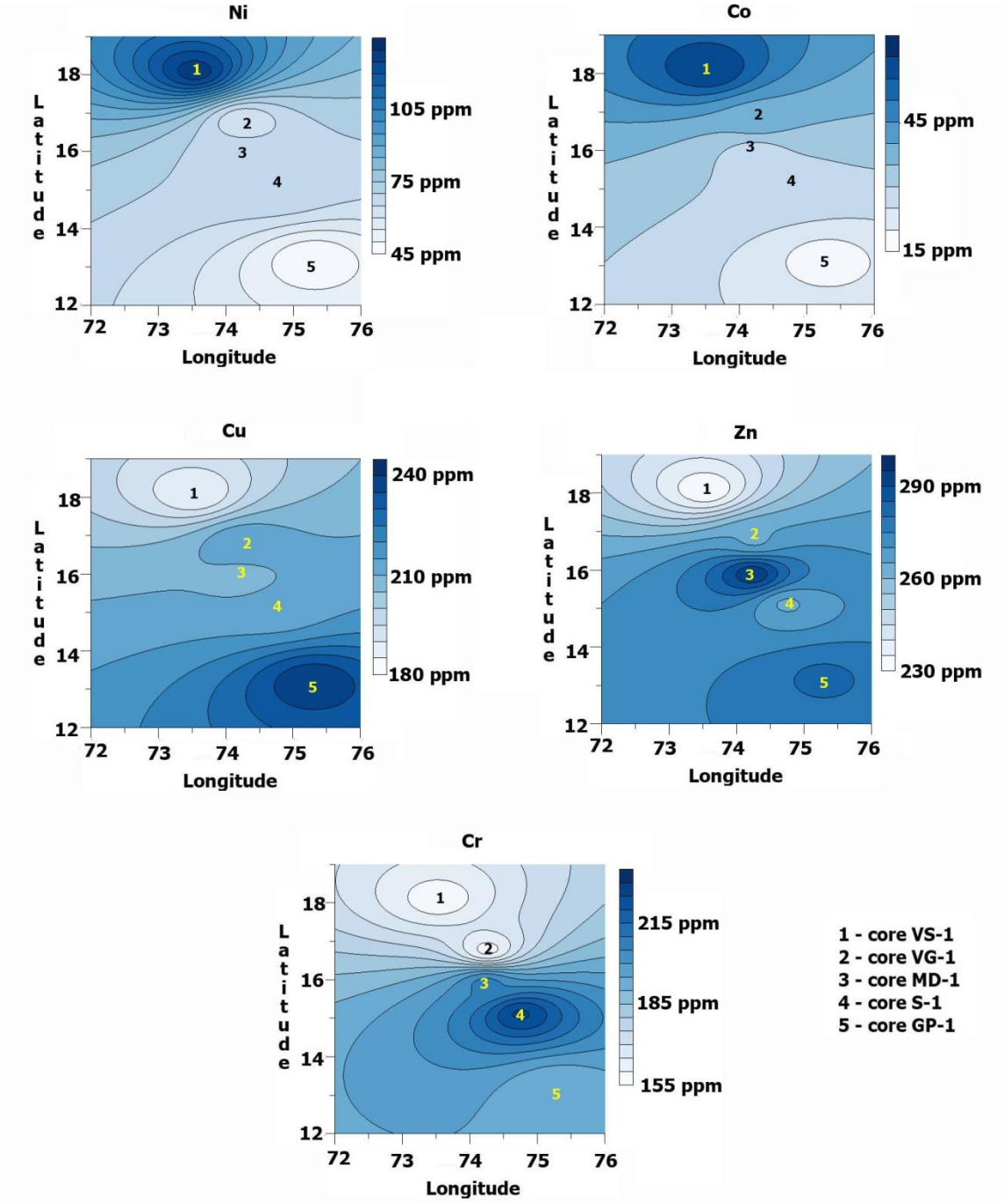

Fig 3.1.11b Distribution of trace metals in the clay fraction along the study area

Pearson's correlation analysis results of the core VS-1 showed significant correlation of smectite with Mn; and of chlorite with Al and Cr (Table 3.1.5a). Among the metals, Cu and Zn exhibited significant correlation with each other.

Table 3.1.5a Correlation between clay minerals and metals in clay fraction incore VS-1 (n=9). Values in bold indicates significant correlation at $p<0.05$

	Smectite (%)	Illite (%)	Kaolinite (%)	Chlorite (%)	Al (%)	Fe (%)	Mn (ppm)	Ni (ppm)	Co (ppm)	Cu (ppm)	Zn (ppm)	Cr (ppm)
Smectite (%)	1.00											
Illite (%)	**-0.78**	1.00										
Kaolinite (%)	-0.61	**0.87**	1.00									
Chlorite (%)	-0.35	-0.01	-0.07	1.00								
Al (%)	0.12	-0.30	-0.22	**0.77**	1.00							
Fe (%)	-0.28	0.06	0.01	-0.23	-0.11	1.00						
Mn (ppm)	**0.95**	**-0.74**	**-0.71**	-0.39	0.05	-0.22	1.00					
Ni (ppm)	0.36	**-0.80**	**-0.75**	0.16	0.11	0.08	0.34	1.00				
Co (ppm)	-0.29	0.35	0.34	0.03	-0.06	0.35	-0.27	-0.13	1.00			
Cu (ppm)	-0.41	0.49	0.14	0.02	0.00	0.37	-0.19	-0.56	0.06	1.00		
Zn (ppm)	-0.11	0.30	0.02	-0.01	0.19	0.29	0.08	-0.58	0.03	**0.93**	1.00	
Cr (ppm)	-0.48	0.20	0.05	**0.71**	0.44	0.06	-0.47	-0.10	0.32	0.34	0.24	1.00

Similar distribution of Cu and Zn throughout the core VS-1 and significant correlation among themselves indicated their association with each other. The significant correlation of smectite with Mn, and chlorite with Al and Cr suggested adsorption of these trace metals onto respective clay minerals or substitute into the lattice structure of clay minerals. Prost and Yaron (2001) stated that clay minerals readily interact with almost all soil contaminants. Further, clay minerals provide binding surfaces for metals in sediment, because of their adsorptive properties (Essa and Faragallah 2006). In core VS-1, the decreasing peak of Co, Cu, Zn and Cr at 18 cm contrasting with increasing peak of major metals indicated that major metals did not involve in regulating distribution of these trace metals between 22 and 10 cm. However, an increasing peak of Cu and Zn, similar to Mn at 6 cm suggested role of Mn oxide and decrease near surface of Co, Cu, Zn and Cr similar to Fe and Mn indicated role of Fe-Mn oxide in distribution of these trace metals in the recent years.

In core VG-1, smectite showed significant correlation with Zn (Table 3.1.5b). Among the metals, Al showed significant correlation with Ni and Co. Metals viz. Ni with Co; Cu with Zn and Cr; and Zn with Cr also exhibited significant correlation.

The similar distribution of Ni and Co to Al in the VG-1 indicated association of these trace metals with Al. The significant correlation of Ni and Co with Al further supported their association. Volvoikar and Nayak (2013a) stated that clay-sized fraction of sediments represents stable weathering product or strong erosion of source rocks and mainly holds metals within lattice structure of alumino-silicate minerals. Alternatively, trace metals may be adsorbed to clay minerals. Among the trace metals, Cu, Zn and Cr showed similar

distribution from 30 cm to surface and agreed largely with the distribution of Mn. Further, significant correlation among them indicated that these metals might have similar sources or enrichment mechanism in the recent years.

Table 3.1.5b Correlation between clay minerals and metals in clay fraction incore VG-1 (n=10). Values in bold indicates significant correlation at p<0.05

	Smectite (%)	Illite (%)	Kaolinite (%)	Chlorite (%)	Al (%)	Fe (%)	Mn (ppm)	Ni (ppm)	Co (ppm)	Cu (ppm)	Zn (ppm)	Cr (ppm)
Smectite (%)	1.00											
Illite (%)	0.03	1.00										
Kaolinite (%)	**-0.89**	-0.36	1.00									
Chlorite (%)	-0.57	-0.61	0.53	1.00								
Al (%)	-0.51	0.28	0.27	0.27	1.00							
Fe (%)	0.23	0.34	-0.30	-0.38	0.33	1.00						
Mn (ppm)	-0.45	0.13	0.37	0.13	-0.04	**-0.67**	1.00					
Ni (ppm)	-0.40	0.40	0.17	0.08	**0.97**	0.48	-0.10	1.00				
Co (ppm)	-0.37	0.38	0.16	0.05	**0.96**	0.53	-0.18	**0.99**	1.00			
Cu (ppm)	0.44	0.57	**-0.72**	-0.33	0.06	0.55	-0.19	0.18	0.17	1.00		
Zn (ppm)	**0.72**	0.29	**-0.77**	-0.49	-0.44	0.43	-0.23	-0.28	-0.31	**0.80**	1.00	
Cr (ppm)	0.22	0.58	-0.34	-0.55	-0.02	0.63	-0.08	0.12	0.14	**0.71**	**0.65**	1.00

In core MD-1, correlation results showed significant correlation of Al with Fe, Mn, Ni, Co and Cr; and Fe with Mn, Ni, Co and Cr (Table 3.1.5c). Metals viz. Ni with Co and Cr; and Co with Cr also exhibited significant correlation.

Table 3.1.5c Correlation between metals in clay fraction incore MD-1 (n=10). Values in bold indicates significant correlation at p<0.05

	Al (%)	Fe (%)	Mn (ppm)	Ni (ppm)	Co (ppm)	Cu (ppm)	Zn (ppm)	Cr (ppm)
Al (%)	1.00							
Fe (%)	**0.96**	1.00						
Mn (ppm)	**0.70**	**0.71**	1.00					
Ni (ppm)	**0.92**	**0.91**	0.42	1.00				
Co (ppm)	**0.95**	**0.94**	0.54	**0.98**	1.00			
Cu (ppm)	0.61	0.61	0.30	0.56	0.63	1.00		
Zn (ppm)	0.56	0.48	0.52	0.44	0.55	0.48	1.00	
Cr (ppm)	**0.84**	**0.85**	0.31	**0.96**	**0.93**	0.57	0.27	1.00

In Mandovi estuary (core MD-1), from bottom to 40 cm similar distribution was observed among Al and Zn; Fe and Cu; and Mn, Ni, Co and Cr. Further, from 40 to 22 cm except Mn, major as well as trace metals showed increasing peak suggesting adsorption of trace metals onto Fe oxide in this section of the core MD-1. Also, from 22 cm to surface except Cu, Cr and Zn, rest of the metals were nearly similar in their distribution. Therefore, the vertical distribution of metals suggested change in their association along the length of the core MD-1. Trace metals get readily adsorbed onto Fe-Mn oxyhydroxides. However, stability of Fe

oxyhydroxides under mild reducing conditions is higher, and faster oxidation kinetics of Fe^{+2} compared to Mn^{+2} occasionally leads to diagenetic enrichment of Fe as compared to diagenetic Mn enrichment (Zwolsman et al. 1993). Such phenomenon can lead to change in trace metal association with time. The correlation results showed significant correlation of Mn, Ni, Co and Cr with Fe indicating role of Fe oxide in distribution of metals.

The correlation results of the core S-1 exhibited, significant correlation of smectite with illite; illite with Ni, Cu and Zn; and kaolinite with Fe and Cr (Table 3.1.5d). Among the metals, Al showed significant correlation with Fe and Cr; while Fe with Cr. All the metals, except Cr exhibited significant correlation among themselves.

Table 3.1.5d Correlation between clay minerals and metals in clay fraction incore S-1 (n=11). Values in bold indicates significant correlation at $p<0.05$

	Smectite (%)	Illite (%)	Kaolinite (%)	Chlorite (%)	Al (%)	Fe (%)	Mn (ppm)	Ni (ppm)	Co (ppm)	Cu (ppm)	Zn (ppm)	Cr (ppm)
Smectite (%)	1.00											
Illite (%)	**0.64**	1.00										
Kaolinite (%)	**-0.83**	**-0.85**	1.00									
Chlorite (%)	-0.28	**-0.63**	0.19	1.00								
Al (%)	-0.28	-0.39	0.37	0.19	1.00							
Fe (%)	**-0.61**	**-0.78**	**0.79**	0.32	**0.73**	1.00						
Mn (ppm)	-0.09	-0.17	0.19	-0.01	0.18	0.40	1.00					
Ni (ppm)	0.39	**0.68**	-0.59	-0.37	0.32	-0.14	0.18	1.00				
Co (ppm)	0.00	0.52	-0.23	-0.48	0.42	0.07	0.24	**0.89**	1.00			
Cu (ppm)	0.20	**0.81**	-0.56	-0.53	-0.17	-0.43	0.17	**0.79**	**0.79**	1.00		
Zn (ppm)	0.02	**0.75**	-0.38	**-0.62**	-0.19	-0.38	0.09	**0.67**	**0.79**	**0.96**	1.00	
Cr (ppm)	**-0.78**	**-0.69**	**0.77**	0.33	**0.66**	**0.73**	0.05	-0.22	0.04	-0.35	-0.23	1.00

The nearly similar distribution pattern of Al, Fe and Cr in the core S-1 indicated adsorption of Cr onto Fe oxides. The significant correlation among these metals further supported the same. Metals viz. Ni, Co, Cu and Zn showed similar distribution pattern and significant correlation among themselves indicated their close association with each other or similar enrichment mechanism. The significant correlation of illite with Ni, Cu and Zn indicated role of illite in their distribution. Further, significant correlation between smectite and illite supported the clay mineral modification from smectite to illite. Manganese oxide did not seem to regulate the distribution of metals in the clay component of the Sharavathi estuary. Kaolinite showed significant correlation with Fe and Cr supporting their terrigenous source.

In core GP-1, correlation analysis results showed significant correlation of kaolinite with Mn, Ni and Co; and chlorite with Ni (Table 3.1.5e). Among the metals, Al exhibited significant

correlation with Fe, Ni and Cr while, Fe with Ni and Cr. Manganese showed significant correlation with Co. Metals viz. Ni with Co and Cr; and Cu with Zn also showed significant correlation.

Table 3.1.5e Correlation between clay minerals and metals in clay fraction in core GP-1 (n=10). Values in bold indicates significant correlation at $p<0.05$

	Smectite (%)	Illite (%)	Kaolinite (%)	Chlorite (%)	Al (%)	Fe (%)	Mn (ppm)	Ni (ppm)	Co (ppm)	Cu (ppm)	Zn (ppm)	Cr (ppm)
Smectite (%)	1.00											
Illite (%)	0.28	1.00										
Kaolinite (%)	0.22	-0.49	1.00									
Chlorite (%)	-0.34	**-0.70**	**0.67**	1.00								
Al (%)	-0.34	-0.29	0.57	0.42	1.00							
Fe (%)	-0.12	-0.14	0.63	0.30	**0.92**	1.00						
Mn (ppm)	-0.01	-0.58	**0.73**	0.55	0.24	0.37	1.00					
Ni (ppm)	-0.29	-0.56	**0.74**	**0.64**	**0.87**	**0.86**	0.61	1.00				
Co (ppm)	-0.13	**-0.66**	**0.69**	0.52	0.44	0.54	**0.92**	**0.78**	1.00			
Cu (ppm)	-0.16	-0.22	-0.47	-0.20	-0.50	-0.47	0.11	-0.29	0.05	1.00		
Zn (ppm)	0.08	-0.36	0.06	0.01	-0.21	-0.01	0.58	0.13	0.60	**0.69**	1.00	
Cr (ppm)	-0.17	-0.16	0.62	0.35	**0.96**	**0.98**	0.28	**0.83**	0.45	-0.56	-0.14	1.00

In core GP-1, distribution pattern of Al, Fe, Ni and Cr was similar to each other indicating role of Fe oxide in distribution of Ni and Cr. The result of correlation analysis supported the same. Manganese seemed to regulate the distribution of Co. All the metals except Cu and Zn, showed an increase towards the surface indicating higher addition of clay bound metals in the recent years. Metals viz. Cu and Zn showed significant correlation between each other indicating they are derived from the similar source. Among the clay minerals, kaolinite showed significant correlation with Mn, Ni and Co, while chlorite with Ni suggesting their adsorption onto respective clay minerals or their substitution within clay lattice structure.

Further, in order to understand difference in clay minerals and metals concentration in the clay fraction among the cores, the data was plotted on the isocon diagram (Fig.3.1.12). On comparison of core VS-1 with core VG-1, smectite, Fe, Ni and Co were higher in the core VS-1, while illite, kaolinite, chlorite, Al, Cu and Zn were higher in the core VG-1. Manganese was slightly higher in the core VS-1, whereas Cr was nearly equal in both the cores. The comparison of cores VS-1 and MD-1 indicated higher smectite, Al, Fe, Co and Ni in the core VS-1, while illite, kaolinite, chlorite, Mn, Zn, Cr and Cu in the core MD-1. Between cores VS-1 and S-1, illite, smectite, Al, Fe, Mn, Ni and Co were higher in the core VS-1, whereas kaolinite, chlorite, Zn, Cr and Cu in the core S-1. Further, between cores VS-1 and GP-1, smectite, Al, Fe, Mn, Ni and Co were higher in the core VS-1, while kaolinite,

chlorite, Zn, Cr and Cu in the core GP-1. Illite had equal concentration in both the cores. On comparison of cores VG-1 and MD-1, smectite, kaolinite, Al and Co were higher in the core

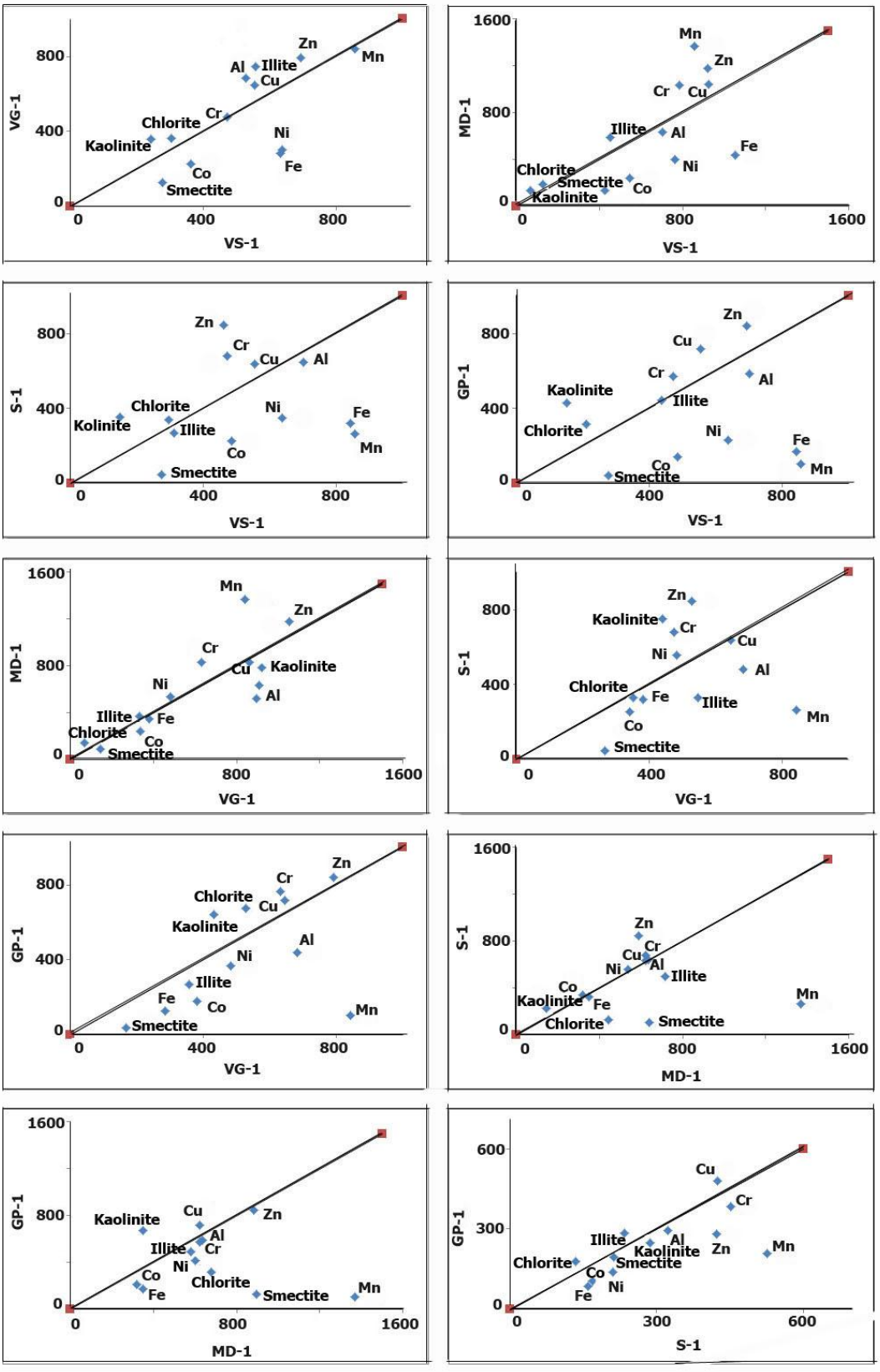

Fig. 3.1.12 Isocon plots for clay minerals and metals in the clay fraction

VG-1, while chlorite, Zn, Cr and Mn in the core MD-1. The concentration of Fe and Cu was slightly higher in the core VG-1, while that of illite and Ni in the core MD-1. Among cores VG-1 and S-1, illite, smectite, Al, Fe, Mn and Co were higher in the core VG-1, while kaolinite, Ni, Cr and Zn in the core S-1. Chlorite and Cu were slightly higher in the core VG-1. Between cores VG-1 and GP-1, illite, smectite, Al, Fe, Mn, Ni and Co were higher in the core VG-1, whereas kaolinite, chlorite, Cu, Zn and Cr in the core GP-1. Further, on comparison of cores MD-1 and S-1, illite, chlorite, smectite, Mn was higher in the core MD-1 while, kaolinite and Zn in the core S-1. Chromium was slightly higher in the core S-1, whereas concentration of Co, Ni, Fe, Cu and Al was nearly equal in both the cores. Similarly among cores MD-1 and GP-1, illite, chlorite, smectite, Fe, Mn, Ni and Co were higher in the core MD-1 while, kaolinite and Cu in the core GP-1. Al, Zn and Cr had slightly higher concentration in the core MD-1. Further, between cores S-1 and GP-1, kaolinite was higher in the core S-1, while illite and chlorite in the core GP-1. Smectite was slightly higher in the core S-1. Among the metals, except Cu, rest all the metals were higher in the core S-1.

From the above described results it was clear that on comparison of core VS-1 with cores S-1 and GP-1 most of the metals were present in higher concentration in the core VS-1. Also, most of the metals exhibited higher concentration in the core VG-1 in comparison to cores S-1 and GP-1. Basalts in the catchment area of Vashishti and Vaghotan estuaries might have contributed higher concentration of metals. Further, in cores collected from Vashishti and Vaghotan estuaries percentage of sand was less than 15 % and that of clay was more than 50 % in the bulk sediments (Table 3.1.1a). On the other hand, sand was more than 60 % and clay was less than 20 % in the bulk sediments of Sharavathi and Gurupur estuaries. This suggested that due to less concentration of clay in Sharavathi and Gurupur estuaries there was larger competition among the metals for absorption sites onto clay size particles than in case of Vashishti and Vaghotan estuaries wherein comparatively sufficient clay size particles were available for the adsorption of metals. Trace metals compete with each other for adsorption sites (McLean and Bledsoe 1992). The difference in clay percentage seemed to have also resulted higher concentration of metals in the Mandovi estuary than the Gurupur estuary. Further, some of the metals were higher in the core MD-1 in comparison to cores VS-1 and VG-1. Also, most of the metals were present in higher concentration in the core S-1 in comparison to cores MD-1 and GP-1.

The average concentration of metals in the bulk sediments for the samples considered for the clay fraction in sediment cores is presented in the Table 3.1.6. Further, when isocon plots of metals in clay fraction and bulk sediments were plotted (Fig 3.1.13), Fe, Mn, Cu and Zn were noted to be higher in the bulk sediments, while rest of the metals were higher in the clay component of the core VS-1. In case of the core VG-1, Fe, Mn, Ni, Co and Cu showed higher average value in the bulk sediments, while Al, Zn and Cr were present in higher average concentration in the clay fraction. In Mandovi estuary (core MD-1), all the metals were present in higher concentration in the clay fraction than the bulk sediments. Among the metals, only Zn showed higher average concentration in the bulk sediments than the clay fraction in the core S-1. In case of the Gurupur estuary (core GP-1), Fe and Zn had higher average concentration in the bulk sediments than the clay fraction, while Al, Ni, Co, Cu and Cr were present in higher average concentration in the clay fraction. Mn showed equal average concentration in bulk sediments and clay fraction in the core GP-1.

Table 3.1.6 Average concentration of metals in the bulk sediments for the samples considered for the clay fraction in sediment cores VS-1, VG-1, MD-1, S-1 and GP-1

	Al (%)	Fe (%)	Mn (ppm)	Ni (ppm)	Co (ppm)	Cu (ppm)	Zn (ppm)	Cr (ppm)
VS-1	8.69	12.01	1061	69	50	277	361	147
VG-1	10.20	13.33	1337	125	84	482	101	106
MD-1	5.02	3.49	731	41	17	22	254	62
S-1	5.36	2.19	126	35	8	15	687	43
GP-1	5.65	3.03	104	37	7	11	720	80

The variation in metal concentration between clay fraction and bulk sediments in the tropical estuaries was attributed to complexity in the admixture of sediment particles and non clastic chemical phases of the estuarine sediments (Padmalal and Seralathan 1995). The association of metals with sediment fractions showed systematic variation. In the Northern part of the study area (Vashishti and Vaghotan estuaries), metals were significantly associated with clay as well as bulk sediments. On the other hand, in middle and lower portion of the study area (Mandovi, Sharavathi and Gurupur estuaries), metals were largely associated with the clay fraction of the sediment. Clay minerals and clay size particles tend to adsorb metal (Liaghati et al. 2003) and therefore metals were associated with clay in all studied tropical estuaries. Higher Zn in Sharavathi and Gurupur estuaries must be from some other source may be anthropogenic. More Fe in the bulk sediments of the Gurupur estuary might be due to

magnetite mining in the catchment area. However, metals were significantly associated with bulk sediments in Vashishti and Vaghotan estuaries which were attributed to the catchment area geology. As discussed earlier, catchment area of Vashishti and Vaghotan estuaries consists of basalts containing olivine, pyroxene, calcium plagioclase and amphibole minerals, whereas catchment area of Mandovi, Sharavathi and Gurupur estuaries varies from meta-volcanic and meta-sedimentary rocks to granites and granite gneisses containing quartz and feldspar. These minerals are present in coarser sand and silt particles in addition to clay size particles. In comparison to quartz and feldspar; olivine, pyroxene and amphibole consist of higher Fe, Mg, Mn and other trace metals, which must be contributing additional metal input to the bulk sediments of Vashishti and Vaghotan estuaries.

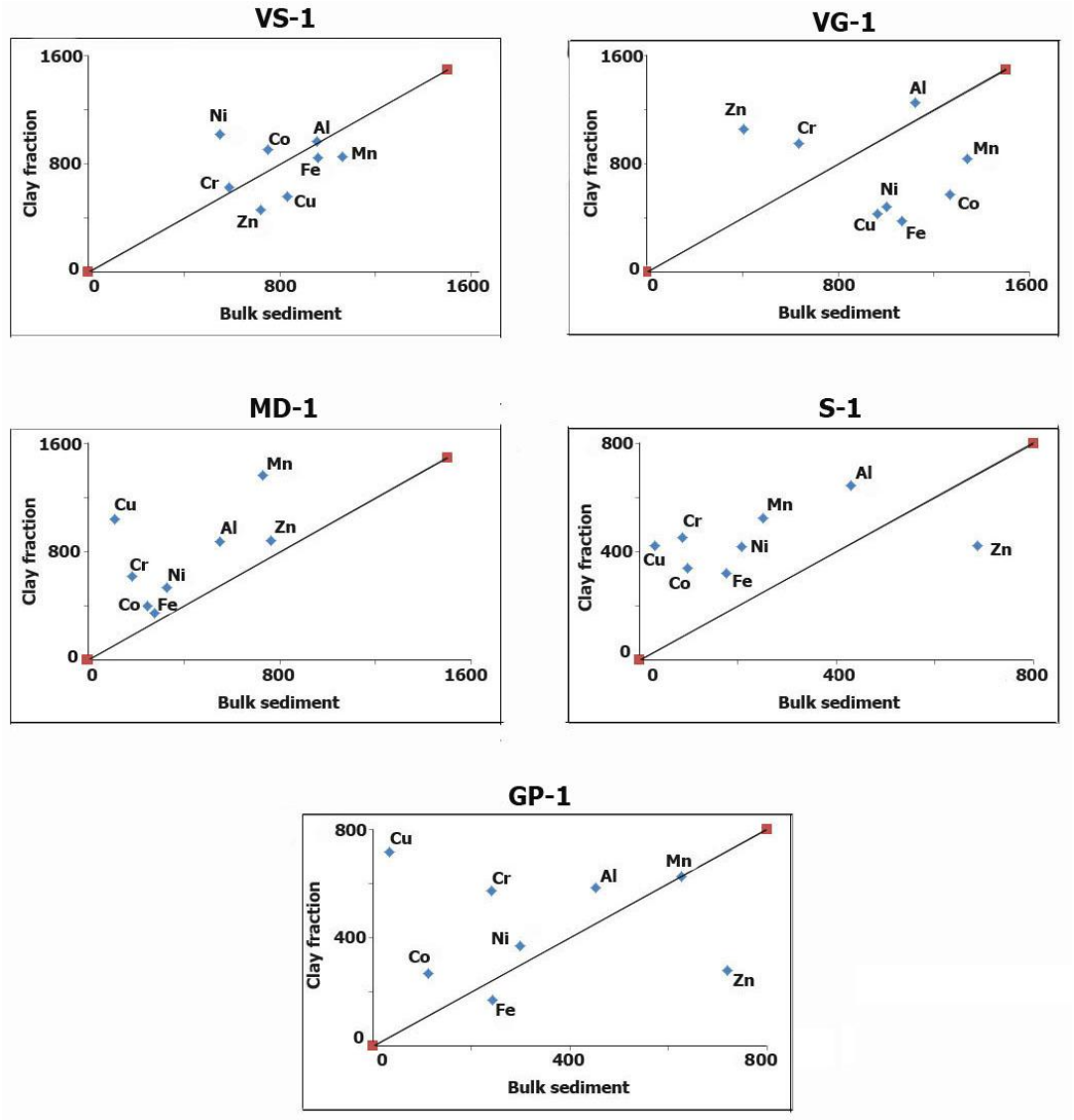

Fig. 3.1.13 Isocon plots for metals in cores VS-1, VG-1, MD-1, S-1 and GP-1

3.1.7 Speciation of elements

The speciation analysis of selected elements whose average value in the bulk sediments exceeded the global average shale value was carried out. The range and average concentration of Fe, Mn, Ni, Co, Cu, Zn and Cr in different fractions in cores VS-1 and VG-1, along with Zn in cores MD-1, S-1 and GP-1 are given in the Table 3.1.7. In order to understand the variations in elemental concentration with depth in different fractions in these cores the chemical partitioning of metals is diagrammatically represented in Figure 3.1.14.

Vashishti estuary

In core VS-1, except Mn all the studied metals were associated with more than 65 % in the residual fraction. Metals viz. Fe and Zn showed least concentration in the exchangeable fraction compared to other fractions, whereas, Ni, Co, Cu and Cr were present in least concentration in the carbonate fraction. Manganese was highest in the Fe-Mn oxide fraction, while showed least concentration in the organic fraction. Next to the residual fraction, Fe, Zn and Co were associated with the Fe-Mn oxide fraction and Cu, Cr and Ni in the organic bound fraction, followed by the Fe/Mn oxide fraction. Manganese was also present in significant concentration in exchangeable and carbonate bound fractions.

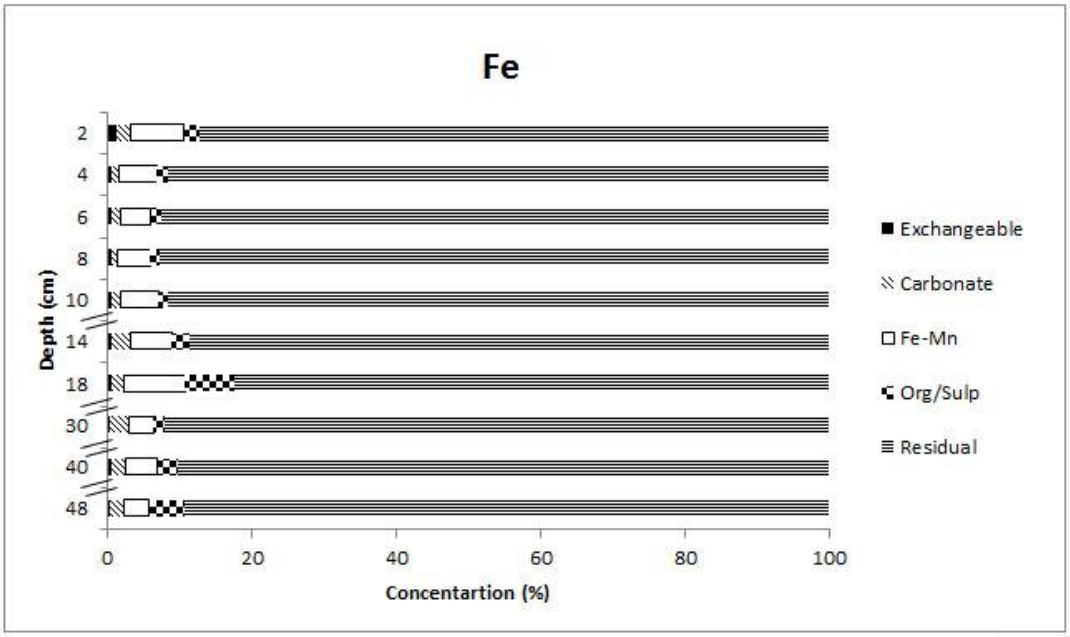

Fig. 3.1.14a Variation of Fe associated with different fractions in core VS-1.

Table 3.1.7 Range and average concentration of Fe, Mn, Ni, Co, Cu, Zn and Cr in different fractions of cores VS-1, VG-1, S-1, MD-1 and GP-1.

VS-1	Exchangeable		Carbonate		Fe-Mn		Organic/Sulphide		Residual	
	Range	Average	Range	Average	Range	Average	Range	Average	Range	Average
Fe (%)	0.31-1.06	0.46	0.86-2.71	1.74	3.28-8.36	5.23	1.27-6.83	2.63	82.56-92.90	89.94
Mn (%)	2.69-16.01	5.82	6.43-15.87	11.34	29.16-55.12	41.71	3.49-7.75	5.56	23.25-45.68	35.57
Ni (%)	3.30-4.01	3.65	2.04-3.11	2.36	3.32-4.60	4.12	5.21-8.14	6.01	81.61-85.47	83.86
Co (%)	5.87-7.50	6.64	3.67-5.96	4.54	10.80-15.24	13.28	6.23-12.12	8.60	63.95-72.62	66.94
Cu (%)	0.19-0.66	0.35	0.05-0.62	0.34	0.95-2.99	1.92	12.87-27.84	18.58	69.07-83.68	78.82
Zn (%)	1.86-5.42	3.50	3.69-9.13	5.46	14.84-18.85	16.80	5.73-10.72	7.33	59.48-70.39	66.91
Cr (%)	0.93-2.13	1.40	0.06-0.35	0.17	2.95-4.84	3.86	5.77-10.25	7.60	82.55-89.01	86.98

VG-1	Exchangeable		Carbonate		Fe-Mn		Organic/Sulphide		Residual	
	Range	Average	Range	Average	Range	Average	Range	Average	Range	Average
Fe (%)	0.002-0.003	0.002	0.001-0.002	0.002	1.29-2.31	1.71	1.08-1.73	1.33	96.13-97.45	96.96
Mn (%)	1.35-9.95	5.02	2.19-9.07	5.90	8.61-24.29	15.47	2.95-7.33	5.13	55.49-81.65	68.49
Ni (%)	1.33-2.13	1.71	2.24-3.34	2.72	1.98-3.54	2.77	3.27-4.39	3.81	86.92-90.81	88.99
Co (%)	0.34-0.59	0.43	0.44-0.89	0.65	1.37-2.54	1.75	0.98-1.86	1.34	94.11-96.71	95.83
Cu (%)	0.05-1.16	0.39	0.57-4.26	2.42	0.31-1.78	1.21	1.14-6.09	4.35	88.76-97.93	91.93
Zn (%)	0.72-3.66	1.82	2.94-6.79	4.27	4.75-12.64	8.40	3.99-6.23	5.22	74.42-86.39	80.29
Cr (%)	2.10-3.78	2.94	0.08-0.48	0.29	3.82-8.69	6.18	3.75-5.61	4.77	83.12-88.97	85.83

MD-1	Exchangeable		Carbonate		Fe-Mn		Organic/Sulphide		Residual	
	Range	Average	Range	Average	Range	Average	Range	Average	Range	Average
Zn (%)	0.26-2.00	1.22	3.75-8.05	6.41	8.41-22.90	17.86	8.20-18.58	13.14	52.54-76.63	61.37

S-1	Exchangeable		Carbonate		Fe-Mn		Organic/Sulphide		Residual	
	Range	Average	Range	Average	Range	Average	Range	Average	Range	Average
Zn (%)	0.50-3.55	1.55	6.98-23.77	13.18	2.19-9.43	7.12	3.84-8.44	6.69	64.56-77.28	71.46

GP-1	Exchangeable		Carbonate		Fe-Mn		Organic/Sulphide		Residual	
	Range	Average	Range	Average	Range	Average	Range	Average	Range	Average
Zn (%)	1.09-3.87	1.88	5.05-13.12	8.06	8.87-17.41	12.79	2.39-6.02	4.43	64.52-77.82	72.84

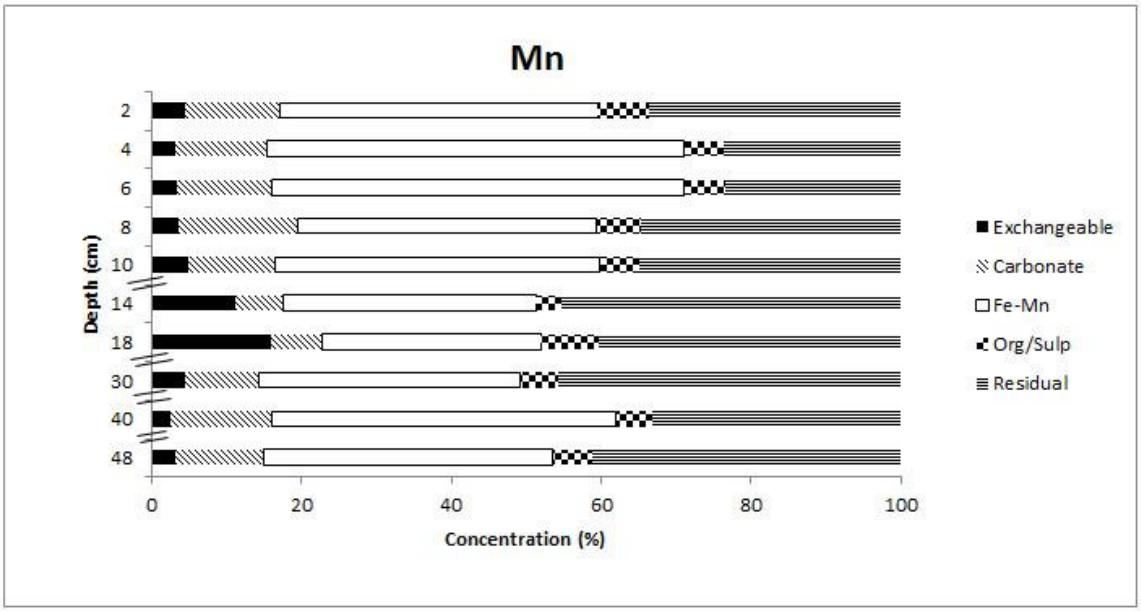

Fig. 3.1.14b Variation of Mn associated with different fractions in core VS-1.

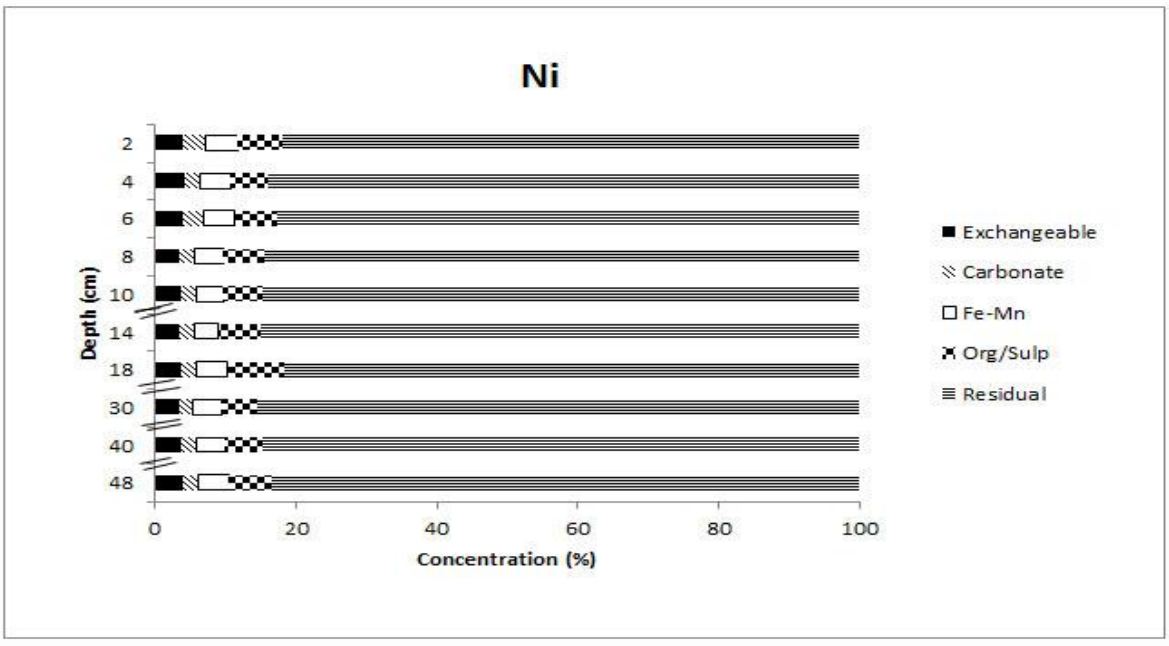

Fig. 3.1.14c Variation of Ni associated with different fractions in core VS-1.

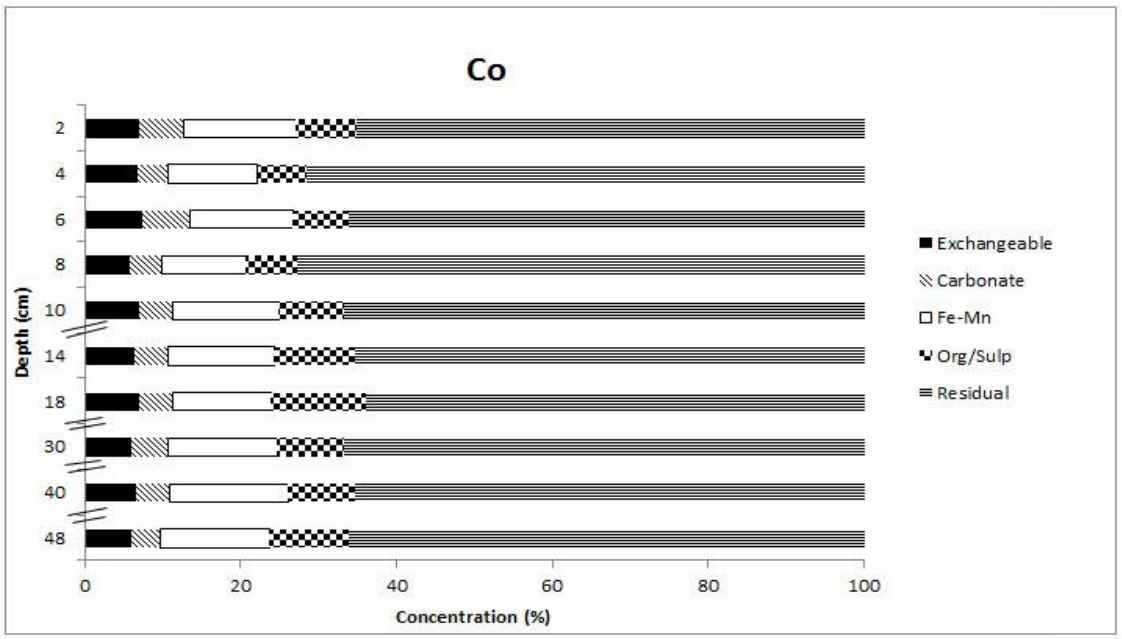

Fig. 3.1.14d Variation of Co associated with different fractions in core VS-1.

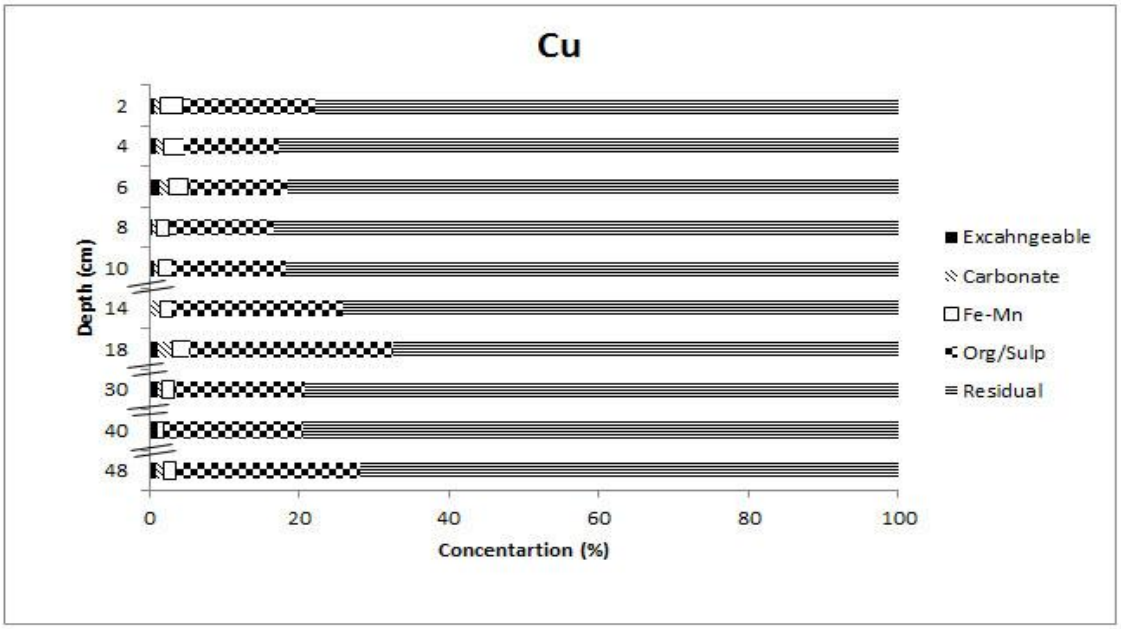

Fig. 3.1.14e Variation of Cu associated with different fractions in core VS-1.

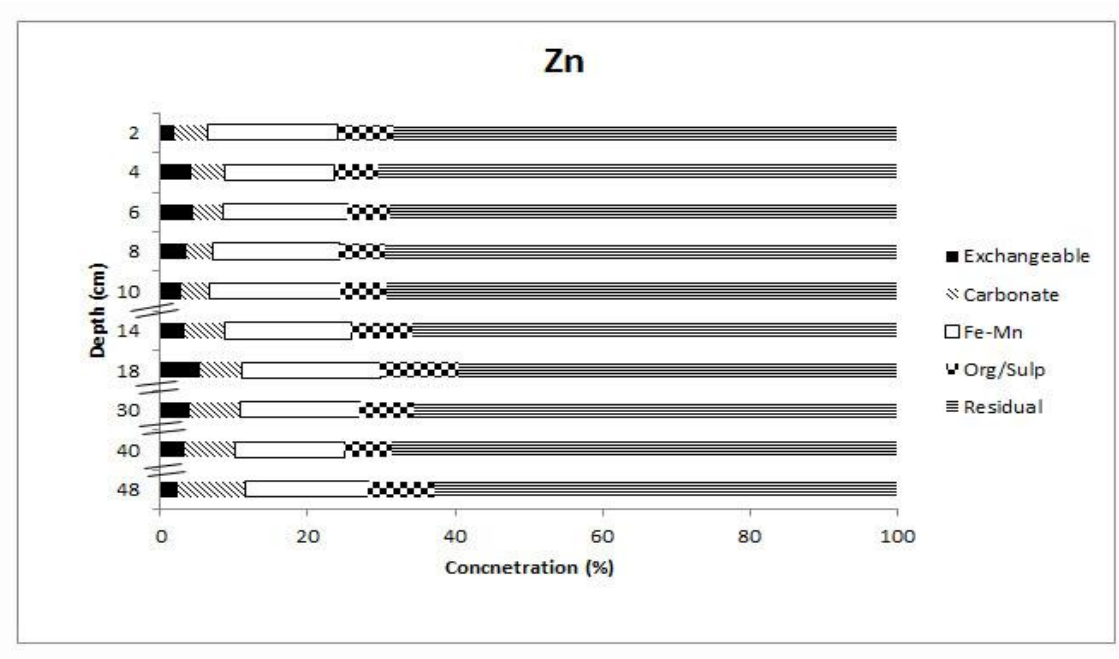

Fig. 3.1.14f Variation of Zn associated with different fractions in core VS-1.

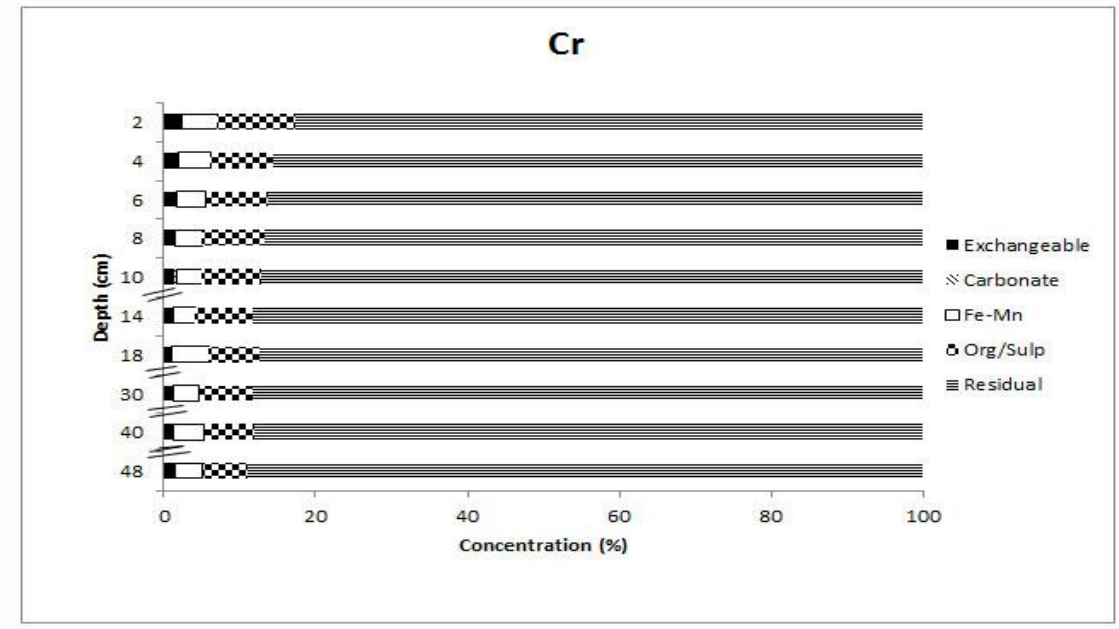

Fig. 3.1.14g Variation of Cr associated with different fractions in core VS-1.

Fe along with Ni and Cr showed almost constant concentration in all the fractions from bottom to surface of the core VS-1. However, at 18 cm depth Fe and Ni showed slightly higher total bioavailable phases. Manganese concentration increased in the Fe-Mn oxide fraction whereas, its concentration decreased in the residual fraction from bottom to surface.

Further, Mn exhibited high concentration at 18 cm depth in the exchangeable phase. Distribution pattern of Fe-Mn oxide phase revealed diagenetic remobilization as a major process involved in the case of Mn. Cobalt concentration remained nearly constant in all the fractions in the core VS-1, however with relatively high concentration in bioavailable phases compared to Fe, Ni and Cr. Metals viz. Zn and Cu also had higher concentration like Co with higher value at 18 cm depth. Metals viz. Co and Zn were available more in the Fe-Mn oxide phase, whereas Cu was bioavailable more in the organic bound fraction. Further, along the depth total bioavailability of Zn and Co was considerably high next to Mn.

Vaghotan estuary

All the metals viz. Fe, Mn, Ni, Co, Cu, Zn and Cr were highest (>65 %) in the residual fraction in the core VG-1. Except Cr, all the metals were present in least concentration in the exchangeable fraction. However, concentration of Fe was equal in exchangeable and carbonate fractions. Chromium was available in least concentration in the carbonate fraction. Next to the residual fraction, Fe, Mn, Co, Zn and Cr were associated with the Fe-Mn oxide while Ni and Cu with the organic bound fraction. Except Mn concentration in the Fe-Mn oxide phase, all the metals in individual bioavailable phases were less than 10 %.

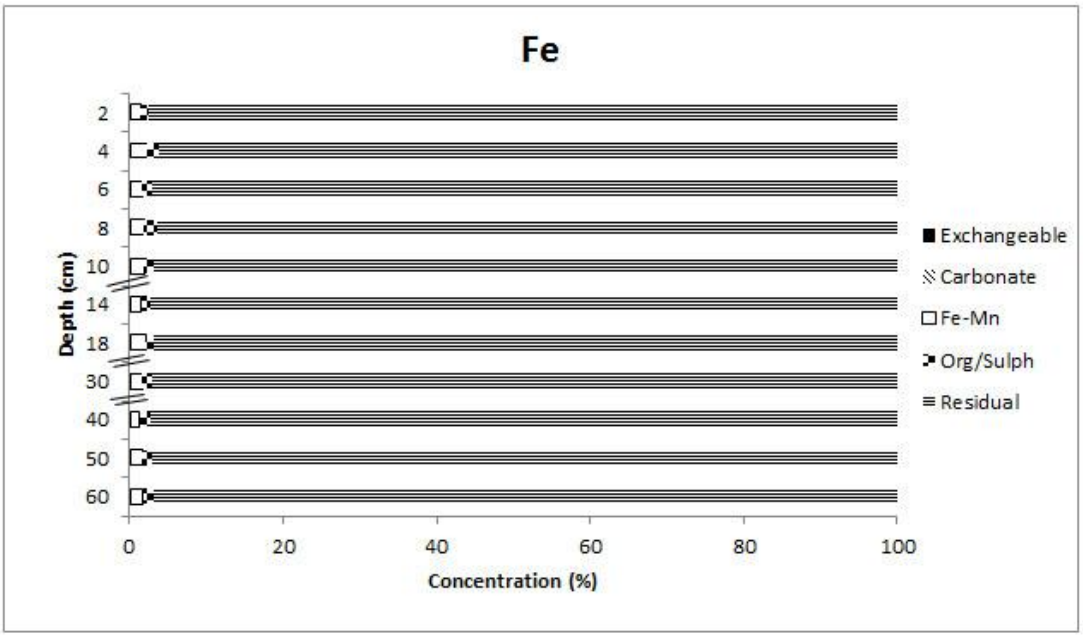

Fig. 3.1.14h Variation of Fe associated with different fractions in core VG-1.

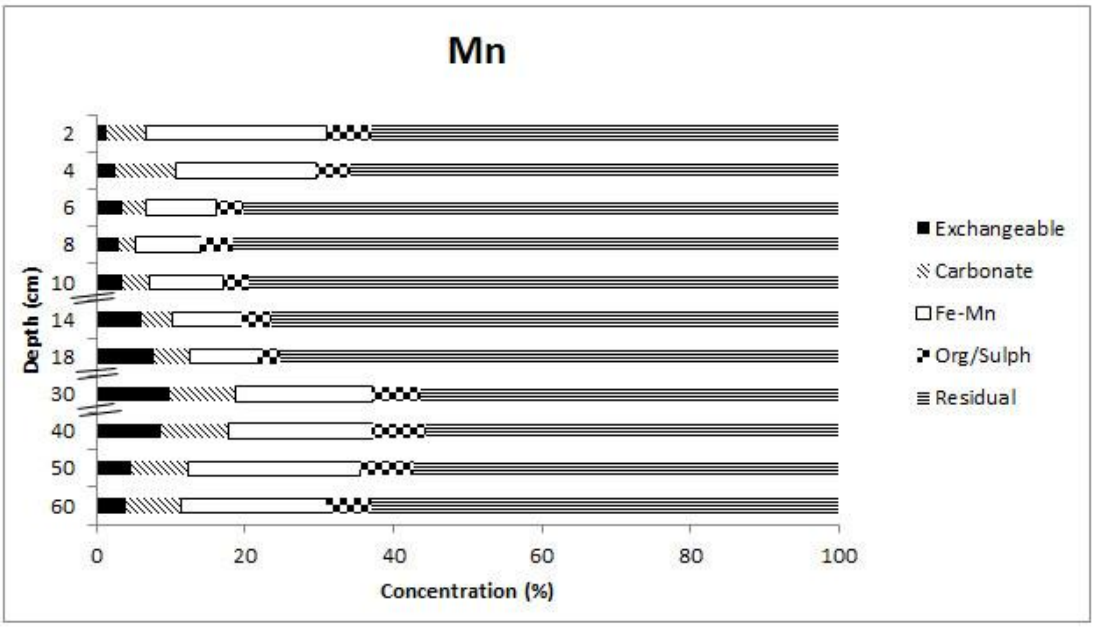

Fig. 3.1.14i Variation of Mn associated with different fractions in core VG-1.

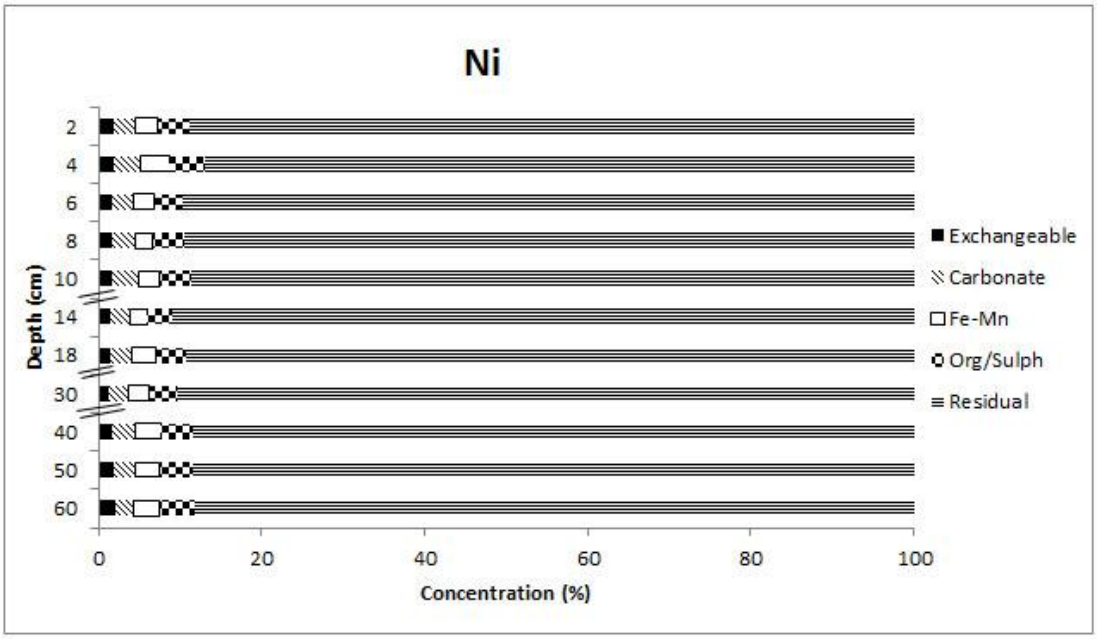

Fig. 3.1.14j Variation of Ni associated with different fractions in core VG-1.

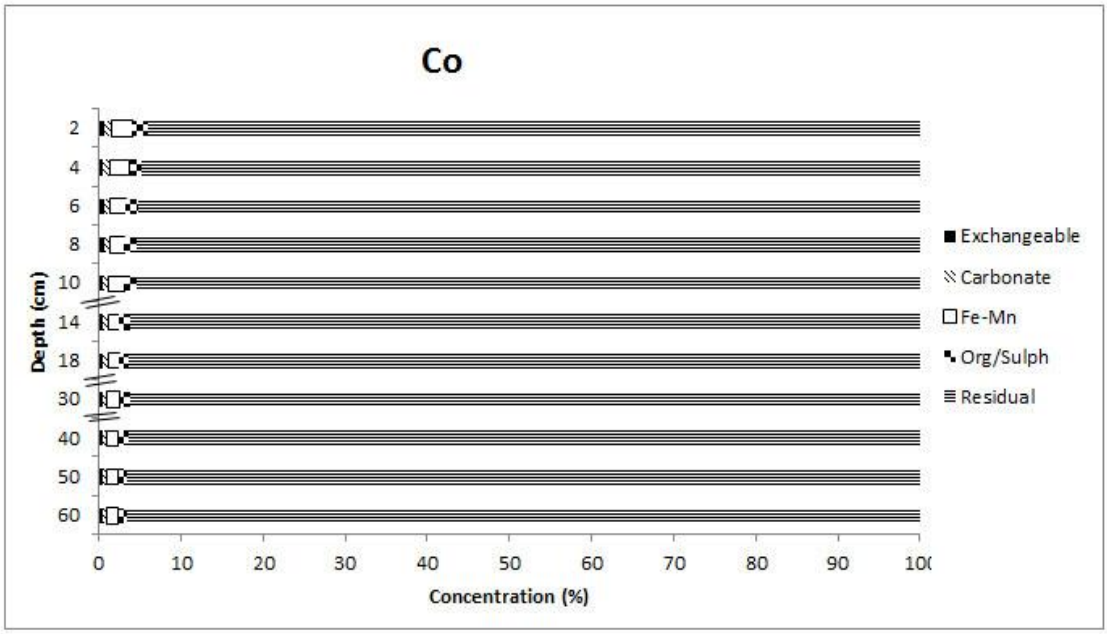

Fig. 3.1.14k Variation of Co associated with different fractions in core VG-1.

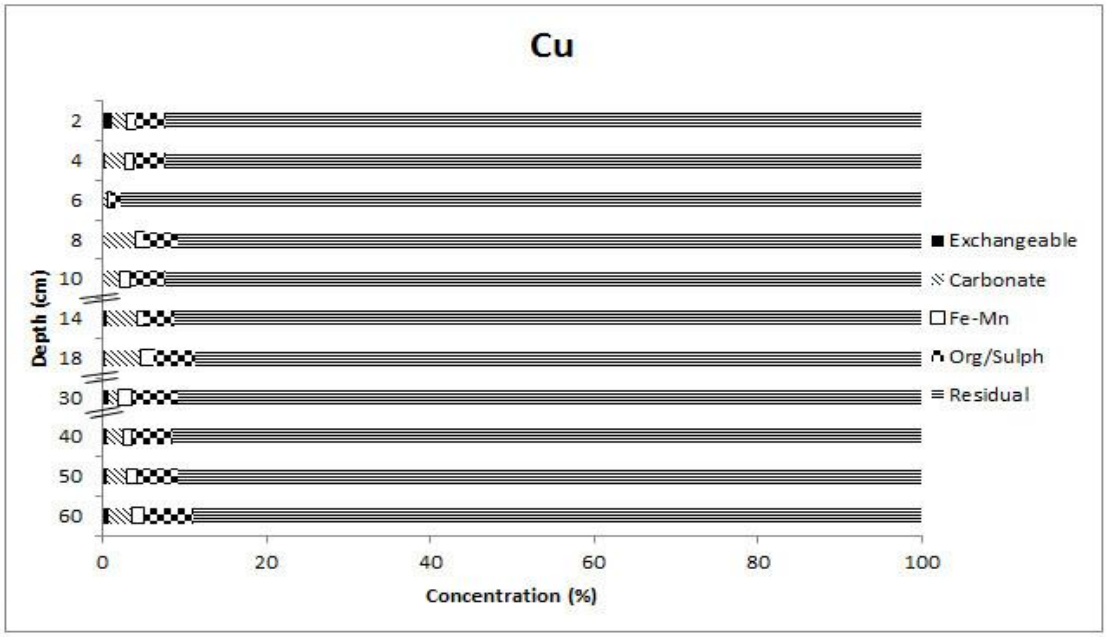

Fig. 3.1.14l Variation of Cu associated with different fractions in core VG-1.

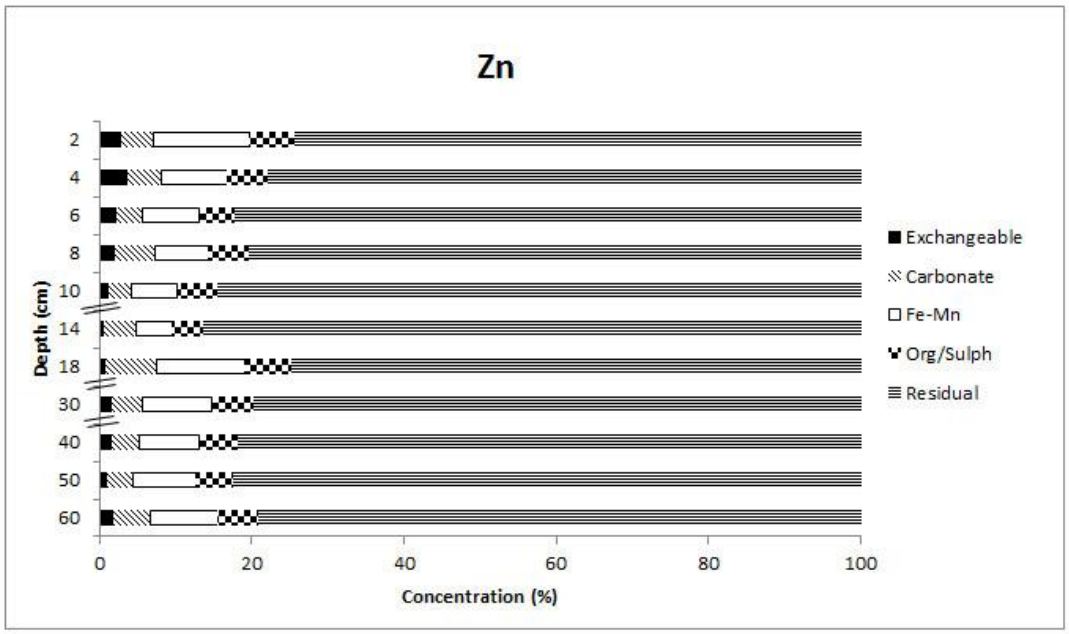

Fig. 3.1.14m Variation of Zn associated with different fractions in core VG-1.

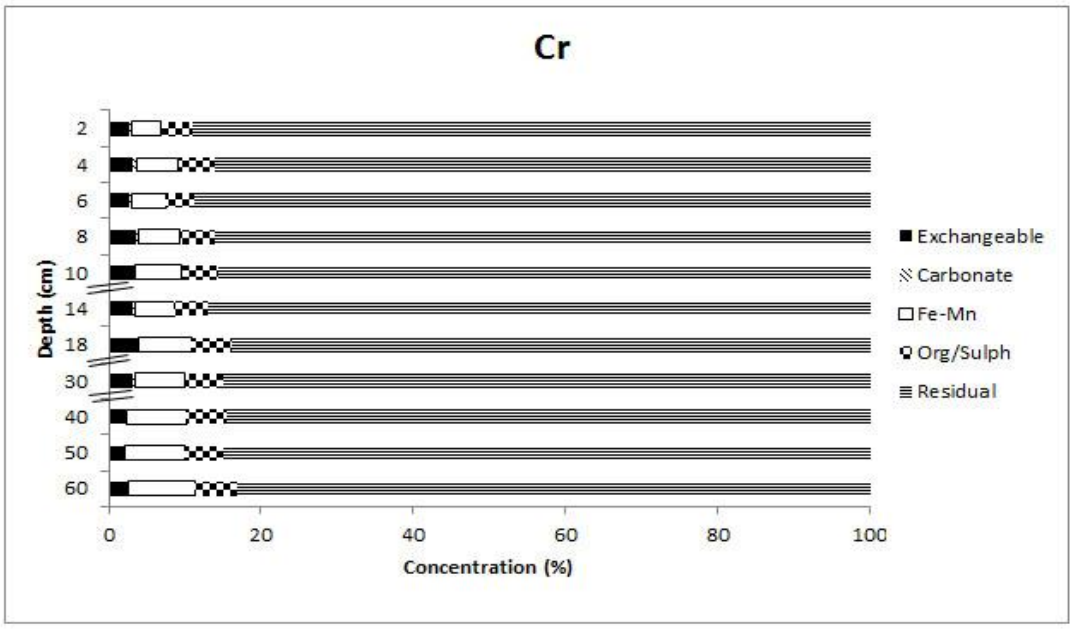

Fig. 3.1.14n Variation of Cr associated with different fractions in core VG-1.

The concentration of sum of bioavailable phases in Fe along with Co remained nearly constant from bottom to surface of the core VG-1. Manganese in all the bioavailable phases increased from bottom to 30 cm. Further, it decreased up to 6 cm followed by increase towards the surface. Exchangeable phase increased up to 30 cm from bottom and then decreased towards the surface. In top 4 cm of the core, large increase in the Fe-Mn oxide

phase indicated diagenetic remobilization. Residual phase compensated increase and decrease in Mn associated with total bioavailable phases. Metals viz. Ni and Cu remained nearly constant throughout the core VG-1, however Cu exhibited an increase in the residual fraction at 6 cm. The total bioavailable Cu and Ni were slightly higher than that of Co and Fe. Zinc in the residual fraction decreased from bottom to 18 cm, while its concentration increased in carbonate, Fe-Mn oxide and organic bound fractions. Zinc bound to the exchangeable fraction was comparatively lower than the other bioavailable phases and does not show much variation. Further, between 18 and 14 cm, there was sharp increase in the residual fraction, while its concentration decreased in the bioavailable phases. Thereafter, Zn associated with the bioavailable phases (oxides, carbonates and exchangeable) showed gradual increase towards the surface and decreased in the residual fraction. Chromium exhibited decrease from bottom to surface in the bioavailable fractions.

Mandovi estuary

In case of the core MD-1, Zn showed highest concentration in the residual fraction and had least concentration in the exchangeable fraction. Next to the residual fraction, Zn was associated with the Fe-Mn oxide fraction, followed by the organic bound fraction. Both these fractions (Fe-Mn oxide and organic/sulphur) represent significant bioavailable concentration of Zn.

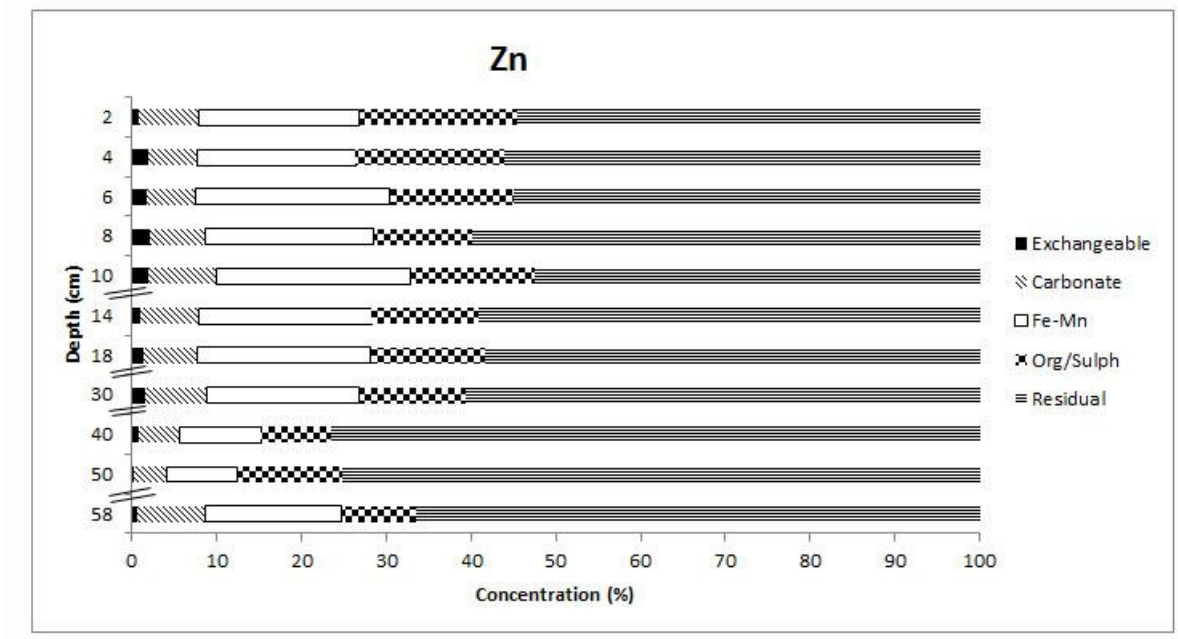

Fig. 3.1.14o Variation of Zn associated with different fractions in core MD-1.

The distribution pattern of Zn showed increase in the residual fraction from bottom to 40 cm, followed by decreasing trend towards the surface of the core MD-1. Zinc associated with carbonate and Fe-Mn oxide fractions decreased from bottom to 50 cm and further, exhibited overall increasing trend towards the surface. Zinc bound to the organic fraction showed less concentration at 40 cm, followed by an increasing trend towards the surface. The concentration of Zn associated with the exchangeable fraction was negligible in comparison to other bioavailable fractions, however, it showed increasing trend from bottom to 4 cm. Distribution pattern of Fe-Mn oxide phase suggested diagenetic remobilization of Zn in this core.

Sharavathi estuary

In the Sharavathi estuary (core S-1), Zn was highest in the residual fraction and showed least concentration in the exchangeable fraction. Among the bioavailable fractions, Zn was present in significant amount in the carbonate fraction. Fe-Mn oxide and organic bound fractions showed considerable amount of Zn.

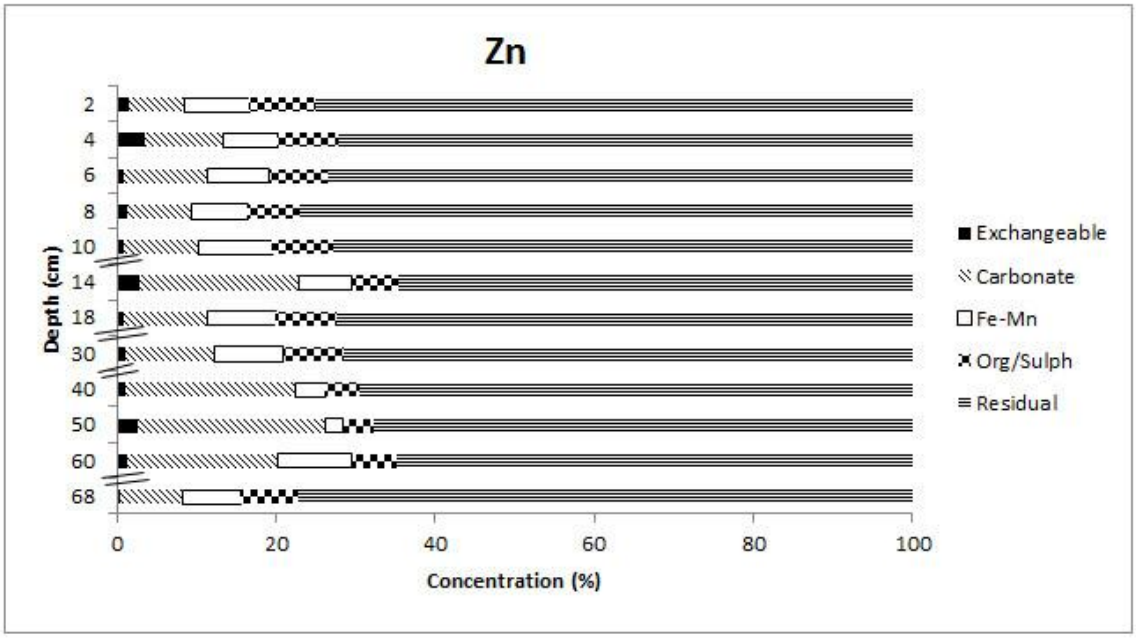

Fig. 3.1.14p Variation of Zn associated with different fractions in core S-1.

Zinc concentration decreased from bottom to 60 cm in the residual phase and further, showed overall increasing trend towards the surface. Zinc associated with carbonate fraction showed

increase from bottom to 60 cm, followed by overall decreasing trend towards the surface. However, its concentration in the bioavailable phases showed increase at 14 cm. Zinc bound to the exchangeable fraction was negligible in comparison to rest of the bioavailable phases and showed fluctuating trend throughout the core S-1.

Gurupur estuary

Zn was present in highest concentration in the residual fraction and had least concentration in the exchangeable fraction in the core GP-1. Next to the residual fraction, Zn was associated with the Fe-Mn oxide fraction. It was available in considerable concentration in the carbonate fraction.

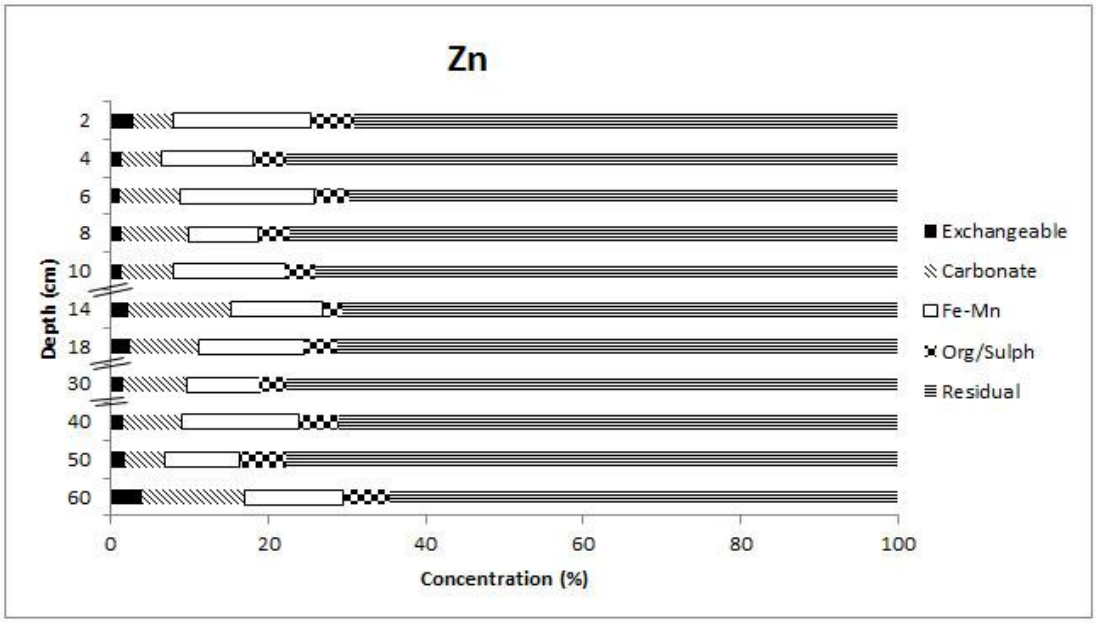

Fig. 3.1.14q Variation of Zn associated with different fractions in core GP-1.

Zinc associated with the residual fraction showed fluctuating distribution pattern from bottom to surface. The concentration of Zn showed overall increase in the Fe-Mn oxide fraction from bottom to surface of the core GP-1, whereas it exhibited decreasing trend in the carbonate phase. Zinc concentration in the organic bound fraction remained almost constant throughout the core GP-1. In the exchangeable fraction, it showed overall decreasing trend from bottom to 4 cm, followed by an increase towards the surface of the core.

All the elements, studied from five estuaries were present in highest percentage in the residual phase, except for Mn in the core VS-1, indicating that these elements were associated with minerals that make up the sediment particles (Fernandes 2012). The residual fraction contains minerals which hold trace metals within their crystal structure derived from the parent rock (Ratuzny et al. 2009). Further, they indicate that the metals were transported in solid form. The metals in this fraction are considered to be of geochemical background rather than the anthropogenic source. The residual phase is generally considered as inert phase as it does not react in the natural conditions. The metals derived from the anthropogenic input are generally associated with the non-residual fraction i.e bioavailable fractions. The metals in bioavailable phases are environmentally reactive with respect to geological and chemical processes (Hseu 2006). The trace metals in the exchangeable fraction include metals weakly adsorbed on sediments or on their essential components namely clays. Metals can also be associated with sediment carbonates which are susceptible to change in pH (Tessier et al. 1979). Metals associated with Fe hydrated oxides and humic acids are metals that can be released by ion-exchange processes and metals that can be co-precipitated in sediment (Marin et al. 1997; Tokalioglu et al. 2000). Changes in ionic composition and pH could cause re-mobilisation of metals from these fractions. Fe-Mn oxide fraction consists of metals adsorbed onto iron-manganese oxide particles or coatings which can be mobilized with changes in redox conditions (Kumar et al. 2011). In addition, trace metals may bound to various forms of organic matter viz. living organisms, detritus, coatings on mineral particles, etc which can be released by degradation of organic matter under oxidizing conditions in natural waters (Tessier et al. 1979). As the concentration of oxygen in sediment decreases, usually because of microbial degradation of organic matter, the metal oxide coatings begin to dissolve, releasing adsorbed metals.

In core VS-1, among the bioavailable fractions, the highest concentration of Mn (41.71 %) and 13.28 % and 16.80 % of Co and Zn respectively were present in the Fe-Mn oxide phase. The low percentage of Mn (35.57 %) in the residual fraction can be attributed to the relatively large ionic radius of Mn which makes its retention by soil silicates difficult (Fernandes 2012). In addition, the considerable concentration of Mn present in the carbonate bound fraction was due to the similarity in ionic radii to that of calcium which allows Mn to substitute for Ca in the carbonate phase (Pedersen and Price 1982; Zhang et al. 1988). Also, concentration of Mn and Zn was highest in the exchangeable fraction at 18 cm indicating diagenetic re-mobilization of Zn along with Mn. The increasing concentration of Mn in the Fe/Mn oxide

fraction from bottom to surface of the core VS-1 indicated its remobilization and re-precipitation. The change in the redox potential and pH may have led to mobilization and re-precipitation of Mn in the recent years in the core VS-1. Yuan et al. (2004) stated that considerable amount of Mn may be released into the environment if conditions become more acidic or if the sediments are subjected to more reducing conditions. The presence of considerable amount of Cu in the organic bound fraction in this core must be due to strong affinity of Cu towards organic matter (Li et al. 2001) and can form highly stable complexes. The source for these metals viz. Mn, Zn, Cu and Co in this core might be anthropogenic viz. industrial, sewage and agricultural in addition to metals released from chemical weathering of parent rock basalt.

In the Vaghotan estuary (core VG-1), Mn was 15.47 % in the Fe-Mn oxide fraction. In addition, among the bioavailable fractions, Zn and Cr were also available in slightly higher concentration in the Fe-Mn oxide fraction. The decrease in concentration of Mn associated with the bioavailable phases, particularly Fe-Mn oxide phase between 30 and 4 cm and further increase towards the surface indicated remobilization of Mn to oxic surface sediments where it is re-precipitated as oxides (Farmer and Lovell 1984). The decrease in concentration of Zn in the Fe-Mn oxide fraction at 14 cm followed by increase in the recent years suggested remobilization and adsorption onto Fe-Mn oxy hydroxides under oxic environment. The trace metals Zn and Cr may be adsorbed onto iron-manganese oxide particles (Zabetoglou et al. 2002) during precipitation.

In core MD-1, Zn was 17.86 and 13.14 % in Fe-Mn oxide and organic bound fractions respectively. Harrington et al. (1998) stated that Zn occurs mainly in the Fe-Mn oxide fraction due to its strong bonding with Fe oxides. Also its increase in Fe-Mn oxide and organic bound phases in the recent years indicated remobilization of Zn and co-precipitation with Fe-Mn oxide near the surface. Among the bioavailable fractions, Zn was highest (13.18 %) in the carbonate fraction in the core S-1. The results indicated the role of carbonates in scavenging Zn introduced into the Sharavathi estuary. However, Zn concentration in the carbonate phase decreased in the recent years. Among the bioavailable phases in the core GP-1, Zn was 12.79 % in the Fe-Mn oxide fraction and it increased towards the surface indicating co-precipitation with Fe-Mn oxide.

3.1.8 Screening quick reference table (SQUIRT)

The concentration of metals in the bulk sediments as well as sum of their bioavailable fractions is given in the Table 3.1.8.

Table 3.1.8 Average concentrations of total metals and bioavailable fractions in selected sub-samples in cores VS-1, VG-1, MD-1, S-1 and GP-1. F1=exchangeable fraction and F2= carbonate fraction.

	VS-1		
	Total metals concentration	Sum of bioavailable fractions	F1+F2(%)
Fe (%)	11.79	0.21	2.20
Mn (ppm)	1058	376	17.09
Ni (ppm)	71	8	6.01
Co (ppm)	48	9	11.18
Cu (ppm)	273	26	1.81
Zn (ppm)	363	25	8.96
Cr (ppm)	144	18	1.51

	VG-1		
	Total metals concentration	Sum of bioavailable fractions	F1+F2(%)
Fe (%)	13.33	0.48	0.004
Mn (ppm)	1291	391	10.91
Ni (ppm)	124	8	4.43
Co (ppm)	84	13	1.08
Cu (ppm)	482	20	2.82
Zn (ppm)	101	15	6.09
Cr (ppm)	101	9	3.23

	MD-1		
	Total metals concentration	Sum of bioavailable fractions	F1+F2(%)
Zn(ppm)	226	18	7.63

	S-1		
	Total metals concentration	Sum of bioavailable fractions	F1+F2(%)
Zn (ppm)	647	7	14.72

	GP-1		
	Total metals concentration	Sum of bioavailable fractions	F1+F2(%)
Zn (ppm)	950	6	9.94

On comparison of Table 3.1.8 with table 2.1.3 a and b, it was observed that the percentage of total Fe and sum of bioavailable Fe was very low compared to apparent effect threshold (AET) in cores VS-1 and VG-1 indicating no harm to the aquatic life from Fe. There are no reported values for Mn and Co for first four classes but the total Mn as well as sum of bioavailable Mn exceeded the AET values in cores VS-1 and VG-1. Total as well as bioavailable Co values exceeded the AET in core VG-1 while, in case of core VS-1 total Co was more than the AET and the sum of the bioavailable Co was very much near to AET. Thus, Mn and Co were potentially bioavailable and might become toxic to environment of Vashishti and Vaghotan estuaries. The value of total Cr fell under effect range low (ERL) to probable effect level (PEL) in these two estuaries, whereas, total Ni fell between effect range medium (ERM) and AET in core VS-1 and was more than the AET in core VG-1. However, sum of the bioavailable fractions of Cr and Ni fell below threshold effect level (TEL) in these estuaries indicating no potential bioavailability of these elements as these elements were observed to be highest in the residual fraction in cores VS-1 and VG-1. The concentration of total Cu fell between ERM and AET in core VS-1, while in case of core VG-1, it exceeded

the AET. The bioavailable fraction of Cu fell between TEL and ERL in both these cores. Hence, Cu was likely to cause concern to associated biota in these estuaries to some extent. The values of total Zn fell under PEL to ERM in the core VS-1, while its value was below TEL in the core VG-1. In case of the core MD-1, value of total Zn fell between ERL to PEL, while its value in cores S-1 and GP-1 exceeded AET. However, sum of the bioavailable fractions of Zn was below TEL in all five estuaries.

The results therefore indicated concern from Mn and Co, and to some extent from Cu to sediment associated organisms in Vashishti and Vaghotan estuaries. Other metals level was lower than the TEL of the neanthes, echinoderm larvae, microtox and oyster larvae, and infaunal community. Benthic invertebrates are an important link in the transfer of substances to higher trophic levels because of their close association with sediments and their ability to accumulate metals (Burgos and Rainbow 2001). However, no standards are available on benthic invertebrates as of now to compare metal toxicity.

3.1.9 Risk assessment code

The risk assessment code indicates the sediment which can release metals from exchangeable and carbonate fractions; % of the total concentration <1: no risk, will be considered safe for the environment, 1-10: low risk, 11-30: medium risk, 31-50: high risk, > 50: very high risk, and can easily enter the food chain (Perin et al. 1985).

When sum of the percentage of metals in exchangeable (fraction 1) and carbonate fractions (fraction 2) of studied cores (Table 3.1.8) were compared with risk assessment code it was noted that Fe, Ni, Co, Cu, Zn and Cr were within the degree of low risk, while Mn was within the degree of medium risk in the core VS-1. All the metals fell under the category of low risk in the core VG-1. Zinc was within the degree of low risk in cores MD-1 and GP-1, whereas in the core S-1 it fell under the category of medium risk.

The results of risk assessment code revealed low to medium risk from metals bound to exchangeable and carbonate phases to associated biota in studied estuaries.

Section II: Middle estuarine region

3.2.1 Sediment components

Vashishti estuary

The percentage of sand in the middle region of the Vashishti estuary (core VS-2) ranged from 9.18 % to 79.58 % (avg. 35.64 %), while silt and clay varied from 12.82 % to 61.22 % (avg. 43.86 %) and 6.44 % to 29.60 % (avg. 20.49 %) respectively (Table 3.2.1a). The core VS-2 was divided into three parts based on the distribution of sediment components, lower 70 to 52 cm, middle 52 to 38 cm and upper section 38 cm to surface (Fig. 3.2.1a). In the lower section, sand varied from 20.78 % to 43.95 % (avg. 31.91 %), while silt and clay varied from 38.77 % to 55.73 % (avg. 47.18 %) and 16.60 % to 28.40 % (avg. 20.92 %) respectively (Table 3.2.1b). In the middle section, sand, silt and clay varied from 29.94 % to 79.58 % (avg. 60.26 %), 12.82 % to 48.54 % (avg. 26.72 %) and 6.44 % to 21.52 % (avg. 13.01 %) respectively, whereas in the upper section sand, silt and clay ranged from 9.18 % to 54.93 % (avg. 28.14 %), 31.83 % to 61.22 % (avg. 48.69 %) and 12.04 % to 29.60 % (avg. 23.17 %) respectively.

Sand showed fluctuating pattern in lower and upper sections of the core VS-2 (Fig. 3.2.1a). In the middle section, there was a large increase in sand and was more than the average. The distribution pattern of sand was largely compensated by finer sediments. The data plotted on the ternary diagram indicated deposition of sediments in violent hydrodynamic energy conditions. It also showed high sand content in the middle section (Fig. 3.2.2a).

Vaghotan estuary

The percentage of sand in the core VG-2 ranged from 0.46 % to 19.57 % (avg. 6.00 %), while silt and clay varied from 10.60 % to 48.60 % (avg. 23.21 %) and 43.72 % to 88.76 % (avg. 70.71 %) respectively (Table 3.2.1a). The core VG-2 was divided into two sections, lower 54 to 30 cm and upper section 30 to surface based on the variations in distribution pattern of sediment components (Fig. 3.2.1b). In the lower section, sand, silt and clay varied from 0.46 % to 3.10 % (avg. 1.60 %), 10.60% to 28.10 % (avg. 20.71 %) and 69.32 % to 88.76 % (avg. 77.85 %) respectively, whereas in the upper section sand, silt and clay ranged from 4.84 % to

Table 3.2.1a Range and average concentration of sediment components, pH and organic carbon in cores VS-2, VG-2, MD-2, S-2 and GP-2

Sediment core	Sand (%)			Silt (%)			Clay (%)			pH			Organic Carbon (%)		
	Range		Avg	Range		Avg	Range		Avg	Range		Avg	Range		Avg
	Min	Max		Min	Max		Min	Max		Min	Max		Min	Max	
VS-2	9.18	79.58	35.64	12.82	61.22	43.86	6.44	29.60	20.49	5.42	6.74	6.22	0.21	2.12	1.19
VG-2	0.46	19.57	6.00	10.60	48.60	23.21	43.72	88.76	70.71	5.95	6.82	6.47	1.21	3.41	2.29
MD-2	4.60	81.70	30.12	13.86	75.40	42.99	0.16	48.48	26.89	5.72	7.71	6.91	0.33	3.00	1.85
S-2	7.98	94.23	38.75	4.57	89.14	43.10	0.64	42.00	18.16	5.50	7.02	6.07	0.09	3.04	1.87
GP-2	4.91	50.20	14.89	27.37	63.77	45.24	21.24	54.72	39.87	6.32	7.66	6.89	0.41	4.28	2.26

Table 3.2.1b Section wise range and average concentration of sediment components, pH and organic carbon in cores VS-2, VG-2, MD-2, S-2 and GP-2, where L=Lower, M=Middle and U=Upper sections

Sediment core	Sand (%)			Silt (%)			Clay (%)			pH			Organic Carbon (%)		
	Range		Avg	Range		Avg	Range		Avg	Range		Avg	Range		Avg
	Min	Max		Min	Max		Min	Max		Min	Max		Min	Max	
VS-2 (L)	20.78	43.95	31.91	38.77	55.73	47.18	16.60	28.40	20.92	5.90	6.38	6.22	0.78	1.64	1.17
(M)	29.94	79.58	60.26	12.82	48.54	26.72	6.44	21.52	13.01	5.93	6.74	6.33	0.21	1.64	0.69
(U)	9.18	54.93	28.14	31.83	61.22	48.69	12.04	29.60	23.17	5.42	6.69	6.17	0.21	2.12	1.40
VG-2 (L)	0.46	3.10	1.60	10.60	28.10	20.71	69.32	88.76	77.85	6.19	6.82	6.54	2.12	3.41	2.81
(U)	4.84	19.57	10.10	14.68	48.60	25.53	43.72	76.12	64.09	5.95	6.72	6.41	1.21	2.53	1.81
MD-2 (L)	8.22	19.32	14.79	37.76	46.42	42.69	36.28	48.48	42.52	7.43	7.58	7.51	2.26	2.61	2.45
(M)	17.47	81.70	66.19	13.86	56.37	26.94	0.16	26.16	6.88	6.18	7.32	6.95	0.33	2.41	1.10
(U)	4.60	39.71	20.93	37.45	75.40	48.40	0.32	41.72	30.67	5.72	7.71	6.79	1.01	3.00	2.00
S-2 (L)	7.99	23.73	12.91	45.31	77.83	60.21	7.32	42.00	26.88	5.52	6.27	5.76	2.21	3.04	2.66
(M)	7.98	94.23	67.07	4.57	89.14	26.11	0.64	15.96	6.82	5.50	6.68	6.22	0.09	2.81	0.81
(U)	36.92	51.79	44.21	27.85	39.88	34.18	20.36	23.20	21.61	6.50	7.02	6.69	1.82	2.69	2.28
GP-2 (L)	4.91	21.05	14.72	33.49	48.24	39.04	37.16	54.72	46.23	6.51	7.66	7.28	1.34	4.28	2.67
(U)	5.79	50.20	15.04	27.37	63.77	50.79	21.24	50.08	34.17	6.32	6.78	6.54	0.41	2.47	1.90

19.57 % (avg. 10.10 %), 14.68 % to 48.60 % (avg. 25.53 %) and 43.72 % to 76.12 % (avg. 64.09 %) respectively (Table 3.2.1b).

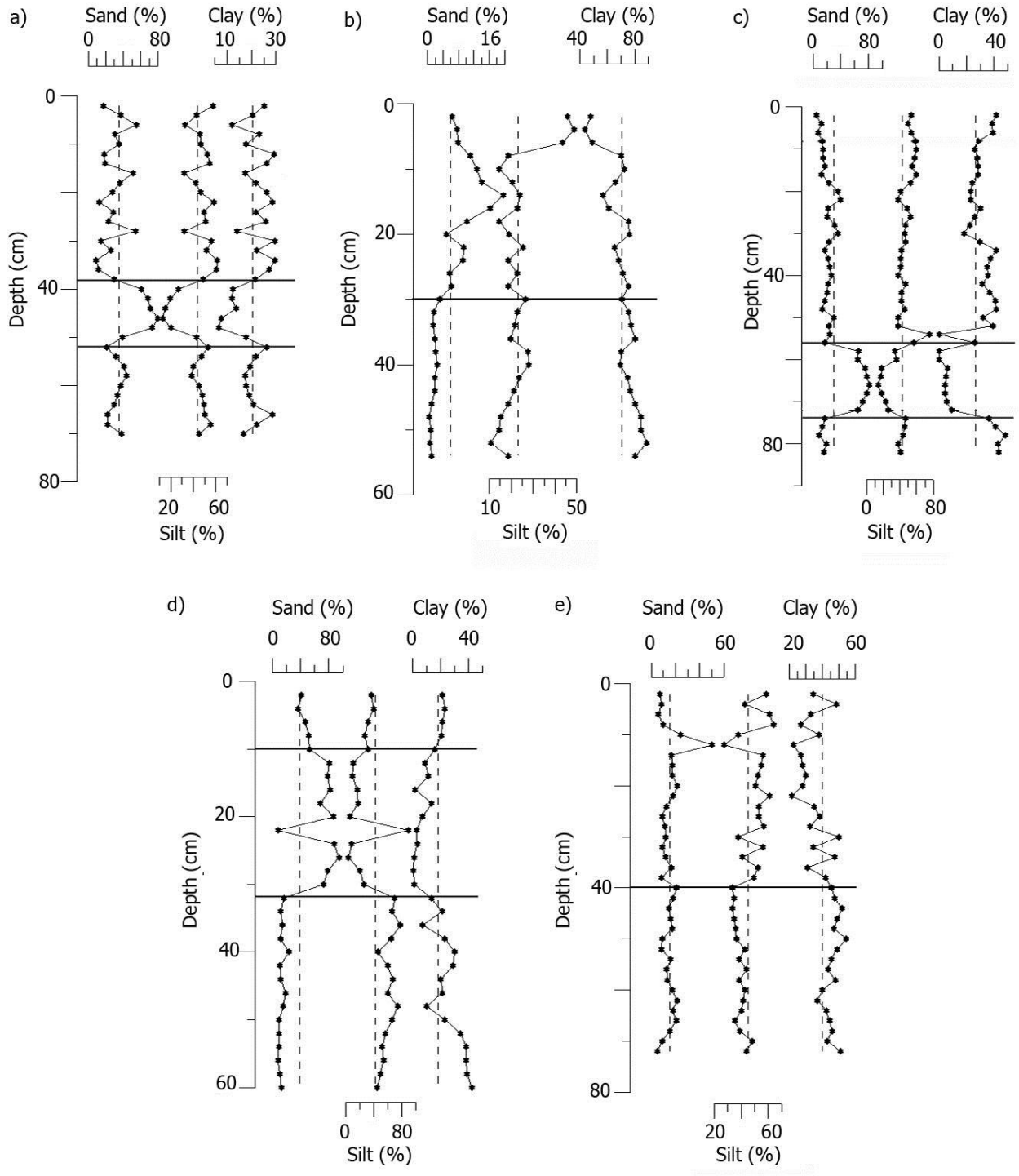

Fig. 3.2.1 Variation of sediment components with average line in sediment cores VS-2 (a), VG-2 (b), MD-2 (c), S-2 (d) and GP-2 (e).

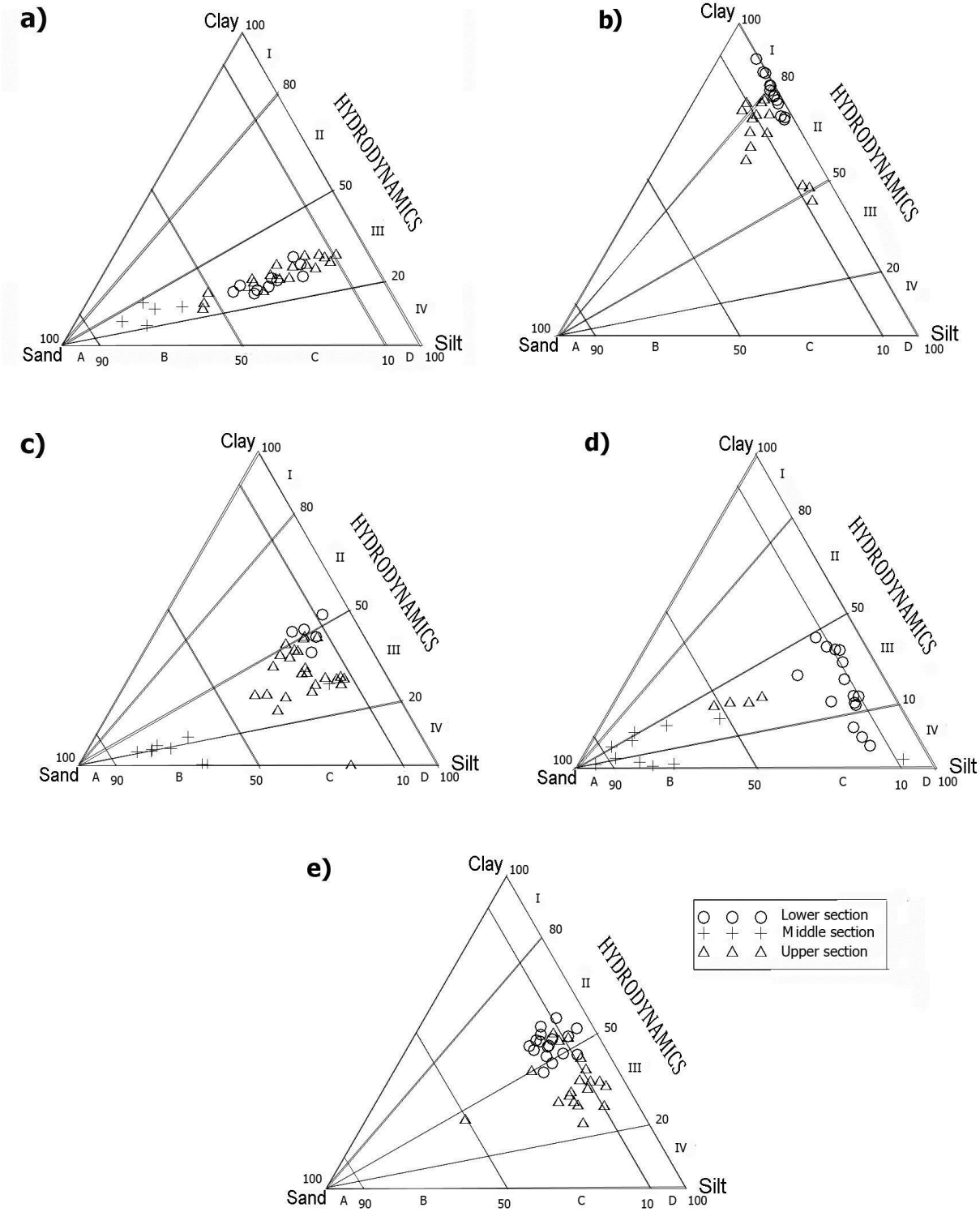

Fig. 3.2.2 Ternary plots for cores VS-2, VG-2, MD-2, S-2 and GP-2.

The percentage of sand did not show much variation in the lower section, while in the upper section its concentration increased from 30 to 14 cm and then decreased towards the surface of the core VG-2 (Fig. 3.2.1b). Silt showed overall increase from bottom to 40 cm. Further, it fluctuated up to 8 cm, followed by sharp increase at 6 cm and then showed overall increase towards the surface. The vertical distribution pattern of clay was largely opposite to that of silt throughout the core. The data plotted on the ternary diagram indicated deposition of sediments of the lower section under calm to relatively violent energy conditions, while majority of the sediments of the upper section were deposited in relatively violent energy conditions (Fig. 3.2.2a). This indicated the change in the deposition environment with time.

Mandovi estuary

Sand in the middle region of the Mandovi estuary (core MD-2) ranged from 4.60 % to 81.70 % (avg. 30.12 %), while silt and clay varied from 13.86 % to 75.40 % (avg. 42.99 %) and 0.16 % to 48.48 % (avg. 26.89 %) respectively (Table 3.2.1a). On the basis of variations in sediment parameters, the core MD-2 (Fig. 3.2.1c) was divided into three sections, the lower 82 to 74 cm, middle 74 to 56 cm and upper section 56 cm to surface. In the lower section, sand varied from 8.22 % to 19.32 % (avg. 14.79 %), while silt and clay varied from 37.76 % to 46.42 % (avg. 42.69 %) and 36.28 % to 48.48 % (avg. 42.52 %) respectively (Table 3.2.1b). In the middle section, sand, silt and clay varied from 17.47 % to 81.70 % (avg. 66.19 %), 13.86 % to 56.37 % (avg. 26.94 %) and 0.16 % to 26.16 % (avg. 6.88 %) respectively, whereas in the upper section sand, silt and clay ranged from 4.60 % to 39.71 % (avg. 20.93 %), 37.45 % to 75.40 % (avg. 48.40 %) and 0.32 % to 41.72 % (avg. 30.67 %) respectively.

In the lower section of the core MD-2, not much variation was observed in sand and silt percentage, while overall decreasing trend was seen in case of clay (Fig. 3.2.1c). In the middle section, however, there was large increase in sand percentage and was more than the average value. Silt and clay compensated distribution of sand in this section. In the upper section, sand did not show much variation from 56 to 22 cm, followed by a gradual decrease towards the surface. Similar to sand, silt also did not show much variation from 56 to 22 cm, except at 54 cm where its sharp increasing peak was seen. Further, there was overall slight increase in silt percentage in the top 22 cm of the core. The concentration of clay varied from more than the average line (54 to 34 cm) to along the average line from 32 to 8 cm. However, clay exhibited sharp decreasing peak at 54 cm. In the top 8 cm of the core, clay showed an

increasing trend towards the surface. The data plotted on the ternary diagram indicated deposition of sediments of lower and upper sections under relatively violent to violent energy conditions (Fig. 3.2.2c). The coarser sediments of the middle section were deposited under violent to extremely violent energy conditions.

Sharavathi estuary

In core S-2, percentage of sand, silt and clay ranged from 7.98 % to 94.23 % (avg. 38.75 %), 4.57 % to 89.14 % (avg. 43.10 %) and 0.64 % to 42.00 % (avg. 18.16 %) respectively (Table 3.2.1a). On the basis of distribution pattern of sediment components (Fig. 3.2.1d), the core S-2 was divided into three sections, the lower (60 to 32 cm), middle (32 to 10 cm) and upper (10 cm to surface) sections. In the lower section, sand varied from 7.99 % to 23.73 % (avg. 12.91 %), while silt and clay vary from 45.31 % to 77.83 % (avg. 60.21 %) and 7.32 % to 42.00 % (avg. 26.88 %) respectively (Table 3.2.1b), whereas in the middle section, sand, silt and clay varied from 7.98 % to 94.23 % (avg. 67.07 %), 4.57 % to 89.14 % (avg. 26.11 %) and 0.64 % to 15.96 % (avg. 6.82 %) respectively. In the upper section, sand, silt and clay ranged from 36.92 % to 51.79 % (avg. 44.21 %), 27.85 % to 39.88 % (avg. 34.18 %) and 20.36 % to 23.20 % (avg. 21.61 %) respectively.

In the lower section of the core, sand was lower than average and not much variation in percentage was seen (Fig. 3.2.1d). The silt and clay showed increasing and decreasing distribution pattern in this section, respectively. In the middle section of the core, sand percentage increased drastically from 32 to 10 cm with a sharp decreasing peak at 22 cm depth. Further, in the upper section, sand percentage decreased towards surface. The variation in sand percentage was compensated by silt and clay, more precisely; silt showed point to point variation compensating sand in the upper two sections. The majority of sediment components of the Sharavathi estuary (Fig. 3.2.2d) fell in group III and IV indicating deposition of sediments under violent to extremely violent hydrodynamic conditions. The ternary diagram clearly suggested deposition of coarser sediments in the middle section of the core S-2.

Gurupur estuary

The percentage of sand in the core GP-2, ranged from 4.91 % to 50.20 % (avg. 14.89 %), while silt and clay varied from 27.37 % to 63.77 % (avg. 45.24 %) and 21.24 % to 54.72 % (avg. 39.87 %) respectively (Table 3.2.1a). On the basis of variations in the distribution pattern of sediment components with depth, the core GP-2 (Fig. 3.2.1e) was divided into two sections, viz. a lower section from bottom to 40 cm and the upper section from 40 cm to surface. In the lower section, sand varied from 4.91 % to 21.05 % (avg. 14.72 %), while silt and clay varied from 33.49 % to 48.24 % (avg. 39.04 %) and 37.16 % to 54.72 % (avg. 46.23 %) respectively (Table 3.2.1b), while in the upper section sand, silt and clay ranged from 5.79 % to 50.20 % (avg. 15.04 %), 27.37 % to 63.77 % (avg. 50.79 %) and 21.24 % to 50.08 % (avg. 34.17 %) respectively.

The sand did not show much variation in lower and upper sections, except at 12 cm depth where a prominent increasing peak of sand was observed (Fig. 3.2.1e). Silt showed overall slightly decreasing distribution pattern in the lower section, while in the upper section its percentage increased towards the surface, with fluctuations. In both the sections, the variation in silt percentage was compensated by clay. In case of the core GP-2 (Fig. 3.2.2e), sediment components varied from group II to III suggesting deposition of sediments in relatively violent to violent energy conditions from lower to upper sections. It also showed an increase in silt percentage in recent times in the core GP-2.

3.2.2 pH

Vashishti estuary

The value of pH in the core VS-2 (Table 3.2.1a) varied from 5.42 to 6.74 (avg. 6.22). In the lower section of the core VS-2, pH ranged from 5.90 to 6.38 (avg. 6.22), whereas it varied from 5.93 to 6.74 (avg. 6.33) in the middle section (Table 3.2.1b). In the upper section, pH ranged from 5.42 to 6.69 (avg. 6.17).

Overall the pH fluctuated around the average line in the core VS-2 (Fig. 3.2.3a).

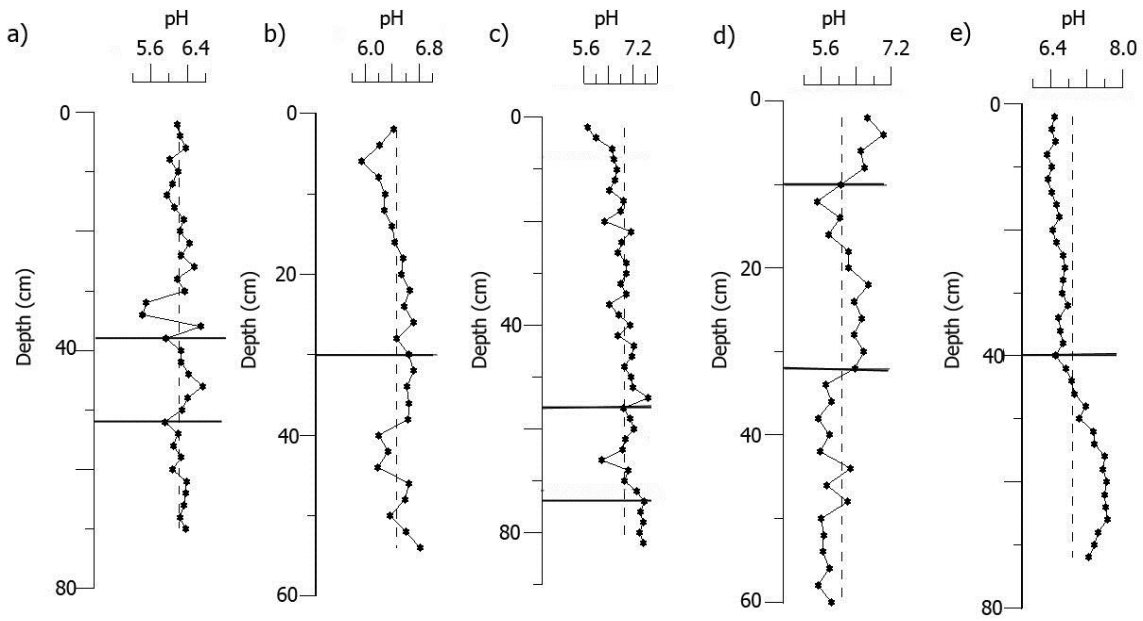

Fig. 3.2.3 Variation of pH with average line in sediment cores VS-2 (a), VG-2 (b), MD-2 (c), S-2 (d) and GP-2 (e).

Vaghotan estuary

In core VG-2 (Table 3.2.1a), pH varied from 5.95 to 6.82 (avg. 6.47). In this core, pH varied from 6.19 to 6.82 (avg. 6.54) and 5.95 to 6.72 (avg. 6.41) in lower and upper sections respectively (Table 3.2.1b).

In core VG-2, pH showed overall decrease from bottom to 40 cm, followed by an increase up to 30 cm (Fig. 3.2.3b). Thereafter, it exhibited overall decreasing trend towards the surface.

Mandovi estuary

The value of pH in the core MD-2 (Table 3.2.1a) varied from 5.72 to 7.71 (avg. 6.91). In the lower section (Table 3.2.1b), it varied from 7.43 to 7.58 (avg. 7.51), whereas in the middle section it ranged from 6.18 to 7.32 (avg. 6.95). In the upper section, pH ranged from 5.72 to 7.71 (avg. 6.79).

Overall decrease in pH was observed from bottom to surface of the core MD-2 (Fig. 3.2.3c).

Sharavathi estuary

In core S-2 (Table 3.2.1a), pH varied from 5.50 to 7.02 (avg. 6.07). It varied from 5.52 to 6.27 (avg. 5.76), 5.50 to 6.68 (avg. 6.22) and 6.50 to 7.02 (avg. 6.69) in lower, middle and upper sections respectively (Table 3.2.1b).

The pH was less than average in the lower section, whereas it varied from more than average to less than average in the middle section (Fig. 3.2.3d). Further, in the upper section, pH increased towards the surface and was more than the average.

Gurupur estuary

In core GP-2 (Table 3.2.1a), pH varied from 6.32 to 7.66 (avg. 6.89). In lower and upper sections of the core GP-2, pH varied from 6.51 to 7.66 (avg. 7.28) and 6.32 to 6.78 (avg. 6.54) respectively (Table 3.2.1b).

The pH was more than average in the lower section which decreased to less than average in the upper section (Fig. 3.2.3e).

3.2.3 Organic carbon

Vashishti estuary

In core VS-2 (Table 3.2.1a), organic carbon percentage ranged from 0.21 % to 2.12 % (avg. 1.19 %). It varied from 0.78 % to 1.64 % (avg. 1.17 %), 0.21 % to 1.64 % (avg. 0.69 %) and 0.21 % to 2.12 % (avg. 1.40 %) in lower, middle and upper sections respectively (Table 3.2.1b).

The distribution pattern of organic carbon was similar to finer sediments in the core VS-2 (Fig. 3.2.4a). It showed fluctuating distribution in lower and upper sections, while decrease in the middle section.

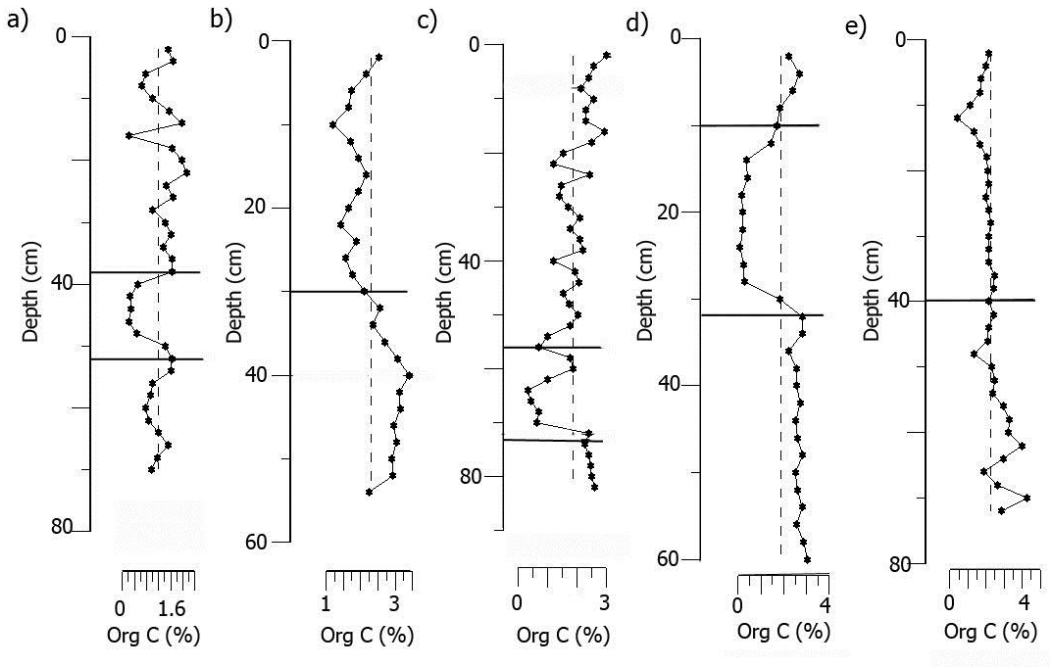

Fig. 3.2.4 Variation of organic carbon with average line in sediment cores VS-2 (a), VG-2 (b), MD-2 (c), S-2 (d) and GP-2 (e).

Vaghotan estuary

The organic carbon percentage in the core VG-2 (Table 3.2.1a) ranged from 1.21 % to 3.41 % (avg. 2.29 %). It varied from 2.12 % to 3.41 % (avg. 2.81 %) and 1.21 % to 2.53 % (avg. 1.81 %) in lower and upper sections respectively (Table 3.2.1b).

Organic carbon was more than the average line in the lower section of the core VG-2, whereas in the upper section it was less than the average line (Fig. 3.2.4b).

Mandovi estuary

In core MD-2 (Table 3.2.1a), organic carbon percentage ranged from 0.33 % to 3.00 % (avg. 1.85 %). In the lower section of the core MD-2 (Table 3.2.1b), organic carbon percentage ranged from 2.26 % to 2.61 % (avg. 2.45 %), whereas in the middle section it varied from 0.33 % to 2.41 % (avg. 1.10 %). In the upper section, organic carbon varied from 1.01 % to 3.00 % (avg. 2.00 %).

A gradual decrease was seen in case of organic carbon from bottom to 74 cm in the lower section of the core MD-2 and was more than the average line (Fig. 3.2.4c). Further, its concentration decreased in the middle section and was less than the average line, largely similar to finer sediments. In the upper section, organic carbon showed overall increase towards the surface with fluctuations.

Sharavathi estuary

The organic carbon percentage in the core S-2 (Table 3.2.1a) ranged from 0.09 % to 3.04 % (avg. 1.87 %). It varied from 2.21 % to 3.04 % (avg. 2.66 %), 0.09 % to 2.81 % (avg. 0.81 %) and 1.82 % to 2.69 % (avg. 2.28 %) in lower, middle and upper sections respectively (Table 3.2.1b).

Organic carbon showed a similar distribution pattern to that of finer sediments in the core S-2 (Fig. 3.2.4d). Organic carbon was more than the average line in lower and upper sections, whereas in the middle section it was less than the average value.

Gurupur estuary

In core GP-2 (Table 3.2.1a), organic carbon percentage ranged from 0.41 % to 4.28 % (avg. 2.26 %). It varied from 1.34 % to 4.28 % (avg. 2.67 %) and 0.41 % to 2.47 % (avg. 1.90 %) in lower and upper sections respectively (Table 3.2.1b).

Organic carbon showed overall decreasing trend from bottom to surface of the core GP-2 with a negative peak at 12 cm (Fig. 3.2.4e).

When average values of sediment components of five estuaries were considered, sand and clay fluctuated from core VS-2 to GP-2. Sand was more than 30 % in cores VS-2, MD-2 and S-2, while clay was highest in the core VG-2 and least in the core S-2. Silt decreased from VS-2 to VG-2 and then increased up to GP-2 i.e. towards the South. Except core VG-2, silt was more than 40 % in rest of the cores. Along the study area, between cores VS-2 and GP-2, pH varied from 6.07 to 6.91, while organic carbon ranged from 1.19 to 2.29 %.

When the sediment components were compared among sections, average sand was higher in the middle section at cores VS-2, MD-2 and S-2. In case of cores VG-2 and GP-2, upper section showed higher sand than the lower section. Silt showed higher value in the upper section at cores VS-2, VG-2, MD-2 and GP-2. However, it showed higher value in the middle section at core S-2. Clay was higher in the upper section at core VS-2, however it maintained higher value in the lower section at cores VG-2, MD-2, S-2 and GP-2.

Using the average values of sand, silt and clay when different sections were compared, it was clear that sand and silt showed increase from lower to upper sections in cores VG-2 and GP-2, whereas a decrease in percentage of clay. This indicated increase in sediment size with time in these cores. In case of cores VS-2, MD-2 and S-2, sand increased while finer sediments decreased from lower to middle sections. However, upper section showed higher value of finer sediments and lower sand. The higher sand value in the middle section suggested additional input of sand material in these estuaries.

pH indicated decrease from lower to upper sections in cores VG-2, MD-2 and GP-2, while its values increased from lower to upper sections in the core S-2. pH was higher in the middle section of the core VS-2. Higher values of organic carbon were seen for the sections with higher finer sediments in cores VS-2 and S-2. In cores VG-2, MD-2 and GP-2, organic carbon was higher in the sections having higher concentration of clay.

In cores VS-2, MD-2 and S-2, increase in sand in the middle section was well represented in profiles (Fig. 3.2.1), which was compensated by decrease in finer sediments. In these cores, organic carbon also decreased in the middle section indicating its dilution by coarser sediments.

3.2.4 Bulk sediment chemistry

Major metals (Al, Fe and Mn)

Vashishti estuary

Metals viz. Al, Fe and Mn varied from 6.68 % to 9.33 % (avg. 8.20 %), 9.46 % to 19.87 % (avg. 15.01 %) and 1344 ppm to 2198 ppm (avg. 1702 ppm) respectively (Table 3.2.2a)

Table 3.2.2a Range and average concentration of major metals in cores VS-2, VG-2, MD-2, S-2 and GP-2

Sediment core	Al (%)			Fe (%)			Mn (ppm)		
	Range		Avg	Range		Avg	Range		Avg
	Min	Max		Min	Max		Min	Max	
VS-2	6.68	9.33	8.20	9.46	19.87	15.01	1344	2198	1702
VG-2	7.67	11.45	10.19	6.22	14.08	10.37	391	761	531
MD-2	5.33	10.20	7.62	10.76	21.33	15.67	1297	6839	3260
S-2	1.84	10.69	8.02	1.51	7.23	4.87	123	2547	1181
GP-2	0.08	15.24	10.18	5.44	14.93	7.86	112	309	157

Table 3.2.2b Section wise range and average concentration of major metals in cores VS-2, VG-2, MD-2, S-2 and GP-2, where L=Lower, M=Middle and U=Upper sections

Sediment core	Al (%)			Fe (%)			Mn (ppm)		
	Range		Avg	Range		Avg	Range		Avg
	Min	Max		Min	Max		Min	Max	
VS-2 (L)	6.74	8.84	8.06	9.46	10.76	10.04	1344	1882	1591
(M)	6.68	8.80	8.04	15.79	19.56	18.04	1566	1750	1654
(U)	7.24	9.33	8.35	13.17	19.87	16.59	1512	2198	1782
VG-2 (L)	7.67	10.76	9.63	6.22	11.01	8.66	391	761	550
(U)	8.21	11.45	10.71	9.76	14.08	11.97	457	656	514
MD-2 (L)	7.55	10.20	9.21	11.87	16.38	13.56	1379	2969	2119
(M)	5.33	8.77	6.31	10.76	16.70	14.16	1298	4920	2180
(U)	5.70	9.88	7.76	12.31	21.33	16.57	1710	6839	3833
S-2 (L)	9.89	10.69	10.40	6..06	7.23	6.52	1323	2072	1762
(M)	1.84	10.10	4.95	1.51	6.45	2.85	123	2547	603
(U)	8.03	9.75	8.86	4.41	6.07	5.15	656	1002	881
GP-2 (L)	4.80	13.93	9.58	5.44	14.93	7.16	112	226	159
(U)	0.08	15.24	10.72	6.15	10.42	8.49	122	309	154

Table 3.2.2c Range and average concentration of trace metals in cores VS-2, VG-2, MD-2, S-2 and GP-2

Sediment core	Ni (ppm)			Co (ppm)			Cu (ppm)			Zn (ppm)			Cr (ppm)		
	Range		Avg	Range		Avg	Range		Avg	Range		Avg	Range		Avg
	Min	Max		Min	Max		Min	Max		Min	Max		Min	Max	
VS-2	60	167	116	36	79	61	313	382	345	378	548	453	135	183	160
VG-2	87	127	111	52	84	71	210	410	293	85	103	94	119	239	160
MD-2	39	118	76	20	38	29	18	117	40	261	3720	1179	156	438	252
S-2	37	148	103	5	54	27	65	190	141	21	100	72	66	183	132
GP-2	33	199	65	24	57	31	18	43	32	75	400	161	309	1602	680

Table 3.2.2d Section wise range and average concentration of trace metals in cores VS-2, VG-2, MD-2, S-2 and GP-2, where L=Lower, M=Middle and U=Upper sections

Sediment core	Ni (ppm)			Co (ppm)			Cu (ppm)			Zn (ppm)			Cr (ppm)		
	Range		Avg	Range		Avg	Range		Avg	Range		Avg	Range		Avg
	Min	Max		Min	Max		Min	Max		Min	Max		Min	Max	
VS-2 (L)	133	167	148	36	73	54	334	367	351	426	548	469	152	171	160
(M)	82	149	128	50	65	59	320	362	337	446	543	473	151	174	162
(U)	60	163	93	53	79	65	314	382	346	378	539	437	135	183	160
VG-2 (L)	87	128	108	52	84	68	210	410	285	90	103	97	119	155	143
(U)	106	121	115	65	78	73	269	344	301	85	98	92	139	239	175
MD-2 (L)	80	95	89	30	34	32	38	45	42	406	434	418	204	243	229
(M)	79	118	99	25	37	30	25	42	35	535	825	656	236	438	308
(U)	39	104	66	20	38	29	18	117	42	261	3721	1495	156	337	238
S-2 (L)	105	148	131	17	54	33	172	190	179	89	101	94	161	183	170
(M)	37	138	69	6	33	21	65	173	97	22	90	46	66	166	92
(U)	94	122	109	20	38	30	129	147	138	66	85	75	111	137	119
GP-2 (L)	44	104	53	24	33	28	23	43	32	75	193	163	309	646	396
(U)	33	199	76	26	57	34	18	43	31	101	400	160	463	1603	935

in the core VS-2. In the lower section (Table 3.2.2b), Al, Fe and Mn varied from 6.74 % to 8.84 % (avg. 8.06 %), 9.46 % to 10.76 % (avg. 10.04 %) and 1344 ppm to 1882 ppm (avg. 1591 ppm) respectively, whereas in the middle section, Al, Fe and Mn ranged from 6.68 % to 8.80 % (avg. 8.04 %), 15.79 % to 19.56 % (avg. 18.04 %) and 1566 ppm to 1750 ppm (avg. 1654 ppm) respectively. In the upper section, Al, Fe and Mn ranged from 7.24 % to 9.33 % (avg. 8.35 %), 13.17 % to 19.87 % (avg. 16.59 %) and 1512 ppm to 2198 ppm (avg. 1782 ppm) respectively.

In core VS-2 (Fig. 3.2.5a), Al concentration fluctuated around an average line from bottom to surface. The concentration of Fe remained nearly constant in the lower section and was less than the average value, while it increased in the middle section and was more than the average value. Further in the upper section, not much variation was seen from 38 to 18 cm, followed by fluctuating trend towards the surface. Manganese showed lower values between 70 and 60 cm depth, almost constant trend in the middle section and overall increasing distribution pattern in the upper section.

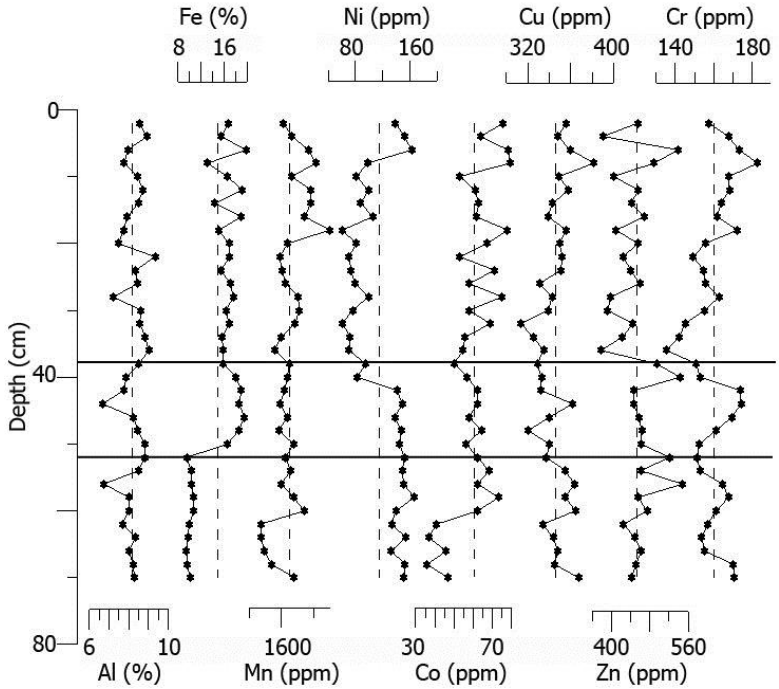

Fig. 3.2.5a Variation of Al, Fe, Mn, Ni, Co, Cu, Zn and Cr with average line in bulk sediments in the core VS-2.

Vaghotan estuary

In core VG-2, Al, Fe and Mn varied from 7.67 % to 11.45 % (avg. 10.19 %), 6.22 % to 14.08 % (avg. 10.37 %) and 391 ppm to 761 ppm (avg. 531 ppm) respectively (Table 3.2.2a). In the lower section (Table 3.2.2b), Al, Fe and Mn ranged from 7.67 % to 10.76 % (avg. 9.63 %), 6.22 % to 11.01 % (avg. 8.66 %) and 391 ppm to 761 ppm (avg. 550 ppm) respectively; while they varied from 8.21 % to 11.45 % (avg. 10.71 %), 9.76 % to 14.08 % (avg. 11.97 %) and 457 ppm to 656 ppm (avg. 514 ppm) respectively in the upper section.

Aluminium showed overall increase from lower to upper sections in the core VG-2 (Fig. 3.2.5b). Iron exhibited overall increasing trend from bottom to 10 cm and then decreased towards the surface. Manganese showed overall increasing trend from bottom to 34 cm and then decreased up to 10 cm. Further it showed increase towards the surface.

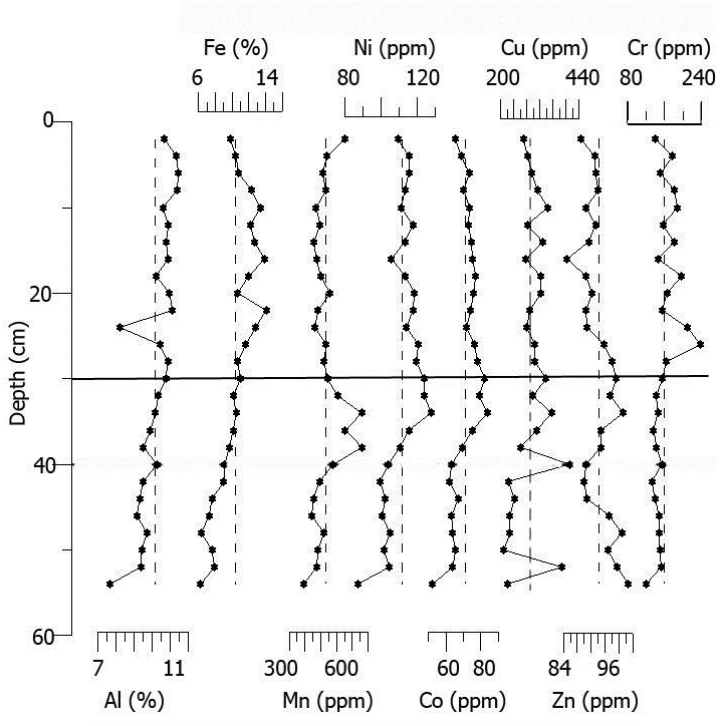

Fig. 3.2.5b Variation of Al, Fe, Mn, Ni, Co, Cu, Zn and Cr with average line in bulk sediments in the core VG-2.

Mandovi estuary

In core MD-2 (Table 3.2.2a), Al, Fe and Mn varied from 5.33 % to 10.20 % (avg. 7.62 %), 10.76 % to 21.33 % (avg. 15.67 %) and 1297 ppm to 6839 ppm (avg. 3260 ppm)

respectively. In the lower section (Table 3.2.2b), Al, Fe and Mn varied from 7.55 % to 10.20 % (avg. 9.21 %), 11.87 % to 16.38 % (avg. 13.56 %) and 1379 ppm to 2969 ppm (avg. 2119 ppm) respectively; while, in the middle section Al, Fe and Mn ranged from 5.33 % to 8.77 % (avg. 6.31 %), 10.76 % to 16.70 % (avg. 14.16 %) and 1298 ppm to 4920 ppm (avg. 2180 ppm) respectively. In the upper section, Al, Fe and Mn varied from 5.70 % to 9.88 % (avg. 7.76 %), 12.31 % to 21.33 % (avg. 16.57 %) and 1710 ppm to 6839 ppm (avg. 3833 ppm) respectively.

Aluminium showed overall decrease from lower to middle section of the core MD-2 (Fig. 3.2.5c). Its concentration was more than average value in the lower section and was less than the average value in the middle section. In the upper section, it increased from 56 to 52 cm and then decreased up to 8 cm. Thereafter, its concentration increased towards the surface. Iron and manganese exhibited overall increase from bottom to 44 cm. Further, concentration of Fe decreased towards the surface, while Mn decreased up to 8 and then increased towards the surface.

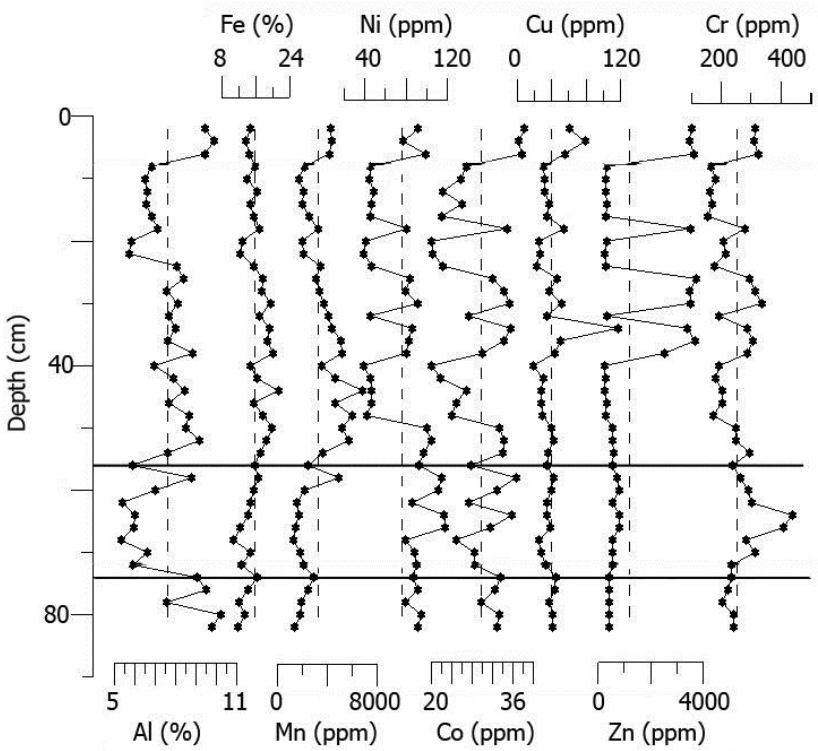

Fig. 3.2.5c Variation of Al, Fe, Mn, Ni, Co, Cu, Zn and Cr with average line in bulk sediments in the core MD-2.

Sharavathi estuary

In core S-2 (Table 3.2.2a), Al, Fe and Mn varied from 1.84 % to 10.69 % (avg. 8.02 %), 1.51 % to 7.23 % (avg. 4.87 %) and 123 ppm to 2547 ppm (avg. 1181 ppm) respectively. In the lower section (Table 3.2.2b), Al, Fe and Mn varied from 9.89 % to 10.69 % (avg. 10.40 %), 6.06 % to 7.23 % (avg. 6.52 %) and 1323 ppm to 2072 ppm (avg. 1762 ppm) respectively, while in the middle section, Al, Fe and Mn ranged from 1.84 % to 10.10 % (avg. 4.95 %), 1.51 % to 6.45 % (avg. 2.85 %) and 123 ppm to 2547 ppm (avg. 603 ppm) respectively. In the upper section, Al, Fe and Mn varied from 8.03 % to 9.75 % (avg. 8.86 %), 4.41 % to 6.07 % (avg. 5.15 %) and 656 ppm to 1002 ppm (avg. 881 ppm) respectively.

Metals viz. Al, Fe and Mn did not show much variation in the lower section and were more than the average value in the core S-2 (Fig. 3.2.5d). In the middle section, these metals decreased from 32 to 28 cm. Further, concentration of Al increased up to 10 cm, while Fe and Mn remained nearly constant up to 14 cm and then increased up to 10 cm. The concentration of these metals was less than the average value in the middle section. In the upper section, these metals showed overall increase towards the surface.

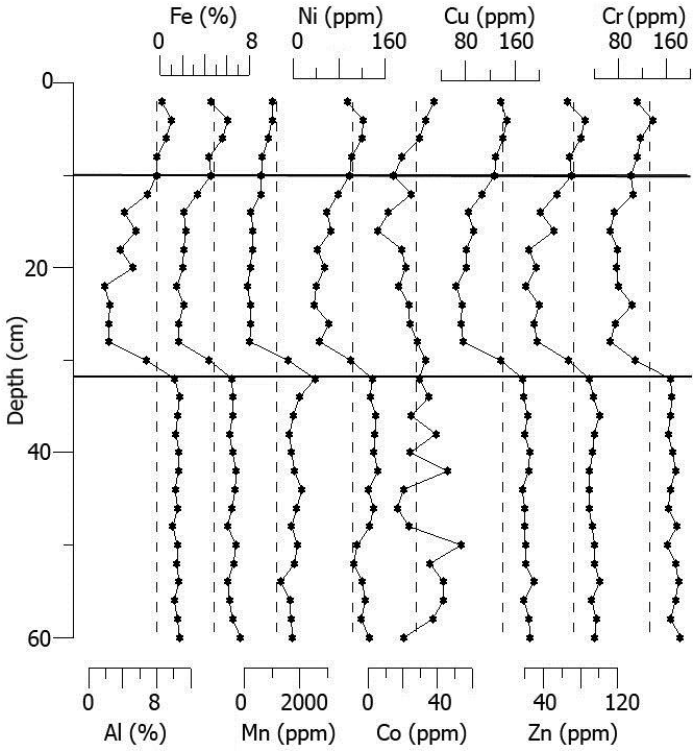

Fig. 3.2.5d Variation of Al, Fe, Mn, Ni, Co, Cu, Zn and Cr with average line in bulk sediments in the core S-2.

Gurupur estuary

In core GP-2 (Table 3.2.2a), Al, Fe and Mn varied from 0.08 % to 15.24 % (avg. 10.18 %), 5.44 % to 14.93 % (avg. 7.86 %) and 112 ppm to 309 ppm (avg. 157 ppm) respectively. In the lower section (Table 3.2.2b), Al, Fe and Mn ranged from 4.80 % to 13.93 % (avg. 9.58 %), 5.44 % to 14.93 % (avg. 7.16 %) and 112 ppm to 226 ppm (avg. 159 ppm) respectively, while in the upper section, Al, Fe and Mn varied from 0.08 % to 15.24 % (avg. 10.72 %), 6.15 % to 10.42 % (avg. 8.49 %) and 122 ppm to 309 ppm (avg. 154 ppm) respectively.

In core GP-2, Al showed overall increase from lower to upper sections, with sharp decreasing peak at 8 cm (Fig. 3.2.5e). Iron did not show much variation in the lower section, except at 46 cm where it showed a prominent increasing peak and increasing trend from 32 cm to surface in the upper section. Manganese concentration showed fluctuating decreasing trend in the lower section, but Mn did not show much variation in the upper section. However, at 12 cm and surface, Mn showed prominent increasing peaks. The distribution pattern of Mn was slightly similar to sand.

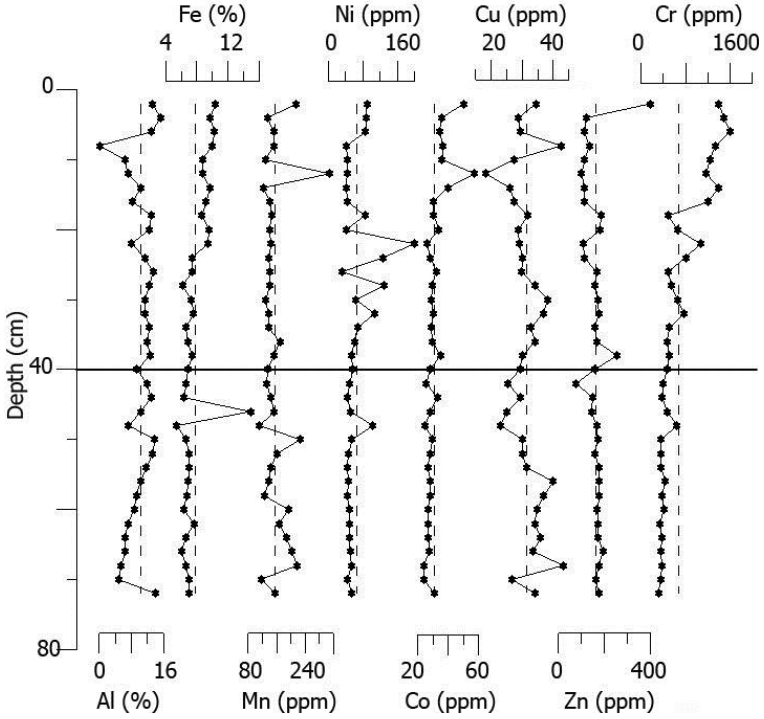

Fig. 3.2.5e Variation of Al, Fe, Mn, Ni, Co, Cu, Zn and Cr with average line in bulk sediments in the core GP-2.

Trace metals (Ni, Co, Cu, Zn and Cr)

Vashishti estuary

In core VS-2 (Table 3.2.2c), Ni, Co, Cu, Zn and Cr varied from 60 ppm to 167 ppm (avg. 116 ppm), 36 ppm to 79 ppm (avg. 61 ppm), 313 ppm to 382 ppm (avg. 345 ppm), 378 ppm to 548 ppm (avg. 453 ppm) and 135 ppm to 183 ppm (avg. 160 ppm) respectively. In the lower section (Table 3.2.2d), Ni, Co, Cu, Zn and Cr varied from 133 ppm to 167 ppm (avg. 148 ppm), 36 ppm to 73 ppm (avg. 54 ppm), 334 ppm to 367 ppm (avg. 351 ppm), 426 ppm to 548 ppm (avg. 469 ppm) and 152 ppm to 171 ppm (avg. 160 ppm) respectively, whereas in the middle section, Ni, Co, Cu, Zn and Cr ranged from 82 ppm to 149 ppm (avg. 128 ppm), 50 ppm to 65 ppm (avg. 59 ppm), 320 ppm to 362 ppm (avg. 337 ppm), 446 ppm to 543 ppm (avg. 473 ppm) and 151 ppm to 174 ppm (avg. 162 ppm) respectively. In the upper section, Ni, Co, Cu, Zn and Cr varied from 60 ppm to 163 ppm (avg. 93 ppm), 53 ppm to 79 ppm (avg. 65 ppm), 314 ppm to 382 ppm (avg. 346 ppm), 378 ppm to 539 ppm (avg. 437 ppm) and 135 ppm to 183 ppm (avg. 160 ppm) respectively.

Nickel did not show much variation from bottom to 42 cm but maintained more than the average value in the core VS-2 (Fig. 3.2.5a). Further, it decreased at 40 cm and up to 8 cm its concentration was less than the average value. From 8 to 6 cm, a sharp increase in Ni was observed, followed by decrease towards the surface. Cobalt showed fluctuations with overall increasing distribution pattern from bottom to surface. Metals viz. Cu and Cr fluctuated around the average line and showed overall increasing trend towards the surface in the top 20 cm. The concentration of Zn exhibited constant trend along the average line up to 40 cm followed by decrease from 40 to 36 cm and then showed gradual increase.

Vaghotan estuary

In core VG-2 (Table 3.2.2c), Ni, Co, Cu, Zn and Cr ranged from 87 ppm to 127 ppm (avg. 111 ppm), 52 ppm to 84 ppm (avg. 71 ppm), 210 ppm to 410 ppm (avg. 293 ppm), 85 ppm to 103 ppm (avg. 94 ppm) and 119 ppm to 239 ppm (avg. 160 ppm), respectively. In the lower section (Table 3.2.2d), Ni, Co, Cu, Zn and Cr ranged from 87 ppm to 128 ppm (avg. 108 ppm), 52 ppm to 84 ppm (avg. 68 ppm), 210 ppm to 410 ppm (avg. 285 ppm), 90 ppm to 103 ppm (avg. 97 ppm) and 119 ppm to 155 ppm (avg. 143 ppm) respectively. On the other hand,

in the upper section, Ni, Co, Cu, Zn and Cr varied from 106 ppm to 121 ppm (avg. 115 ppm), 65 ppm to 78 ppm (avg. 73 ppm), 269 ppm to 344 ppm (avg. 301 ppm), 85 ppm to 98 ppm (avg. 92 ppm) and 139 ppm to 239 ppm (avg. 175 ppm) respectively.

Metals viz. Ni, Co and Cu showed overall increase from bottom to 34 cm and then showed gradual decrease towards the surface of the core VG-2 (Fig. 3.2.5b). Zinc fluctuated from bottom to 34 cm which was followed by decreasing trend towards the surface. Chromium did not exhibit much variation from bottom to 28 cm, followed by positive peak at 26 cm. Further, it showed fluctuations along average line.

Mandovi estuary

In core MD-2 (Table 3.2.2c), Ni, Co, Cu, Zn and Cr ranged from 39 ppm to 118 ppm (avg. 76 ppm), 20 ppm to 38 ppm (avg. 29 ppm), 18 ppm to 117 ppm (avg. 40 ppm), 261 ppm to 3720 ppm (avg. 1179 ppm) and 156 ppm to 438 ppm (avg. 252 ppm) respectively. In the lower section (Table 3.2.2d), Ni, Co, Cu, Zn and Cr varied from 80 ppm to 95 ppm (avg. 89 ppm), 30 ppm to 34 ppm (avg. 32 ppm), 38 ppm to 45 ppm (avg. 42 ppm), 406 ppm to 434 ppm (avg. 418 ppm) and 204 ppm to 243 ppm (avg. 229 ppm) respectively; while in the middle section, Ni, Co, Cu, Zn and Cr ranged from 79 ppm to 118 ppm (avg. 99 ppm), 25 ppm to 37 ppm (avg. 30 ppm), 25 ppm to 42 ppm (avg. 35 ppm), 535 ppm to 825 ppm (avg. 656 ppm) and 236 ppm to 438 ppm (avg. 308 ppm) respectively. In the upper section, Ni, Co, Cu, Zn and Cr ranged from 39 ppm to 104 ppm (avg. 66 ppm), 20 ppm to 38 ppm (avg. 29 ppm), 18 ppm to 117 ppm (avg. 42 ppm), 261 ppm to 3721 ppm (avg. 1495 ppm) and 156 ppm to 337 ppm (avg. 238 ppm) respectively.

Metals viz. Ni and Co did not show much variation in the lower section of the core MD-2 (Fig. 3.2.5c). Further, they exhibited fluctuations in the middle section. From 32 to 8 cm they showed fluctuating decreasing trend and then increased towards the surface. Copper maintained along the average line up to 8 cm, however sharp increasing peak was seen at 34 cm. Further, it showed overall increase towards the surface in the top 8 cm. Zinc concentration remained nearly constant from bottom to 40 cm, followed by wide fluctuations up to 6 cm and further, remained almost constant towards the surface with higher value. Chromium maintained almost constant concentration in the lower section which was followed by increase in the middle section. In the upper section, its concentration decreased

up to 8 cm and then sharply increased at 6 cm, followed by constant value towards the surface.

Sharavathi estuary

In core S-2 (Table 3.2.2c), Ni, Co, Cu, Zn and Cr varied from 37 ppm to 148 ppm (avg. 103 ppm), 5 ppm to 54 ppm (avg. 27 ppm), 65 ppm to 190 ppm (avg. 141 ppm), 21 ppm to 100 ppm (avg. 72 ppm) and 66 ppm to 183 ppm (avg. 132 ppm) respectively. In the lower section (Table 3.2.2d), Ni, Co, Cu, Zn and Cr varied from 105 ppm to 148 ppm (avg. 131 ppm), 17 ppm to 54 ppm (avg. 33 ppm), 172 ppm to 190 ppm (avg. 179 ppm), 89 ppm to 101 ppm (avg. 94 ppm) and 161 ppm to 183 ppm (avg. 170 ppm) respectively, while in the middle section, Ni, Co, Cu, Zn and Cr ranged from 37 ppm to 138 ppm (avg. 69 ppm), 6 ppm to 33 ppm (avg. 21 ppm), 65 ppm to 173 ppm (avg. 97 ppm), 22 ppm to 90 ppm (avg. 46 ppm) and 66 ppm to 166 ppm (avg. 92 ppm) respectively. In the upper section, Ni, Co, Cu, Zn and Cr varied from 94 ppm to 122 ppm (avg. 109 ppm), 20 ppm to 38 ppm (avg. 30 ppm), 129 ppm to 147 ppm (avg. 138 ppm), 66 ppm to 85 ppm (avg. 75 ppm) and 111 ppm to 137 ppm (avg. 119 ppm) respectively.

Nickel exhibited overall increasing trend in the lower section of the core S-2, whereas Cu, Zn and Cr maintained nearly constant concentration in this section (Fig. 3.2.5d) with higher than average value. In the middle section, these metals decreased from 32 to 28 cm, followed by increase up to 10 cm. Further, these metals showed increase towards the surface. Cobalt exhibited fluctuating trend in the lower section and was largely more than the average value which decreased to less than the average value in the middle section. It increased towards the surface in the upper section.

Gurupur estuary

In core GP-2 (Table 3.2.2c), Ni, Co, Cu, Zn and Cr varied from 33 ppm to 199 ppm (avg. 65 ppm), 24 ppm to 57 ppm (avg. 31 ppm), 18 ppm to 43 ppm (avg. 32 ppm), 75 ppm to 400 ppm (avg. 161 ppm) and 309 ppm to 1602 ppm (avg. 680 ppm) respectively. In the lower section (Table 3.2.2d), Ni, Co, Cu, Zn and Cr varied from 44 ppm to 104 ppm (avg. 53 ppm), 24 ppm to 33 ppm (avg. 28 ppm), 23 ppm to 43 ppm (avg. 32 ppm), 75 ppm to 193 ppm (avg. 163 ppm) and 309 ppm to 646 ppm (avg. 396 ppm) respectively, while in the upper section

Ni, Co, Cu, Zn and Cr ranged from 33 ppm to 199 ppm (avg. 76 ppm), 26 ppm to 57 ppm (avg. 34 ppm), 18 ppm to 43 ppm (avg. 31 ppm), 101 ppm to 400 ppm (avg. 160 ppm) and 463 ppm to 1603 ppm (avg. 935 ppm) respectively.

Nickel did not vary in the lower section of the core GP-2, except at 48 cm it showed an increasing peak (Fig. 3.2.5e). In the upper section, Ni showed large fluctuations from 34 to 16 cm, followed by a constant trend up to 8 cm. Further, Ni increased towards the surface. Like Ni, the concentration of Co did not vary in the lower section. The concentration of Co was similar to sand and Mn in the upper section. Cobalt concentration was highest at 12 cm depth and coincided with sand and Mn peak at this depth. The fluctuating distribution pattern of Cu was observed in both the sections. Zinc concentration remained nearly constant in the lower section with prominent decreasing peak at 42 cm. In the upper section, Zn showed overall decrease up to 4 cm, followed by a sudden increase towards the surface. Like rest of the trace metals, Cr concentration did not vary in the lower section. However, in the upper section it showed overall increase towards the surface.

When the average values of major elements were considered, Al was highest in the core VG-2 and lowest in the core MD-2 (Table 3.2.2a). However, its value was also higher in the core GP-2. Metals viz. Fe and Mn were highest in the core MD-2. Iron was lowest in the core S-2, while Mn in the core GP-2.

When average values were compared between the sections (Table 3.2.2b) in core VS-2, Al and Mn were higher in the upper section, while Fe in the middle section. In core VG-2, Al and Fe were higher in the upper section, while Mn was higher in the lower section. In core MD-2, Al was higher in the lower section, while Fe and Mn remained higher in the upper section. In core S-2, all the three elements viz. Al, Fe and Mn were higher in the lower section. Metals viz. Al and Fe were higher in the upper section of the core GP-2, while Mn in the lower section.

In case of trace metals when five estuaries were compared highest value was recorded in core VS-2 for Ni, Cu and Zn, while in core VG-2 for Co (Table 3.2.2c). Chromium was highest in the core GP-2. Lowest value for Ni and Cu was seen in the core GP-2, whereas Co, Zn and Cr were lowest in the core S-2.

When the average value of the sections was compared (Table 3.2.2d), in core VS-2, Ni and Cu were highest in the lower section, whereas Zn and Cr in the middle section. Cobalt was highest in the upper section. In core VG-2, Ni, Co, Cu and Cr were highest in the upper section, while Zn was reported highest in the lower section. In case of core MD-2, Ni and Cr were highest in the middle section, Co in the lower section and Zn in the upper section. The value of Cu was equal in lower and upper sections and was highest in these sections. In core S-2, all the trace metals were highest in the lower section. In core GP-2, Ni, Co and Cr were highest in the upper section, while Cu and Zn remained highest in the lower section.

When the sediment components of five estuaries were compared at middle estuarine regions, it was noted that sand varied from 6.00 % to 38.75 %, while silt and clay ranged from 23.21 % to 45.24 % and 18.16 % to 70.71 % respectively (Table 3.2.1a). It was seen from the contour diagram (Fig. 3.2.6a) that sand and clay fluctuated from North to South in the middle estuarine mudflats along central west coast of India. Silt with initial decrease from Vashishti to Vaghotan estuaries, further exhibited overall increase up to Gurupur estuary. Sediment components in the middle region of the studied estuaries did not show systematic pattern, unlike lower estuarine region. The lower estuary is in free connection with the open sea and is dominated by marine processes regulated by waves and tides (Dalrymple et al. 1992), and the upper estuary is dominated by freshwater input derived from river and its tributaries. The middle estuary, however, is exposed to mixing of sea and river water and hence is subjected to greater variations in depositional processes. Among the studied estuaries, the length of estuaries from mouth to middle region were 21, 15, 19, 16 and 14 km in Vashishti, Vaghotan, Mandovi, Sharavathi and Gurupur estuaries respectively. The higher length indicated higher tidal range in the Vashishti estuary and lesser distance suggested lower tidal range in the Gurupur estuary. However, slightly lower distance from mouth to middle region in core VG-2 might be due to change in geomorphology. Further, more the tidal influence more is the mixing of fresh and saline water (US DA 1963) retaining finer sediments in suspension for a longer period of time which eventually coagulates and later settles down to form mudflats. Hence, larger tidal range helps in the formation of well-developed mudflats in the Vashishti estuary than the Gurupur estuary. With this approach higher finer sediments are expected in the estuaries towards North. In the present study, silt showed less variation among the estuaries, except the Vaghotan estuary. However, large variation in sand and clay was seen. Tambi and Jagbudi tributaries join Vashisthi in the middle estuarine region. The average water depth near the confluence point of Tambi and Vashishti was 10 m and near the

confluence point of Jagbudi and Vashisthi was 5 m (Nair et al. 1998). The more water depth near the confluence point of tributary and river suggests higher energy associated with runoff of the tributary. Higher energy runoff seem to have brought along with it coarser particles from surrounding catchment area into the middle region of the Vashishti estuary carrying away finer sediments. On the other hand, release of higher sand particles towards the Southern part of the study area from the parent rock, as discussed earlier must have increased sand percentage in Mandovi and Sharavathi estuaries. However, decrease in sand was observed in the Gurupur estuary. Therefore, factors viz. runoff from tributaries and catchment area geology may have resulted variation in sand and clay percentage in the present study.

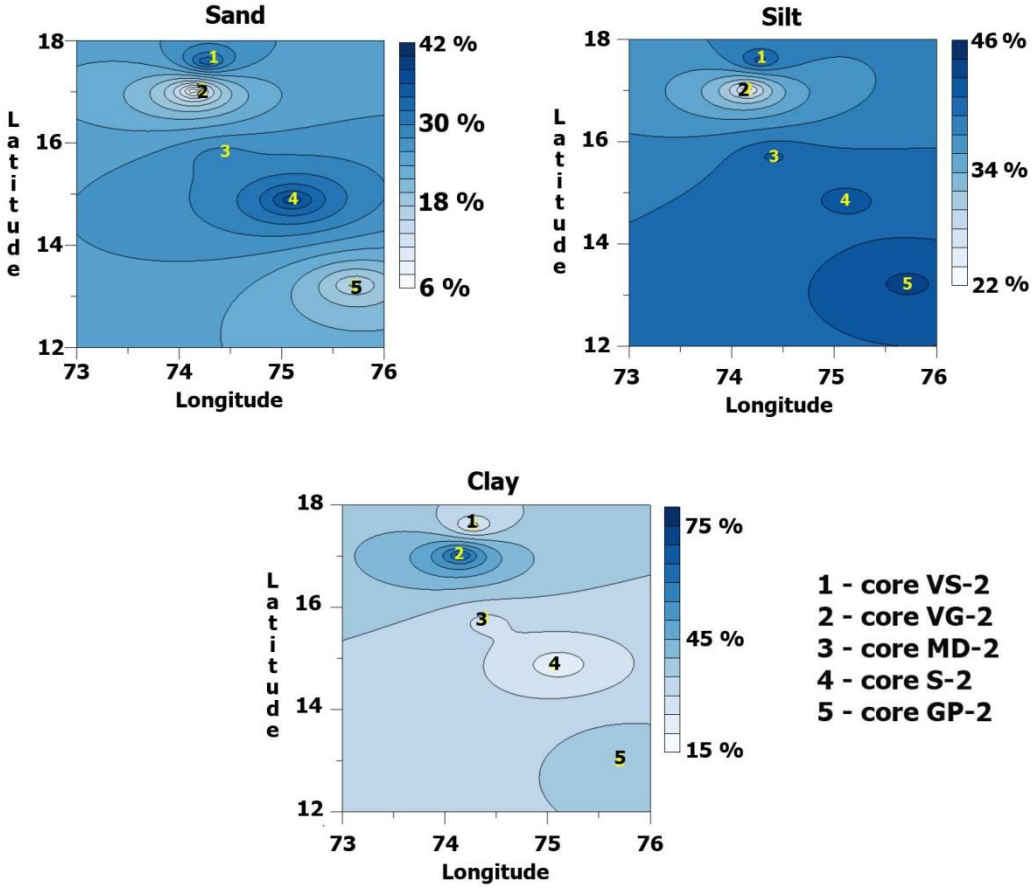

Fig. 3.2.6a Distribution of sediment components along the study area.

In the lower section of core VS-2 sand fluctuated around the average value, while was less than the average value in cores MD-2 and S-2 (Fig. 3.2.1). Further, sand percentage was more than the average value in the middle section of these cores. This suggested relatively higher hydrodynamic environment experienced by the middle section of cores VS-2, MD-2 and S-2. In the upper section, however sand decreased compared to the middle section in these cores. The higher percentage of sand in the middle section in cores VS-2 and MD-2 must have been

received during flood events which occurred in the past probably as a result of heavy rainfall. Further, sediment dredging for sand mining in the Sharavathi estuary might have decreased sand in the recent years. In the Vaghotan estuary, increase in sand percentage from lower to upper sections suggested higher hydrodynamic conditions in the recent years might be due to human activities in the catchment area. In case of the Gurupur estuary, sand did not show much variation between the sections, however percentage of silt increased in the upper section. It was already seen in the core GP-1, collected from the lower region of the Gurupur estuary, an increase in sand between 30 and 10 cm. This suggested that higher hydrodynamic conditions near the mouth of the estuary must have facilitated higher deposition of coarser sediments carrying away finer sediments (silt) towards the middle region (Siraswar and Nayak 2011).

pH at middle estuarine regions in five estuaries varied from 6.07 to 6.91 (Table 3.2.1a). It showed varying pattern from North to South along central west coast of India (Fig. 3.2.6b). In cores VG-2, MD-2 and GP-2 there was change in pH towards more acidic nature from bottom to surface, whereas in the core S-2, pH varied from acidic to basic nature. In the Vashishti estuary, however, pH varied with a small range.

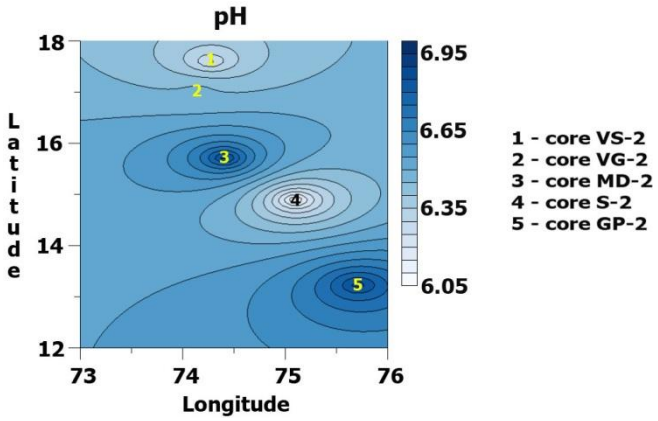

Fig. 3.2.6b Distribution of pH along the study area.

When organic carbon of five estuaries was compared at middle estuarine regions, it was observed that organic carbon varied from 1.19 % to 2.29 % (Table 3.2.1a). The percentage of organic carbon showed variation from Vashishti to Gurupur estuaries (Fig. 3.2.6c).

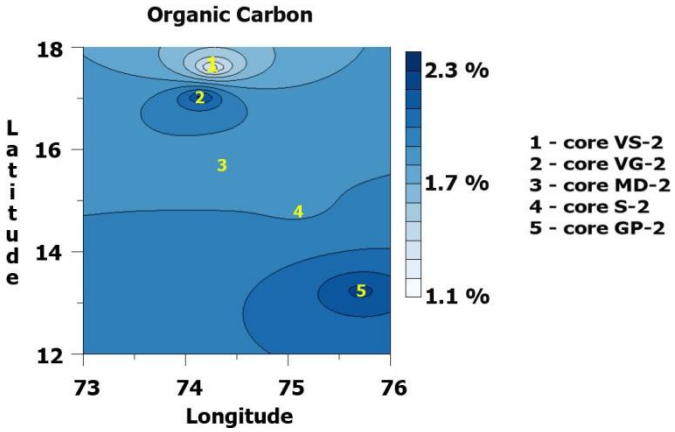

Fig. 3.2.6c Distribution of organic carbon along the study area.

The distribution pattern of organic carbon was similar to silt and clay in cores VS-2, MD-2 and S-2 suggesting its association with finer sediments. In core GP-2, organic carbon decreased from lower to upper sections, similar to clay. The similar distribution pattern of organic carbon to that of silt and/or clay in cores VS-2, MD-2, S-2 and GP-2 reflected the incorporation of organic matter into the finer fractions of sediment by adsorption phenomena (Keil et al. 1994) due to similar settling velocity (Raj et al. 2013) and larger surface area of finer sediments. In case of core VG-2, organic carbon was more than average value in the lower section and less than average value in the upper section, opposite to that of sand. This suggested that higher sand input in the upper section must have diluted the organic matter content.

In the present study, major metals in the bulk sediments varied with a range for Al from 7.62 % to 10.19 %, Fe from 4.87 % to 15.67 % and Mn from 157 ppm to 3260 ppm, while trace metals varied with a range for Ni from 65 ppm to 116 ppm, Co from 27 ppm to 71 ppm, Cu from 32 ppm to 345 ppm, Zn from 72 ppm to 453 ppm and Cr from 132 ppm to 680 ppm (Table 3.2.2a and c). Metals viz. Fe and Co along with Cu showed overall decrease from North to South in the middle region of estuaries along central west coast of India (Fig. 3.2.6d and e), while Cr exhibited overall increase towards the South. Rest of the metals, however showed fluctuating distribution pattern.

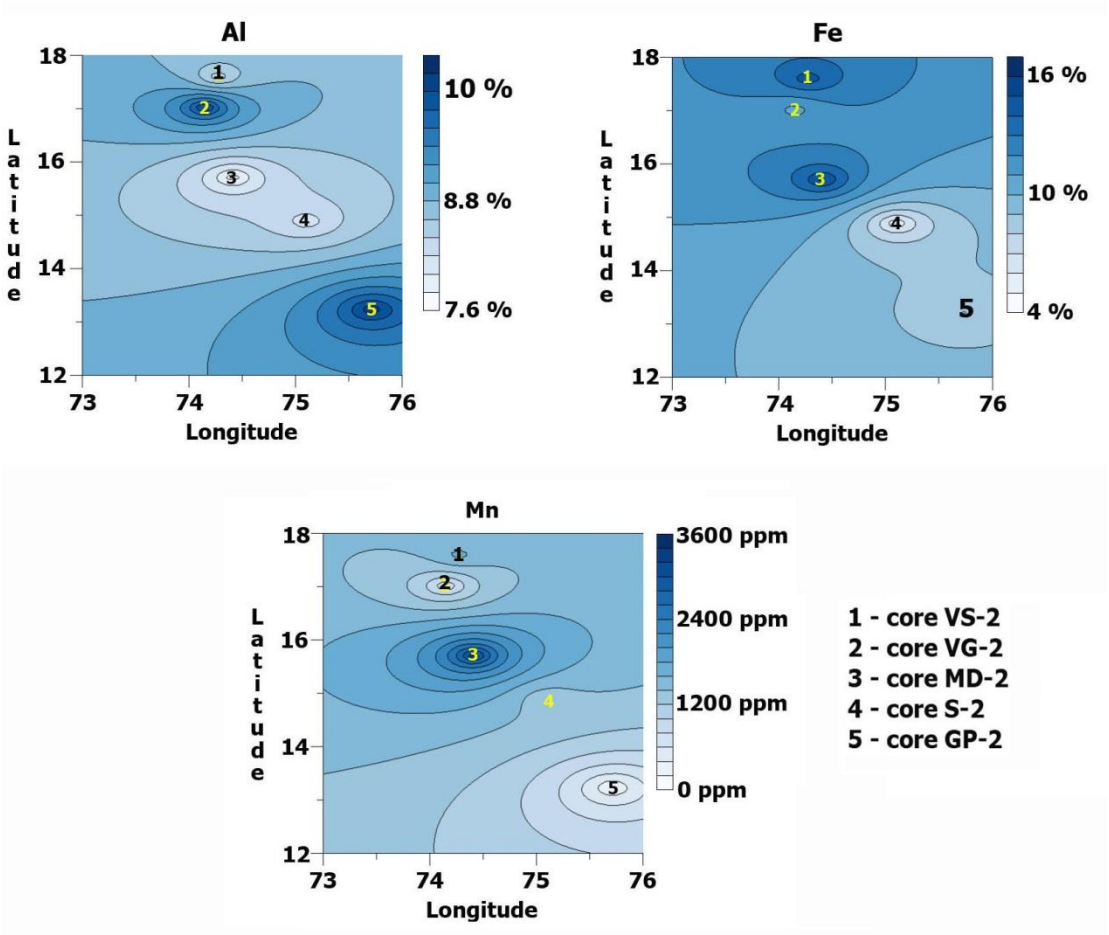

Fig. 3.2.6d Distribution of major metals in the bulk sediments along the study area.

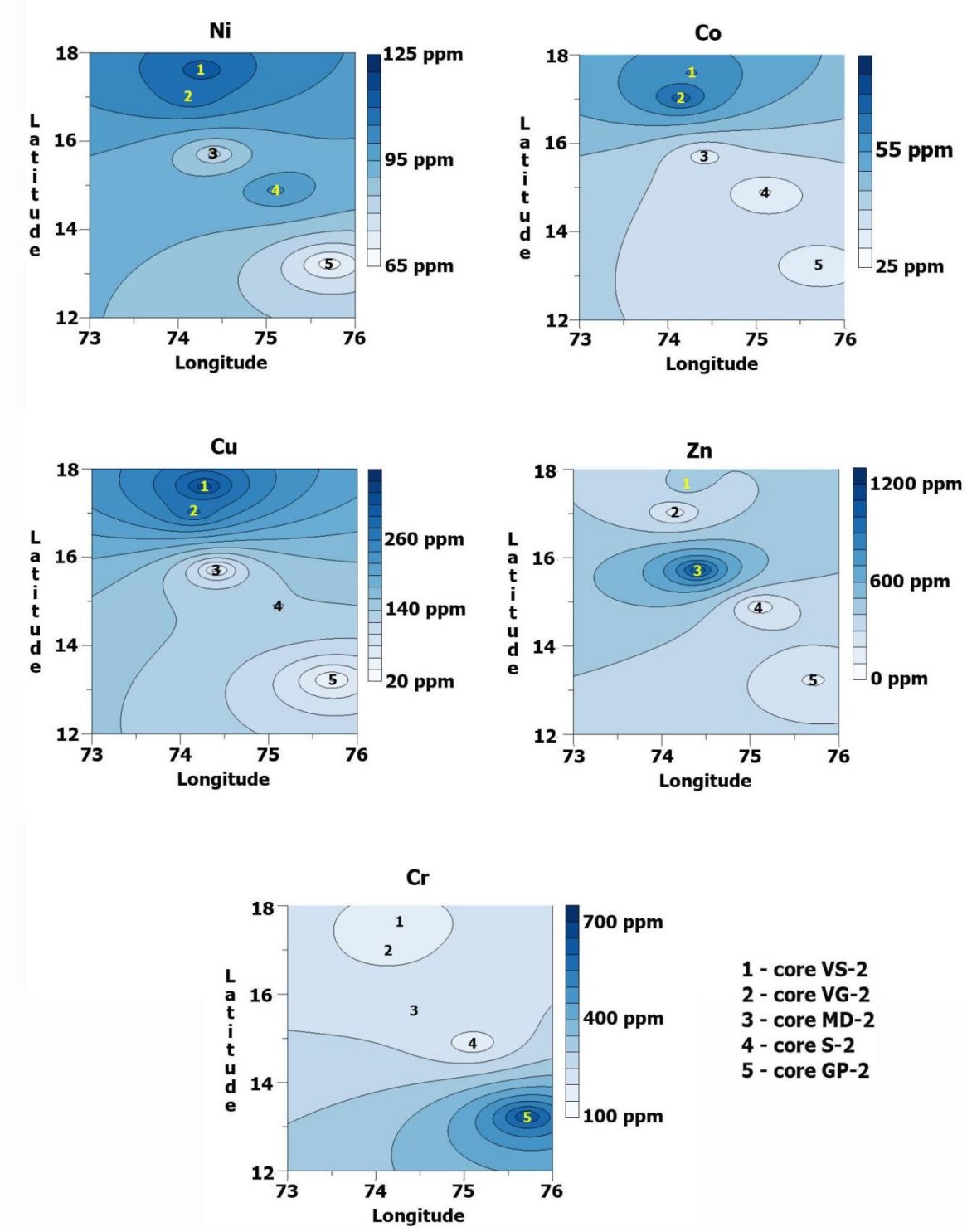

Fig. 3.2.6e Distribution of trace metals in the bulk sediments along the study area.

Pearson's correlation analysis of the core VS-2 (Table 3.2.3a) revealed significant correlation of sand with pH, Fe, Ni and Cr; silt with clay, organic carbon and Al; clay with organic carbon and Al; and organic carbon with Al. Further, Fe exhibited significant correlation with

Co, while Mn with Co, Cu and Cr. Also, Ni with Zn and Cr; and Cu with Cr showed significant correlation.

Table 3.2.3a Correlation between sediment components, pH, organic carbon and metals in bulk sediments in core VS-2 (n=35). Values in bold indicates significant correlation at $p<0.05$

	Sand (%)	Silt (%)	Clay (%)	Org C (%)	pH	Al (%)	Fe (%)	Mn (ppm)	Ni (ppm)	Co (ppm)	Cu (ppm)	Zn (ppm)	Cr (ppm)
Sand (%)	1.00												
Silt (%)	**-0.99**	1.00											
Clay (%)	**-0.95**	**0.89**	1.00										
Org C (%)	**-0.81**	**0.79**	**0.79**	1.00									
pH	**0.35**	**-0.35**	-0.32	-0.20	1.00								
Al (%)	**-0.53**	**0.57**	**0.43**	**0.53**	-0.09	1.00							
Fe (%)	**0.38**	**-0.41**	-0.28	-0.20	0.12	0.04	1.00						
Mn (ppm)	0.06	-0.08	-0.02	0.01	-0.24	-0.05	0.31	1.00					
Ni (ppm)	**0.41**	**-0.38**	**-0.46**	**-0.40**	0.22	-0.23	**-0.38**	-0.27	1.00				
Co (ppm)	0.20	-0.22	-0.13	-0.03	-0.17	-0.22	**0.37**	**0.66**	-0.12	1.00			
Cu (ppm)	-0.02	0.03	0.05	-0.08	0.18	**-0.34**	-0.28	**0.35**	0.28	0.28	1.00		
Zn (ppm)	0.27	-0.27	-0.26	-0.28	-0.17	-0.31	-0.10	0.05	**0.35**	0.12	0.16	1.00	
Cr (ppm)	**0.50**	**-0.52**	**-0.44**	**-0.51**	0.19	**-0.52**	0.06	**0.44**	**0.38**	0.28	**0.58**	0.14	1.00

In core VS-2, similar distribution pattern of Fe, Mn, Co, Cu and Cr, and good correlation of Co, Cu and Cr with Mn, and Co with Fe suggested adsorption of Co, Cu and Cr onto Fe and/or Mn oxy-hydroxides. Further, Fe, Ni and Cr showed good correlation with sand in this core. According to Achyuthan et al. (2002), in the sediments of estuarine and near shore regions, iron oxide (hematite) occurs as a coating of 5-7 μm size around the coarser quartz and feldspar grains which could facilitate adsorption of Ni and Cr onto coarser sediments. Although, clay and silt fractions of the sediments and organic matter have been considered as the main adsorbing agents for metals, the contribution of the coarser fraction of the sediments cannot be ignored (Jain and Ram 1997). Presence of Lote Parshuram industrial estate in proximity of the middle estuary makes it prone to maximum effect of industrial wastes which might have accumulated in the surrounding mudflat sediments. It further suggested that excess metals from non-natural sources may have accumulated in the sand-sized fraction. Zinc seemed to be from different source may be anthropogenic. The significant correlation of Al with silt and clay indicated that the finer sediments are lithogenous along with silicates.

The results of correlation analysis of the core VG-2 showed significant correlation of sand with Al, Fe and Cr; silt with Al; clay with pH and Zn; and pH with Zn (Table 3.2.3b). Among the metals, Al showed significant correlation with Fe, Ni, Co and Cu; while Fe with Ni, Co, Cu and Cr. Also, Mn exhibited significant correlation with Ni and Co. Further, Ni showed significant association with Co, Cu and Cr, while Co with Cu.

Table 3.2.3b Correlation between sediment components, pH, organic carbon and metals in bulk sediments in core VG-2 (n=27). Values in bold indicates significant correlation at $p<0.05$

	Sand (%)	Silt (%)	Clay (%)	Org C (%)	pH	Al (%)	Fe (%)	Mn (ppm)	Ni (ppm)	Co (ppm)	Cu (ppm)	Zn (ppm)	Cr (ppm)
Sand (%)	1.00												
Silt (%)	0.11	1.00											
Clay (%)	**-0.58**	**-0.87**	1.00										
Org C (%)	**-0.67**	-0.02	0.35	1.00									
pH	-0.35	**-0.41**	**0.50**	0.05	1.00								
Al (%)	**0.51**	**0.44**	**-0.57**	**-0.49**	**-0.46**	1.00							
Fe (%)	**0.81**	0.10	**-0.49**	**-0.76**	-0.15	**0.60**	1.00						
Mn (ppm)	-0.29	0.30	-0.09	0.21	0.15	0.22	0.02	1.00					
Ni (ppm)	0.24	0.18	-0.26	**-0.51**	0.06	**0.63**	**0.60**	**0.50**	1.00				
Co (ppm)	0.34	0.01	-0.17	**-0.52**	0.08	**0.58**	**0.67**	**0.38**	**0.92**	1.00			
Cu (ppm)	0.19	-0.03	-0.06	-0.22	-0.08	**0.41**	**0.40**	0.27	**0.49**	**0.47**	1.00		
Zn (ppm)	**-0.61**	-0.29	**0.54**	0.17	**0.49**	-0.35	**-0.58**	0.12	0.02	-0.09	-0.05	1.00	
Cr (ppm)	**0.46**	-0.09	-0.17	**-0.58**	-0.03	0.22	**0.54**	-0.16	**0.40**	0.38	0.31	-0.21	1.00

The increase in Al, Fe and Cr concentration in the recent years (upper section), similar to sand indicated their association with coarser sediments in the Vaghotan estuary. This was further verified from the correlation analysis where in good correlation of these metals with sand was observed. Metals viz. Mn, Ni, Co, Cu and Zn concentration decreased towards the surface that suggested diffusion of these metals in the recent years. Trace metals can be mobilized after their deposition and then relocalized in the sediment column (Gobeil and Cossa 1993) or diffuse to the water column (Morfett et al. 1998). Trace metals showed good correlation with Fe and/or Mn suggesting their adsorption onto Fe and/or Mn oxy-hydroxides. According to Duchart et al. (1973), trace metals are first sorbed or precipitated onto the Fe/Mn oxides forming films or layers near the sediment surface. Zinc distribution seemed to be regulated by clay and influenced by pH.

The results of correlation analysis of the core MD-2 (Table 3.2.3c) revealed significant correlation of sand with Ni and Cr; silt with clay and organic carbon; clay with organic carbon, Al and Mn; and organic carbon with Al. Among the metals, Al showed significant correlation with Fe, Mn, Co, Cu and Zn, while Fe with Mn and Zn. Further, all the trace metals showed significant correlation with each other.

In case of core MD-2, concentration of Al and Mn was low in the middle section, similar to clay. Also, these elements showed significant correlation with clay. This indicated dilution of these metals by higher coarser sediments in the middle section. However, distribution of rest of the metals did not seem to be influenced by higher sand percentage in the middle section. Higher Cr in this section was associated with coarser sediments. In the upper section (from 56 to 8 cm), trace metals viz. Ni, Co, Zn and Cr exhibited wide fluctuations in their distribution

pattern suggesting their mobilization from sediments. Further, increase in metal concentration (except Fe) in the top 8 cm suggested their adsorption in oxic conditions. However, Mandovi estuary being a reservoir of mining wastes, addition of metals in the recent years from mining related activities cannot be ignored. Also, sewage sludge dump sites, municipal waste discharge, antifouling paints, agricultural and industrial wastes contributed additional input. Further, the significant correlation among the trace metals suggested their similar source or similar enrichment mechanism (Bibi et al. 2007).

Table 3.2.3c Correlation between sediment components, pH, organic carbon and metals in bulk sediments in core MD-2 (n=41). Values in bold indicates significant correlation at $p<0.05$

	Sand (%)	Silt (%)	Clay (%)	Org C (%)	pH	Al (%)	Fe (%)	Mn (ppm)	Ni (ppm)	Co (ppm)	Cu (ppm)	Zn (ppm)	Cr (ppm)
Sand (%)	1.00												
Silt (%)	**-0.81**	1.00											
Clay (%)	**-0.85**	**0.38**	1.00										
Org C (%)	**-0.67**	**0.51**	**0.61**	1.00									
pH	0.07	-0.07	-0.04	-0.08	1.00								
Al (%)	**-0.56**	0.30	**0.61**	**0.56**	0.10	1.00							
Fe (%)	-0.27	0.28	0.17	0.08	0.04	**0.32**	1.00						
Mn (ppm)	**-0.37**	0.23	**0.39**	0.21	-0.07	**0.54**	**0.77**	1.00					
Ni (ppm)	**0.43**	**-0.37**	**-0.35**	-0.23	0.16	0.22	0.01	-0.09	1.00				
Co (ppm)	0.01	-0.01	0.03	0.12	-0.01	**0.54**	0.23	0.20	**0.82**	1.00			
Cu (ppm)	-0.25	0.13	0.27	0.26	-0.22	**0.42**	0.26	0.24	**0.37**	**0.65**	1.00		
Zn (ppm)	-0.19	0.17	0.14	0.15	**-0.43**	**0.32**	**0.33**	0.29	**0.32**	**0.63**	**0.68**	1.00	
Cr (ppm)	**0.53**	**-0.45**	**-0.43**	**-0.47**	-0.19	0.02	0.04	-0.07	**0.78**	**0.69**	**0.37**	**0.55**	1.00

The correlation analysis results of the core S-2 showed significant correlation of sand with pH; silt with clay and organic carbon, and clay with organic carbon (Table 3.2.3d). Further, finer sediments and organic carbon showed significant correlation with all the metals. Among the metals, Al, Fe and Mn exhibited significant correlation with all the trace metals. Also, trace metals showed significant correlation among themselves.

The distribution patterns of most of the trace elements agreed with the distribution patterns of finer sediments and organic carbon in the core S-2 which suggested that sediment grain size regulates the vertical distribution of metals. Association of metals with finer sediment particles was attributed to co-precipitation and complexation of metals on particle surfaces and this determines the distribution pattern of metals in sediments (Ho et al. 2010). These trace metals, along with finer sediments and organic carbon, showed significant positive correlation with Al. Aluminium is a geochemical proxy and a strong correlation of it with metals further suggested that particle size contributes significantly to the variations of these elements (Zhang et al. 2007). Further, a similar point-to-point distribution of Fe and Mn was

observed from bottom to 14 cm depth in the core S-2. This was supported by strong positive correlation between Fe and Mn which Jonathan et al. (2010) attributed to the strong association of the geochemical matrix between Fe and Mn. From the overall distribution pattern, a prominent increase in concentration of Fe from 14 cm towards the surface was seen which must be the result of higher supply during recent years or remobilization of Fe which later associated with finer sediments and organic carbon in surface section.

Table 3.2.3d Correlation between sediment components, pH, organic carbon and metals in bulk sediments in core S-2 (n=30). Values in bold indicates significant correlation at $p<0.05$

	Sand (%)	Silt (%)	Clay (%)	Org C (%)	pH	Al (%)	Fe (%)	Mn (ppm)	Ni (ppm)	Co (ppm)	Cu (ppm)	Zn (ppm)	Cr (ppm)
Sand (%)	1.00												
Silt (%)	**-0.93**	1.00											
Clay (%)	**-0.69**	**0.36**	1.00										
Org C (%)	**-0.81**	**0.65**	**0.75**	1.00									
pH	**0.37**	-0.24	**-0.46**	-0.35	1.00								
Al (%)	**-0.77**	**0.61**	**0.75**	**0.97**	**-0.46**	1.00							
Fe (%)	**-0.83**	**0.68**	**0.75**	**0.97**	**-0.42**	**0.97**	1.00						
Mn (ppm)	**-0.79**	**0.72**	**0.56**	**0.89**	**-0.41**	**0.87**	**0.92**	1.00					
Ni (ppm)	**-0.76**	**0.65**	**0.62**	**0.94**	**-0.38**	**0.95**	**0.95**	**0.89**	1.00				
Co (ppm)	**-0.49**	**0.36**	**0.51**	**0.54**	-0.27	**0.48**	**0.52**	**0.50**	**0.43**	1.00			
Cu (ppm)	**-0.83**	**0.68**	**0.75**	**0.97**	**-0.49**	**0.97**	**0.98**	**0.93**	**0.95**	**0.54**	1.00		
Zn (ppm)	**-0.80**	**0.65**	**0.72**	**0.96**	**-0.47**	**0.97**	**0.98**	**0.89**	**0.95**	**0.51**	**0.99**	1.00	
Cr (ppm)	**-0.86**	**0.72**	**0.74**	**0.92**	**-0.49**	**0.90**	**0.95**	**0.91**	**0.89**	**0.54**	**0.96**	**0.93**	1.00

The correlation analysis results of the core GP-2 revealed significant correlation of sand with Mn and Co; silt with Ni and Cr; clay with organic carbon and pH, and organic carbon with pH and Cu (Table 3.2.3e). Also, pH showed significant correlation with Cu. Among the metals, Fe exhibited significant correlation with Co and Cr, while Mn with Co. In addition, Co showed significant correlation with Cr, while Cu with Zn.

Table 3.2.3e Correlation between sediment components, pH, organic carbon and metals in bulk sediments in core GP-2 (n=36). Values in bold indicates significant correlation at $p<0.05$

	Sand (%)	Silt (%)	Clay (%)	Org C (%)	pH	Al (%)	Fe (%)	Mn (ppm)	Ni (ppm)	Co (ppm)	Cu (ppm)	Zn (ppm)	Cr (ppm)
Sand (%)	1.00												
Silt (%)	**-0.46**	1.00											
Clay (%)	**-0.38**	**-0.65**	1.00										
Org C (%)	**-0.41**	-0.01	**0.36**	1.00									
pH	-0.11	**-0.39**	**0.51**	**0.68**	1.00								
Al (%)	**-0.37**	0.05	0.27	-0.03	-0.21	1.00							
Fe (%)	0.04	0.31	**-0.35**	-0.32	**-0.48**	0.01	1.00						
Mn (ppm)	**0.49**	-0.27	-0.14	-0.19	0.09	-0.13	0.02	1.00					
Ni (ppm)	-0.15	**0.43**	-0.32	-0.14	-0.26	0.14	0.06	-0.15	1.00				
Co (ppm)	**0.38**	0.11	**-0.44**	**-0.58**	**-0.56**	0.08	**0.40**	**0.51**	-0.10	1.00			
Cu (ppm)	**-0.45**	0.25	0.13	**0.43**	**0.36**	-0.17	-0.25	-0.02	-0.03	-0.29	1.00		
Zn (ppm)	-0.32	0.14	0.13	0.25	0.17	0.19	-0.04	0.21	-0.04	0.21	**0.36**	1.00	
Cr (ppm)	0.07	**0.48**	**-0.57**	**-0.61**	**-0.69**	-0.07	**0.57**	0.02	0.27	**0.63**	-0.22	-0.13	1.00

A gradual increase in Fe concentration towards the surface in the core GP-2 must be due to additional supply from industrial input (Bhagure and Mirgane 2010) in the recent years. Iron was associated with silt at this location. The slight similarity in Mn and sand distribution patterns along with a peak value at 12 cm depth in the core GP-2 indicated association of Mn with coarser sediments. This was also supported by the significant positive correlation of Mn with sand. In core GP-2, Fe and Mn exhibited different distribution pattern and insignificant correlation (Table 2c), unlike core S-2. The differences in Fe and Mn distribution pattern and their associations could be due to difference in elemental behaviour with respect to physico-chemical conditions and source of supply (Volvoikar and Nayak 2013a). The similar distribution pattern of Co to that of sand in the core GP-2 suggested its association with coarser sediments. The significant correlation of Co with sand further supported their association (Table 2c). Also, significant correlation of Co with Mn was observed. Although metals are usually associated with finer fractions they have also been shown to accumulate on the surface of coarser materials like sand (Kljakovic-Gaspic et al. 2009) possibly when received from non-natural sources. The coarser sediments sometimes develop oxide coatings as they stay in place for a longer period of time (Tessier and Campbell 1982). This must have facilitated adsorption of Co onto the Mn oxide coatings on the sand grains (Badr et al. 2009). Iron also showed good correlation with Co, however its poor correlation with sand limits its role in the regulation of Co. The increase in Cr concentration towards the surface suggested its higher addition in recent years, probably from anthropogenic sources. Chromium showed good correlation with silt and Fe indicating their close association. Further, core GP-2 was in close proximity to the Baikhampady industrial area accommodating major refineries, storage of crude and finished petroleum products, LPG storage and bottling, fertilizer plant, pharmaceutical industry, brewery, edible oil processing units, sea food processing units, lead refining unit, cashew processing units, paint and dispersion unit, iron ore pelletization plant and pig iron plant apart from few engineering, fabrication, plywood plants and ready-mix plants (MOEF 2011). Although, these industries discharge their effluents through lined pipes into the Arabian Sea (Adiga and Poornananda 2013), there is no proper drainage system for storm water drains and surface runoff within the industrial cluster and the adjacent area. Since the topography of the area is sloping towards the river course, the storm water/surface runoff flow towards the Gurupur River through nalas/other natural drains (MOEF 2011). This must have caused anthropogenic addition of metals. However, the absence of elevated concentration of metals (except Fe and Cr) in the Gurupur estuary in the recent years indicated not much change in industrial effluent discharge with time. This may be mainly due

to the implementation of environmental protection policies, improvement in waste treatment systems and discharge of wastes into the Arabian Sea by the Karnataka state pollution control board (KSPCB) in co-ordination with the central pollution control board and Baikampady industrial cluster.

Further, in order to understand difference between estuaries in sediment components, pH, organic carbon, metals concentration in the bulk sediments, the data was plotted on the isocon diagram (Fig.3.2.7). On comparison of core VS-2 with core VG-2, sand, silt, Fe, Mn Cu and Zn were higher in the core VS-2, while clay, organic carbon, Al and Co were higher in the core VG-2. Nickel was slightly higher in the core VS-2, while pH in the core VG-2. The concentration of Cr was equal in both the cores. The comparison of cores VS-2 and MD-2 indicated higher sand, Co, Cu and Ni in the core VS-2, while Clay, organic carbon, pH, Cr, Zn and Mn were higher in the core MD-2. Silt and Al were slightly higher in the core VS-2, while Fe in the core MD-2. Between cores VS-2 and S-2, clay, Fe, Mn, Ni, Co, Cu, Zn and Cr were higher in the core VS-2, whereas sand and organic carbon in the core S-2. Silt, pH and Al were slightly higher in the core VS-2. Further, between cores VS-2 and GP-2, sand, Fe, Mn, Ni, Co, Cu and Zn were higher in the core VS-2, while clay, organic carbon, pH, Al and Cr in the core GP-2. Silt was slightly higher in the core GP-2. On comparison of cores VG-2 and MD-2, clay, Al, Ni, Co and Cu were higher in the core VG-2, while sand, silt, pH, Fe, Mn, Zn and Cr in the core MD-2. The concentration of organic carbon was slightly higher in the core VG-2. Among cores VG-2 and S-2, clay, pH, Al, Fe, Ni, Co, Cu, Zn and Cr were higher in the core VG-2, while sand, silt and Mn in the core S-2. Organic carbon was slightly higher in the core VG-2. Between cores VG-2 and GP-2, clay, Fe, Mn, Ni, Co and Cu were higher in the core VG-2, whereas sand, silt, Zn and Cr in the core GP-2. Organic carbon and Al were nearly equal in both the cores, while pH was slightly higher in the core GP-2. Further, on comparison of cores MD-2 and S-2, clay, pH, Fe, Mn, Co, Zn and Cr were higher in the core MD-2, while sand, Ni and Cu in the core S-2. Silt, organic carbon and Al were nearly equal in both the cores. Among cores MD-2 and GP-2, sand, pH, Fe, Mn, Ni, Cu and Zn were higher in the core MD-2 while, clay, organic carbon, Al and Cr in the core GP-2. Silt and Co were slightly higher in the core GP-2. Further, between cores S-2 and GP-2, sand, Mn, Ni and Cu were higher in the core S-2, whereas clay, organic carbon, pH, Al, Fe, Co, Zn and Cr in the core GP-2. Silt was slightly higher in the core GP-2.

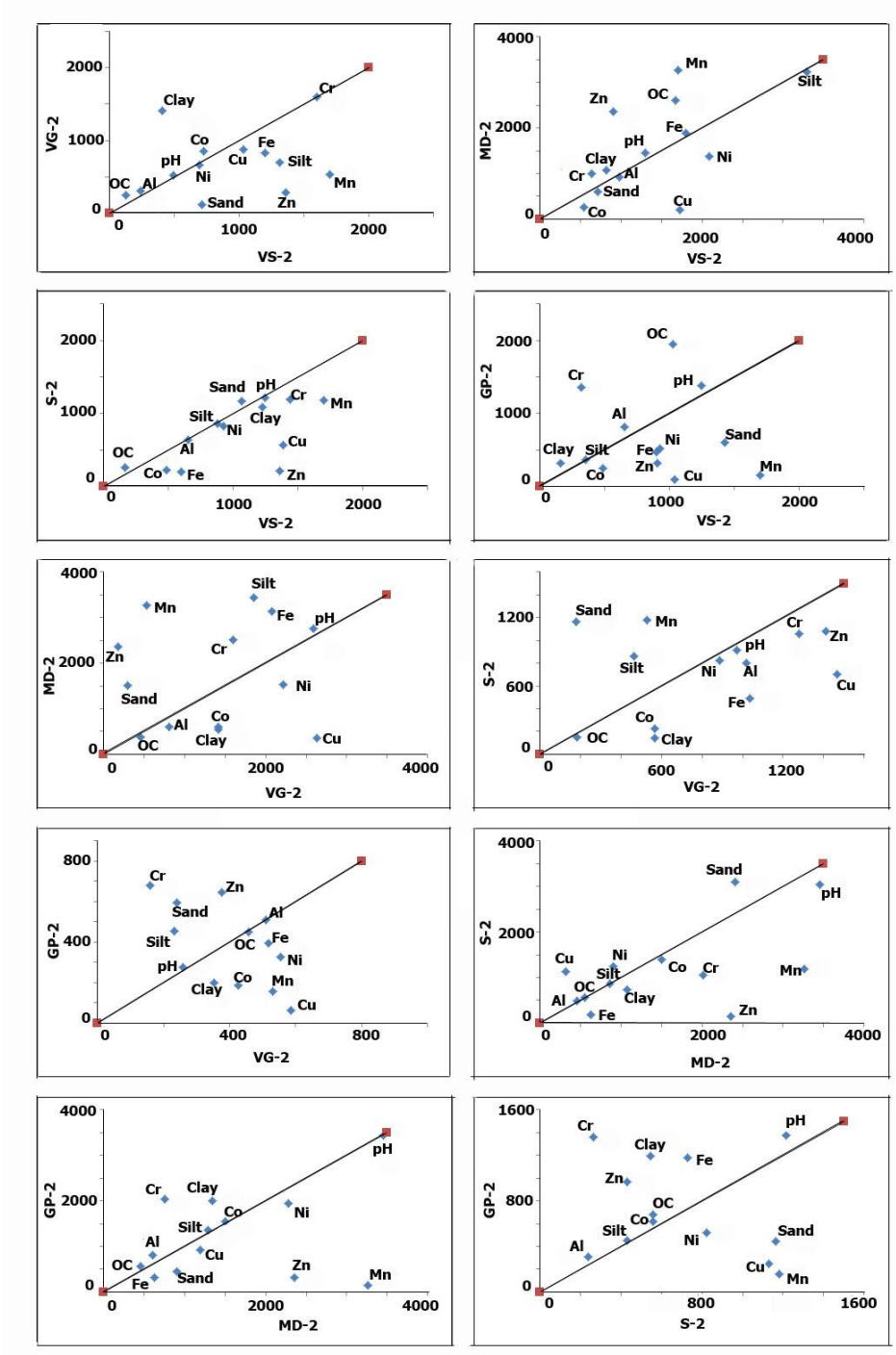

Fig. 3.2.7 Isocon plots for sediment components, pH, organic carbon and metals in the bulk sediments.

The core VS-2 has higher concentration of sand than the rest of the cores (except core S-2), however, the concentration of most of the metals was higher in the Vashishti estuary than Vaghotan, Sharavathi and Gurupur estuaries. The concentration of Al, Ni, Co and Cu was also higher in the Vashisthi estuary than the Mandovi estuary. Although clay and silt components adsorb metal ions much better than sediment fractions of higher size, one should

take into account that most rivers and tributaries sediment contain 90-95 % of sand and only 0-10 % of clay and silt (Jain and Ram 1997). Therefore, as the Vashishti estuary received coarser sediment input from tributaries (as discussed earlier) in the middle region, the overall contribution of the sand content to adsorption of metal ions could be comparable to or even higher than that of clay and silt fraction. On the other hand, concentration of most of the metals was higher in the Vaghotan estuary than Sharavathi and Gurupur estuaries. Also, Al, Ni, Co and Cu were higher in the Vaghotan estuary than the Mandovi estuary. This suggested adsorption of metals onto clay rich sediments (70.71 %) of the Vaghotan estuary. In addition, as stated earlier the rock types vary from basalts to granites and gneisses from North to South along the study area. Basalts generally contain higher Fe, Mn and other associated metals compared to granites and gneisses which must have resulted in higher concentration of metals in Vashishti and Vaghotan estuaries than rest of the estuaries. Further, on comparison of cores MD-2 and GP-2 with core S-2, most of the metals were higher in the cores MD-2 and GP-2 than core S-2 which indicated dilution of metals concentration by higher sand in the core S-2. However, concentration of most of the metals was higher in the core MD-2 than the core GP-2.

3.2.5 Clay mineralogy

Vashishti estuary

In core VS-2, the abundance of clay minerals was in the order of smectite > kaolinite > illite > chlorite (Table 3.2.4a). The percentage of smectite, illite, kaolinite and chlorite ranged from 28.36 % to 52.70 % (avg. 41.26 %), 3.32 % to 41.56 % (avg. 20.19 %), 11.68 % to 49.60 % (avg. 29.00 %) and 4.70 % to 12.19 % (avg. 9.55 %) respectively.

Distribution of clay minerals in the core VS-2 is presented in the figure 3.2.8a. The distribution pattern of smectite showed decrease from bottom to 60 cm, followed by slight increasing trend up to 30 cm. Further, it exhibited fluctuating distribution pattern around average line up to the surface. Kaolinite and illite showed slight fluctuating distribution pattern around the average line with overall slight decreasing trend from bottom to 14 cm. Further, they showed positive peak at 4 cm. Chlorite exhibited fluctuating distribution pattern throughout the core VS-2.

Table 3.2.4a Range and average concentration of clay minerals in cores VS-2, VG-2, S-2 and GP-2.

Sediment core	Smectite (%)			Illite (%)			Kaolinite (%)			Chlorite (%)		
	Range		Avg	Range		Avg	Range		Avg	Range		Avg
	Min	Max		Min	Max		Min	Max		Min	Max	
VS-2	28.36	52.7	41.26	3.32	41.56	20.19	11.68	49.6	29	4.7	12.19	9.55
VG-2	10.92	37.12	18.34	9.35	22.49	16.41	27.63	58.44	49.33	9.28	23.03	15.92
*Middle Mandovi estuary			14.16			20.44			42.02			23.38
S-2	1.71	14.72	5.85	4.9	20.3	8.72	59.31	88.38	77.6	3.29	10.87	7.82
GP-2	2.53	7.62	4.96	8.84	19.79	12.93	63.91	79.85	72.38	5.57	13.34	9.73

*Average concentration of clay minerals in the middle Mandovi estuary was referred from Singh (2008)

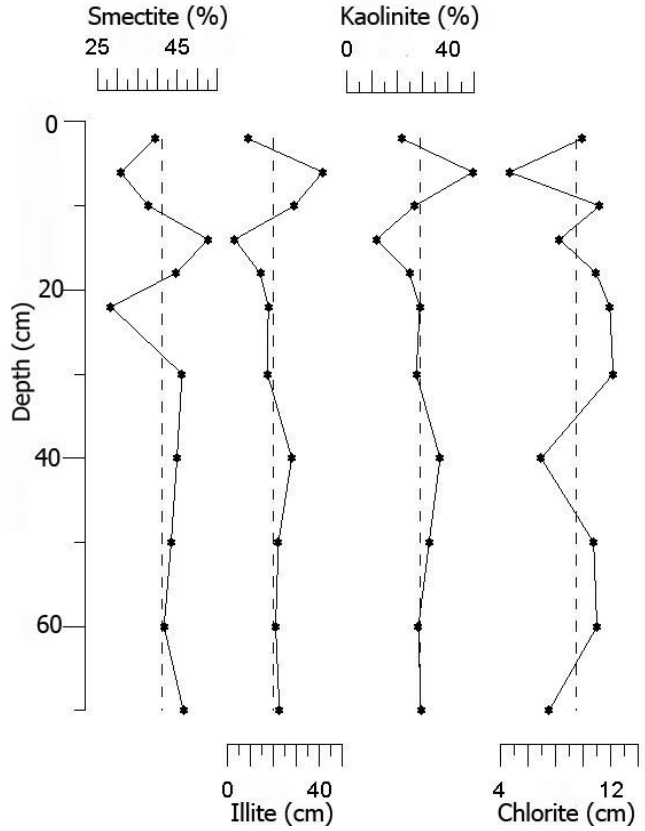

Fig. 3.2.8a Variation of clay minerals with average line in sediment core VS-2

Vaghotan estuary

In the vaghotan estuary (core VG-2), the abundance of clay minerals was in the order of kaolinite > smectite > illite > chlorite (Table 3.2.4a). The percentage of smectite and illite varied from 10.92 % to 37.12 % (avg. 18.34 %) and 9.35 % to 22.49 % (avg. 16.41 %) respectively, whereas kaolinite and chlorite ranged from 27.63 % to 58.44 % (avg. 49.33 %) and 9.28 % to 23.03 % (avg. 15.92 %) respectively.

Distribution of clay minerals in the core VG-2 is presented in the figure 3.2.8b. The clay minerals exhibited fluctuating distribution between bottom and 30 cm which has resulted in positive peak at 40 cm for smectite and chlorite, while negative peak for illite and kaolinite. Above 30 cm, concentration of smectite and kaolinite showed overall decreasing and increasing trend towards the surface, respectively. The concentration of illite increased from 30 to 10 cm and then decreased towards the surface, whereas chlorite showed overall increase towards the surface with fluctuations.

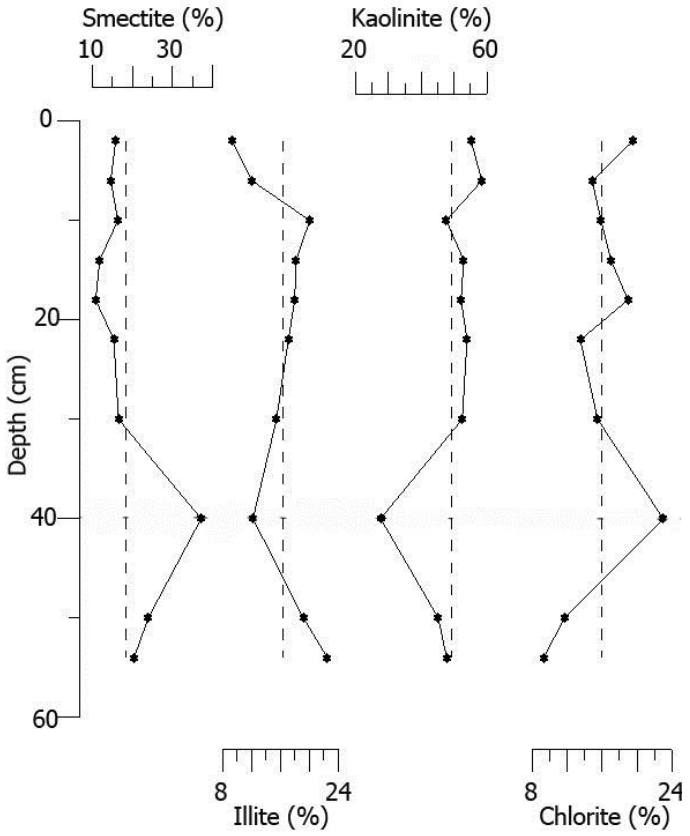

Fig. 3.2.8b Variation of clay minerals with average line in sediment core VG-2

Mandovi estuary

The average concentration of smectite, illite, kaolinite and chlorite in the middle region of the Mandovi estuary was 14.16 %, 20.44 %, 42.02 % and 23.38 %, respectively (Singh 2008).

Sharavathi estuary

In the middle estuarine region of the Sharavathi estuary (core S-2) the abundance of clay minerals was in the order of kaolinite > illite > chlorite > smectite (Table 3.2.4a). The concentration of smectite ranged from 1.71 % to 14.72 % (avg. 5.85 %), while illite varied from 4.90 % to 20.30 % (avg. 8.72 %) in the core S-2. Kaolinite and chlorite ranged from 59.31 % to 88.38 % (avg. 77.60 %) and 3.29 % to 10.87 % (avg. 7.82 %) respectively.

Distribution of clay minerals in the core S-2 is presented in the figure 3.2.8c. The concentration of smectite, illite and kaolinite fluctuated from bottom to 30 cm. Further, smectite and illite showed sharp increasing peak at 22 cm, while kaolinite exhibited

decreasing peak. Above 22 cm, smectite and illite showed overall decease towards the surface, whereas kaolinite exhibited overall increase. Chlorite concentration fluctuated throughout the core S-2.

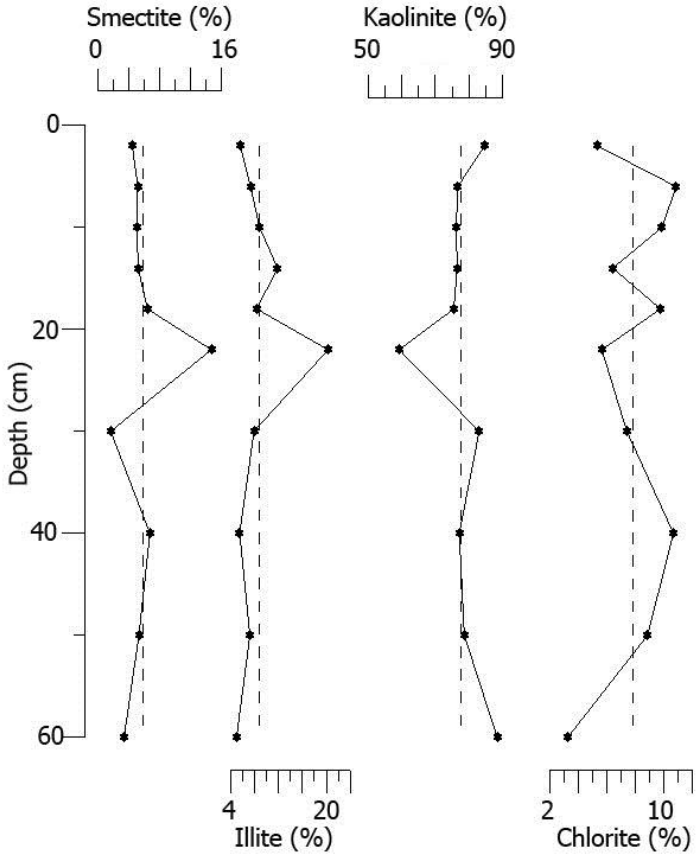

Fig. 3.2.8c Variation of clay minerals with average line in sediment core S-2

Gurupur estuary

In core GP-2, the abundance of clay minerals was in the order of kaolinite > chlorite > illite > smectite (Table 3.2.4a). The percentage of smectite, illite, kaolinite and chlorite ranged from 2.53 % to 7.62 % (avg. 4.96 %), 8.84 % to 19.79 % (avg. 12.93 %), 63.91 % to 79.85 % (avg. 72.38 %) and 5.57 % to 13.34 % (avg. 9.73 %) respectively.

Distribution of clay minerals in the core GP-2 is presented in the figure 3.2.8d. The clay minerals fluctuated around average line from bottom to 30 cm in this core. Further, towards surface, all the minerals showed overall increase with fluctuations.

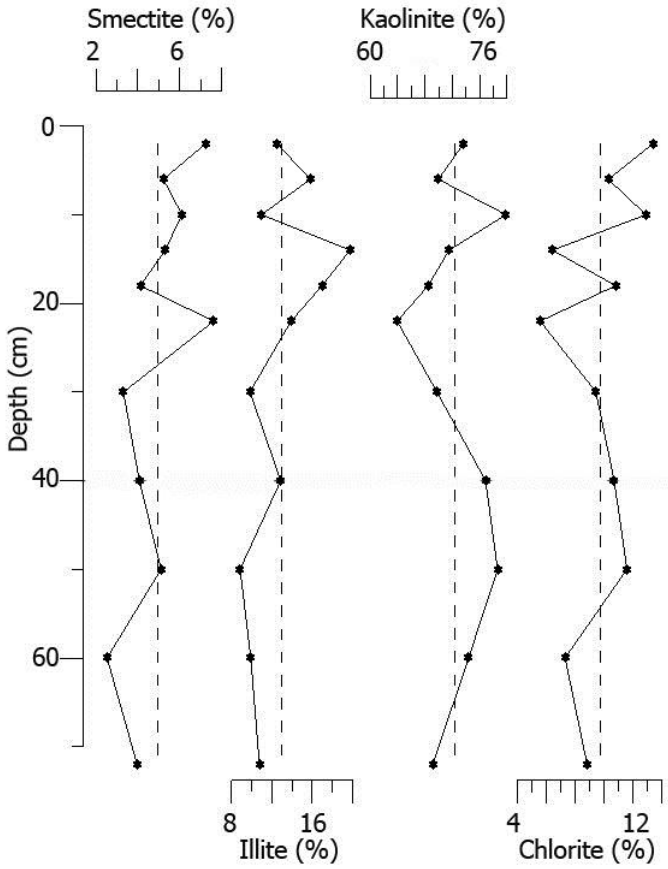

Fig. 3.2.8d Variation of clay minerals with average line in sediment core GP-2

When average values of clay minerals of five estuaries were considered, smectite decreased from VS-2 to GP-2 i.e. from North to South. Kaolinite, in general increased towards South with some exceptions, namely Mandovi and Gurupur, wherein slightly lower values were recorded. Illite and chlorite showed highest percentage in the Mandovi and lowest in the Sharavathi estuary.

3.2.6 Clay chemistry

Major metals (Al, Fe and Mn)

Vashishti estuary

In core VS-2, the concentration of Al, Fe and Mn in the clay fraction varied from 4.46 % to 9.00 % (avg. 7.57 %), 7.11 % to 10.73 % (avg. 9.77 %) and 1184 ppm to 1759 ppm (avg. 1527 ppm) respectively (Table 3.2.4b).

Table 3.2.4b Range and average concentration of major metals in clay fraction in cores VS-2, VG-2, MD-2, S-2 and GP-2

Sediment core	Al (%)			Fe (%)			Mn (ppm)		
	Range		Avg	Range		Avg	Range		Avg
	Min	Max		Min	Max		Min	Max	
VS-2	4.46	9.00	7.57	7.11	10.73	9.77	1184	1759	1527
VG-2	4.97	11.05	8.80	3.51	5.60	4.69	154	412	306
MD-2	0.55	9.91	7.31	0.36	5.85	4.49	227	6413	3248
S-2	0.87	13.18	8.18	0.29	6.08	3.84	97	1106	692
GP-2	11.83	17.25	13.66	2.66	4.92	3.83	87	173	140

Table 3.2.4c Range and average concentration of trace metals in clay fraction in cores VS-2, VG-2, MD-2, S-2 and GP-2

Sediment core	Ni (ppm)			Co (ppm)			Cu (ppm)			Zn (ppm)			Cr (ppm)		
	Range		Avg	Range		Avg	Range		Avg	Range		Avg	Range		Avg
	Min	Max		Min	Max		Min	Max		Min	Max		Min	Max	
VS-2	79	127	112	39	65	48	189	292	244	199	350	266	71	133	113
VG-2	36	73	62	14	43	34	163	207	186	153	288	192	107	159	141
MD-2	14	80	63	9	34	27	38	193	151	82	354	252	24	204	162
S-2	12	183	81	7	95	42	51	418	204	60	428	227	27	440	236
GP-2	65	251	129	21	37	28	108	251	176	201	367	249	259	1517	714

Element distribution profile in the clay component of the core VS-2 is presented in the figure 3.2.9a. Metals viz. Al and Fe decreased from bottom to 40 cm and then exhibited overall increase up to 22 cm. Further, they showed sharp decrease up to 6 cm and later increased towards the surface. Manganese showed fluctuating distribution throughout the core VS-2 with overall increase.

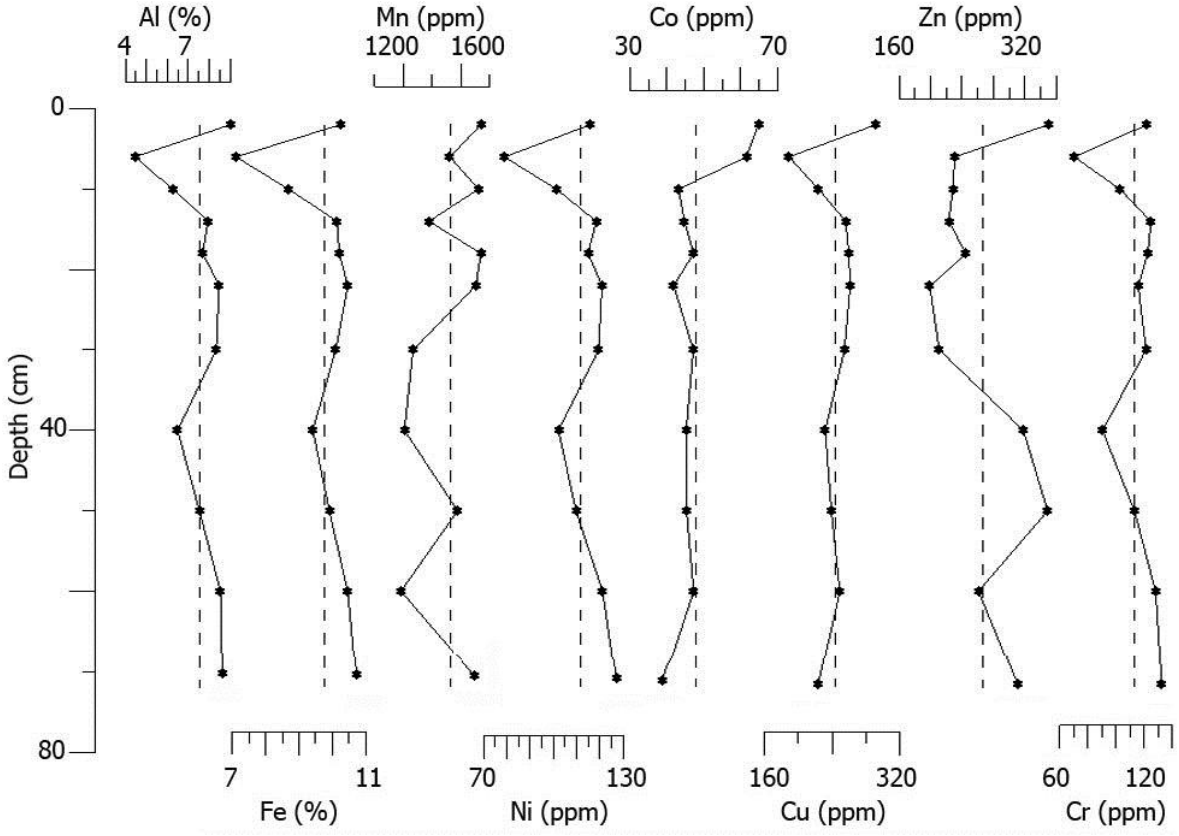

Fig. 3.2.9a Variation of metals in clay fraction with average line in sediment core VS-2

Vaghotan estuary

In core VG-2, Al, Fe and Mn in the clay fraction varied from 4.97 % to 11.05 % (avg. 8.80 %), 3.51 % to 5.60 % (avg. 4.69 %) and 154 ppm to 412 ppm (avg. 306 ppm) respectively (Table 3.2.4b).

Element distribution profile in the clay component of the core VG-2 is presented in the figure 3.2.9b. Metals viz. Al, Fe and Mn showed decrease from bottom to 40 cm and then increased up to 30 cm. Further, they exhibited overall decrease up to 10 cm and then increased towards the surface.

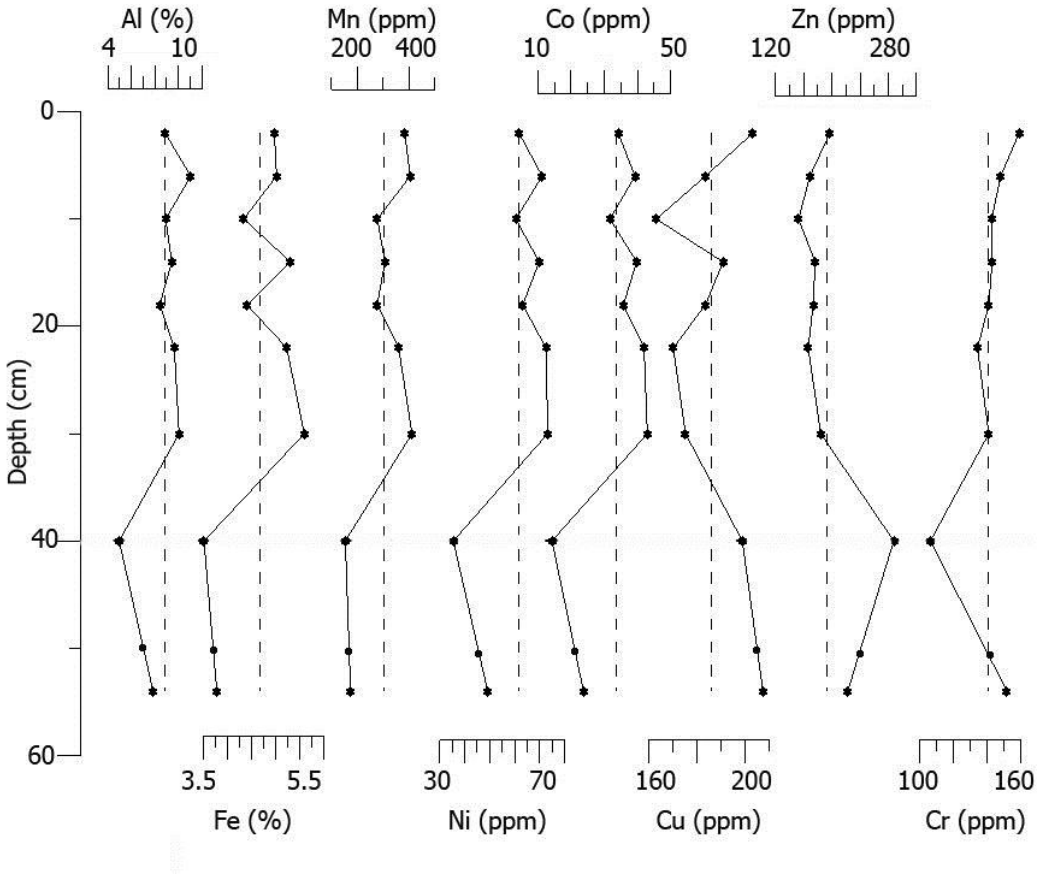

Fig. 3.2.9b Variation of metals in clay fraction with average line in sediment core VG-2

Mandovi estuary

The concentration of Al, Fe and Mn ranged from 0.55 % to 9.91 % (avg. 7.31 %), 0.36 % to 5.85 % (avg. 4.49 %) and 227 ppm to 6413 ppm (avg. 3248 ppm) respectively in the core MD-2 (Table 3.2.4b).

Element distribution profile in the clay component of the core MD-2 is presented in the figure 3.2.9c. The major metals viz. Al, Fe and Mn showed decrease in their concentration between bottom and 60 cm. Further, they exhibited increase up to 50 cm and then showed gradual decrease towards surface, except Mn which showed increase in top 10 cm.

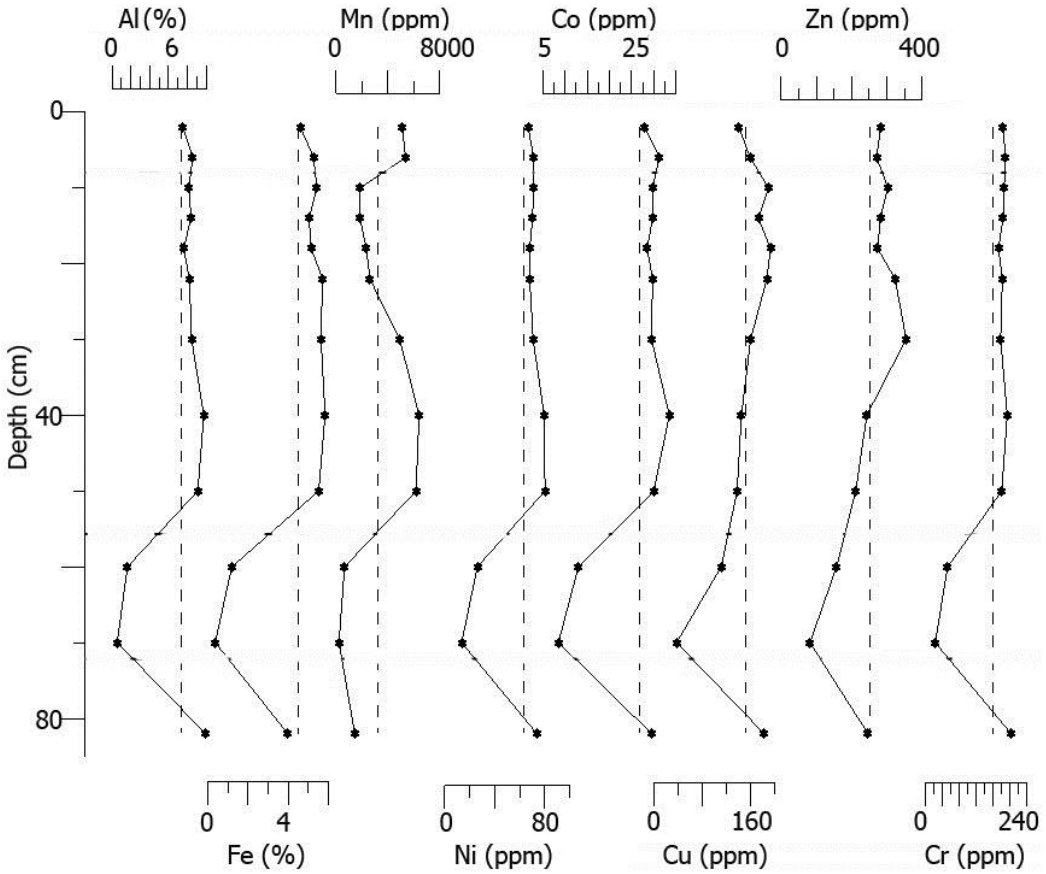

Fig. 3.2.9c Variation of metals in clay fraction with average line in sediment core MD-2

Sharavathi estuary

In this estuary (core S-2), concentration of Al, Fe and Mn in the clay fraction ranged from 0.87 % to 13.18 % (avg. 8.18 %), 0.29 % to 6.08 % (avg. 3.84 %) and 97 ppm to 1106 ppm (avg. 692 ppm) respectively (Table 3.2.4b).

Distribution of metals in the clay component of the core S-2 is presented in the figure 3.2.9d. From bottom up to 40 cm, Al and Fe did not show much variation, while Mn exhibited overall increasing trend. However, concentration of all the three metals was more than the average value. Further, Al, Fe and Mn decreased to less than the average value up to 22 cm which was followed by sharp increase up to 18 cm. Thereafter, concentration of these metals showed overall decrease up to 10 cm. In the top 10 cm of the core S-2, Al did not show much variation, while Fe and Mn exhibited overall increase towards the surface.

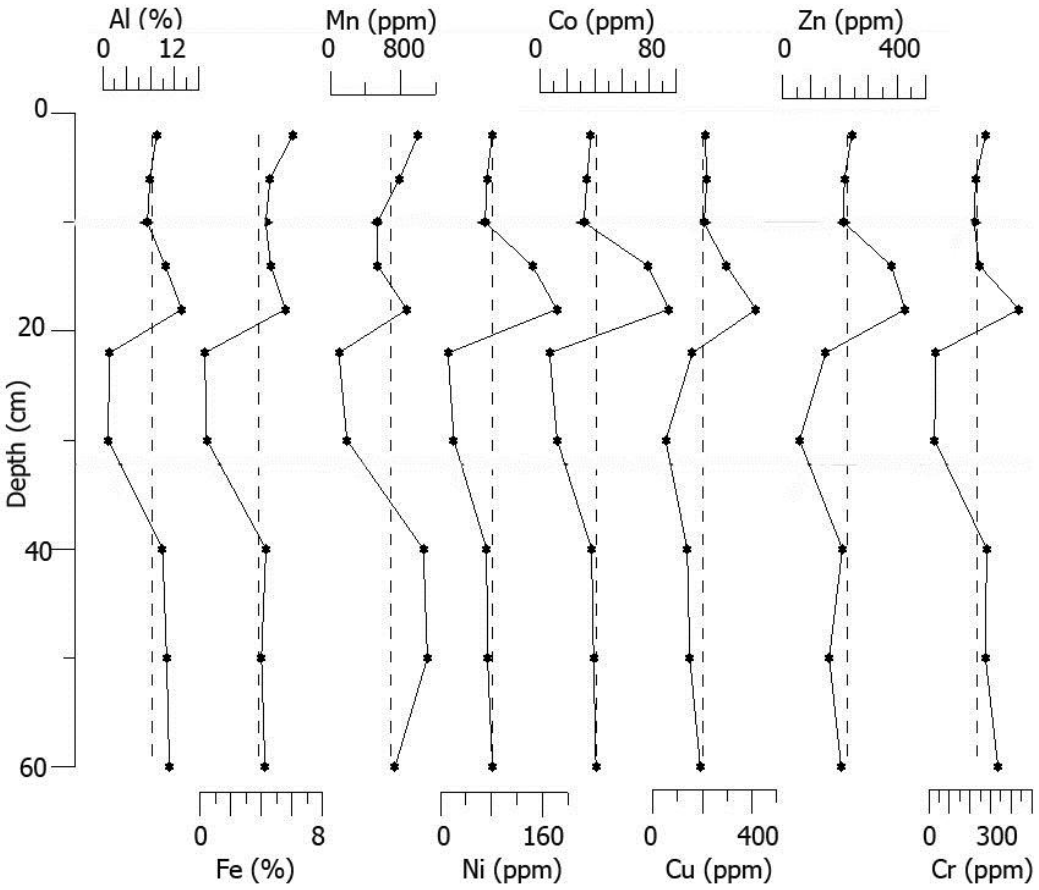

Fig. 3.2.9d Variation of metals in clay fraction with average line in sediment core S-2

Gurupur estuary

In core GP-2, Al, Fe and Mn in the clay fraction varied from 11.83 % to 17.25 % (avg. 13.66 %), 2.66 % to 4.92 % (avg. 3.83 %) and 87 ppm to 173 ppm (avg. 140 ppm) respectively (Table 3.2.4b).

Element distribution profile of clay component in the core GP-2 is presented in the figure 3.2.9e. Metals viz. Al and Fe exhibited decrease from bottom to 60 cm which was followed by increase up to 50 cm. Aluminium further exhibited decreasing trend up to surface. Iron however showed constant values along average line from 50 to 14 cm. Then Fe exhibited sharp increase up to 10 cm and maintained higher values above average line in the upper 10 cm. Manganese showed increase from bottom to 50 cm followed by decrease up to 30 cm. Further, it increased with fluctuations up to 4 cm and then exhibited decreasing trend towards surface.

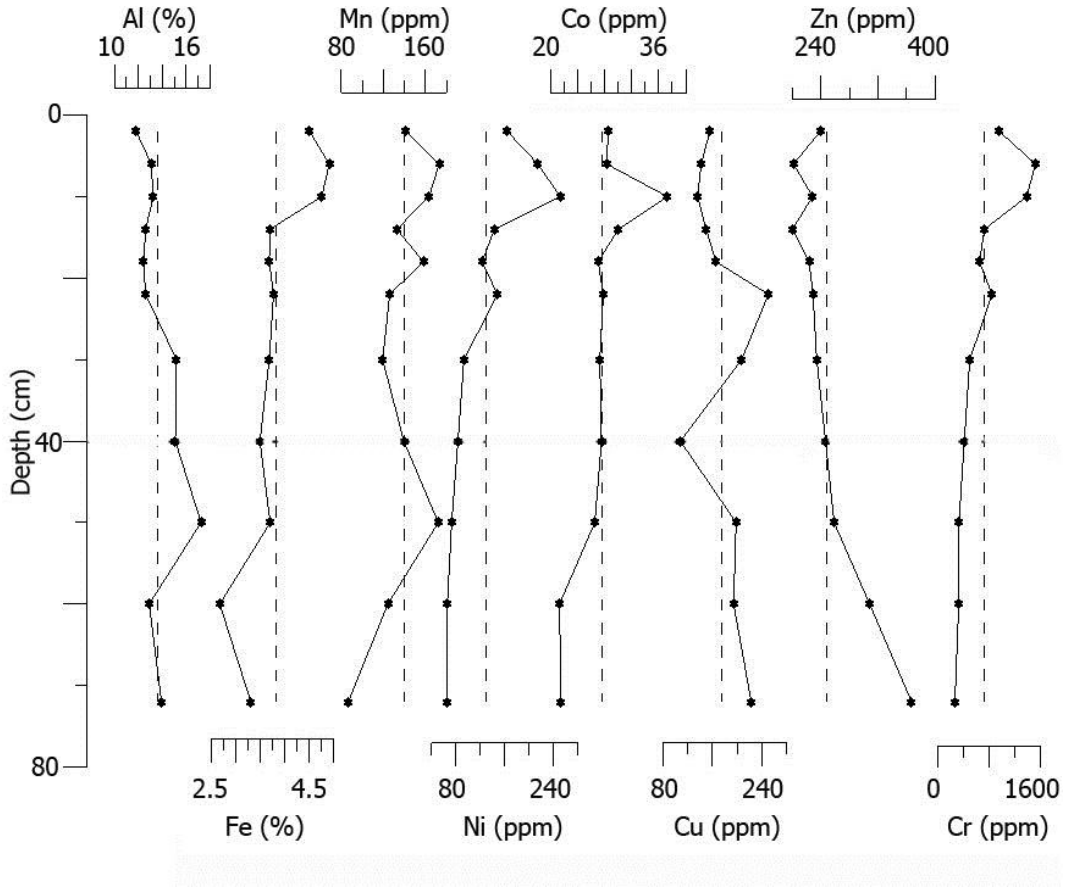

Fig. 3.2.9e Variation of metals in clay fraction with average line in sediment core GP-2

Trace metals (Ni, Co, Cu, Zn and Cr)

Vashishti estuary

In core VS-2, the concentration of Ni, Co, Cu, Zn and Cr in the clay fraction varied from 79 ppm to 127 ppm (avg. 112 ppm), 39 ppm to 65 ppm (avg. 48 ppm), 189 ppm to 292 ppm (avg. 244 ppm), 199 ppm to 350 ppm (avg. 266 ppm) and 71 ppm to 133 ppm (avg. 113 ppm) respectively (Table 3.2.4c).

The distribution pattern of Ni and Cr was similar to major elements viz. Al and Fe throughout the core VS-2 (Fig 3.2.9a). Copper increased from bottom to 60 cm and further, its concentration was similar to that of Al, Fe, Ni and Cr but with less fluctuation. Trace metals viz. Ni, Cu and Cr exhibited decreasing peak at 6 cm. Cobalt showed increase from bottom to 60 cm, similar to distribution of Cu and then it maintained constant value along average line up to 10 cm. In top 10 cm, Co exhibited sharp increase. Zinc exhibited overall decrease with

large fluctuations from bottom to 20. Thereafter, its concentration was almost constant up to 4 cm. In the upper 4 cm, it exhibited sharp increase.

Vaghotan estuary

In core VG-2, Ni, Co, Cu, Zn and Cr in the clay fraction varied from 36 ppm to 73 ppm (avg. 62 ppm), 14 ppm to 43 ppm (avg. 34 ppm), 163 ppm to 207 ppm (avg. 186 ppm), 153 ppm to 288 ppm (avg. 192 ppm) and 107 ppm to 159 ppm (avg. 141 ppm) respectively.

The distribution pattern of Ni and Co was similar to major elements in the core VG-2 (Fig 3.2.9b). Copper showed overall decrease from bottom to 20 cm and then showed increasing value at 14 cm. Further, its concentration decreased up to 10 cm and then increased towards the surface. Zinc with initial increase from bottom to 40 cm showed overall decrease up to 10 cm and then increased towards the surface. Chromium decreased from bottom to 40 cm and then exhibited increasing trend towards the surface.

Mandovi estuary

The concentration of Ni, Co, Cu, Zn and Cr ranged from 14 ppm to 80 ppm (avg. 63 ppm), 9 ppm to 34 ppm (avg. 27 ppm), 38 ppm to 193 ppm (avg. 151 ppm), 82 ppm to 354 ppm (avg. 252 ppm) and 24 ppm to 204 ppm (avg. 162 ppm) respectively.

All the trace metals showed decrease in their concentration between bottom and 70 cm, similar to major metals (Fig 3.2.9c). Further, they showed increase up to 40 cm, except Ni which showed decrease between 50 and 40 cm. From 40 cm to surface, Ni and Cu showed decreasing trend similar to Al and Fe. Chromium exhibited constant trend whereas Cu increased up to 20 cm and then decreased towards surface. Zinc increased from 40 to 30 cm and then decreased up to 20 cm followed by constant trend.

Sharavathi estuary

In this estuary (core S-2), concentration of Ni, Co, Cu, Zn and Cr in the clay fraction ranged from 12 ppm to 183 ppm (avg. 81 ppm), 7 ppm to 95 ppm (avg. 42 ppm), 51 ppm to 418 ppm

(avg. 204 ppm), 60 ppm to 428 ppm (avg. 227 ppm) and 27 ppm to 440 ppm (avg. 236 ppm) respectively.

In core S-2, distribution pattern of trace metals was largely similar to major metals (Fig 3.2.9d). Trace metals showed slight decrease between bottom and 40 cm which was followed by decrease in their concentration up to 22 cm. Further, trace metals exhibited sharp increasing peak at 18 cm and then showed overall decrease up to 10 cm. In the top 10 cm of the core S-2, trace metals did not show much variation in their concentration.

Gurupur estuary

In core GP-2, Ni, Co, Cu, Zn and Cr in the clay fraction varied from 65 ppm to 251 ppm (avg. 129 ppm), 21 ppm to 37 ppm (avg. 28 ppm), 108 ppm to 251 ppm (avg. 176 ppm), 201 ppm to 367 ppm (avg. 249 ppm) and 259 ppm to 1517 ppm (avg. 714 ppm) respectively.

Nickel showed overall increase from bottom to 20 cm and then showed slight decrease followed by sharp positive peak at 10 cm and then decreased towards the surface of the core GP-2 (Fig 3.2.9e). Cobalt exhibited overall increasing trend from bottom to 50 cm followed by constant values up to 20 cm and then it showed sharp increasing peak at 10 cm. The concentration of Cu fluctuated from bottom to surface of the core S-2, whereas Zn exhibited overall decrease towards the surface. Chromium showed overall increasing distribution from bottom to surface, however, increase was more prominent in the top 14 cm, similar to distribution of Fe and Mn.

When the average values of major elements in the clay fraction of five estuaries were considered, Al was highest in the core GP-2, Fe in the core VS-2 and Mn in the core MD-2. Aluminium was lowest in the core MD-2, while Fe and Mn in the core GP-2. Average concentration of Fe decreased from North to South in the studied estuaries.

On comparison of average values of trace metals in the clay fraction of five estuaries highest value was recorded in the core VS-2 for Co, Cu and Zn. Core GP-2 showed highest value for Ni and Cr. Metals viz. Ni and Zn exhibited lowest value in the core VG-2, while Co and Cu in the core MD-2. Chromium was lowest in the core VS-2. Average Cr value increased from North to South.

In the present study, clay minerals varied with a range for smectite from 4.96 % to 41.26 %, illite from 8.72 % to 20.44 %, kaolinite from 29.00 % to 77.60 % and chlorite from 7.82 % to 23.38 % (Table 3.2.4a). When the data of clay minerals for middle region of five estuaries was compared it revealed decrease in percentage of smectite from Vashishti to Gurupur estuary, while, there was overall increase in percentage of kaolinite from North towards the South in the study area (Fig 3.2.10), similar to lower estuarine region. Such a variation in percentage of these clay minerals can be attributed to change in the catchment area source rocks of rivers from North to South of the study area (as discussed earlier). The production, supply and composition of clay minerals in the estuarine environment largely depend on geology and drainage of the hinterland area, and climate variations (Chamley 1989). The processes governing clay minerals abundance and distribution may differ between lower and middle stretch of estuaries in the study area, however, it does not seem to have affected spatial distribution of clay minerals in the present study. Further, Illite showed overall decrease in its concentration from North towards the South in the study area. Such a distribution of illite which is largely similar to smectite suggested their close association as illite could be transformed from smectite during diagenesis of argillaceous sediments (Li et al. 1997).

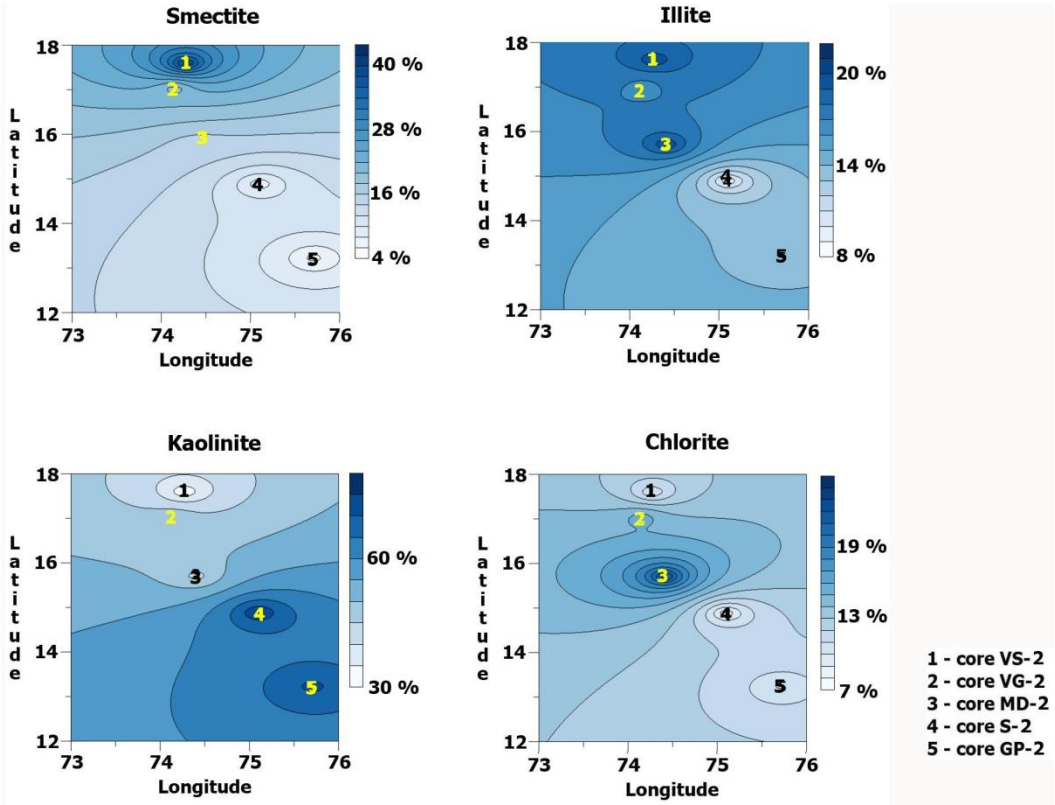

Fig 3.2.10 Distribution of clay minerals along the study area

The variation in clay minerals concentration in cores VS-2, VG-2, S-2 and GP-2 was similar to their distribution in lower estuarine regions. The small size of the clay minerals makes them prone to erosion, transport and redistribution by factors viz. wind transport, fluviatile transport, as well as transport and erosion by currents (Ehrmann et al. 1992). One or more of these factors along with physico-chemical factors like salinity, pH etc might have led to variations in concentration of clay minerals within the studied sediment cores.

The major metals in the clay component varied with a range for Al from 7.31 % to 13.66 %, Fe from 3.83 % to 9.77 % and Mn from 140 ppm to 3248 ppm, while trace metals varied with a range for Ni from 62 ppm to 129 ppm, Co from 27 ppm to 48 ppm, Cu from 151 ppm to 244 ppm, Zn from 192 ppm to 266 ppm and Cr from 113 ppm to 714 ppm (Table 3.2.4b and c). Iron showed overall decrease from North to South along central west coast of India, while Cr exhibited overall increase from Vashishti to Gurupur estuaries (Fig. 3.2.11a and b). Metals viz. Al, Mn, Ni, Co, Cu and Zn exhibited fluctuating distribution pattern.

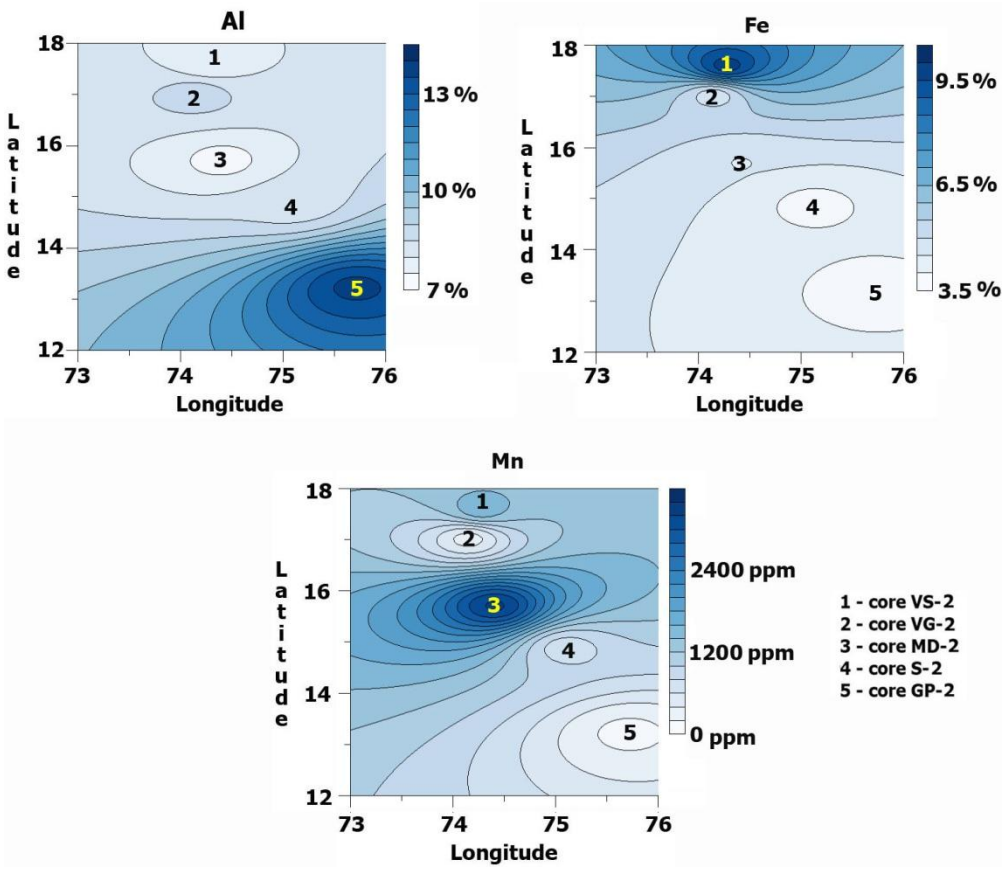

Fig 3.2.11a Distribution of major metals in the clay fraction along the study area

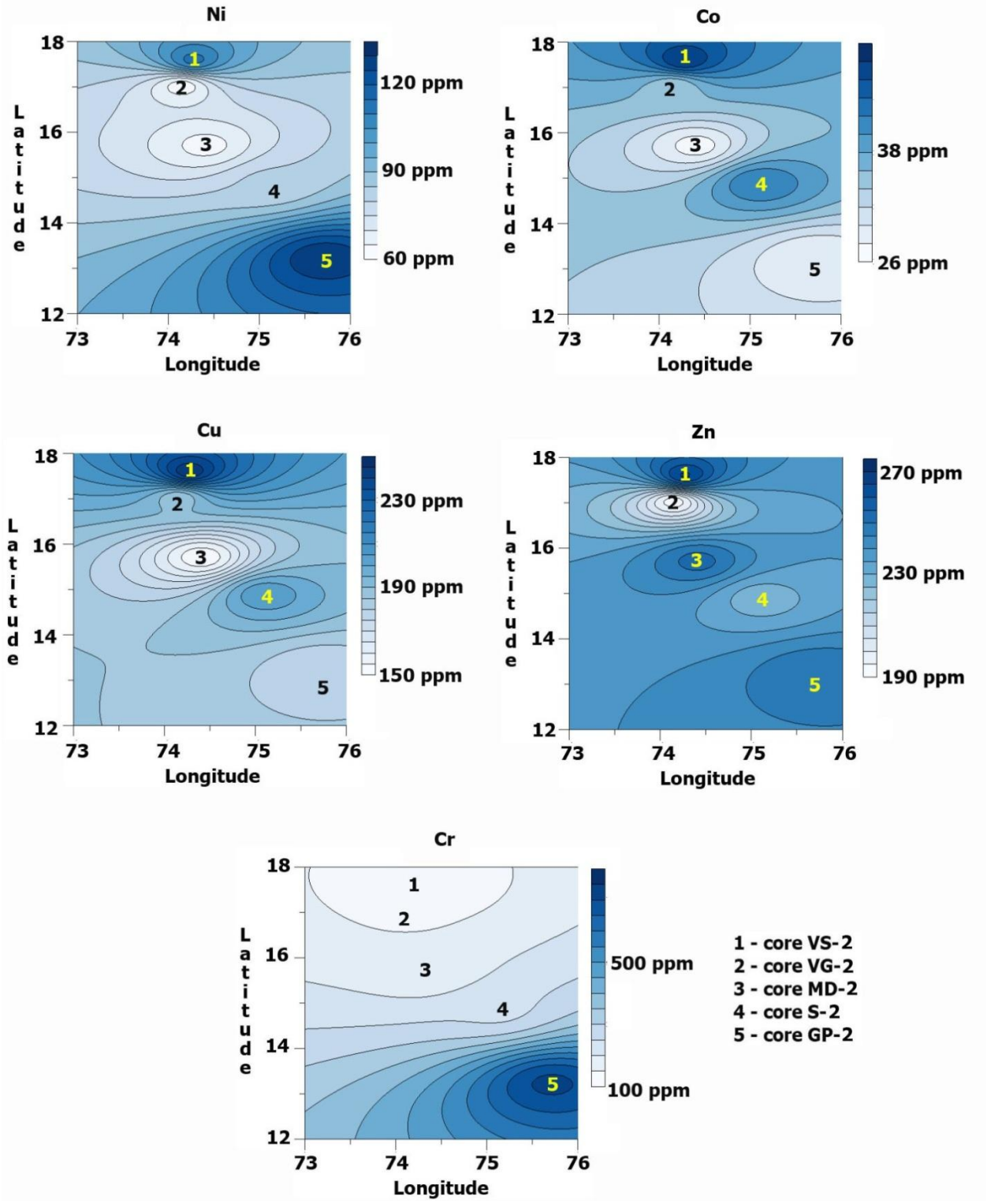

Fig 3.2.11b Distribution of trace metals in the clay fraction along the study area

Pearson's correlation analysis results of the core VS-2 showed significant correlation of illite with Kaolinite; and of chlorite with Cu (Table 3.2.5a). Among the metals, Al exhibited

significant correlation with Fe. Further, Al and Fe showed significant correlation with Ni, Cu and Cr. Trace metals viz. Ni, Cu and Cr exhibited significant correlation among themselves.

Table 3.2.5a Correlation between clay minerals and metals in clay fraction in core VS-2 (n=11). Values in bold indicates significant correlation at $p<0.05$

	Smectite (%)	Illite (%)	Kaolinite (%)	Chlorite (%)	Al (%)	Fe (%)	Mn (ppm)	Ni (ppm)	Co (ppm)	Cu (ppm)	Zn (ppm)	Cr (ppm)
Smectite (%)	1.00											
Illite (%)	-0.53	1.00										
Kaolinite (%)	-0.57	**0.93**	1.00									
Chlorite (%)	0.00	-0.47	-0.50	1.00								
Al (%)	0.35	**-0.79**	**-0.70**	0.60	1.00							
Fe (%)	0.45	**-0.76**	**-0.69**	0.57	**0.96**	1.00						
Mn (ppm)	-0.34	-0.05	-0.09	0.10	0.08	0.03	1.00					
Ni (ppm)	0.44	**-0.75**	**-0.72**	0.58	**0.96**	**0.98**	0.05	1.00				
Co (ppm)	-0.33	0.10	0.26	-0.31	-0.25	-0.45	0.05	-0.49	1.00			
Cu (ppm)	0.22	**-0.87**	**-0.74**	**0.63**	**0.81**	**0.73**	0.09	**0.68**	0.10	1.00		
Zn (ppm)	0.25	-0.03	0.07	-0.20	0.19	0.20	0.11	0.07	0.21	0.14	1.00	
Cr (ppm)	0.51	**-0.79**	**-0.79**	0.59	**0.93**	**0.93**	0.12	**0.96**	-0.39	**0.68**	0.09	1.00

The similar distribution pattern of Al, Fe, Ni, Cu and Cr in the core VS-2 indicated their similar source and adsorption of Ni, Cu and Cr onto Fe oxides. The significant correlation of Al, Fe, Ni, Cu and Cr among themselves further supported the same. Further, increased value of these metals towards surface indicated role of diagenetic mobilization. Within a sediment profile, the dissolved pore-water Fe (II) and Mn (II) cations produced by bacterial reduction of Fe-Mn oxides at greater depths migrate upwards. These cations then get re-precipitated under oxic conditions and thereby scavenge other pore-water trace metals (Spencer 2002). Hence, distribution of trace metals in sediments is often regulated by diagenetic elements which are susceptible to change in redox potential. The significant correlation of chlorite with Cu indicated role of chlorite in its distribution.

In core VG-2, smectite showed significant correlation with Zn, while kaolinite with Al, Fe, Mn, Ni, Co and Cr (Table 3.2.5b). Among the metals, Al, Fe and Mn exhibited significant correlation with each other. Further, these major metals showed significant correlation with Ni and Co. Also, Al exhibited significant correlation with Cr. In addition, Ni exhibited significant correlation with Co, while Cu with Zn.

Metals viz. Ni and Co showed similar distribution to that of Al, Fe and Mn in the core VG-2 and significant correlation of these trace metals with major metals suggested role of Fe and Mn oxides in distribution of Ni and Co. Further, significant correlation of Zn with smectite and of Al, Fe, Mn, Ni, Co and Cr with kaolinite indicated their lithogenic source. Clay

minerals play important role in sorption of metals by soils and sediments as they act as mechanical substrate for precipitation and flocculation of organics and secondary minerals (Jenne 1976).

Table 3.2.5b Correlation between clay minerals and metals in clay fraction in core VG-2 (n=10). Values in bold indicates significant correlation at p<0.05

	Smectite (%)	Illite (%)	Kaolinite (%)	Chlorite (%)	Al (%)	Fe (%)	Mn (ppm)	Ni (ppm)	Co (ppm)	Cu (ppm)	Zn (ppm)	Cr (ppm)
Smectite (%)	1.00											
Illite (%)	-0.17	1.00										
Kaolinite (%)	**-0.92**	-0.02	1.00									
Chlorite (%)	0.25	**-0.66**	-0.37	1.00								
Al (%)	**-0.84**	-0.06	**0.93**	-0.33	1.00							
Fe (%)	**-0.69**	-0.31	**0.71**	0.09	**0.82**	1.00						
Mn (ppm)	**-0.67**	-0.47	**0.78**	0.09	**0.87**	**0.93**	1.00					
Ni (ppm)	**-0.85**	-0.11	**0.85**	-0.10	**0.93**	**0.94**	**0.91**	1.00				
Co (ppm)	**-0.84**	-0.13	**0.83**	-0.05	**0.90**	**0.95**	**0.91**	**0.98**	1.00			
Cu (ppm)	0.43	-0.11	-0.31	-0.03	-0.53	-0.53	-0.52	**-0.64**	-0.63	1.00		
Zn (ppm)	**0.91**	-0.12	**-0.82**	0.17	**-0.87**	**-0.75**	**-0.74**	**-0.90**	**-0.88**	**0.73**	1.00	
Cr (ppm)	**-0.76**	0.08	**0.83**	-0.42	**0.68**	0.43	0.50	0.53	0.51	0.02	-0.61	1.00

In core MD-2, correlation results showed significant correlation of Al, Fe and Mn with each other (Table 3.2.5c). Further, Al and Fe exhibited significant correlation with all the trace metals, while Mn with Ni, Co and Cr. Also, trace metals showed significant correlation among themselves. The distribution pattern of metals in the core MD-2 and results of correlation analysis indicated role of Fe-Mn oxides in distribution of trace metals. Elements are readily scavenged by Fe-Mn oxides (Takematsu et al. 1993). Major as well as trace metals exhibited decrease in their concentration between bottom and 50 cm which suggested their dilution by input of coarser material in the core MD-2 (Fig. 3.2.1c). Further, significant correlation among trace metals indicated their common source in the estuary.

Table 3.2.5c Correlation between metals in clay fraction in core MD-2 (n=12). Values in bold indicates significant correlation at p<0.05

	Al (%)	Fe (%)	Mn (ppm)	Ni (ppm)	Co (ppm)	Cu (ppm)	Zn (ppm)	Cr (ppm)
Al (%)	1.00							
Fe (%)	**0.92**	1.00						
Mn (ppm)	**0.61**	**0.67**	1.00					
Ni (ppm)	**0.99**	**0.95**	**0.66**	1.00				
Co (ppm)	**0.98**	**0.97**	**0.65**	**0.99**	1.00			
Cu (ppm)	**0.80**	**0.80**	0.19	**0.80**	**0.82**	1.00		
Zn (ppm)	**0.76**	**0.86**	0.40	**0.77**	**0.82**	**0.85**	1.00	
Cr (ppm)	**0.98**	**0.93**	**0.58**	**0.98**	**0.99**	**0.85**	**0.82**	1.00

The correlation results of the core S-2 exhibited significant correlation of smectite with illite (Table 3.2.5d). Among the metals, major metals viz. Al, Fe and Mn showed significant

correlation among themselves. Further, Al and Fe exhibited significant correlation with all the trace metals, while Mn with Cr. Trace metals showed significant correlation with each other.

Table 3.2.5d Correlation between clay minerals and metals in clay fraction in core S-2 (n=10). Values in bold indicates significant correlation at $p<0.05$

	Smectite (%)	Illite (%)	Kaolinite (%)	Chlorite (%)	Al (%)	Fe (%)	Mn (ppm)	Ni (ppm)	Co (ppm)	Cu (ppm)	Zn (ppm)	Cr (ppm)
Smectite (%)	1.00											
Illite (%)	**0.83**	1.00										
Kaolinite (%)	**-0.92**	**-0.89**	1.00									
Chlorite (%)	-0.03	-0.19	-0.21	1.00								
Al (%)	-0.29	-0.56	0.40	0.15	1.00							
Fe (%)	-0.35	-0.60	0.45	0.19	**0.89**	1.00						
Mn (ppm)	-0.31	**-0.71**	0.45	0.31	**0.82**	**0.81**	1.00					
Ni (ppm)	-0.21	-0.26	0.19	0.17	**0.83**	**0.75**	0.47	1.00				
Co (ppm)	-0.19	-0.22	0.16	0.16	**0.80**	**0.69**	0.43	**0.99**	1.00			
Cu (ppm)	0.10	0.03	-0.10	0.13	**0.66**	**0.64**	0.27	**0.91**	**0.89**	1.00		
Zn (ppm)	0.04	-0.03	-0.04	0.12	**0.73**	**0.69**	0.34	**0.95**	**0.94**	**0.96**	1.00	
Cr (ppm)	-0.27	-0.57	0.40	0.16	**0.97**	**0.88**	**0.79**	**0.83**	**0.79**	**0.71**	**0.73**	1.00

The similar distribution pattern of trace metals to that of major metals (Fig 3.2.9d) in the core S-2 and significant correlation of trace metals with Fe suggested their adsorption onto Fe oxides. Also, significant correlation among trace metals indicated that they may have originated from the common source. Further, peak values of metals in the clay fraction obtained between 22 and 10 cm revealed that the metals brought to the estuary got selectively associated with the clay fraction. Smectite seemed to be closely associated with illite in this core.

In core GP-2, correlation analysis results showed significant association of smectite with Fe and Ni, while kaolinite with chlorite (Table 3.2.5e). Among the metals, Fe exhibited significant correlation with Ni, Co and Cr. Further, Ni, Co and Cr showed significant correlation among themselves.

In core GP-2, Ni, Co and Cr exhibited nearly similar distribution to that of Fe. Also, these trace metals showed significant correlation with Fe indicating their adsorption onto Fe oxy-hydroxides in the clay fraction. Anderson and Benjamin (1990) reported that Fe oxides constitute significant sinks of metals in aquatic systems. In this core, smectite seemed to regulate the distribution of Fe and Ni as clay minerals with smaller size and large specific surfaces, possess the ability to adsorb cations (Bradl 2002).

Table 3.2.5e Correlation between clay minerals and metals in clay fraction in core GP-2 (n=11). Values in bold indicates significant correlation at $p<0.05$

	Smectite (%)	Illite (%)	Kaolinite (%)	Chlorite (%)	Al (%)	Fe (%)	Mn (ppm)	Ni (ppm)	Co (ppm)	Cu (ppm)	Zn (ppm)	Cr (ppm)
Smectite (%)	1.00											
Illite (%)	0.24	1.00										
Kaolinite (%)	-0.12	-0.42	1.00									
Chlorite (%)	0.14	-0.30	**0.62**	1.00								
Al (%)	-0.34	-0.57	0.43	0.18	1.00							
Fe (%)	**0.64**	0.23	0.12	0.56	-0.22	1.00						
Mn (ppm)	0.28	0.17	0.44	0.53	0.12	0.60	1.00					
Ni (ppm)	**0.62**	0.35	0.07	0.32	-0.49	**0.89**	0.53	1.00				
Co (ppm)	0.55	0.24	0.35	0.41	-0.14	**0.75**	0.56	**0.83**	1.00			
Cu (ppm)	0.03	-0.34	-0.57	-0.53	0.09	-0.42	-0.52	-0.41	-0.50	1.00		
Zn (ppm)	-0.44	-0.58	0.04	-0.11	0.20	**-0.61**	**-0.67**	**-0.62**	**-0.70**	0.44	1.00	
Cr (ppm)	0.58	0.36	0.00	0.30	-0.48	**0.90**	0.56	**0.98**	**0.72**	-0.40	**-0.63**	1.00

Further, in order to understand variation between estuaries in clay minerals and metals concentration in the clay fraction, the data was plotted on the isocon diagram (Fig.3.2.12). On comparison of core VS-2 with core VG-2, smectite, illite Fe, Mn, Ni, Cu and Zn were higher in the core VS-2, while kaolinite, chlorite, Al and Co were higher in the core VG-2. Chromium was present in equal concentration in both the cores. On comparison of cores VS-2 and MD-2, smectite, Ni, Co and Cu were higher in the core VS-2, while kaolinite, chlorite, Mn, Cr and Zn in the core MD-2. Aluminium was slightly higher in the core VS-2, while Fe in the core MD-2. The concentration of illite was equal in both the cores. Between cores VS-2 and S-2, smectite, illite, chlorite, Fe, Mn, Ni, Co, Cu, Zn and Cr were higher in the core VS-2, while kaolinite in the core S-2. Aluminium was present in equal concentration in both the cores. Further, between cores VS-2 and GP-2, smectite, illite, Fe, Mn, Ni, Co, Cu and Zn were higher in the core VS-2, while kaolinite, Al and Cr in the core GP-2. Chlorite had equal concentration in both the cores. On comparison of cores VG-2 and MD-2, smectite, kaolinite, Al, Ni, Co and Cu were higher in the core VG-2, while chlorite, illite, Fe, Mn, Zn and Cr in the core MD-2. Among cores VG-2 and S-2, smectite, illite, chlorite, Al, Fe, Ni, Co, Cu, Zn and Cr were higher in the core VG-2, while kaolinite and Mn in the core S-2. Between cores VG-2 and GP-2, smectite, illite, chlorite, Fe, Mn, Ni, Co and Cu were higher in the core VG-2, whereas kaolinite, Zn and Cr in the core GP-2. Aluminium had equal concentration in both the cores. Further, on comparison of cores MD-2 and S-2, smectite, illite, chlorite, Fe, Mn, Co, Cr and Zn were higher in the core MD-2 while, kaolinite, Ni and Cu in the core S-2. Aluminium was slightly higher in the core S-2. Similarly among cores MD-2 and GP-2, smectite, illite, chlorite, Fe, Mn, Ni, Cu and Zn were higher in the core MD-2, while kaolinite, Al and Cr in the core GP-2. Cobalt was slightly higher in the core GP-2. Further,

between cores S-2 and GP-2, smectite, kaolinite, Mn, Ni and Cu were higher in the core S-2, while illite, chlorite, Al, Fe, Co, Zn and Cr in the core GP-2.

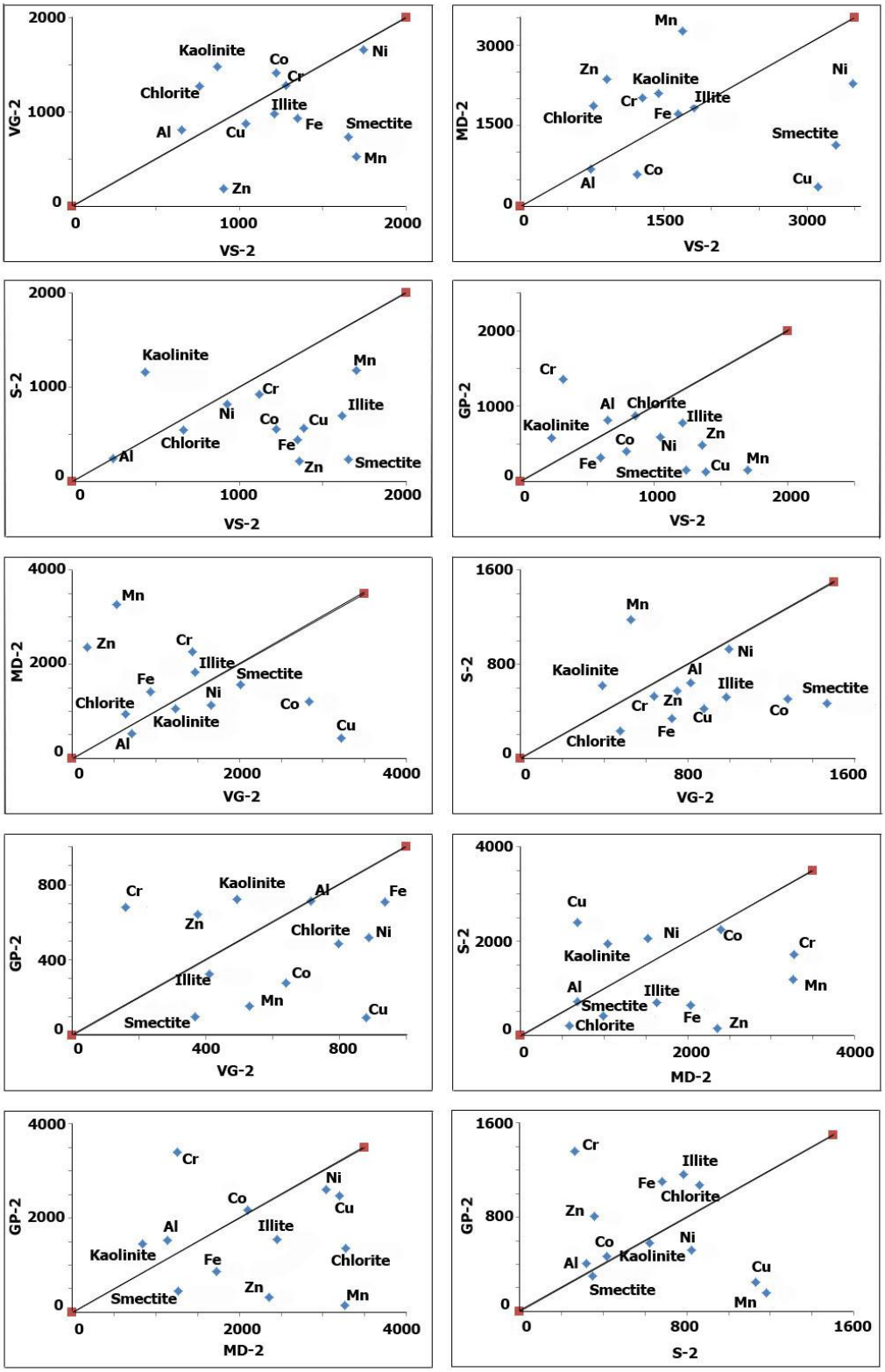

Fig. 3.2.12 Isocon plots for clay minerals and metals in the clay fraction

On comparison of core VS-2 with cores S-2 and GP-2, most of the metals were present in higher concentration in the core VS-2. Also cores VG-2 and MD-2 showed higher concentration of metals than cores S-2 and GP-2. The rock types in the catchment area being basalts in case of Vashishti and Vaghotan, meta-sediments in the Mandovi and granites and granitic gneisses in case of Sharavathi and Gurupur, metals released to estuaries are expected to vary considerably. Further, as discussed earlier, higher tidal range in Vashishti, Vaghotan and Mandovi estuaries in comparison to Sharavathi and Gurupur estuaries favours retention of higher finer sediments in suspension for a longer period of time. This might have facilitated higher adsorption of metal onto clay particles in Vashishti, Vaghotan and Mandovi estuaries than Sharavathi and Gurupur estuaries. In addition, smectite, a finer size clay mineral (Bican-Brisan and Hosu 2006) has higher concentration in cores VS-2, VG-2 and MD-2 than cores S-2 and GP-2 which might have favoured additional adsorption of metals. Further, core VS-2 had higher concentration of metals than core VG-2, while comparison of core VS-2 with MD-2 indicated considerable number of metals in higher concentration in both the cores. Also, considerable numbers of metals were present in higher concentration in cores MD-2 and GP-2 in comparison to cores VG-2 and S-2, respectively.

The average concentration of metals in the bulk sediments for the samples considered for the clay fraction in sediment cores is presented in the Table 3.2.6. Further, when isocon plots of metals in clay fraction and bulk sediments were plotted (Fig 3.2.13), Al, Fe, Mn, Co, Cu, Zn and Cr were noted to be higher in the bulk sediments, while Ni was slightly higher in the clay component of the core VS-2. In case of the core VG-2, Al, Fe, Mn, Ni, Co, Cu and Cr showed higher average value in the bulk sediments, while Zn was present in higher average concentration in the clay fraction. In Mandovi estuary (core MD-2), Fe, Ni, Co, Cr and Zn were present in higher concentration in the bulk sediments, while Mn and Cu in the clay fraction. Aluminium was slightly higher in the bulk sediments. In core S-2, Fe, Mn and Ni showed higher average concentration in the bulk sediments, while Al, Co, Cu, Zn and Cr in the clay fraction. In case of the Gurupur estuary (core GP-2), Fe, Mn, Co and Cr had higher average concentration in the bulk sediments than the clay fraction, while Al, Ni, Zn and Cu were present in higher average concentration in the clay fraction.

Table 3.2.6Average concentration of metals in the bulk sediments for the samples considered for the clay fraction in sediment cores VS-2, VG-2, MD-2, S-2 and GP-2

	Al (%)	Fe (%)	Mn (ppm)	Ni (ppm)	Co (ppm)	Cu (ppm)	Zn (ppm)	Cr (ppm)
VS-2	8.37	15.61	1809	109	61	351	453	160
VG-2	10.40	11.01	510	110	71	313	93	160
MD-2	7.63	15.27	2952	77	30	40	1477	259
S-2	7.39	4.54	1008	94	26	131	65	118
GP-2	10.98	8.30	159	75	33	31	171	852

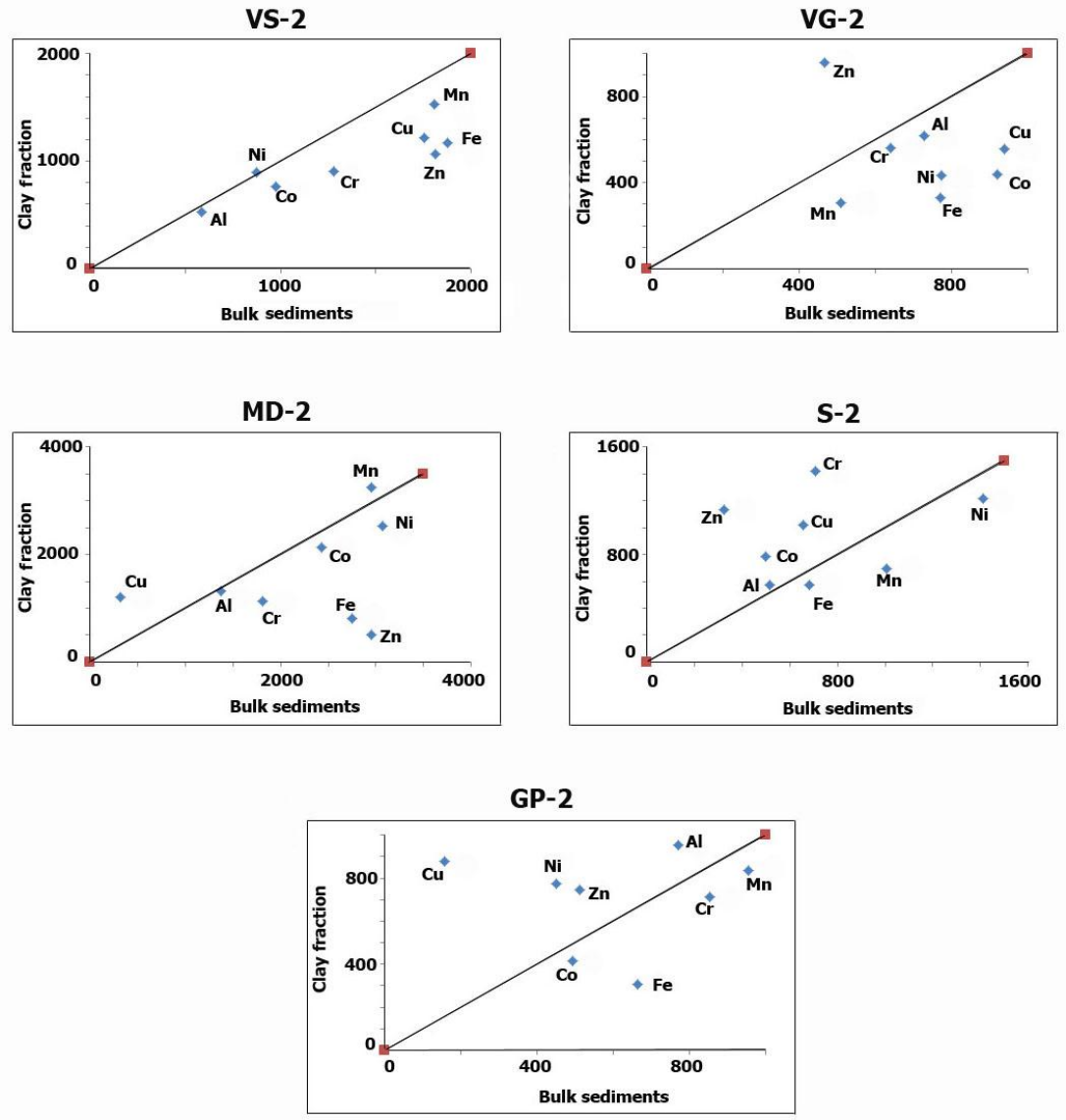

Fig. 3.2.13 Isocon plots for metals in cores VS-2, VG-2, MD-2, S-2 and GP-2

The sediment cores collected from the middle estuarine region showed higher concentration of most of the metals in the bulk sediments of Vashishti, Vaghotan and Mandovi estuaries,

while higher concentration of most of the metals in the clay fraction of the Sharavathi estuary. Gurupur estuary also showed considerable number of metals with higher concentration in the clay fraction. Such a distribution of metals in the tropical estuaries was attributed to change in catchment area geology along the study area. Coarser sediments released from basalts and meta-sediments might be ferromagnesian minerals which are responsible for higher metal concentration in the bulk sediments.

3.2.7 Speciation of elements

The speciation analysis of selected elements whose average value in the bulk sediments exceeded the global average shale value was carried out. The range and average concentration of Fe, Mn, Ni, Co, Cu, Zn and Cr in different fractions in the core VS-2 and Fe, Ni, Co, Cu and Cr in the core VG-2, Fe, Mn, Ni, Co, Zn and Cr in the core MD-2, Fe, Mn, Ni, Co, Cu and Cr in the core S-2, along with Fe, Ni, Co, Zn and Cr in the core GP-2 are given in the Table 3.2.7. In order to understand the variations in elemental concentration with depth in different fractions in these cores the chemical partitioning of metals is diagrammatically represented in Figure 3.2.14.

Vashishti estuary

Metals viz. Fe, Mn, Ni, Co, Cu, Zn and Cr were highest (>70 %, except Mn) in the residual fraction in the core VS-2. Manganese in the residual phase was 47.99 %. Next to the residual fraction, Fe, Co and Zn were associated with the Fe-Mn oxide fraction, while Cu and Cr with organic bound fraction. Nickel concentration was low in the bioavailable fractions. Among the bioavailable fractions, Mn was highest in the exchangeable fraction, present in significant level in the Fe-Mn oxide fraction and lowest in the organic fraction. Metals viz. Fe, Cu and Zn showed least concentration in the exchangeable fraction, while Ni, Co and Cr in the carbonate fraction.

In residual as well as bioavailable fractions, Fe and Ni did not show much variation from bottom to surface of the core VS-2. Manganese in exchangeable, carbonate and Fe-Mn oxide fractions together showed overall increase from bottom to 18 cm and then decreased up to 8 cm. Further, its concentration increased towards the surface. Manganese exhibited high concentration at 18 cm depth and near surface in exchangeable and Fe-Mn oxide fractions

Table 3.2.7 Range and average concentration of Fe, Mn, Ni, Co, Cu, Zn and Cr in different fractions of cores VS-2, VG-2, MD-2, S-2 and GP-2.

VS-2	Exchangeable		Carbonate		Fe-Mn		Organic/Sulphide		Residual	
	Range	Average	Range	Average	Range	Average	Range	Average	Range	Average
Fe (%)	0.09-0.39	0.20	1.02-3.78	1.96	4.91-7.66	6.44	0.30-0.99	0.64	87.86-92.69	90.76
Mn (%)	22.06-40.89	28.57	2.40-9.40	6.21	12.25-20.34	16.4	0.36-2.09	0.84	30.03-61.67	47.99
Ni (%)	1.28-2.77	2.10	1.12-2.25	1.58	1.73-2.77	2.24	1.28-3.19	2.33	90.15-94.19	91.75
Co (%)	3.15-9.80	6.41	3.13-6.77	4.86	9.97-15.95	12.13	3.66-8.88	6.35	63.86-77.28	70.25
Cu (%)	0.06-0.41	0.21	0.01-0.79	0.34	2.42-5.82	4.30	4.40-11.69	8.09	83.47-91.35	87.06
Zn (%)	1.58-3.59	2.40	3.21-9.27	5.05	7.08-14.17	10.28	2.77-6.53	4.21	71.56-83.88	78.07
Cr (%)	1.09-1.64	1.22	0.07-0.26	0.17	4.08-8.76	5.66	3.90-9.28	5.91	84.15-89.81	87.04
VG-2	Exchangeable		Carbonate		Fe-Mn		Organic/Sulphide		Residual	
	Range	Average	Range	Average	Range	Average	Range	Average	Range	Average
Fe (%)	0.0005-0.0016	0.0011	0.001-0.002	0.002	0.95-2.38	1.42	0.95-3.82	1.85	93.80-98.04	96.72
Ni (%)	1.83-15.89	5.06	3.13-5.84	4.01	2.99-4.77	3.72	4.06-5.31	4.72	70.63-87.22	82.49
Co (%)	3.36-4.85	4.09	5.40-7.02	6.14	13.25-19.03	16.65	11.10-14.62	12.81	55.13-64.85	60.31
Cu (%)	0.30-2.66	1.11	2.10-8.53	4.41	0.10-1.20	0.47	2.96-5.46	4.35	83.35-92.40	89.66
Cr (%)	0.37-1.78	1.04	0.10-0.37	0.23	2.23-7.03	3.32	0.29-1.82	1.00	89.11-96.16	94.41
MD-2	Exchangeable		Carbonate		Fe-Mn		Organic/Sulphide		Residual	
	Range	Average	Range	Average	Range	Average	Range	Average	Range	Average
Fe (%)	0.005-0.0074	0.0013	0.0001-0.0024	0.0006	1.45-4.10	2.25	1.37-4.51	2.35	92.35-96.59	95.40

Mn (%)	1.38-34.18	11.29	2.06-16.99	11.18	5.60-50.05	30.74	2.29-12.31	6.72	22.06-61.71	40.08
Ni (%)	2.46-28.41	5.77	2.65-4.62	3.75	5.03-11.74	7.94	4.75-8.94	7.33	57.23-80.95	75.21
Co (%)	3.94-14.60	6.38	3.87-5.86	5.08	5.20-18.94	14.56	2.62-11.17	8.86	56.68-72.87	65.13
Zn (%)	1.48-8.86	3.26	4.67-9.97	6.87	5.37-15.89	11.19	4.56-10.89	8.68	63.31-74.24	70.00
Cr (%)	0.52-2.92	1.67	0.18-1.33	0.73	5.31-9.41	6.66	4.32-11.69	8.72	78.79-86.31	82.22
S-2	Exchangeable		Carbonate		Fe-Mn		Organic/Sulphide		Residual	
	Range	Average	Range	Average	Range	Average	Range	Average	Range	Average
Fe (%)	0.0002-0.0070	0.0014	0.001-0.006	0.004	6.77-10.90	8.58	0.07-0.86	0.43	88.93-93.12	90.98
Mn (%)	2.27-20.99	16.25	1.80-6.84	3.58	8.48-25.91	16.66	0.71-11.28	2.88	46.57-84.76	60.62
Ni (%)	1.50-7.13	3.70	2.82-9.83	4.67	5.32-9.96	7.04	4.48-6.34	5.28	68.64-84.51	79.31
Co (%)	4.19-14.24	8.10	5.52-15.13	8.28	13.30-24.84	19.27	1.19-36.52	8.42	38.01-62.89	55.93
Cu (%)	0.16-1.50	0.65	3.91-23.13	8.86	0.96-2.06	1.48	0.73-12.97	8.75	70.62-86.25	80.25
Cr (%)	1.07-3.89	2.07	0.39-6.65	2.89	4.21-9.84	7.33	7.21-13.89	10.86	67.93-86.59	76.86
GP-2	Exchangeable		Carbonate		Fe-Mn		Organic/Sulphide		Residual	
	Range	Average	Range	Average	Range	Average	Range	Average	Range	Average
Fe (%)	0.0002-0.0100	0.0021	0.0004-0.0010	0.0006	1.11-9.23	4.90	0.47-11.51	3.70	79.26-98.30	91.40
Ni (%)	0.58-3.51	1.75	0.89-5.15	2.26	2.72-7.37	4.06	2.08-5.43	3.20	79.31-93.38	88.73
Co (%)	6.22-18.37	10.32	3.49-6.75	4.61	5.66-19.39	12.58	5.80-9.91	8.37	51.27-70.19	64.12
Zn (%)	0.32-14.98	5.55	4.50-9.15	6.25	6.58-23.09	12.25	2.25-7.32	4.57	64.00-78.53	71.39
Cr (%)	0.44-7.56	2.26	0.18-2.15	0.65	0.61-12.92	3.55	0.99-18.95	5.59	58.42-97.77	87.95

indicating diagenetic remobilization. The residual fraction compensated variations in Mn in the bioavailable fractions. Cobalt exhibited increase from bottom to surface in exchangeable and carbonate fractions. Its concentration was slightly higher at 18 to 14 cm depth and in the top 4 cm in Fe-Mn oxide and organic phases. Metals viz. Cu and Cr associated with Fe-Mn oxide and organic phases showed similar distribution. In the organic phase, they were higher between 30 and 14 cm and in top 4 cm. Zinc bound to the exchangeable phase did not show much variation in this core, however, slight increase at 30 cm and near the surface was seen in the carbonate phase. Zinc concentration in Fe-Mn oxide and organic phases had increased between 18 and 14 cm, and in top 4 cm.

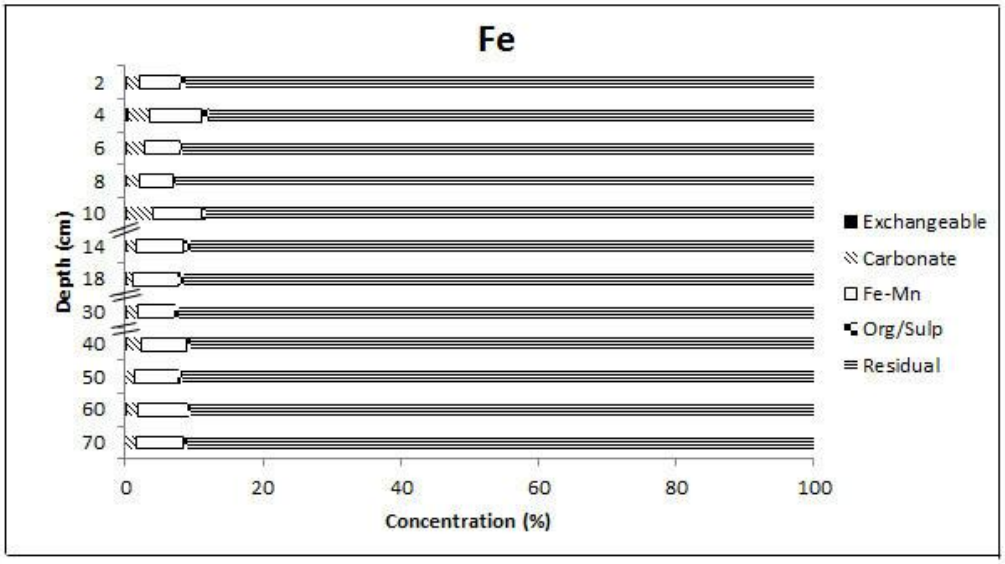

Fig. 3.2.14a Variation of Fe associated with different fractions in core VS-2.

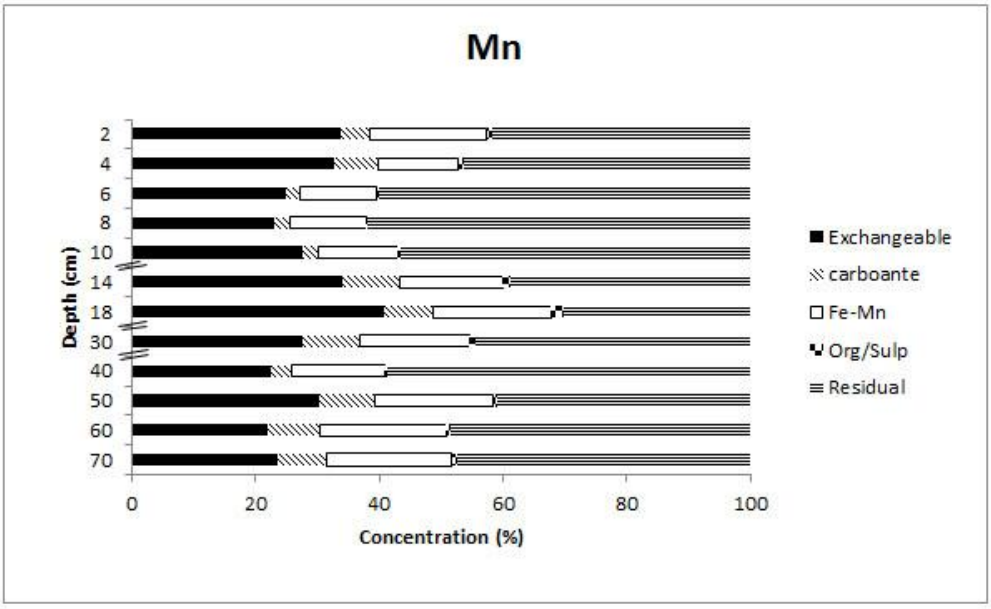

Fig. 3.2.14b Variation of Mn associated with different fractions in core VS-2.

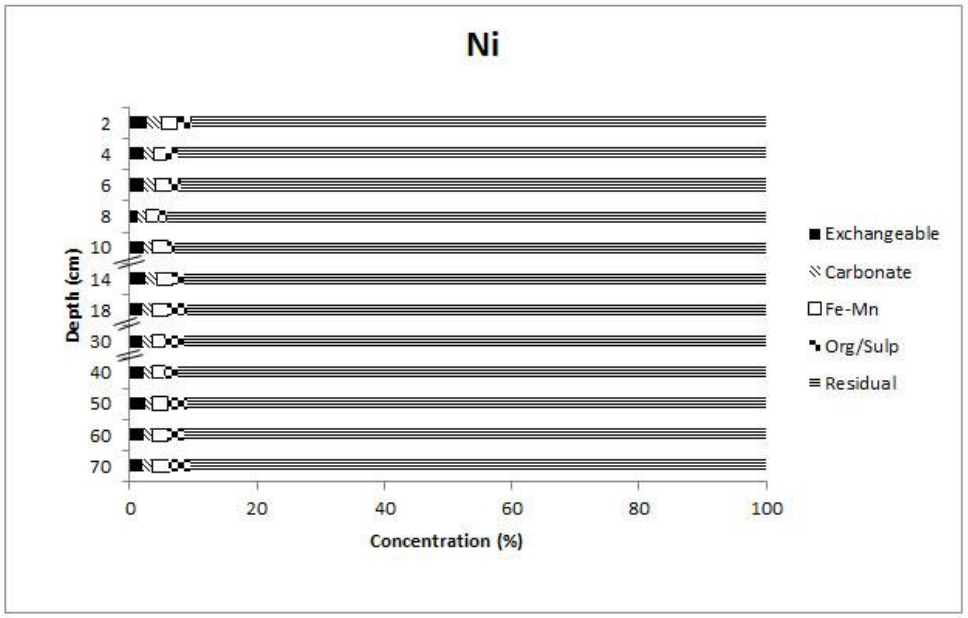

Fig. 3.2.14c Variation of Ni associated with different fractions in core VS-2.

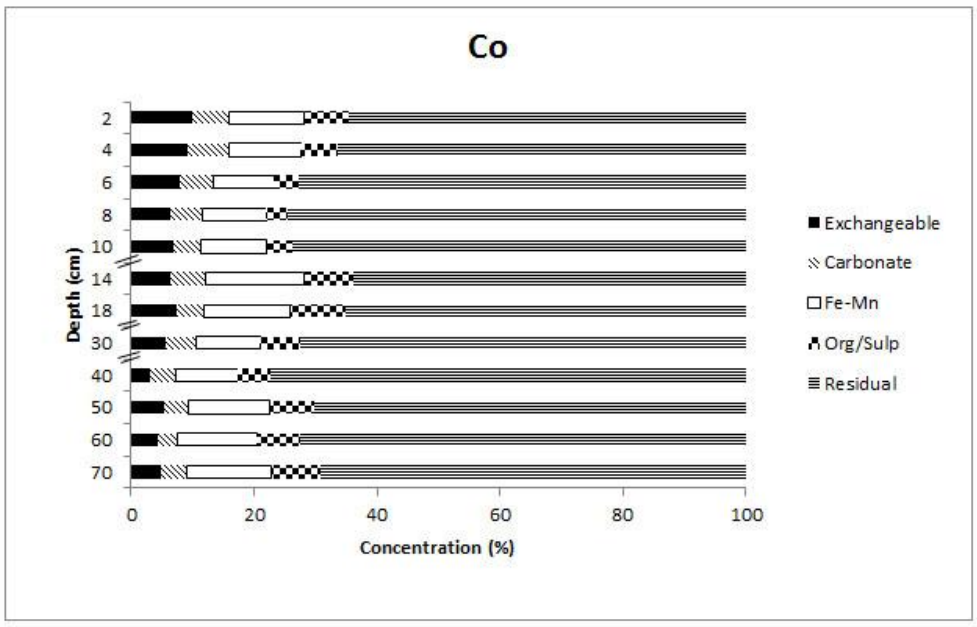

Fig. 3.2.14d Variation of Co associated with different fractions in core VS-2.

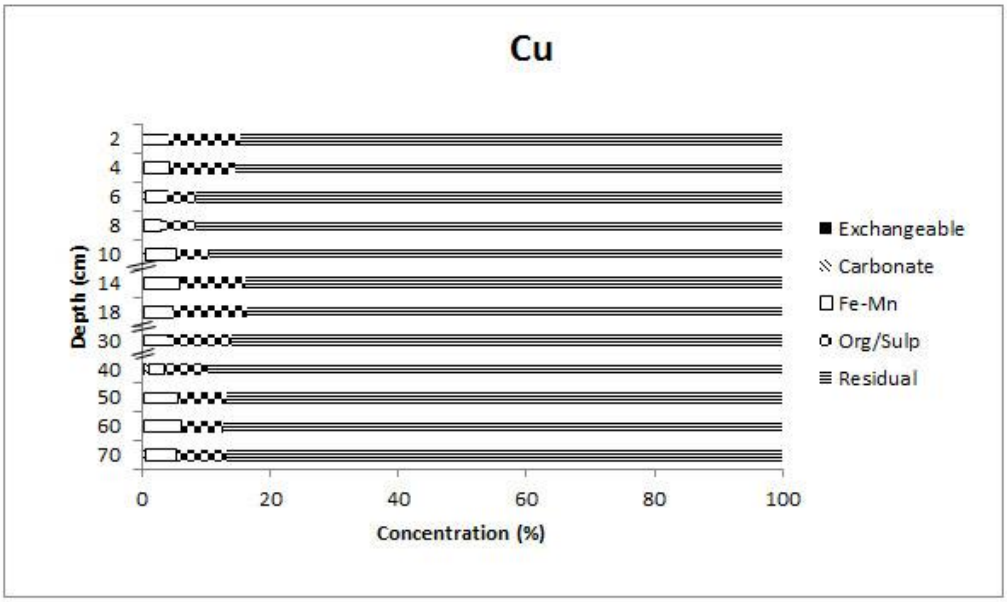

Fig. 3.2.14e Variation of Cu associated with different fractions in core VS-2.

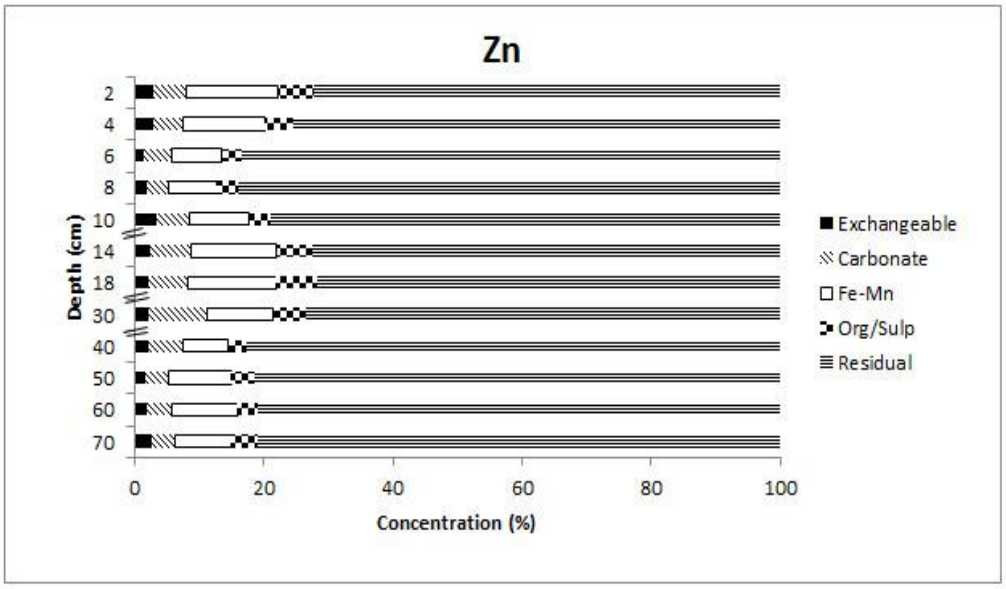

Fig. 3.2.14f Variation of Zn associated with different fractions in core VS-2.

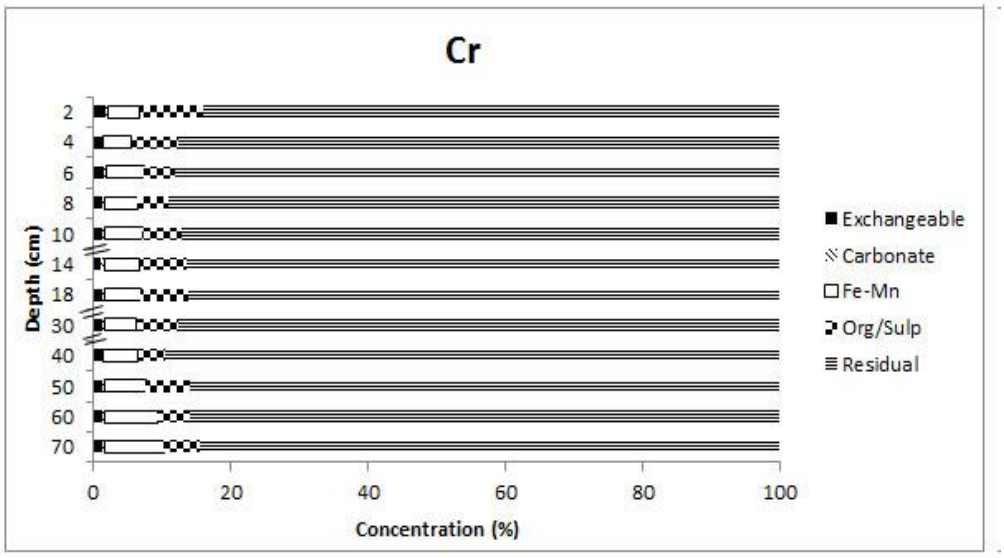

Fig. 3.2.14g Variation of Cr associated with different fractions in core VS-2.

Vaghotan estuary

In core VG-2, Fe, Ni, Cu and Cr were associated more than 80 %, except Co which was 60.31 % in the residual fraction. Next to the residual fraction, Co was associated with the Fe-Mn oxide fraction and also available in more than 10 % in the organic bound fraction. Metals viz. Fe, Ni, Cu and Cr were present in less than 6 % in individual bioavailable phases. Iron and cobalt were least in the exchangeable fraction, while Ni and Cu in the Fe-Mn oxide fraction. Chromium was present in least concentration in the carbonate fraction.

The distribution of Fe in the core VG-2 showed two sections, lower from bottom to 40 cm and upper from 40 cm to surface. The concentration of Fe was slightly higher in the bioavailable (organic) phases in the lower section than the upper section indicating formation of Fe sulphide at deeper anoxic level. Similar to Fe, Ni showed increase in bioavailable phases from bottom to 40 cm. It showed increasing trend in the exchangeable fraction, whereas decreasing trend in the residual fraction from bottom to 40 cm. However, did not show much variation in carbonate, Fe-Mn oxide and organic phases. From 40 cm to surface, Ni concentration decreased in stages in the bioavailable phases and increased in the residual phase. However, its concentration remained nearly constant in different phases. In core VG-2, Co concentration in the bioavailable phases was around 40 %. Cobalt did not show much variation in exchangeable and carbonate phases but showed variation in Fe-Mn oxide and organic phases. Cobalt in Fe-Mn oxide and organic phases increased from bottom to 40 cm

followed by decrease up to 14 cm and then increased towards surface, indicating remobilization in these phases. Copper associated with the exchangeable fraction was slightly higher in the bottom half of the core which was negligible towards the surface. In carbonate and organic phases, Cu was more concentrated and slight increase was seen at 50 cm, 18 cm, 10 cm and near surface. Chromium in bioavailable phases was seen in exchangeable and Fe-Mn oxide phases. It was relatively higher in the Fe-Mn oxide phase. At 40 cm, slight increase in Cr in the Fe-Mn oxide phase was observed, compared to other depths.

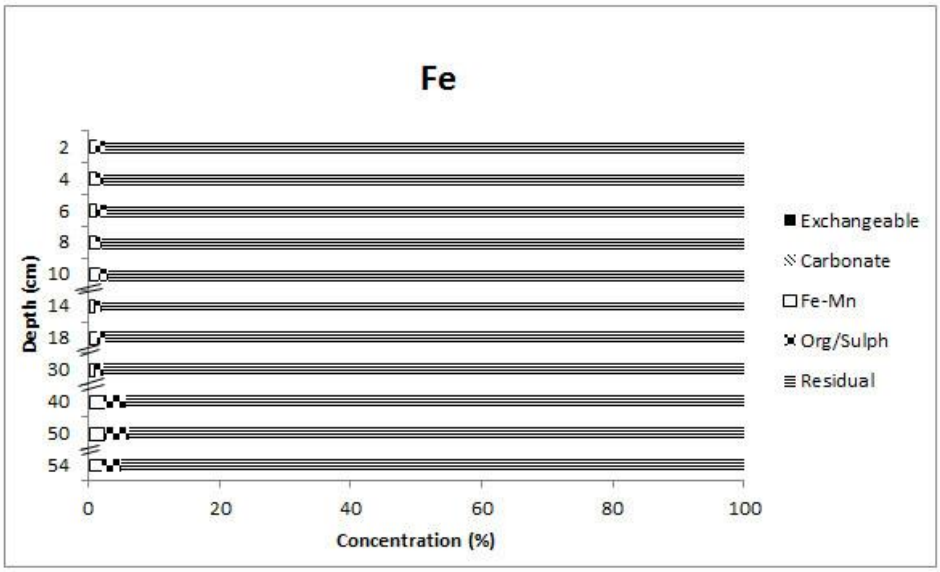

Fig. 3.2.14h Variation of Fe associated with different fractions in core VG-2.

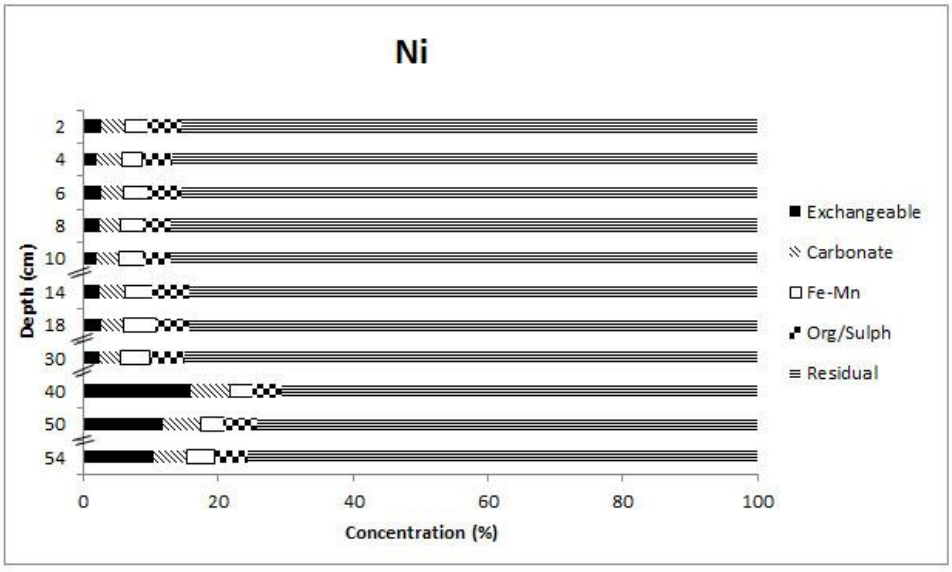

Fig. 3.2.14i Variation of Ni associated with different fractions in core VG-2.

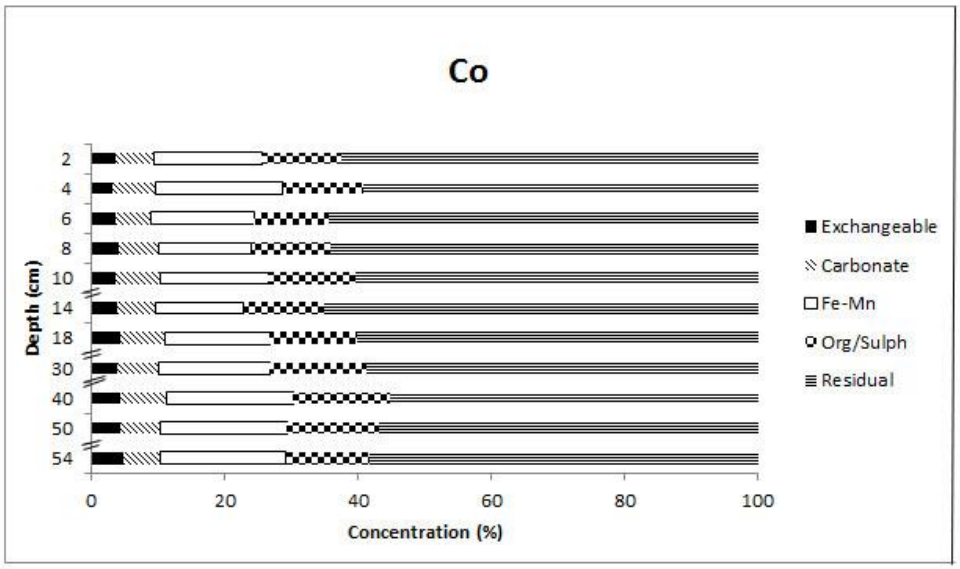

Fig. 3.2.14j Variation of Co associated with different fractions in core VG-2.

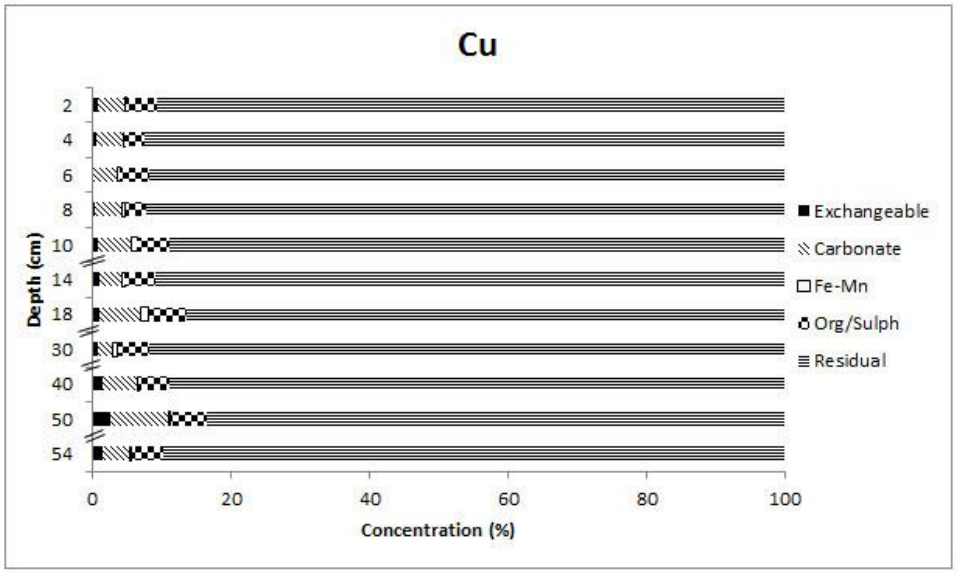

Fig. 3.2.14k Variation of Cu associated with different fractions in core VG-2.

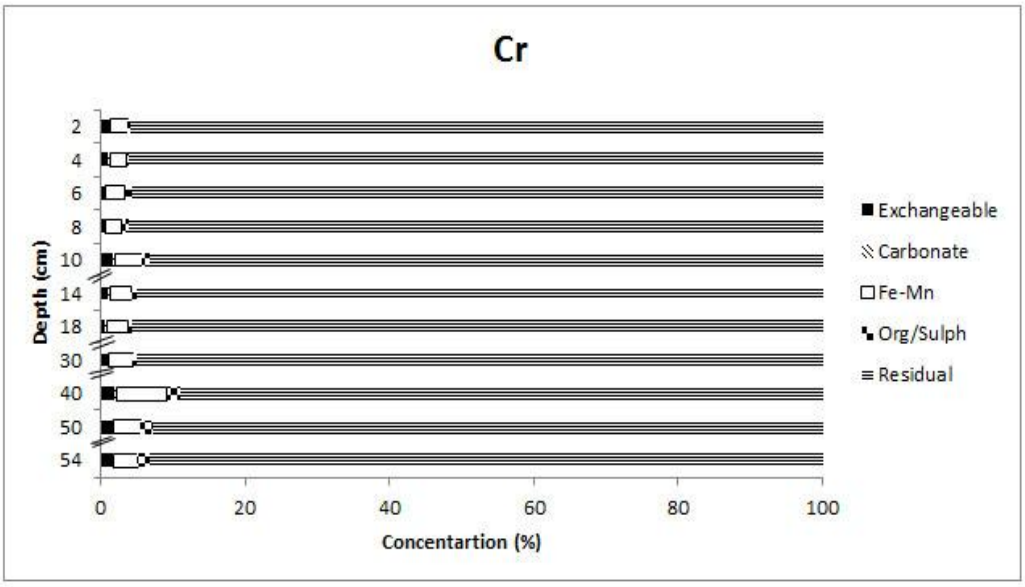

Fig. 3.2.14l Variation of Cr associated with different fractions in core VG-2.

Mandovi estuary

In core MD-2, Fe, Mn, Ni, Co, Zn and Cr were highest in the residual fraction. Metals viz. Fe, Ni, Co, Zn and Cr were present in more than 65 % in the residual fraction, while Mn was around 40 %. Next to the residual fraction, Mn, Ni, Co and Zn were present in the Fe-Mn oxide fraction, while Fe and Cr in the organic bound fraction. Metals viz. Fe, Ni, Co and Cr were available in least concentration in the carbonate fraction. Manganese was least in the organic bound fraction, whereas Zn in the exchangeable fraction. The concentration of Fe was the lowest in the bioavailable fractions.

Iron did not show much variation in any of the fractions in the core MD-2. Manganese associated with the exchangeable fraction showed overall decrease from bottom to surface except very high values at 60, 18 and 10 cm depths. In carbonate and Fe-Mn oxide fractions, Mn concentration increased from bottom to 30 cm followed by overall decrease up to 10 cm. Further, it exhibited increasing trend towards the surface in these fractions. Manganese bound to the organic fraction showed overall increase towards the surface. The vertical distribution of Ni did not show much variation in any of the fractions in the core MD-2. However, at 60 cm increase in the exchangeable phase and at 4 cm large increase in the exchangeable and decrease in the residual phase was seen. Cobalt in the exchangeable phase exhibited slight increase at 60, 18 and 10 cm, similar to Mn. Cobalt associated with the carbonate fraction

remained nearly constant in the core MD-2. Its concentration decreased from bottom to 60 cm in the organic phase and then showed slightly increasing values towards the surface. Cobalt in the Fe-Mn oxide phase was higher in the middle portion of the core between 50 and 14 cm, and also at 8 cm and surface. Similar to Mn, Zn exhibited slight increase at 60 and 10 cm in the exchangeable fraction. Zinc bound to the organic phase exhibited overall increase from bottom to surface. Fe-Mn oxide and carbonate phases showed variation with slightly higher values in the middle portion of the core. Chromium in different phases did not show much variations except in the organic phase in which it exhibited higher values towards surface.

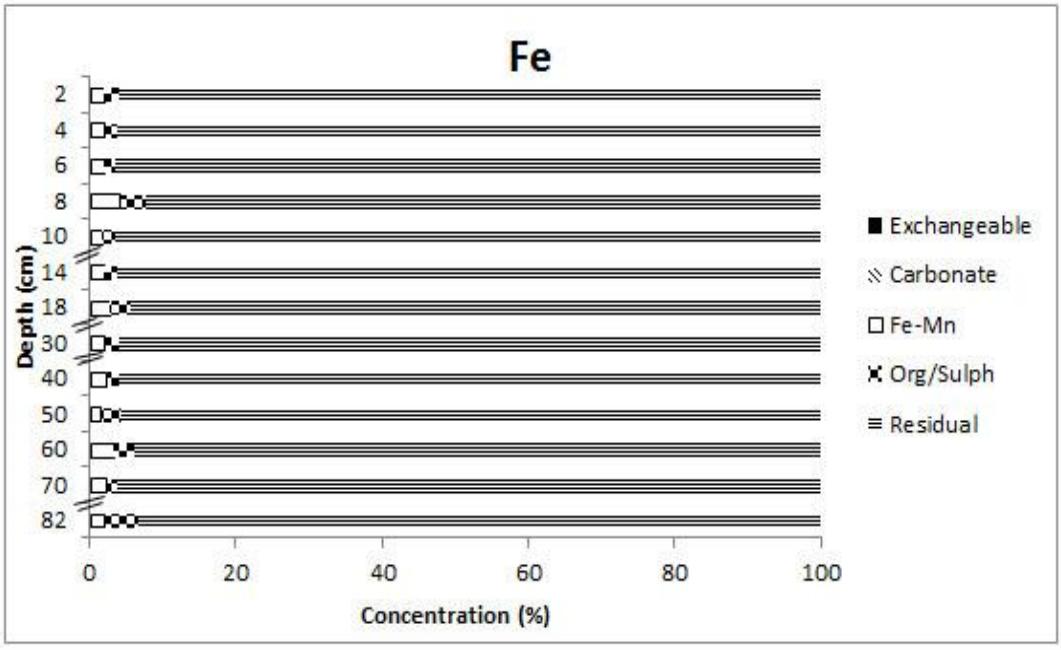

Fig. 3.2.14m Variation of Fe associated with different fractions in core MD-2.

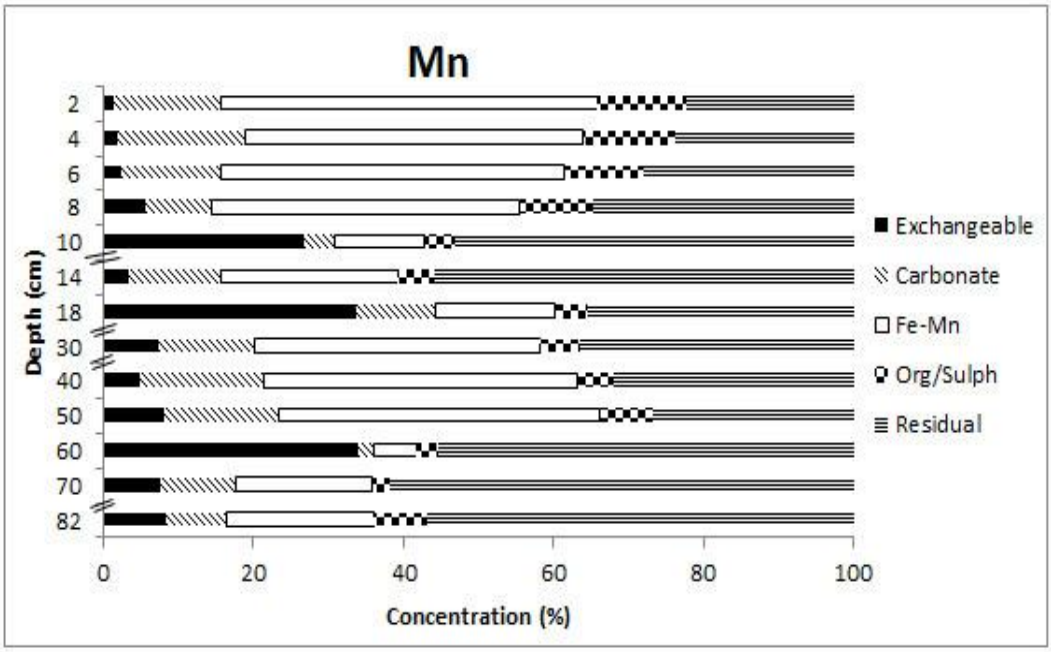

Fig. 3.2.14n Variation of Mn associated with different fractions in core MD-2.

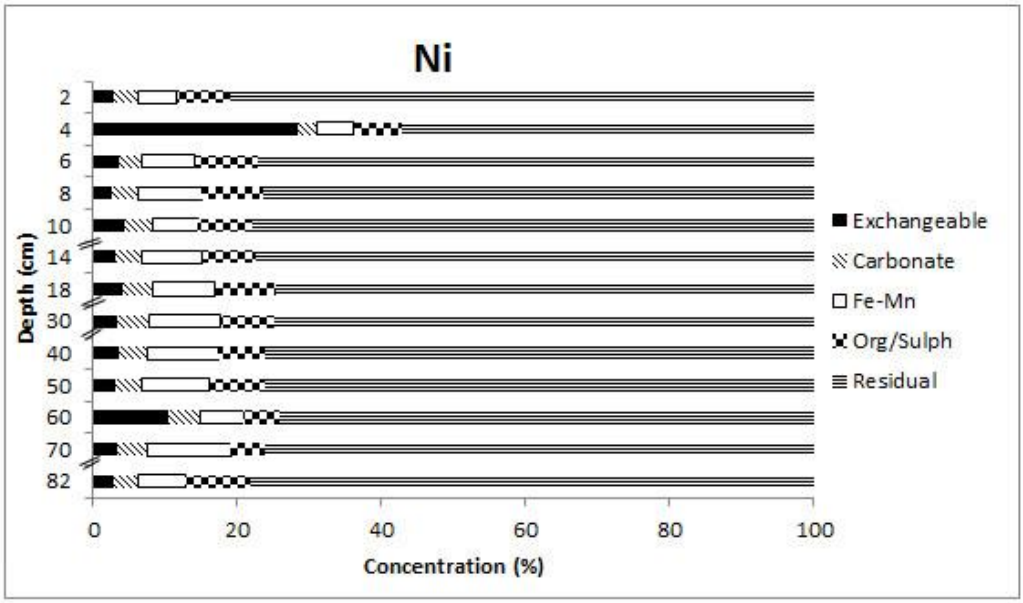

Fig. 3.2.14o Variation of Ni associated with different fractions in core MD-2.

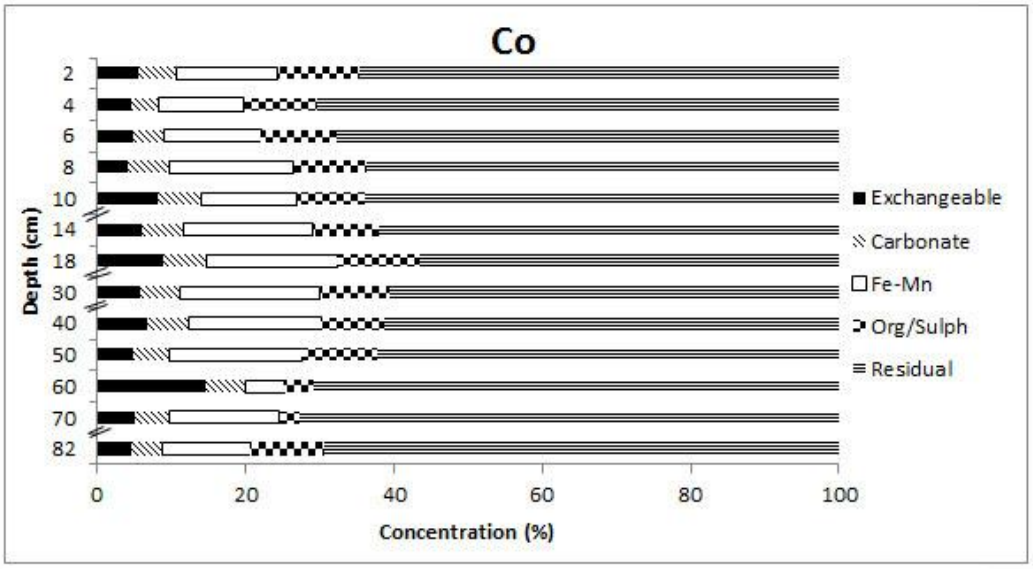

Fig. 3.2.14p Variation of Co associated with different fractions in core MD-2.

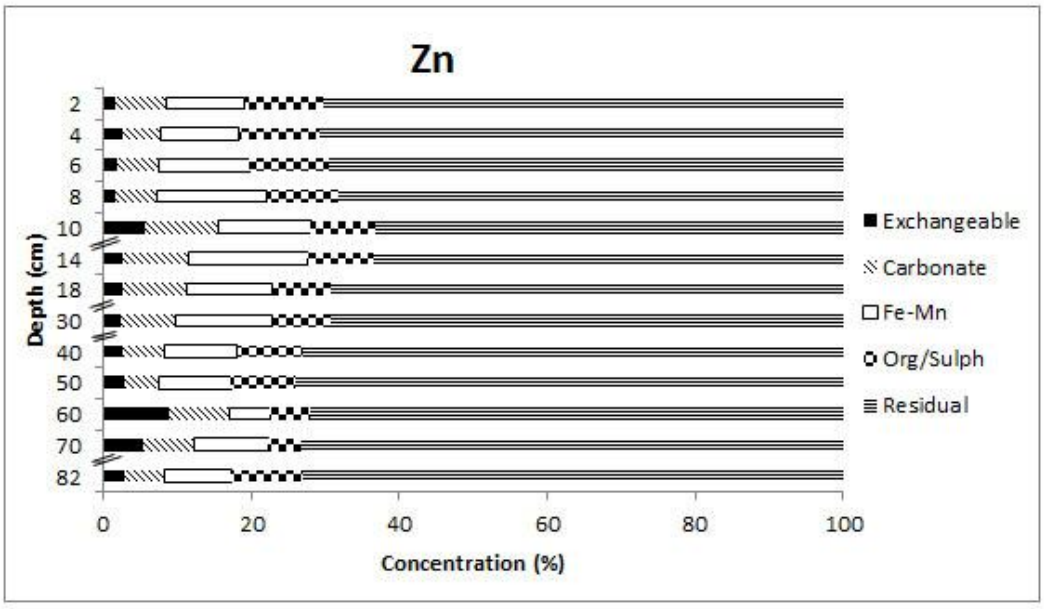

Fig. 3.2.14q Variation of Zn associated with different fractions in core MD-2.

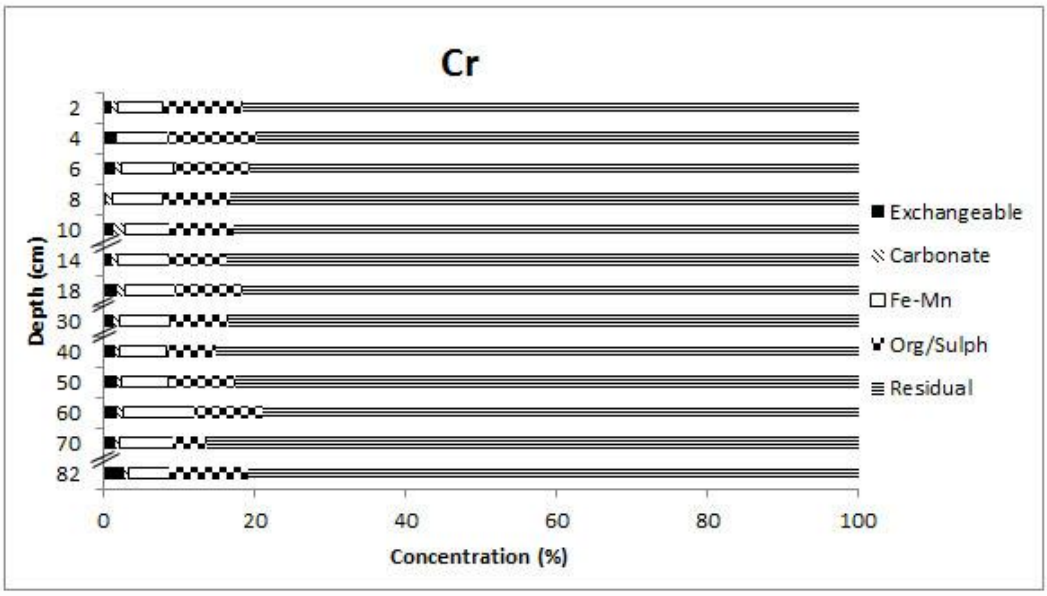

Fig. 3.2.14r Variation of Cr associated with different fractions in core MD-2.

Sharavathi estuary

In core S-2, Fe, Mn, Ni, Co, Cu and Cr were highest (> 70 %) in the residual phase, except Mn and Co which were 60.62 and 55.93 % respectively. Next to the residual fraction, Fe, Mn, Ni and Co was associated with the Fe-Mn oxide phase, Cu with the carbonate phase and Cr with the organic phase. Manganese was available in considerable concentration in the exchangeable fraction and Cu in the organic phase. Metals viz. Fe, Ni, Co, Cu and Cr showed least concentration in the exchangeable phase, while Mn in the organic phase.

The distribution of Fe from bottom to 30 cm was slightly higher in the Fe-Mn oxide phase than from 30 cm to surface. Manganese was with high concentration in the exchangeable fraction, except between 18 to 14 cm where it showed less concentration. Manganese in carbonate and organic bound fractions was almost constant with depth, except higher value at 30 and 18 cm, respectively. Manganese in the Fe-Mn oxide phase showed slight increase from bottom to 30 cm which was followed by sharp decrease at 18 cm. Further, it maintained low concentration up to 10 cm and showed slightly higher values from 8 cm to surface. Sum of the bioavailable phases was higher in the lower part from bottom to 30 cm. From 14 cm to surface, bioavailable Mn increased towards surface. Nickel exhibited increase in the bioavailable fractions from bottom to 18 cm. It was highest and constant between 18 and 14 cm, and then gradually decreased towards surface. Cobalt in the exchangeable fraction

increased from bottom to 18 cm and then showed overall decrease towards the surface. Its concentration in both exchangeable and carbonate fractions was much higher between 18 and 14 cm. In the Fe-Mn oxide fraction, it decreased from bottom to 8 cm followed by increase towards the surface. Cobalt exhibited very high concentration at 8 cm in the organic phase. Copper in exchangeable and Fe-Mn oxide phases was negligible. Carbonate phase showed high values between 18 and 14 cm. Compared to other depths organic phase was almost constant except from 18 to 14 cm depth wherein it was very less. Chromium showed overall increase from bottom to 14 cm in exchangeable, carbonate and organic phases and then exhibited overall decrease towards the surface. The organic phase showed slightly higher values at 6 cm. Fe-Mn oxide phase was high between 18 and 14 cm.

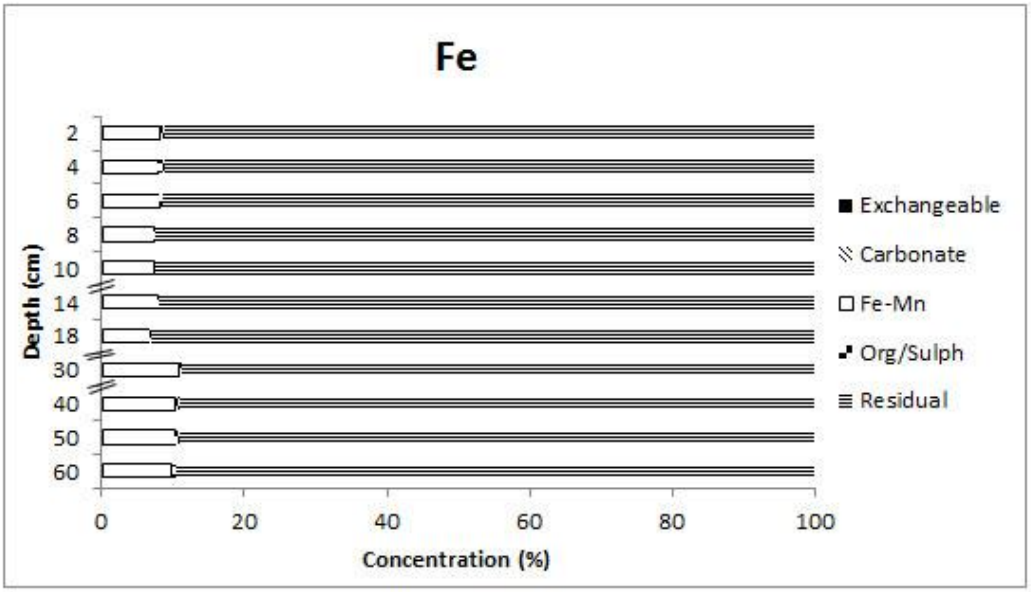

Fig. 3.2.14s Variation of Fe associated with different fractions in core S-2.

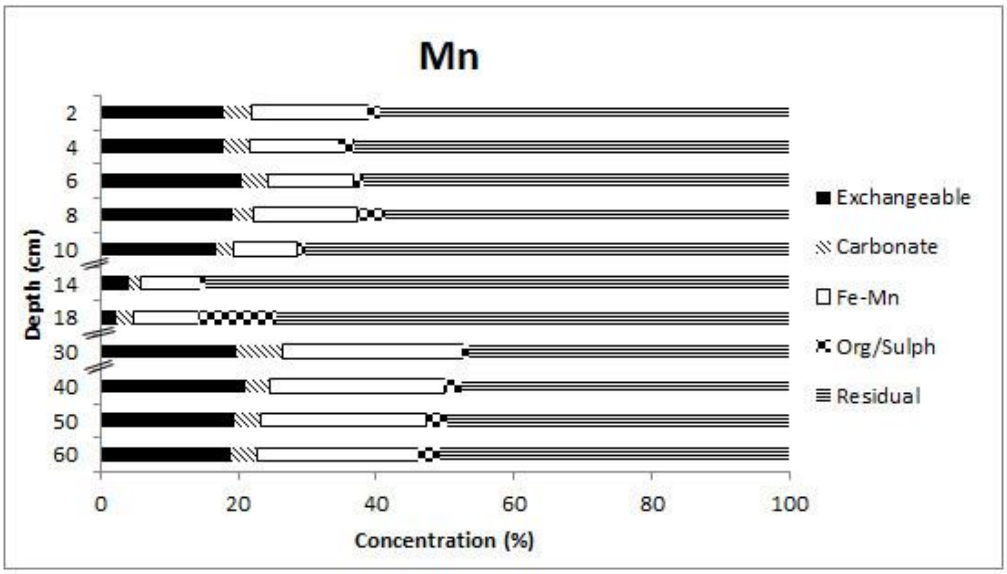

Fig. 3.2.14t Variation of Mn associated with different fractions in core S-2.

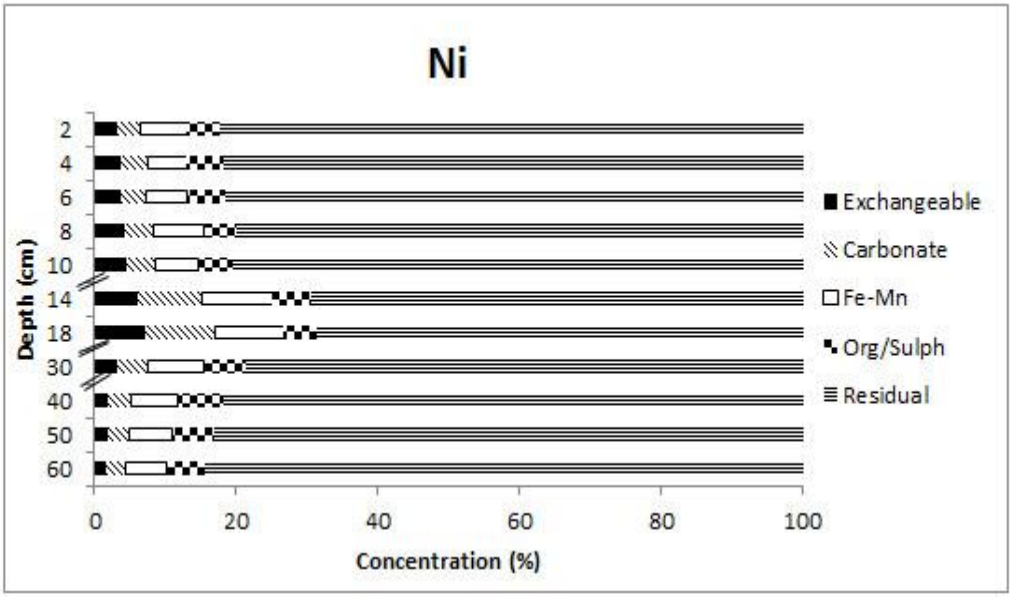

Fig. 3.2.14u Variation of Ni associated with different fractions in core S-2.

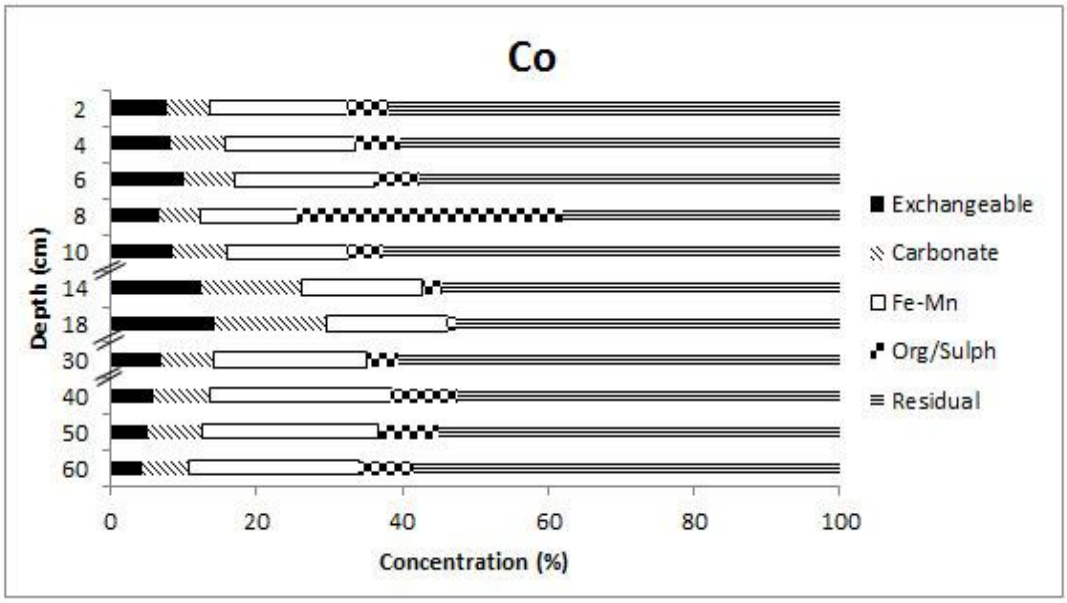

Fig. 3.2.14v Variation of Co associated with different fractions in core S-2.

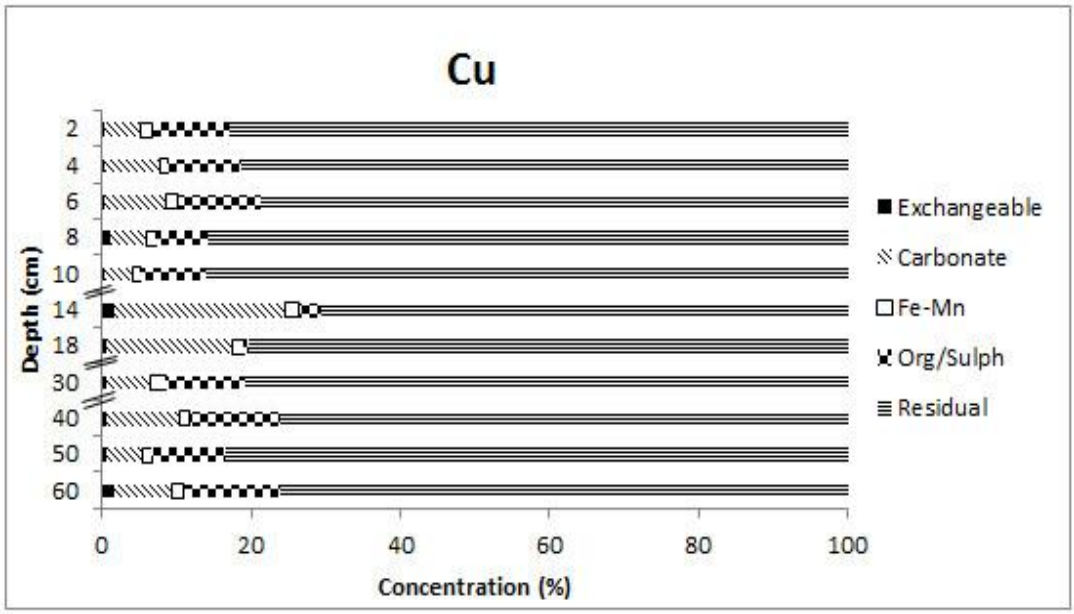

Fig. 3.2.14w Variation of Cu associated with different fractions in core S-2.

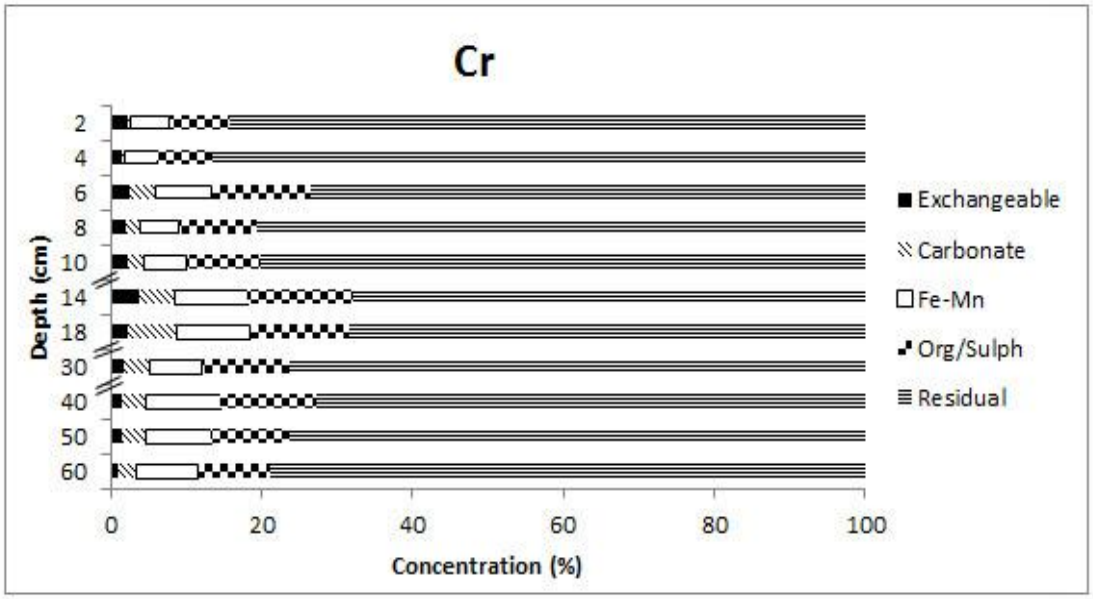

Fig. 3.2.14x Variation of Cr associated with different fractions in core S-2.

Gurupur estuary

In core GP-2, Fe, Ni, Co, Zn and Cr were associated more than 70 %, except Co which was 64.12 % with the residual fraction. Among the bioavailable phases, Fe, Ni, Co and Zn were highest in the Fe-Mn oxide fraction, while Cr was associated more with the organic fraction. Metals viz. Fe, Co and Cr were present in least concentration in the carbonate fraction, while Ni in the exchangeable fraction and Zn were least in the organic bound fraction.

The concentration of Fe and Ni associated with the residual fraction increased from 60 cm to surface and Cr from 50 cm to surface of the core GP-2. Iron bound to Fe-Mn oxide and organic phases, Ni bound to carbonate, Fe-Mn oxide and organic phases were higher at 60 cm depth, and Cr bound to exchangeable, Fe-Mn oxide and organic phases was higher at 50 cm of the core GP-2. The bioavailable concentration was much higher in case of Co and Zn when compared to Fe, Ni and Cr. Metals viz. Co and Zn associated with the exchangeable fraction showed higher concentration between 40 and 18 cm in this core. Cobalt showed less concentration associated with carbonate, Fe-Mn oxide and organic phases between 40 and 18 cm. Also, Zn exhibited overall decrease in its bioavailable concentration between 40 and 14 cmbound to carbonate, Fe-Mn oxide and organic phases. Zinc associated with carbonate, Fe-Mn oxide and organic phases increased from 14 cm to surface. Cobalt associated with the carbonate phase increased, Fe-Mn oxide phase decreased from 10 cm to surface.

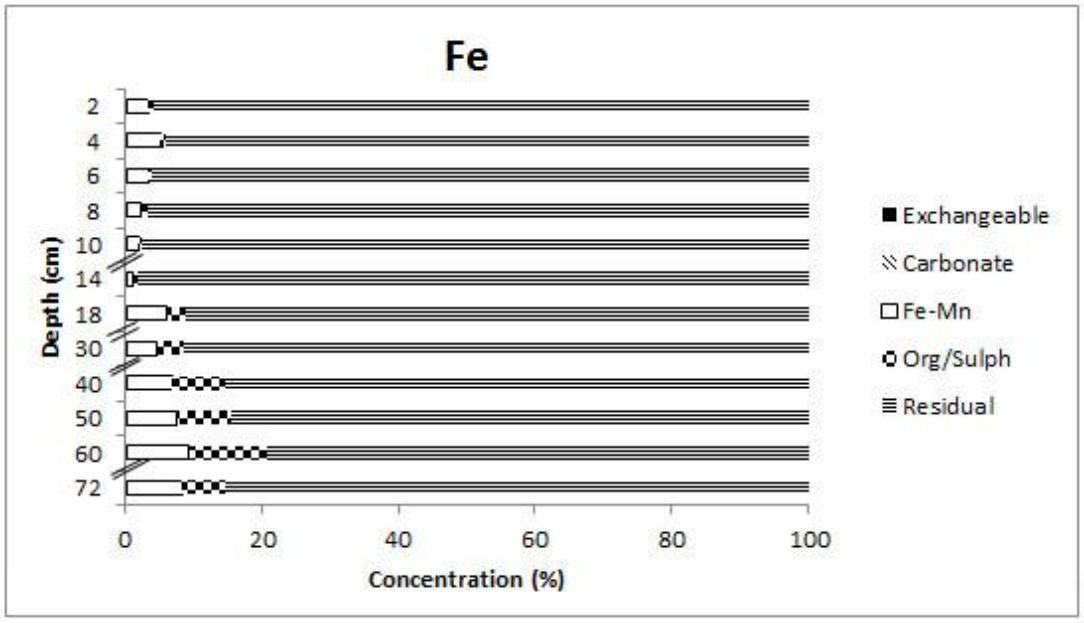

Fig. 3.2.14y Variation of Fe associated with different fractions in core GP-2.

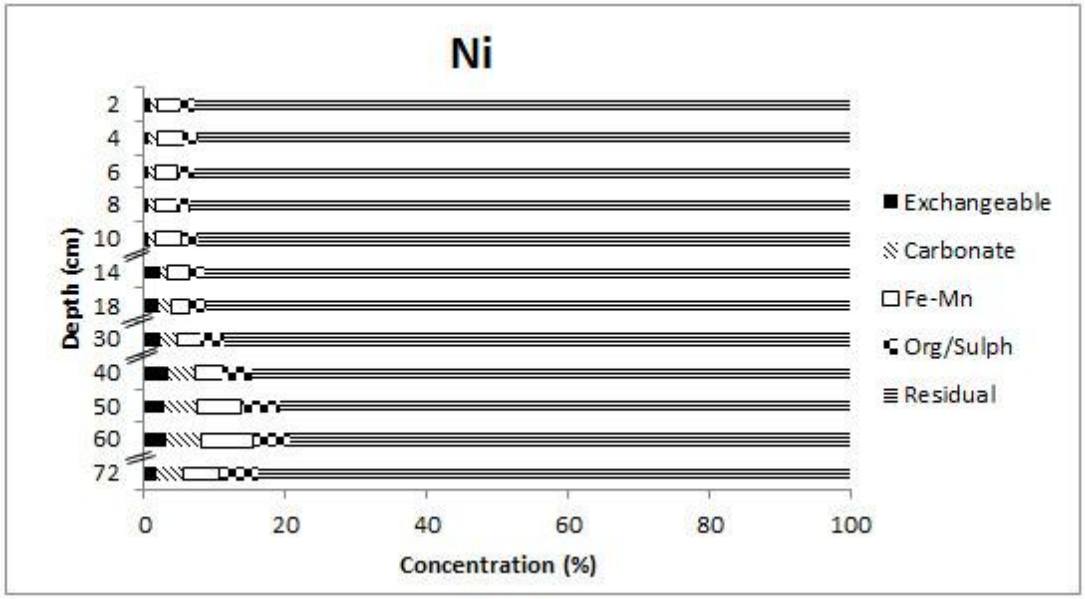

Fig. 3.2.14z Variation of Ni associated with different fractions in core GP-2.

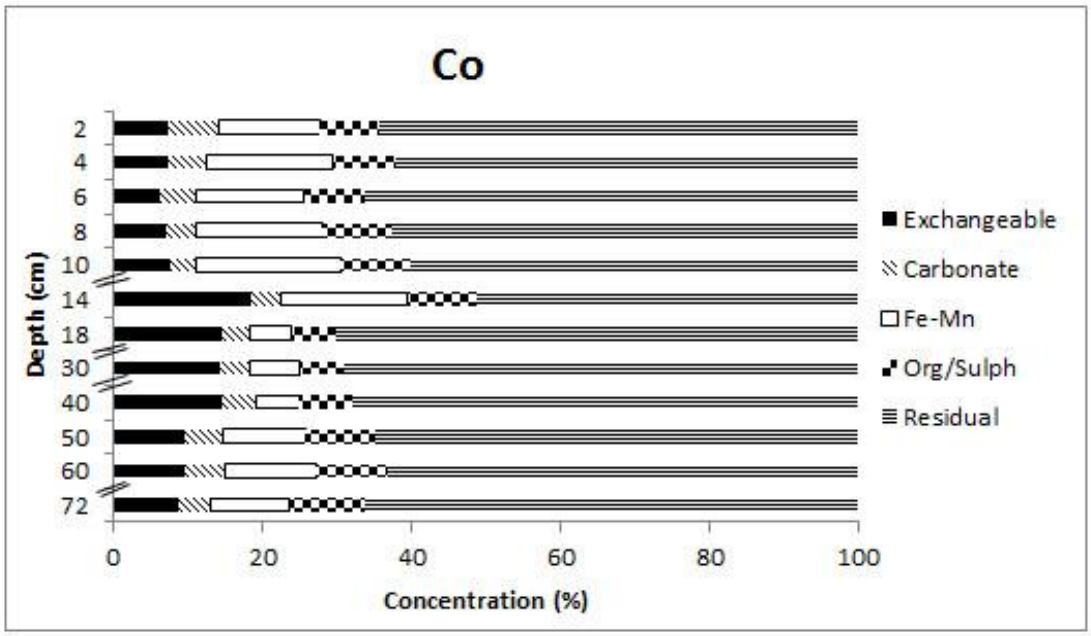

Fig. 3.2.14aa Variation of Co associated with different fractions in core GP-2.

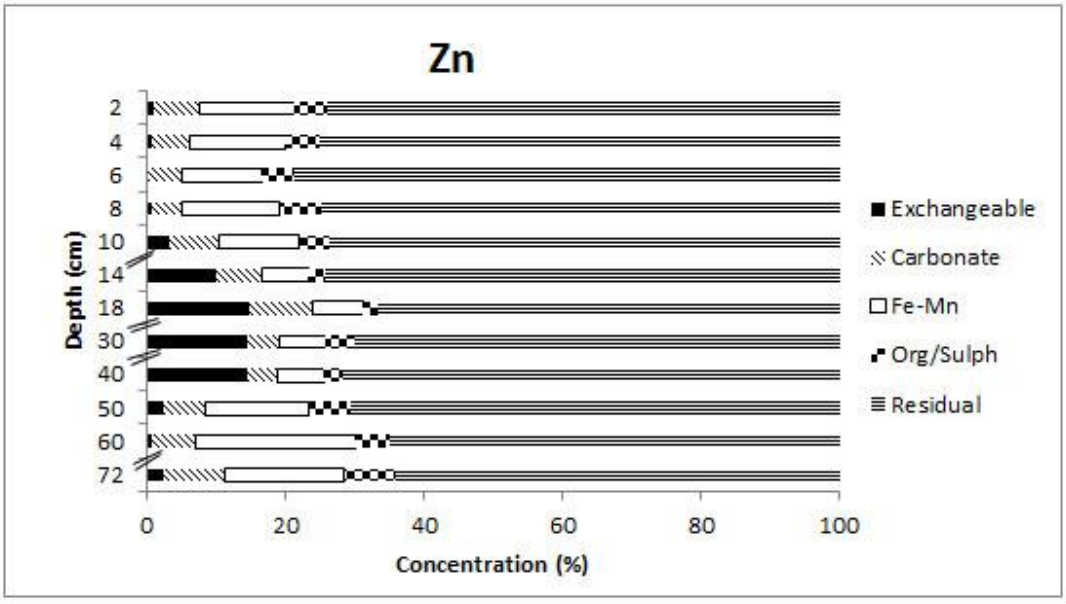

Fig. 3.2.14ab Variation of Zn associated with different fractions in core GP-2.

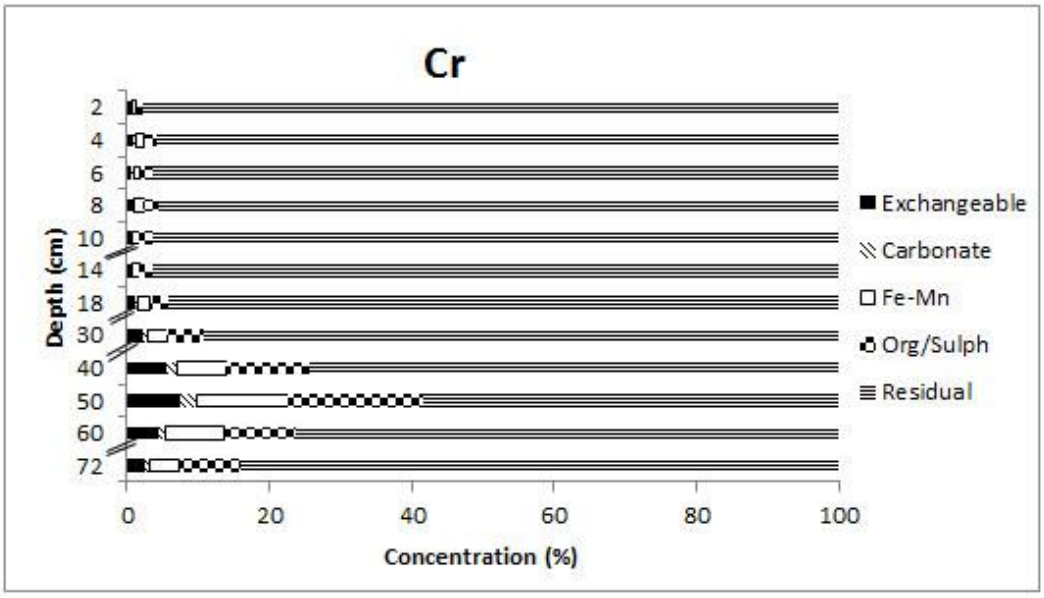

Fig. 3.2.14ac Variation of Cr associated with different fractions in core GP-2.

The speciation study of selected sub-samples of sediment cores collected from five estuaries showed highest concentration of all the analysed metals in the residual phase indicating their natural occurrence to large extent as derived from the parent rock (Ratuzny et al. 2009). However, some metals with very high concentration in the bioavailable phases indicated anthropogenic origin.

In core VS-2, among the bioavailable fractions, Mn was highest in the exchangeable phase and also its concentration was higher near the surface. Also, it exhibited increase in the Fe-Mn oxide phase near the surface. Cobalt bound to exchangeable and Fe-Mn oxide phases also showed increase near the surface. Increase in Co and Zn, similar to Mn near the surface in the Fe-Mn oxide phase revealed diagenetic remobilization of these metals. Distribution of sum of bioavailable phases of Mn, Co, Cu and Zn along with Cr showed enrichment of these metals near the surface and decrease between 10 and 6 cm, indicating remobilization of bioavailable phases. Metals migrate through pore water towards the surface and get adsorb onto sediments under oxic conditions (Brown et al. 2000).

Metals viz. Fe, Ni, Cu and Cr were less than 18 % in the bioavailable phases and exhibited overall decrease in their concentration from bottom to surface of the core VG-2. Cobalt in Fe-Mn oxide (16.65 %) and organic (12.81 %) phases in the core VG-2 were considerably high. Cobalt was most mobile in the surface environment under acidic and reducing conditions, where the formation of high valence phases of Fe and Mn is inhibited. Cobalt is rapidly

removed from solution by co-precipitation and sorption in most oxidising, near-neutral or alkaline stream water as the dissolved Fe and Mn precipitate out as secondary oxides, hydrous Mn oxides having a particularly strong sorption affinity for cobalt (Longhinos 2011). Also Co can be organically bound (McBride 1994). High Co concentration in all the bioavailable phases indicated that it was from different source might be anthropogenic. Typically metals of anthropogenic inputs tend to reside in the first four fractions (Ratuzny et al. 2009) which are accessible to organisms. Cobalt concentration in the first two phases was around 10 %.

In core MD-2, Mn was present in significant concentration (30.74 %) in the Fe-Mn oxide phase. Moreover, increase in distribution of Mn in the Fe-Mn oxide phase towards the surface reflected its diagenetic mobilization and precipitation in the near surface sediments. Due to constantly varying Eh within the aquatic environment, metals do not remain permanently sequestered within the aquatic environment (Depledge and Fossi 1994). This results in the mobilization of sediment-bound metals (Fytianos and Lourantou 2004) and later precipitation in oxic conditions. Manganese also exhibited increase near the surface in carbonate and organic phases and was therefore environmentally significant for mobility, availability for uptake by aquatic biota and possible toxicity (Yuan et al. 2004). Zinc bound to the organic phase showed increase in the surface sediments in this core. Apart from Mn and Zn, rest of the metals did not exhibit increase in bioavailability at surface. However, decrease in exchangeable phase of Mn, Ni, Co and Zn near surface revealed diffusion of these metals from sediments to water column. The distribution of sum of bioavailable phases of Co and Zn were higher at 18 and 10 cm, and later decreased towards surface. Further, higher concentration of metals in the bioavailable phases indicated their different source might be anthropogenic.

In core S-2, Mn and Co increased towards the surface in the Fe-Mn oxide phase. In addition, Mn was also considerably high towards the surface in the exchangeable fraction. Further, in this core between 18 and 14 cm, drastic decrease in Mn and increase in Ni, Co, Cu and Cr was seen in some of the bioavailable fractions which suggested no role of Mn in regulating distribution of these trace metals. Distribution of Mn and to some extent Co in bioavailable phases indicated diagenetic mobilization. From 18 to 14 cm, most of the trace metals were trapped in carbonate and organic phases. The higher concentration of Mn, Co and Cr towards surface indicated their anthropogenic source. The high concentration of Fe in the residual

fraction of the core S-2 suggested that it was largely present in the immobile state and not available for the biota. Rest of the metals were in considerable concentration in the bioavailable phases. Metals bound to the residual phase are most strongly bound and so least available for uptake by organisms, while those metals in the exchangeable phase are most available for uptake (Davies 1984).

In core GP-2, less and decrease in concentration of Fe, Ni and Cr in the bioavailable phases towards surface was noted. Among these metals, Cr was bound to the organic phase in the lower half of the core suggesting adsorption onto sulphides under anoxic conditions. In anoxic conditions, sulphides produced from sulphate reducing bacteria are either re-oxidized or precipitated with numerous trace metals and therefore, sulphides play a predominant role in the distribution of trace elements (Saulnier and Mucci 2000). Further, the sulphide results in a more efficient scavenging of trace metals in anoxic conditions (Lesven et al. 2008). The concentration of Co and Zn was much higher in the exchangeable fraction between 40 and 14 cm which further decreased towards the surface. The concentration of Co and Zn in the Fe-Mn oxide and Co in the organic phase was higher from 14 cm to surface. The distribution pattern of Co and Zn therefore suggested their mobilization from the exchangeable phase in the recent sediments to adsorb onto Fe-Mn oxides or organic coatings on inorganic mineral particles (Tessier et al. 1979).

3.2.8 Screening quick reference table (SQUIRT)

The concentration of metals in the bulk sediments as well as sum of their bioavailable fractions is given in the Table 3.2.8.

On comparison of table 3.2.8 with table 2.3 a and b, it was observed that the percentage of total Fe and sum of bioavailable Fe was lower than the apparent effect threshold (AET) in all the estuaries indicating no harm from Fe to the sediment associated biota. Total Mn as well as sum of bioavailable Mn in Vashishti, Mandovi and Sharavathi estuaries exceeded AET suggesting its probable toxicity to the sediment associated organisms. In the Gurupur estuary, value of total Ni ranged from effect range median (ERM) to AET, whereas bioavailable Ni varied from threshold effect level (TEL) to effect range low (ERL) demonstrating its concern to the sediment associated biota. Although, total Ni in rest of the estuaries exceeded

Table 3.2.8 Average concentrations of total metals and bioavailable fractions in selected sub-samples in cores VS-2, VG-2, MD-2, S-2 and GP-2. F1=exchangeable fraction and F2=carbonate fraction.

	VS-2		
	Total metals concentration	Sum of bioavailable fractions	F1+F2 (%)
Fe (%)	15.28	0.27	2.15
Mn (ppm)	1840	572	34.91
Ni (ppm)	114	4	3.68
Co (ppm)	64	10	11.28
Cu (ppm)	353	26	0.50
Zn (ppm)	452	23	7.45
Cr (ppm)	164	19	1.55

	VG-2		
	Total metals concentration	Sum of bioavailable fractions	F1+F2 (%)
Fe (%)	10.49	0.51	0.002
Ni (ppm)	110	11	9.07
Co (ppm)	70	13	10.23
Cu (ppm)	303	16	5.52
Cr (ppm)	163	4	1.27

	MD-2		
	Total metals concentration	Sum of bioavailable fractions	F1+F2 (%)
Fe (%)	15.42	0.76	0.001
Mn (ppm)	3069	1596	22.46
Ni (ppm)	77	15	9.52
Co (ppm)	31	7	11.45
Zn (ppm)	1634	14	10.12
Cr (ppm)	259	19	2.40

	S-2		
	Total metals concentration	Sum of bioavailable fractions	F1+F2 (%)
Fe (%)	4.94	0.80	0.004
Mn (ppm)	1056	365	19.83
Ni (ppm)	102	10	8.37
Co (ppm)	27	9	16.38
Cu (ppm)	139	16	9.51
Cr (ppm)	123	22	4.94

	GP-2		
	Total metals concentration	Sum of bioavailable fractions	F1+F2 (%)
Fe (%)	8.47	0.45	0.002
Ni (ppm)	63	19	4.01
Co (ppm)	34	8	14.93
Zn (ppm)	168	10	11.80
Cr (ppm)	927	31	2.91

the TEL, sum of bioavailable Ni was lower than the TEL suggesting not much concern to associated biota from Ni. Total as well as bioavailable Co exceeded the AET in the core VG-2 while, in case of the core VS-2 total Co was more than the AET and the sum of the bioavailable Co equals AET value. Therefore, indicated concern from Co to sediment associated biota in Vashishti and Vaghotan estuaries. In case of Mandovi, Sharavathi and Gurupur estuaries, total Co exceeded the AET, while sum of bioavailable Co was lower than the AET revealing not much concern to the aquatic life of these estuaries from these metals. Associated organisms of the Vashishti estuary seemed to be at concern from Cu as its concentration in bulk sediments ranged from ERM to AET, while sum of bioavailable Cu varied from TEL to ERL. Bioavailable Cu in Vaghotan and Sharavathi estuaries was lower than the TEL. The concentration of total Zn in Vashishti and Mandovi estuaries was more than the AET while, in the Gurupur estuary it ranged from ERL to probable effect level (PEL). However, sum of bioavailable Zn in these estuaries was lower than the TEL suggesting not much concern to the sediment associated biota. Total Cr ranged from PEL to ERM in Vashishti, Vaghotan and Mandovi estuaries, whereas in the Sharavathi estuary, it ranged from ERL to PEL. In the Gurupur estuary, total Cr was more than the ERM. In all these estuaries, however sum of bioavailable Cr was lower than the TEL indicating not much concern to the associated organisms.

The speciation of elements therefore indicated concern from Mn, Co and Cu to sediment associated organisms in the Vashishti estuary. Cobalt concentration suggested concern to sediment associated biota in the Vaghotan estuary, while biota from Mandovi and Sharavathi estuaries was at concern from Mn. Nickel was likely to cause concern to aquatic life of the Gurupur estuary. Exposure of sediment-dwelling organisms to metals may occur via uptake of interstitial waters, ingestion of sediment particles and via the food chain (Luoma 1989). Therefore, necessary steps are required to reduce the effect and also reduce the further input of the anthropogenic material to these estuaries.

3.2.9 Risk assessment code

When sum of the percentage of metals in exchangeable (fraction 1) and carbonate fractions (fraction 2) at studied cores (Table 3.2.8) were compared with risk assessment code it was noted that in core VS-2 Fe, Ni, Cu, Zn and Cr were within the degree of low risk, Co within the degree of medium risk and Mn in the category of high risk. In core VG-2, all the metals

were within the degree of low risk. In core MD-2, Fe, Ni, Zn and Cr fell under the category of low risk, while Mn and Co within the degree of medium risk. Metals viz. Fe, Ni, Cu and Cr were within the degree of low risk in the core S-2, whereas Mn and Co fell under the category of medium risk. In core GP-2, Fe, Ni and Cr were within the degree of low risk, while Co and Zn fell under the category of medium risk.

Among the metals studied, only Mn in the core VS-2 showed higher degree of risk associated with exchangeable and carbonate phases.

Section III: Comparison of lower and middle estuarine regions

3.3.1 Sediment components, pH, organic carbon and metals in bulk sediments

In order to understand difference between lower and middle regions of estuaries, the data of sediment components, pH, organic carbon, metals in the bulk sediments was plotted on isocon diagram (Fig.3.3.1). On comparison of core VS-1 with core VS-2, clay, organic carbon and pH were higher in the core VS-1, while sand, silt, Fe, Mn, Ni, Co, Cu and Zn were higher in the core VS-2. Aluminium was slightly higher in the core VS-1, whereas Cr in the core VS-2. Among cores VG-1 and VG-2, sand, silt, organic carbon, Fe, Mn, Ni, Co and Cu were higher in the core VG-1, while clay and Cr in the core VG-2. pH and Al were nearly equal in both the cores, while Zn was present in slightly higher concentration in the core VG-1. In case of cores MD-1 and MD-2, sand and pH were higher in the core MD-1, whereas silt, Al, Fe, Mn, Ni, Co, Cu, Zn and Cr were higher in the core MD-2. Clay and organic carbon were slightly higher in the core MD-1. On comparison of cores S-1 and S-2, sand, pH and Zn were higher in the core S-1, while silt, organic carbon, Al, Fe, Mn, Ni, Co, Cu and Cr were higher in the core S-2. Clay was equal in both the cores. Among the cores GP-1 and GP-2, sand and Zn were higher in the core GP-1, whereas silt, clay, organic carbon, Al, Fe, Mn, Ni, Co, Cu and Cr were higher in the core GP-2. pH was equal in both the cores.

In Vaghotan, Mandovi, Sharavathi and Gurupur estuaries sand was higher in the lower estuarine region than the middle estuarine region, whereas silt was higher in the middle estuarine region of Vashishti, Mandovi, Sharavathi and Gurupur estuaries. In general in any given estuarine system, lower estuary with more marine influence, high waves, tides and

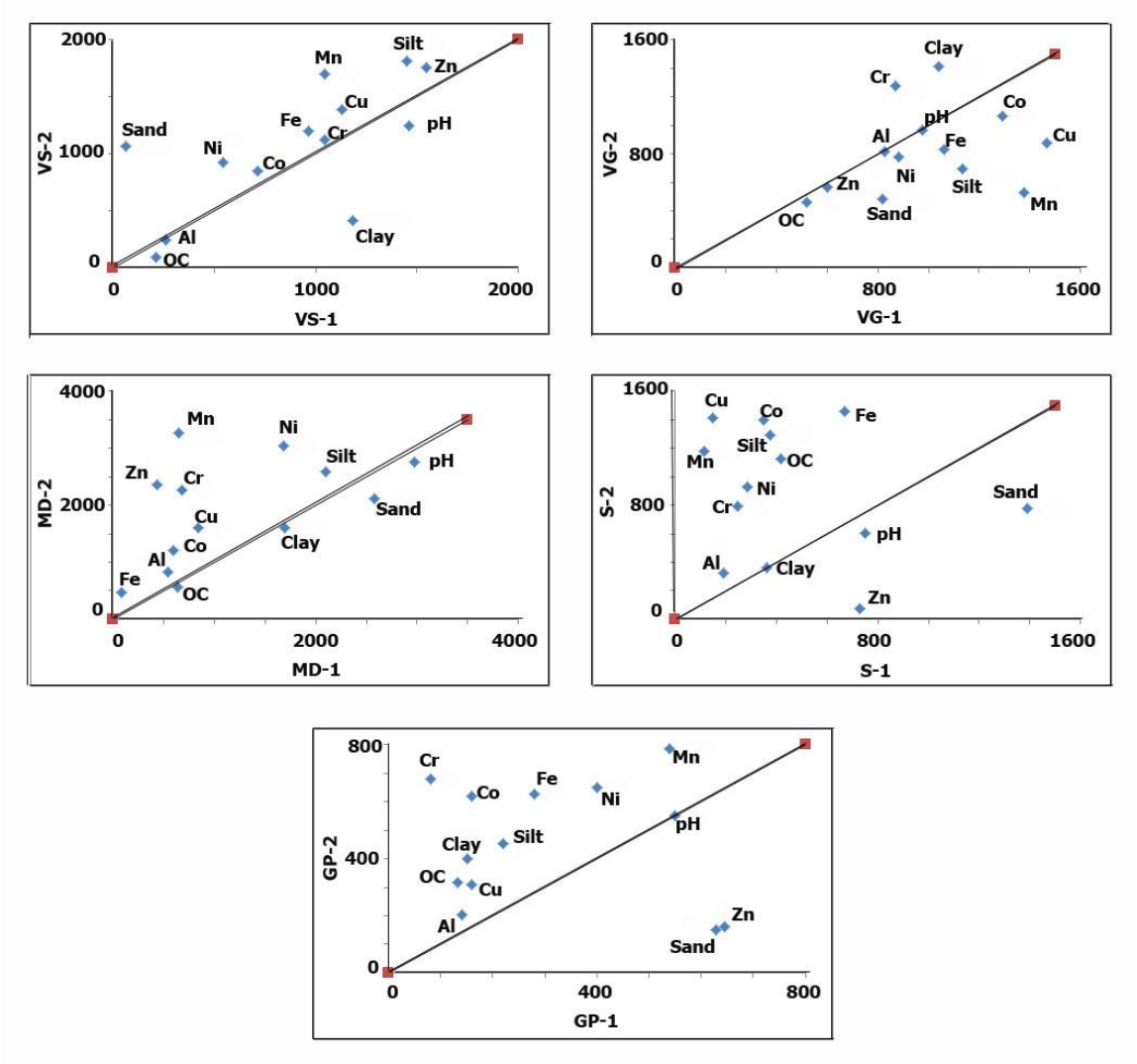

Fig. 3.3.1 Isocon plots for comparing sediment components, pH, organic carbon and metals in the bulk sediments in Vashishti (VS-1 v/s VS-2), Vaghotan (VG-1 v/s VG-2), Mandovi (MD-1 v/s MD-2) Sharavathi (S-1 v/s S-2) and Gurupur estuaries (GP-1 v/s GP-2).

currents maintains high energy and facilitates deposition of coarser sediments. Middle estuarine region is known for mixing of fresh and saline waters which facilitates calm conditions and therefore helps in deposition of finer sediments, organic matter and metals. However, in the present study, clay and organic carbon did show higher concentration in the middle region of all the estuaries. Further, in Vashishti, Mandovi, Sharavathi and Gurupur estuaries, concentration of most of the metals was higher in the middle region than the lower region which was attributed to their retention on finer sediments which remain in suspension for longer period of time in the middle estuarine region. In addition, the Lote Parshuram industrial estate in the catchment area of the Vashisthi estuary, Baikampady industrial area near Mangalore in the catchment area of the Gurupur estuary and mining related activities in

the catchment area of Mandovi and Sharavathi estuaries are located in proximity to middle region of these estuaries. Therefore, middle region of these estuaries is prone to maximum input of metals from such anthropogenic activities compared to lower estuarine region. In addition, metals transported to the lower estuarine region often get discharge into nearby sea by strong tides and currents (Karbassi et al. 2013) that might have decreased their concentration in the lower estuarine region. On the other hand, most of the metals were higher in the lower region than the middle region of the Vaghotan estuary. The core VG-1 was collected from the sheltered portion of the lower Vaghotan estuary. The decrease in tidal current velocities in the sheltered portion compared to the main estuarine channel might have facilitated higher deposition of metals at this location.

3.3.2 Clay minerals and metals in the clay fraction

To understand difference between estuaries in clay minerals and metals in the clay fraction, the data was plotted on the isocon diagram (Fig.3.3.2). When cores VS-1 and VS-2 were compared smectite, Al and Ni were higher in the core VS-1, while illite, kaolinite, chlorite, Fe, Mn, Cu and Zn were higher in the core VS-2. Metals viz. Co and Cr were nearly equal in both the cores. Further, on comparison of cores VG-1 and VG-2 smectite, illite, Mn and Zn were present in higher concentration in the core VG-1, while chlorite, Fe, Ni, Co and Cu were higher in the core VG-2. Aluminium was slightly higher in the core VG-1, while kaolinite in the core VG-2. Chromium was available in nearly equal concentration in these cores. Among the cores MD-1 and MD-2, smectite and Cu were higher in the core MD-1, while illite, kaolinite, chlorite, Fe, Mn, Ni, Zn and Cr were higher in the core MD-2. Aluminium was slightly higher in the core MD-1, while Co in the core MD-2. In case of cores S-1 and S-2, illite, chlorite, Al, Cu, Zn and Cr were higher in the core S-1, while smectite, Fe, Mn and Ni in the core S-2. Cobalt was slightly higher in the core S-1, while kaolinite in the core S-2. On comparison of cores GP-1 and GP-2, illite, Zn and Cu were observed in higher concentration in the core GP-1, whereas in the core GP-2 Al, Fe, Mn, Ni, Co and Cr were present in higher concentration. Chlorite was slightly higher in the core GP-1, while smectite and kaolinite in the core GP-2.

Among the clay minerals, smectite was higher in the lower region of Vashishti, Vaghotan and Mandovi estuaries, while in Sharavathi and Gurupur estuaries it was slightly higher in the middle estuarine region. Illite was higher in lower region in Shravathi and Gurupur estuaries

indicating transformation of smectite to illite. Kaolinite on the other hand was slightly higher in the middle region of all the estuaries. The variation in percentage of clay minerals within an estuary was attributed to processes governing flocculation of clay minerals. For instance, a rapid flocculation of kaolinite takes place under a 2 ‰ of salinity, leading to fast sedimentation in slightly saline waters (Deconinck and Stresser 1987) whereas, smectite flocculates in normal saline waters. Further, metals in the clay fraction were higher in the middle region than the lower region in Vashishti, Mandovi and Gurupur estuaries. As stated earlier, finer sediments stay in suspension for a longer period of time in the middle estuarine region compared to the lower estuarine region. Therefore, clay size particles might have favoured higher adsorption of metals in the middle estuarine region. In case of Vaghotan and Sharavathi estuaries, however, numbers of metals were present in higher concentration in the lower estuarine region, as well, indicating their association with smectite and illite.

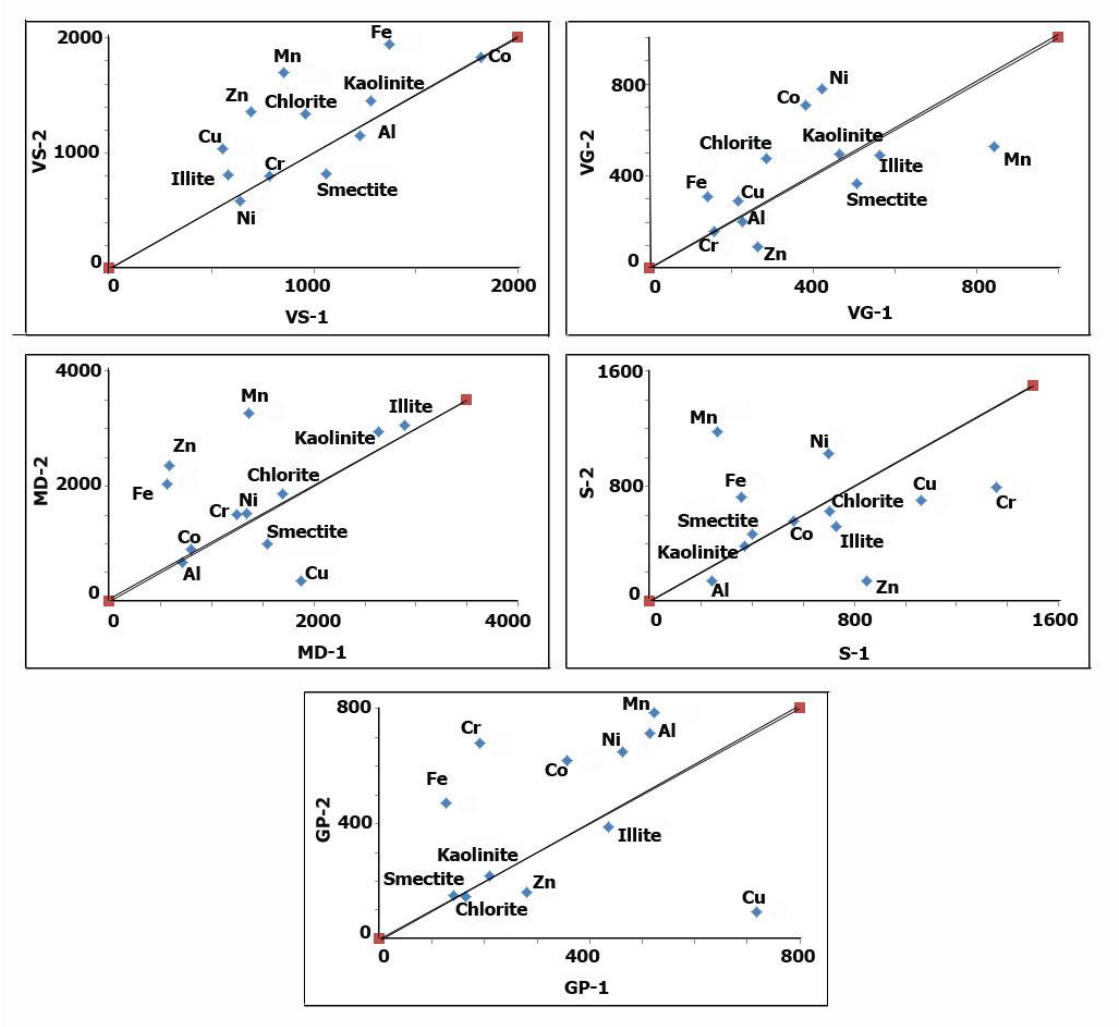

Fig. 3.3.2 Isocon plots for comparing clay minerals and metals in the clay fraction in Vashishti (VS-1 v/s VS-2), Vaghotan (VG-1 v/s VG-2), Mandovi (MD-1 v/s MD-2) Sharavathi (S-1 v/s S-2) and Gurupur estuaries (GP-1 v/s GP-2).

3.3.3 Speciation of elements

The data of speciation of elements in lower and middle regions of studied estuaries was used for understanding the possible concern from metals to associated biota (SQUIRT). Further, results obtained individually for lower as well as middle regions of estuaries were compared. In case of Vashishti estuary, Mn, Co and to some extent Cu was likely to cause concern to sediment associated biota in lower as well as middle regions. Metals viz. Mn, Co and to some extent Cu also indicated concern to sediment associated biota in the lower Vaghotan estuary, while biota in the middle estuarine region was at concern from Co. In the lower region of Mandovi, Sharavathi and Gurupur estuaries speciation of Zn was carried out and it did not reveal concern to sediment associated biota. On the other hand, in the middle region of Mandovi and Sharavathi estuaries Mn indicated concern to sediment associated organisms, while sediment associated biota of the middle Gurupur estuary was at concern from Ni.

Chapter 4

SUMMARY AND CONCLUSION

Estuaries are the transitional zones between marine and terrestrial environments and are divided into lower, middle and upper regions based on the variations in sea-river water mixing. The lower estuary has open access to sea and therefore the processes operating in this region are governed by wave and tidal energy, while fresh water influx derived from river and its tributaries dominate the upper estuary. The middle estuary, on the other hand is subjected to mixing of sea and river water. The material brought into an estuary through rivers is modified under changing physical, chemical and biological conditions and allowed to deposit in quiet environment within estuaries like mangroves and mudflats. A large quantity of organic and inorganic material enters the estuarine mudflats through natural processes as well as from pollutants released by human activities. The lower and middle regions of an estuary are significant with respect to the biogeochemical processes as waves and tides are forcing factors for mixing. The processes and factors regulating the distribution and abundance of metals, however, differ between lower and middle estuarine regions. Hence, study of mudflat sediments with time from lower and middle estuarine regions is important in understanding factors and processes involved in distribution and abundance of metals under varying depositional conditions.

The central west coast of India is known for smaller rivers/estuaries, micro to meso tidal range estuaries, monsoon controlled tropical climate, varying geological formations in the catchment area and rapid industrialization and urbanization region in the last two decades. In addition, with growing population, increase in land use-land cover, increase in agricultural activities, construction of dam must have altered the rate of sediment discharge to the estuaries. Further, to meet the needs of growing population, freshwater from rivers and its tributaries is diverted which has decreased river flow and resulted in enhanced tidal surge and changed mixing processes. Rise in mean sea level is also indicated in the recent years along the Indian coast. Additionally, activities viz. sand mining, fishing of benthic species and increasing use of estuarine channel by barges for transportation purpose has resulted in disturbing bottom sediments. All these processes and factors are capable of bringing change in deposition pattern of estuarine sediments and distribution of metals. As a consequence of this, estuaries along central west coast of India are considered as sink as well as source for material, metal and pollutants. With this background, in the present study an attempt was made to understand the depositional environment within lower and middle regions of estuaries along central west coast of India with following objectives.

- To study the distribution (spatial and temporal) and abundance of sediment components from selected locations within estuaries along central west coast of India.

- To understand the source and the factors influencing the distribution of sediment components along central west coast of India.

In order to accomplish the objectives, sediment cores representing lower and middle regions from five selected estuaries were collected and sub-sampled at 2 cm interval. In the laboratory, analysis for sediment components (Folk 1974), pH, organic carbon content (Gaudette et al. 1974), bulk element chemistry (Jarvis and Jarvis 1985), clay mineralogy (Biscaye 1965), clay chemistry (Jarvis and Jarvis 1985) and speciation of elements (Tessier et al. 1979; Dessai and Nayak 2009) were carried out. Statistical analyses involving Pearson's correlation matrix was attempted to understand the association of metals in sediments. Further, total metal concentration in the bulk sediments and metal concentration in the bioavailable fractions were compared with the sediment quality values (SQV's) using SQUIRT's table (Buchman 1999) to understand the pollution status with respect to associated biota. In addition, risk assessment code (RAC) (Perin et al. 1985) was used to evaluate the risk of metals released from the labile and readily bioavailable fractions (exchangeable and carbonate) to the associated biota. The data obtained was used to understand source of sediment components and processes involved.

Lower estuarine regions

The sediment components when compared within the lower region of tropical estuaries along central west coast of India indicated increase in sand and overall decrease in finer sediments from North to South. Such a distribution pattern of grain size was attributed to variation in the product of weathering of rock types from basalts to granites and granitic gneisses in catchment area of studied estuaries. The weathering of basalts released higher finer sediments to the Vashishti and Vaghotan estuaries, while weathering of granites and granitic gneisses released higher sand to the estuaries towards the South of the study area. In addition, higher tidal range towards North led to the deposition of higher finer sediments, whereas, higher rainfall and associated runoff towards the South helped in retaining the coarser sediments. pH exhibited fluctuating trend along the study area. The distribution of organic carbon in the lower estuarine region from Vashishti (North) to Gurupur (South) estuaries showed

decreasing trend, similar to finer sediments. Thus, suggested the role of grain size in distribution of organic matter in sediments. Major as well as trace metals (except Zn) showed overall decrease from North to South along central west coast of India and therefore, suggested that sediment grain size along with organic carbon regulated the distribution of metals in the lower region of tropical estuaries.

Further, the study of grain size in sediment cores collected from the lower estuarine regions of Vashishti (VS-1), Vaghotan (VG-1), Mandovi (MD-1) and Sharavathi (S-1) estuaries indicated increase in sand in the lower section followed by an increase in finer sediments. Thus, suggested presence of relatively higher hydrodynamic environment in the past along central west coast of India which has changed from relatively higher to lower energy environment. This has led to decrease in sand in the upper section of Vashishti, Mandovi and Sharavathi estuaries and in the middle section of the Vaghotan estuary. However, human induced activities in the catchment area of the Vaghotan estuary seem to have resulted in an increase in coarser size sediments in the recent years. In the lower region of the Gurupur estuary (GP-1), however, different pattern of distribution of sediment components in comparison to other studied estuaries was attributed to the change in morphology of the Gurupur estuary with time. The vertical distribution of organic carbon in all the sediment cores was similar to either silt or clay which indicated its association with finer sediments. Most of the metals in Mandovi and Sharavathi estuaries, Ni and Zn in the Vashishti, Ni and Cu in the Vaghotan and Zn and Cr in the Gurupur estuaries were higher in sections with higher percentage of silt and/or clay and therefore, indicated role of grain size in the distribution of metals. Further, Fe and Cr in the core VS-1 and Co and Zn in the core VG-1, collected from lower Vashishti and Vaghotan estuaries respectively, were found to be associated with sand indicating formation of Fe coating on sand grains. In core VG-1, overall decrease in metals towards the surface indicated their diffusion from sediments. In core MD-1, collected from the lower Mandovi estuary, finer sediments, organic carbon and Fe oxides mainly regulated distribution of metals. Diagenetic enrichment of Fe and Mn was also noted in this core which influenced the distribution of trace metals. In core S-1, collected from the lower Sharavathi estuary, metal distribution seemed to be largely governed by finer sediments, organic carbon and Mn oxides. Mobilization of metals from sand rich lower section to finer sediments rich upper section was observed in this core. In core GP-1, collected from the lower Gurupur estuary, metal distribution was regulated by finer sediments, organic carbon and Fe-Mn oxides. The decrease in metal concentration (except

Zn) in the middle section of the core GP-1 was attributed to dilution of concentration by input of coarser sediments. In general, inter comparison of lower estuarine cores indicated increase in metals concentration released from weathering of basalts in Vashishti and Vaghotan estuaries and decrease in metals in estuaries with granite and granitic gneisses in the catchment area along Southern portion of the study area. Therefore, suggested catchment area geology as the major source and sediment size, organic matter and Fe-Mn oxide as factors regulating the distribution of metals in the lower region of the tropical estuaries.

The clay minerals data of the study area along lower estuarine regions revealed decrease in percentage of smectite from Vashishti to Gurupur estuary, while overall increase in percentage of kaolinite. The systematic variation in percentage of these clay minerals was due to the change in source rocks from North to South in the catchment area of rivers studied. The distribution of metals in the clay fraction of sediments showed overall decrease in Fe, Ni and Co and fluctuating trend for rest of the metals from North to South along the study area.

The vertical distribution of clay minerals indicated role of processes operated with time, such as size sorting during transport and differential flocculation. Smectite and chlorite in the core VS-1, smectite to a lesser extent in the core VG-1, Fe oxide in the core MD-1, illite, kaolinite and to some extent Fe oxide in the core S-1, and kaolinite, chlorite along with Fe-Mn oxides in the core GP-1 provided important binding sites for metals in the clay fraction. In addition, Cu, Zn and Cr in the core VG-1, Ni, Co, Cu and Zn in the core S-1, and Cu and Zn in the core GP-1 showed similar distribution pattern and significant correlation among themselves and therefore, indicated their close association with each other or had undergone similar post-depositional changes. Further, on comparison of metals in the clay fraction among the cores, most of the metals showed higher concentration in cores VS-1 and VG-1 in comparison to cores S-1 and GP-1 which was attributed to release of metals from rock types in the catchment area and percentage of clay among these cores. The comparison of metals in the clay fraction with that of bulk sediments revealed systematic variation. In the Vashishti and Vaghotan estuaries metals were significantly associated with clay as well as bulk sediments, while in Mandovi, Sharavathi and Gurupur estuaries metals were largely associated with the clay fraction of the sediment. Such a distribution pattern of metals was due to metals associated with minerals within the rock types in the catchment area.

Further, speciation of selected elements whose average value in the bulk sediments exceeded the global average shale value was carried out. In core VS-1, Mn was significantly high, while Co and Zn were available in considerable amount in the Fe-Mn oxide phase and thus indicated their strong bioavailability. Manganese in the Fe/Mn oxide fraction showed increase from bottom to surface of the cores VS-1 and thus suggested increase in Mn of anthropogenic origin in recent years. In core VG-1, considerable concentration of Mn, Zn and Cr in the Fe-Mn oxide phase indicated their bioavailability. In the Fe-Mn oxide phase, increase in Mn in the core VS-1, and increase in Mn and Zn in the core VG-1 near the surface suggested their diagenetic mobilization. Zinc also indicated its considerable bioavailability in cores MD-1, S-1 and GP-1. The results of speciation of elements when compared with the screening quick reference table suggested concern from Mn, Co, and to a lesser extent from Cu to the sediment associated organisms in Vashishti and Vaghotan estuaries. Further, risk assessment code revealed low to medium risk to the sediment associated biota from metals bound to the first two phases.

Middle estuarine regions

The sediment components in the middle estuarine region of tropical estuaries along central west coast of India indicated fluctuating trend of sand and clay, while silt with initial decrease from Vashishti to Vaghotan estuaries, further exhibited overall increase up to Gurupur estuary from North to South. The fluctuating trend of sand and clay along the study area was attributed to various factors involved in mixing which includes fresh water addition, catchment area geology and physico-chemical factors in the estuaries. pH, organic carbon and most of the metals viz. Al, Mn, Ni and Zn also showed fluctuating distribution pattern. However, Fe, Co and Cu showed overall decrease from North to South along central west coast of India, while Cr exhibited overall increase towards the South. The spatial variation in concentration of organic carbon and some of the metals along the study area was attributed to the location of the core sample from which they were collected. The middle regions of Vashishti and Gurupur estuaries were in close proximity to industries. The input of industrial waste material in these estuaries and mining waste from mines operating in the catchment area of Mandovi, Sharavathi and Gurupur estuaries contributed to variation in percentage of sediment components, organic carbon and metals viz. Mn, Ni and Zn along the study area.

Further, the grain size in sediment cores collected from the middle estuarine regions of Vashishti (VS-2), Mandovi (MD-2) and Sharavathi (S-2) estuaries indicated increase in sand in the middle section, while in the upper section in case of the Vaghotan estuary (VG-2). The higher sand in certain sections of these cores was attributed to input from natural as well as human induced activities in the catchment area. In cores VS-2 and S-2, finer sediments compensated distribution pattern of sand from bottom to surface, whereas in the core MD-2, finer sediments compensated increase in sand in the middle section. In core VG-2, silt showed overall increase from bottom to surface which was largely compensated by clay. In core GP-2, collected from middle estuarine region of the Gurupur estuary, sand did not show much variation between the sections. However, increase in silt in the upper section of the core GP-2, reflected role of tidal and wave energy in carrying away finer sediments from lower estuarine region and depositing the same in the middle estuarine region. The distribution pattern of clay was opposite to that of silt in this core. The vertical distribution of organic carbon in cores VS-2, MD-2, S-2 and GP-2 was similar to silt and/or clay and thus suggested incorporation of organic carbon into finer sediments. In core VS-2, sand showed significant association with Fe, Ni and Cr. The coatings of iron oxide onto coarser sediments helped in adsorption of Ni and Cr. Also, correlation analysis indicated that Mn regulated the distribution of Co, Cu and Cr. The presence of Lote Parshuram industrial estate in the proximity of the middle Vashishti estuary provided additional metal input. Metals viz. Al, Fe, Ni, Co, Cu and Cr in sediments of the core VG-2 indicated their association with sand and/or Fe-Mn oxides. The vertical distribution of Mn, Ni, Co, Cu and Zn in this core revealed their diffusion from sediments in the recent years. In core MD-2, Ni and Cr were associated with sand, while Al and Mn were associated with clay. Further, vertical distribution of trace metals viz. Ni, Co, Zn and Cr indicated mobilization from deeper layer to shallow depth which latter adsorbed under oxic conditions. The significant correlation among the trace metals indicated their common source and/or similar enrichment mechanism in this core. The similar distribution of metals and their significant association with finer sediments and organic carbon suggested role of finer sediments and organic carbon in distribution of metals in the core S-2. Further, Fe and Mn indicated similar point-to-point distribution from bottom to 14 cm depth which indicated strong association among Fe and Mn. In core GP-2, sand regulated the distribution of Mn and Co. The slight increase in Fe and Cr towards the surface suggested their anthropogenic input in the Gurupur estuary. The inter comparison of middle estuarine cores indicated increase in metals concentration in Vashishti and Vaghotan estuaries when compared with Mandovi, Sharavathi and Gurupur estuaries. The higher concentration of

metals in estuaries along Northern part of the study area was attributed to input of metals from weathering of basalts brought by tributaries, and clay enriched sediments of Vaghotan estuary favouring adsorption of metals.

Similar to lower estuarine region, the clay minerals data along the middle estuarine regions of the study area revealed decrease in percentage of smectite from Vashishti to Gurupur estuary, while overall increase in percentage of kaolinite which was attributed to change in catchment area geology along the study area. The distribution of metals in the clay fraction of sediments showed overall decrease in Fe from North to South along central west coast of India, while Cr exhibited overall increase from Vashishti to Gurupur estuaries. Metals viz. Al, Mn, Ni, Co, Cu and Zn showed fluctuating distribution pattern.

The clay minerals distribution showed variation along the length of cores VS-2, VG-2, S-2 and GP-2. Iron oxides and to some extent chlorite in the core VS-2, kaolinite and to some extent smectite along with Fe-Mn oxides in the core VG-2, Fe-Mn oxides in the core MD-2, Fe oxide in the core S-2, and smectite and Fe oxides in the core GP-2 played important role in the distribution of trace metals in the clay fraction. Further, diagenetic remobilization was evident at 6 cm depth in the core VS-2. Trace metals showed significant correlation among themselves in cores MD-2 and S-2 which suggested their common source in these estuaries. In addition, peak values of metals in the clay fraction obtained between 22 and 10 cm i.e. portion of the core representing higher sand percentage in the bulk sediments in the core S-2 indicated that the metals brought to the estuary got selectively associated with the clay fraction. On comparison of metals in the clay fraction among the cores, most of the metals showed higher concentration in the cores VS-2 and VG-2 than MD-2, S-2 and GP-2. The higher concentration of metals in cores VS-2 and VG-2 was attributed to release of metals from their catchment area rich in basalts and adsorption of metals onto clay particles which remained in suspension for a longer period of time as a result of higher tidal range in Vashishti and Vaghotan estuaries. Further, the comparison of metals in the clay fraction with that of bulk sediments in the middle estuarine region indicated higher concentration of metals in bulk sediments in Vashishti, Vaghotan and Mandovi estuaries, while metals were associated with bulk as well as clay fraction of the sediment in Sharavathi and Gurupur estuaries. Thus, suggested role of catchment area geology and physico-chemical conditions of depositing site in the distribution of metals.

Metal speciation within the sediments of the core VS-2 indicated considerable concentration of Mn and Co in the bioavailable fractions (exchangeable and/or Fe-Mn oxide). The increase in concentration of these metals towards the surface of the core indicated concern to sediment associated biota. In core VG-2, Co was available in considerable concentration in Fe-Mn oxide and organic phases, while metals viz. Fe, Ni, Cu and Cr were present in negligible levels in the bioavailable phases. The concentration of Mn in carbonate, Fe-Mn oxide and organic phases in the core MD-2 reflected its environmental significance with respect to associated biota. Also, Zn in the organic phase to some extent indicated its bioavailability. In core S-2, Mn and Co were bound to the Fe-Mn oxide phase and to some extent Mn associated with the exchangeable fraction indicated increase towards the surface and thus suggested their availability to sediment associated organisms. In case of core GP-2, the vertical distribution of Co and Zn in the bioavailable fractions revealed their mobilization from the exchangeable phase which got adsorbed onto Fe-Mn oxides and organic phases. Diagenetic mobilization of Mn, Co and Zn in the core VS-2, Mn in the core MD-2, and Mn and to some extent Co in the core S-2 was evident.

The data of speciation of elements when compared with the screening quick reference table indicated concern to sediment associated organisms in the Vashishti estuary from Mn, Co and Cu. Cobalt concentration suggested concern to biota in the Vaghotan estuary, while biota from Mandovi and Sharavathi estuaries was at concern from Mn. Nickel was available higher in the Gurupur estuary in the bioavailable phases. Further, risk assessment code revealed higher degree of risk from Mn bound to exchangeable and carbonate phases to associated biota in the middle Vashishti estuary.

Lower v/s middle estuarine regions

Sand in most of the estuaries viz. Vaghotan, Mandovi, Sharavathi and Gurupur estuaries was higher in the lower estuarine region than the middle estuarine region which was attributed to waves and tidal energy facilitating retention of coarser particles. On the other hand, silt in most of the estuaries viz. Vashishti, Mandovi, Sharavathi and Gurupur was higher in the middle estuarine region which was attributed to mixing of fresh and saline waters facilitating deposition of finer sediments. However, clay and organic carbon did not reveal higher concentration in the middle region of all the estuaries. The concentration of most of the metals in the bulk sediments was higher in the middle region of Vashishti, Mandovi,

Sharavathi and Gurupur estuaries than the lower region. The higher concentration of metals in the middle region of these estuaries was attributed to mixing which facilitated retention of metals onto finer sediments which remain in suspension for a longer period of time. Input from industries and mining related activities located in the proximity also contributed metals. On the other hand, higher metal concentration in the lower region of the Vaghotan estuary was explained with reference to location of the core from which it was collected. The variation in percentage of clay minerals between lower and middle regions of an estuary was attributed to processes governing flocculation of clay minerals. Further, metals in the clay fraction were higher in the middle region than the lower region in most of the estuaries (Vashishti, Mandovi and Gurupur) which suggested role of mixing and associated processes. The results of speciation of elements between lower and middle estuarine regions were compared. It indicated concern from Mn, Co and to some extent from Cu to the sediment associated biota in lower as well as middle estuarine regions of the Vashishti estuary. Metals viz. Mn, Co and to some extent Cu also indicated concern to sediment associated biota in the lower Vaghotan estuary, while biota in the middle Vaghotan estuary was at concern from Co. In the lower region of Mandovi, Sharavathi and Gurupur estuaries, speciation of Zn did not reveal concern to sediment associated biota. On the other hand, in the middle region of Mandovi and Sharavathi estuaries Mn indicated concern to sediment associated organisms, while Ni concentration suggested concern to sediment associated biota in the middle Gurupur estuary.

References

Abdullah NA, Abdullah LI, Shazili NAM, Sokiman S (2015) Clay minerals on recent surface estuarine sediments from selected rivers of Terengganu, Malaysia. Journal of Earth Sciences 1:8-16.

Achyuthan H, Richardmohan D, Srinivasalu S, Selvaraj K (2002) Trace metals concentrations in the sediment cores of estuary and tidal zones between Chennai and Pondicherry, along the east coast of India. Indian Journal of Geo-Marine Sciences 31(2):141-149.

Adiga S, Poornananda DS (2013) Environmental movement and the media in Dakshina Kannada. Global Media Journal 4(1):1-29.

Aloupi M, Angelidis MO (2002) The significance of coarse sediments in metal pollution studies in the coastal zone. Water Air Soil Pollution 133:121-131.

Anand JBD, Kala MJS (2015) Seasonal distribution of heavy metals in the coastal waters and sediments along the major zones of south east coast of India. International Research Journal of Environmental Sciences 4(2):22-31.

Anderson PR, Benjamin MM (1990) Constant capacitance surface complexation model: Adsorption in silica-iron binary suspensions. In: Melchior DC, Bassett RL (eds.), Chemical Modelling of Aqueous Systems II, pp. 272-281. ACS Symposium Series 416, American Chemical Society, Washington, DC.

Avinash KG, Diwakar PG, Joshi NV, Ramachandra TV (2008) Landslide susceptibility mapping in the downstream region of Sharavathi river basin, Central Western Ghats. In: Proceedings of the 24th annual symposium on space and technology ISRO-IISc technology cell, Indian Institute of Science, Bangalore.

Badr NBE, El-Fiky AA, Mostafa AR, Al-Mur BA (2009) Metal pollution records in core sediments of some Red Sea coastal areas, Kingdom of Saudi Arabia. Environmental Monitoring and Assessment 155:509-526.

Baeyens W, Monteny F, Leermaakers M, Boullion S (2003) Evaluation of sequential extractions on dry and wet sediments. Analytical and Bioanalytical Chemistry 376:890-901. doi:10.1007/s00216-003-2005-z.

Banerjee K, Senthilkumar B, Purvaja R, Ramesh R (2012) Sedimentation and trace metals distribution in selected locations of the Sundarban Mangroves and Hoogly estuary, north east coast of India. Environmental Geochemistry and Health 34:27-42.

Bannur CR, Sherieff AN, Basappa RM, Shreedhara V (1991) Application of remote sensing technique in detection of morphological changes in the vicinity of estuarine mouths - a case study pertaining to D.K. district. Workshop on Indian remote sensing satellite mission and its application.

Bhagure GR, Mirgane SR (2010) Heavy metal concentrations in groundwaters and soils of Thane region of Maharashtra, India. Environmental Monitoring and Assessment 173(1-4):643-652. doi:10.1007/s10661-010-1412-9.

Bibi MH, Ahmed F, Ishiga H (2007) Assessment of metal concentrations in lake sediments of southwest Japan based on sediment quality guidelines. Environmental Geology 52:625-639.

Bican-Brisan N, Hosu A (2006) Clay mineral association in the salt formation of the Transylvanian basin and its paleo-environmental significance. Studia Universitatis Babes-Bolyai, Geologia 51(1-2):35-41.

Billen G, Lancelot C, Meybeck M (1991) N, P and Si retention along the aquatic continuum from land to ocean. In: Mantoura RFC, Martin JM, and Wollast R (eds), Ocean margin processes in global change, John Wiley and Sons Limited, London, pp. 19-44.

Binning K, Baird D (2001) Survey of heavy metals in the sediments of the Swartkops River Estuary, Port Elizabeth South Africa. Water 27(4):461-466.

Biscaye PE (1965) Mineralogy and sedimentation of recent deep-sea clay in the Atlantic Ocean and adjacent seas and oceans. Geological Society of America Bulletin 76:803-832.

Boldt KV, Nittrouer CA, Ogston AS (2013) Seasonal transfer and net accumulation of fine sediment on a muddy tidal flat: Willapa Bay, Washington. Continental Shelf Research 60:157-172.

Boothroyd JC (1978) Mesotidal inlets and estuaries. In: Davis RA (ed.), Coastal sedimentary environments, Springer-Verlag, New York, pp. 287-360.

Bradl H (2002) Adsorption of Heavy Metal Ions on Clays. Encyclopedia of Surface and Colloid Science, Marcell-Dekker, Inc., New York, pp. 1-13.

Brown ET, Callonnec LL, German CR (2000) Geochemical cycling of redox-sensitive metals in sediments from Lake Malawi: A diagnostic paleotracer for episodic changes in mixing depth. Geochimica Cosmochimica Acta 64(20):3515-3523.

Buchman MF (1999) NOAA screening quick reference tables. NOAA HAZMAT Report 99-1, (pp. 12). Seattle, WA, Coastal Protection and Restoration Division, National Oceanic and Atmospheric Administration.

Burban PY, Lick W, Lick J (1989) The flocculation of fine-grained sediments in estuarine waters. Journal of Geophysical Research 94(C6):8323-8330.

Burgos MG, Rainbow PS (2001) Availability of cadmium and zinc from sewage sludge to the flounder, Platichthys flesus via a marine food chain. Marine Environmental Research 51:417-431.

Calmano W, Hong J, Forstner U (1993) Binding and mobilization of heavy metals in contaminated sediments affected by pH and redox potential. Water Science and Technology 28:223-235.

Cao L, Hong GH, Liu S (2015) Metal elements in the bottom sediments of the Changjiang Estuary and its adjacent continental shelf of the East China Sea. Marine pollution bulletin 95:458-468.

Chakraborty P, Sarkar A, Krushna V, Naik R, Nagender B (2015) Organic matter-A key factor in controlling mercury distribution in estuarine sediment. Marine Chemistry 173:302-309.

Chamley H (1989) Clay Sedimentology. Springer, Berlin, pp. 623.

Chapman PM, Wang FY (2001) Assessing sediment contamination in estuaries. Environmental Toxicology and Chemistry 20(1):3-22.

Chassagne C, Mietta F, Winterwerp JC (2009) Electrokinetic study on kaolinite suspensions. Journal of Colloid and Interface Science 336(1):352-359.

Chatterjee M, Filho EVS, Sarkar SK, Sella SM, Bhattacharya A, Satpathy KK, Prasad MVR, Chakraborty S, Bhattacharya BD (2007) Distribution and possible source of trace elements in the sediment core of a tropical macrotidal estuary and their ecotoxicological significance. Environment International 33(3):346-356.

Chauhan, OS, Vogelsang E (2006) Climate induced changes in the circulation and dispersal patterns of the fluvial sources during late Quaternary in the middle Bengal Fan. Journal of Earth System Science 115(3):379-386.

Chunyan MA, Chen J, Zhou Y, Wang Z (2010) Clay minerals in the major Chinese coastal estuaries and their provenance implications. Frontiers of Earth Science in China 4(4):449-456.

Clark M (1992) The physical and geochemical controls on heavy metal cycling in Mangal sediments, Wynnum, Brisbane. Thesis submitted to University of Canterbury.

Dalrymple RW, Zaitlin BA, Boyd R (1992) Estuarine facies models: conceptual basis and stratigraphic implications. Journal of Sediment Petrology 62:1130-1146.

Dandekar P (2010) River stories from Maharashtra: many morals to learn from. National river conservation plan ministry of environment and forest 1-52. http://sandrp.in/rivers/Rivers_of_Maharashtra_Dec_2011.pdf. Accesses 18 May 2015.

Davies JA (1984) Complexation of trace metals by adsorbed natural organic matter. Geochimica Cosmochimica Acta 48:679-691.

Deconinck JF, Stresser A (1987) Sedimentology, clay mineralogy and depositional environment of Purbeckian green marls (Swiss and French Jura). Ecologae Geologicae Helvetiae 80(3):753-772.

Delgado J, Barba-Brioso C, Nieto J, Boski T (2011) Speciation and ecological risk of toxic elements in estuarine sediments affected by multiple anthropogenic contributions (Guadiana saltmarshes, SW Iberian Peninsula): I. surficial sediments. Science of the Total Environment 409:3666-3679.

Depledge MH, Fossi MC (1994) The role of biomarkers in environmental assessment. Ecotoxicology 3:161-172.

Dessai VGD, Nayak GN (2009) Distribution and speciation of selected metals in surface sediments, from the tropical Zuari estuary, central west coast of India. Environmental Monitoring and Assessment 158:117-137.

Duchart P, Calvert SE, Price NB (1973) Distribution of trace metals in the pore waters of shallow water marine sediments. Limnology Oceanography 18:605-610.

Dulaiova H, Gonneea ME, Henderson PB, Charette MA (2008) Geochemical and physical sources of radon variation in a subterranean estuary-Implications for groundwater radon activities in submarine groundwater discharge studies. Marine Chemistry 110(1-2):120-127.

Dyer KR, Christie MC, Wright EW (2000) The classification of intertidal mudflats. Continental Shelf Research 20:1039-1060.

Eberl DD (1984) Clay mineral formation and transformation in rocks and soils. Philosophical Transactions of the Royal Society A 311:241-257.

Ehrmann WE, Melles M, Kuhn G, Grobe H (1992) Significance of clay mineral assemblages in the Antarctic ocean. Marine Geology 107:249-273.

Essa MA, Farragallah MA (2006) Clay minerals and their interactions with heavy metals and microbes of soil irrigated by various water resources at Assiut, Egypt. Assiut University Bulletin for Environmental Research 9(2):73-90.

Fagela N, Boskib T, Likhoshwayc L, Oberhaenslid H (2003) Late Quaternary clay mineral record in Central Lake Baikal (Academician Ridge, Siberia). Palaeogeography, Palaeoclimatology, Palaeoecology 193(1):159-179.

Fairbridge RW (1980) The estuary: Its definition and geodynamic cycle. In: Olausson E and Cato I (eds.), Chemistry and biogeochemistry of estuaries, John Wiley and Sons limited, Chichester, pp. 1-36.

Farmer JG, Lovell MA (1984) Massive diagenetic enhancement of manganese in Loch Lomond sediments. Environmental Technology letters 5:257-270.

Feng Y, Huang X, Zhang D, Tian L, Zeng L (2012) Distribution of heavy metals in sediments of the Pearl River Estuary, Southern China: Implications for sources and historical changes. Journal of Environmental Sciences 24:1-10.

Fernandes L (2012) Reconstructing pollution history from intertidal regions of estuaries along Mumbai coast, India, Thesis submitted to Goa University.

Fernandes L, Nayak GN (2010) Sources and factors controlling the distribution of metals in mudflat sedimentary environment, Ulhas estuary, Mumbai. Indian Association of Sedimentologists 29:71-83.

Fernandes L, Nayak GN (2009) Distribution of sediment parameters and depositional environment of mudflats of Mandovi estuary, Goa, India. Journal of Coastal Research 25(2):273-284.

Fernandes MC, Nayak (2015) Role of sediment size in the distribution and abundance of metals in a tropical (Sharavathi) estuary, west coast of India. Arabian Journal of Geosciences. doi:10.1007/s12517-015-2127-6.

Folk RL (1974) Petrology of sedimentary rocks. Hemphill, Austin, Texas, pp. 177.

Fytianos K, Lourantou A (2004) Speciation of elements in sediment samples collected at lakes. Environment International 30:11-17.

Ganesh B, Naidu AGSS, Rao MJ, Karudu TK, Avatharam P (2013) Studies on textural characteristics of sediments from Gosthani River Estuary-Bheemunipatnam, Andhra Pradesh, East Coast of India. Journal of Indian Geophysical Union 17(2):139-151.

Gangadhar BH (1995) Long-term shoreline changes of Mulki-Pavanje and Nethravati-Gurpur estuaries, Karnataka. Journal of Indian Society of Remote Sensing 23:147-153.

Gaudette HE, Flight WR, Toner L (1974) An inexpensive titration method for the determination of organic carbon in recent sediment. Journal of Sedimentary Petrology 44 (1):249-253.

German J, Svensson G (2002) Metal content and particle size distribution of street sediments and street sweeping waste. Water Science Technology 46 (6-7):191-198.

Gobeil C, Cossa D (1993) Mercury in sediments and sediment pore water in the Aurentian Trough. Canadian Journal of Fisheries and Aquatic Sciences 50:1794-1800.

Gujar AR (1996) Heavy mineral placers in the nearshore areas of south Konkan, Maharashtra: Their nature of distribution, origin and economic evaluation. Ph.D. Thesis submitted to Tamil University, Thanjavur.

Gujar AR, Angusam N, Rajamanickam V (2008) Wave refraction patterns and their role in sediment redistribution along South Konkan, Maharashtra, India. Geochemica Acta 7:69-79.

Gujar AR, Borole DV, Parthiban G, Rajamanickam GV (2005) ^{210}Pb geochronology in changing coastal environment: A case study of Vijaydurg, central west coast of India. 7th Marine Archeology Seminar at NIO, Abstract vol. 17.

Guo Y, Yang S (2015) Heavy metal enrichments in the Changjiang (Yangtze River) catchment and on the inner shelf of the East China Sea over the last 150 years. Science of the total environment 543(Pt A):105-115.

Harringtoin JM, Laforce MJ, Rember WC, Fendorf SE, Rosenzweig RF (1998) Phase associations and mobilization of iron and trace elements in Coeur d'Alene Lake, Idaho. Environmental Science and Technology 32:650-656.

Hedge JI, Keil RG, Cowie GL (1993) Sedimentary diagenesis: organic perspectives with inorganic overlays. Chemical Geology 107:487-492.

Hegde AV, Raveendra B (2000) Short-term and long-term geomorphological dynamics of Mangalore spits using IRS-1A/1C data. Journal of Indian Society of Remote Sensing 28(4):233-247.

Helios-Rybicka E, Kyziol J (1990) Clays and clay minerals as the natural barriers for heavy metals in pollution mechanisms-illustrated by Polish rivers and soils. Themenband Umweltgeologie 83:163-176.

Hizal H, Apak R (2006) Modeling of copper (II) and lead (II) adsorption on kaolinite based clay minerals individually and in the presence of humic acid. Journal of Colloid and Interface Science 295:1-13.

Ho HH, Swennen R, Van Damme A (2010) Distribution and contamination status of heavy metals in estuarine sediments near Cua Ong Harbor, Ha Long Bay, Viatinam. Geologica Beligica 13(1):37-47.

Hseu ZY (2006) Extractability and bioavailability of zinc over time in three tropical soils incubated with biosolids. Chemosphere 63:762-771.

Ingole B, Rodrigues N, Ansari ZA (2002) Macrobenthic communities of the coastal waters of Dabhol, west coast of India. Indian Journal of Geo-Marine Sciences 31(2):93-99.

Jain CK, Ram D (1997) Adsorption of metal ions on bed sediments. Hydrological Sciences Journal 42(5):713-723. doi:10.1080/02626669709492068.

Jarvis IJ, Jarvis K (1985) Rare earth element geochemistry of standard sediments: a study using inductively coupled plasma spectrometry. Chemical Geology 53:335-344.

Jenne EA (1976) Trace element sorption by sediments and soils-sites and processes. In: Chappel W, Petersen K(eds.), Symposium on Molybdenum, Marcel Dekker, New York, pp. 425-553.

Jonathan MP, Sarkar SK, Roy PD, Alam A, Chatterjee M, Bhattacharya BD, Bhattacharya A, Satpathy KK (2010) Acid leachable trace metals in sediment cores from Sunderban mangrove wetland, India: an approach towards regular monitoring. Ecotoxicology 19:405-418. doi:10.1007/s10646-009-0426-y.

Jordao CP, Pereira MG, Bellato CR, Pereira JL, Matos AT (2002) Assessment of water systems for contaminants from domestic and industrial sewages. Environmental Monitoring and Assessment 79(1):75-100.

Kappler A, Straub KL (2005) Geomicrobiological cycling of iron. Reviews in Mineralogy and Geochemistry 59:85-105.

Karbassi AR, Bassam SS, Ardestani M (2013) Flocculation of Cu, Mn, Ni, Pb, and Zn during estuarine mixing (Caspian Sea). International Journal of Environmental Research 7(4):917-924.

Keil RG, Montlucon DB, Prahl FG, Hedges JI (1994) Sorptive preservation of labile organic matter in marine sediments. Nature 370:549-552.

Kenjale C (1993) The morphology and sedimentology of Yelavane tidal inlet. In: Karlekar S (ed.), Coastal Geomorphology of Konkan, Aparna Publications, Pune, pp. 217-218.

Klavins M, Briede A, Rodinov V, Kokorite I, Parele E, Klavina I (2000) Heavy metals in rivers of Latvia. Science of the Total Environment 262:175-184.

Kljakovic-Gaspic Z, Bogner D, Ujevic I (2009) Trace metals (Cd, Pb, Cu, Zn and Ni) in sediment of the submarine pit Dragon ear (Soline Bay, Rogoznica, Croatia). Environmental Geology 58:751-760. doi:10.1007/s00254-008-1549-9.

Kranck K (1984) The role of flocculation in the filtering of particulate matter in estuaries. In:Kennedy V (ed.), The Estuary as a Filter, Academic Press, Orlando Inc., Florida, pp. 159-175.

Kristiansen KD, Kristensen E, Jensen MH (2002) The influence of water column hypoxia on the behaviour of manganese and iron in sandy coastal marine sediment. Estuarine Coastal and Shelf Science 55:645-654.

Krone RB (1963) A study of rheological properties of estuarial sediments. Hydraulic engineering laboratory and sanitary engineering laboratory, University of California, Berkeley. Report No. 63-68.

Kumar A, Jayappa KS, Deepika B, Dinesh AC (2010) Hydrological-drainage analysis for evaluation of groundwater potential in a watershed basin of southern Karnataka, India: A remote sensing and GIS approach. In: Proceedings of the 1st international applied geological congress, department of geology, Islamic Azad University-Mashad Branch, Iran.

Kumar B, Kumar S, Mishra M, Singh SK, Prakash D, Sharma CS, Mukherjee DP (2011) Geochemical fractionation of some heavy metals in soils in the vicinity of sukinda mining Area, Orissa. Advances in Applied Science Research 2(5):263-272.

Kumar SP, Edward JKP (2009) Assessment of metal concentration in the sediment cores of Manakudy estuary, south west coast of India. Indian Journal of Marine Sciences 38(2):235-248.

Kumar VS, Dora GU, Philip S, Pednekar P, Singh J (2011) Variations in tidal constituents along the nearshore waters of Karnataka, west coast of India. Journal of Coastal Research 27(5):824-829.

Kunte PD, Wagle BG (1991) Spit evolution and shore drift direction along south Karnataka coast, India. Giornale di Geologia 53:71-80.

Lak R, Saeedi M, Vosoogh A (2015) Heavy metals distribution in fractioned river sediments-Case Study: Shafaroud River-South West of Caspian Sea. International Journal of Environmental Science and Development 6(7):530-534.

Lan X, Zhang Z, Li R, Wang Z, Chen X, Tian Z (2012) Distribution of clay minerals in surface sediments off Yangtze River estuary. Marine Science Bulletin 14(2):56-69.

Larumbe I, Casado A (1989) Speciation of particulate trace metals in sediments of Aarbe reservoir. Toxicological and Environmental Chemistry 23:135-141.

Lasheen MR, Ammar NS (2009) Speciation of some heavy metals in River Nile sediments, Cairo, Egypt. Environmentalist 29:8-16.

Leedy P, Ormrod J(2001) Practical Research: Planning and Design.Saga Publications, New Jersey.

Lesven L, Gao Y, Billon G, Leermakers M, Ouddane B, Fischer JC, Baeyens W (2008) Early diagenetic processes aspects controlling the mobility of dissolved trace metals in three riverine sediment columns. Science of the Total Environment 407:447-459.

Li G, Peacor DR, Coombs DS (1997) Transformation of smectite to illite in bentonite and associated sediments from Kaka point, New Zealand: contrast in rate and mechanism. Clay and Clay Minerals 45(1):54-67.

Li X, Poon C, Liu PS (2001) Heavy metal contamination of urban soils and street dusts in Hong Kong. Applied Geochemistry 16:1361-1368. doi:10.1016/S0883-2927(01)00045-2.

Liaghati T, Preda M, Cox M (2003) Heavy metal distribution and controlling factors within coastal plain sediments, Bells Creek catchment, southeast Queensland, Australia. Environmental International 29:935-948.

Lin CY, Abdullah MH, Musta B, Praveena MS, Aris AZ (2011) Stability behaviour and thermodynamic states of iron and manganese in sandy soil aquifier Manukan island, Malaysia. Natural Resources Research. doi:10.1007/s11053-011-9136-2.

Liu BL, Hu K, Jiang Z, Yang J, Luo X, Liu A (2011) Distribution and enrichment of heavy metals in a sediment core from the Pearl River Estuary. Environmental Earth Science 62:265-275.

Longhinos B (2011) Geology and geochronology of Silica sands of coastal plain of Thiruvanthapuram district, Kerala, India, with special reference to late quaternary environment. Thesis submitted to Department of Marine Geology and Geophysics, School of Marine Sciences, Cochin University of Science & Technology, Kochi.

Luoma SN (1989) Can we determine the biological availability of sediment-bound trace metals. Hydrobiologia 176-177:379-396.

Madkour HA (2013) Impacts of human activities and natural inputs on heavy metal contents of many coral reef environments along the Egyptian Red Sea coast. Arabian Journal of Geosciences 6:1739-1752. doi:10.1007/s12517-011-0482-5.

Manning AJ (2004a) The observed effects of turbulence on estuarine flocculation. Journal of Coastal Research 41:90-104.

Marin B, Valladon M, Polve M, Monaco A (1997) Reproducibility testing of a sequential extraction scheme for the determination of trace metal speciation in a marine reference sediment by inductively coupled plasma-mass spectrometry. Analytica Chimica Acta 342:91-112.

Martin G, George R, Shaiju P, Muraleedharan K, Nair S, Chandramohanakumar N (2012) Toxic metals enrichment in the surficial sediments of a eutrophic tropical estuary (Cochin backwaters, Southwest coast of India). Scientific World Journal. doi:10.1100/2012/972839.

McAnally WH, Mehta AJ (2001) Collisional aggregation of fine estuarine sediments. In: McAnally WH, Mehta AJ (eds.), Coastal and estuarine fine sediment processes, Proceedings in Marine Science 3, Elsevier, Amsterdam, pp. 19-39.

Mcbride MB (1994) Environmental Chemistry of Soils. Oxford University Press, New York, pp. 397.

McLean JE, Bledsoe BE (1992) Ground water issue: Behavior of metals in soil. United States environmental protection agency. EPA/540/S-92/018.

Mehta AJ (1989) On estuarine cohesive sediment suspension behaviour. Journal of Geophysical Research 94(C10):14303-14314.

Mikulic N, Orescanin V, Elez L, Pavicic L, Pezelj D, Lovrencic I, Lulic S (2008) Distribution of trace elements in the coastal sea sediments of Maslinica Bay, Croatia. Environmental Geology 53:1413-1419. doi:10.1007/s00254-007-0750-6.

MOEF (2011) Comprehensive environmental pollution abatement action plan Mangalore industrial cluster-Karnataka. Action plan for critically polluted area. http://cpcb.nic.in/divisionsofheadoffice/ess/Mangalore.pdf. Accessed 2 December 2014.

Morfett K, Davison W, Hamilton-Taylor J (1998) Trace metals dynamics in a seasonally anoxic lake. Environmental Geology and Water Science 11:107-114.

Mudge SM, Norris CE (1997) Lipid biomarkers in the Conwy Estuary (North Wales, UK): a comparison between fatty alcohols and sterols. Marine Chemistry 57(1-2):61-84.

Mukhopadhyay R, Karisiddaiah SM (2014) The Indian Coastlines: Processes and Landforms. In: Kale VS (ed.), Landscapes and Landforms of India, Springer, Dordrecht, Heidelberg, New York, London, pp. 91-105.

Muzuka ANN, Shaghude YW (2000) Grain size distribution along the Msasani Beach, North of Dar es Salaam Harbour. Journal of African Earth Sciences 30:417-426.

Naidu AS, Mowatt TC, Somayajulu BLK, Rao KS (1985) Characteristics of the clay minerals in the bed loads of major rivers of India. Mitteilungen Geologisch Palaontologishes Institut Umversitat Hamburg SCOPE/UNEP Sonderband 58:559-568.

Nair VR, Mustafa S, Mehta P, Govindan K, Ram MJ, Gajbhiye SN (1998) Biological characteristic of Vashishti estuary, Maharashtra. Indian Journal of Geo-Marine Sciences 27:310-316.

Naqvi SM (2005) Geology and evolution of the Indian Plate (from Hadean to Holocene - 4 Ga to 4 Ka). Capital publishing company, New Delhi, pp. 450.

Nasnodkar MR, Nayak GN (2015) Processes and factors regulating the distribution of metals in mudflat sedimentary environment within tropical estuaries, India. Arabian Journal of Geosciences 8:9389-9405. doi:10.1007/s12517-015-1823-6.

Nobi EP, Dilipan E, Thangaradjou T, Sivakumar K, Kannan L (2010) Geochemical and geo-statistical assessment of heavy metal concentration in the sediments of different coastal ecosystems of Andaman islands, India. Estuarine Coastal and Shelf Science 87:253-264.

O'Brien DJ, Whitehouse RJS, Cramp A (2000) The cyclic development of a macrotidal mudflat on varying timescales. Continental Shelf Science 20:1593-1619.

Okuku EO, Mubiana VK, Hagos KG, Peter HK, Blust R (2010) Bioavailability of sediment-bound heavy metals on the East African Coast. Western Indian Ocean Journal of Marine Science 9(1):31-42.

Osakwe JO, Adowei P, Horsfall Jnr M (2014) Evaluation of Heavy Metal Species in Bottom Sediments from Imo River System, Southeastern Nigeria. Research Journal of Chemical Sciences 4(6):23-30.

Oyedotun TDT, Burningham H, French JR (2013) Sediment sorting and mixing in the Camel estuary, UK. Journal of Coastal Research. doi:10.2112/SI65-264.

Padmalal D, Seralathan P (1995) Geochemistry of Fe and Mn in surficial sediments of a tropical river and estuary, India - a granulometric approach. Environmental Geology 25:270-276.

Panchang (2014) Sand mining and industrial effluents threaten mangroves along central west coast of India. Open journal of ocean and coastal sciences 1(1):35-49.

Pande A, Nayak GN (2013) Understanding distribution and abundance of metals with space and time in estuarine mudflat sedimentary environment. Environmental Earth Science 70:2561-2575.

Parthasarathy G, Choudary BM, Sreedhar B, Kunwar AC, Srinivasan R (2003) Ferrous saponite from the Deccan trap, India, and its application in adsorption and reduction of hexavalent chromium. American Mineralogy 88:1983-1988.

Patchineelam SM, Neto JAB (2007) Spatial distribution of clay minerals in Guanabara Bay sediemnts and its relationship with the estuary hydrodynamics. Geochimica Brasiliensis 21(1):1-8.

Pathak MC, Kotnala KL, Prabaharan N (1988) Effects of bridge piers on a tropical estuary in Goa, India. Journal of Coastal Research 4(3):475-481.

Pedersen TF, Price NB (1982) The geochemistry of manganese carbonate in Panama Basin sediments. Geochimica Cosmochimica Acta 46:59-68. doi:10.1016/0016-7037(82)90290-3.

Pejrup M (1988) The triangular diagram for classification of estuarine sediments: A new approach. In:de Boer PL, van Gelder A, Nios SD (eds.), Tide influenced sedimentary environments and facies, Reidel, Dordrecht, pp. 289-300.

Perin G, Craboledda L, Lucchese M, Cirillo R, Dotta L, Zanette ML, Orio AA (1985) Heavy metal speciation in the sediments of Northern Adriatic Sea. A new approach for

environmental toxicity determination. In Lekkas TD (ed.), Heavy metals in the environment 2, CEP Consultants, Edinburgh.

Perin G, Fabris R, Manente S, RebelloWagener A, Hamacher C, Scotto S (1997) A five-year study on the heavy metal pollution of Guanabara Bay sediments (Rio de Janeiro, Brazil) and evaluation of the metal bioavailability by means of geochemical speciation. Water Research 31:3017-3028.

Pethick J (1984) An introduction to Coastal Geomorphology. Arnold-Heinemann Publication, London.

Pritchard DW (1955) Estuarine circulation pattern. Proceedings of American Society of Civil Engineering 81(717):7-11.

Pritchard DW (1967) What is an estuary: Physical view point. In: Lauff GH (ed.), Estuaries, American Association for the Advancement of Science 83, pp. 3-5.

Prost R, Yaron B (2001) Use of modified clays for controlling soil environmental quality. Social Science 166:880-894.

Rabouille C, Stahl H, Bassinot F, Tengberg A, Brunnegard J, Hall P, Kiriakoulakis K, Reyss JL, Dezileau L, Crassous P, Roos P, Lampitt RS (2001) Imbalance in the carbonate budget of surficial sediments in the North Atlantic Ocean: Variations over the last millennium. Progress in Oceanography 50:201-221.

Radhakrishna BP, Vaidyanadhan R (1994) Geology of Karnataka: Geological Society of India, Bangalore, pp. 9-17.

Radheshyam B, Rao S, Shirlal KG (2010) On numerical modelling of waves, currents and sediment movement around Gurupur-Netravathi river mouth. International Journal of Earth Science Engineering 3(4):538-552.

Raghavan BR, Vinod BT, Dimple KA, Prabhu HV, Udayashankar HN, Murthy TRS (2001) Evaluation of the Nethravathi spit complex, west coast of India: Integrated change detection

study using topographic and remotely sensed data. Indian Journal of Geo-Marine Sciences 30(4):268-270.

Raj S, Jee PK, Panda CR (2013) Textural and heavy metal distribution in sediments of Mahanadi estuary, east coast of India. Indian Journal of Geo-Marine Sciences 42(3):370-374.

Ram A, Borole DV, Rokade MA, Zingde MD (2009) Diagenesis and bioavailability of mercury in the contaminated sediments of Ulhas Estuary, India. Marine Pollution Bulletine 58(11):1685-1693.

Ramachandra TV, Subhashchandran MD, Sreekantha DM, Rao GR, Ali S (2004) Cumulative impact assessment in the Sharavathi river basin. International Journal of Environment and Development 1(1):113-135.

Rao VP, Rao BR (1995) Provenance and distribution of clay minerals in the continental shelf and slope sediments of the west coast of India. Continental Shelf Research 15:1757-1771.

Rao VP, Shynu R, Kessarkar PM, Sundar D, Michael GS, Narvekar T, Blossom V, Mehra P (2011) Suspended sediment dynamics on a seasonal scale in the Mandovi and Zuari estuaries, central west coast of India. Estuarine Coastal and Shelf Science 91:78-86.

Ratuzny T, Gong Z, Wilke BM (2009) Total concentrations and speciation of heavy metals in soils of the Shenyang Zhangshi Irrigation Area, China. Environmental Monitoring and Assessment 156(1-4):171-180.

Reddy NPC, Durga Prasad Rao NVN, Dora YL (1992) Clay mineralogy of inner shelf sediments off Cochin, west coast of India. Indian Journal of Marine Sciences 21:152-154.

Rhein M, Rintoul SR, Aoki S, Campos E, Chambers D, Feely RA, Gulev S, Johnson GC, Josey SA, Kostianoy A, Mauritzen C, Roemmich D, Talley LD, Wang F (2013) Observations: Ocean. In: Climate Change 2013: The Physical Science Basis. Contribution of Working Group I to the Fifth Assessment Report of the Intergovernmental Panel on Climate Change, Cambridge University Press, Cambridge, United Kingdom and New York, NY, USA.

Rodriguez CA, Flessa KW, Dettman DL (2001) Effects of upstream diversion of Colorado River water on the estuarine bivalve mollusc Mulinia coloradoensis. Conservation Biology 15(1):249-258.

Roussiez V, Ludwig W, Monaco A, Probst JL, Bouloubassi I, Buscail R, Saragoni G (2006) Sources and sinks of sediment-bound contaminants in the Gulf of Lions (NW Mediterranean Sea): a multi-tracer approach. Continental Shelf Research 26:1843-1857.

Salomons W, Forstner U (1984) Metals in the Hydrocycle. Springer, Berlin, pp. 349.

Saulnier I, Mucci A (2000) Trace metal remobilization following the re-suspension of estuarine sediments: Saguenay Fjord, Canada. Applied Geochemistry 15:191-210.

Sharmin S, Zakir HM, Shikazono N (2010) Fractionation profile and mobility pattern of trace metals in sediments of Nomi River, Tokyo, Japan. Journal of Soil Science and Environmental Management 1:1-14.

Shi W, Sun MY, Molina M, Hodson RE (2001) Variability in the distribution of lipid biomarkers and their molecular isotopic composition in Altamaha estuarine sediments: implications for the relative contribution of organic matter from various sources. Organic Geochemistry 32:453-467.

Singer A (1984) The paleoclimatic interpretation of clay minerals in sediments - a review. Earth-Science Reviews 21:251-293.

Singh KT (2008) Geochemistry and sedimentology of tidal mudflats along central west coast of India. Thesis submitted to Goa University.

Singh KT, Nayak GN (2009) Sedimentary and geochemical signatures of depositional environment of sediments in mudflats from a microtidal Kalinadi estuary, central west coast of India. Journal of Coastal Research 25(3):641-650.

Singh KT, Nayak GN, Fernandes L (2013) Geochemical evidence of anthropogenic impacts in sediment cores from mudflats of a tropical estuary, central west coast of India. Soil and Sediment Contamination: An International Journal 22(3):256-272. doi:10.1080/15320383.2013.726291.

Singh KT, Nayak GN, Fernandes L, Borole DV, Basavaiah N (2014) Changing environmental conditions in recent past - Reading through the study of geochemical characteristics, magnetic parameters and sedimentation rate of mudflats, central west coast of India. Palaeogeography, Palaeoclimatology, Palaeoecology 397:61-74.

Siraswar R, Nayak GN (2011) Mudflats in lower middle estuary as a favorable location for concentration of metals, west coast of India. Indian Journal of Geo-Marine Sciences 40(3):372-385.

Sondi I, Pravdic V (1998) The colloid and surface chemistry of clays in natural waters. Croatia Chemica Acta 71:1061-1074.

Spencer KL (2002) Spatial variability of metals in the inter-tidal sediments of theMedway Estuary, Kent, UK. Marine Pollution Bulletin 44:933-944.

Takematsu N, Sato Y, Kato Y, Okabe S (1993) Factors Regulating the Distribution of Elements in Marine Sediments Predicted by a Simulation Model. Journal of Oceanography 49:425-441.

Tam NFY, Wong WS (2000) Spatial variation of heavy metals in surface sediments of Hong Kong mangrove swamps. Environmental Pollution 110:195-205.

Tessier A, Campbell PGC (1982) Particulate trace metal speciation in stream sediments and relationship with grain size: implications for geochemical exploration. Journal of Geochemical Exploration 6:77-104.

Tessier A, Campbell PGC, Auclair JC, Bisson M (1984) Relationships between the partitioning of trace metals in sediments and their accumulation in the tissues of the

freshwater mollusc Elliptio complanata in a mining area. Canadian Journal of Fisheries and Aquatic Sciences 41:1463-1472.

Tessier A, Campbell PGC, Bisson M (1979) Sequential extraction procedure for the speciation of particulate trace metals. Analytical Chemistry 51(7):844-851. doi: 10.1021/ac50043a017.

Thamdrup B (2000) Bacterial manganese and iron reduction in aquatic sediments. Advances in Microbial Ecology 16:41-84.

Tokalioglu S, Kartal S, Elci L (2000) Determination of heavy metals and their speciation in lake sediments by flame atomic absorption spectrometry after a four-stage sequential extraction procedure. Analytica Chimica Acta 413:33-40.

Trefry JH, Presley BJ (1976) Heavy metals in sediments from San Antonio Bay and the northwest Gulf of Mexico. Environmental Geology 1:283-294.

Tripati S, Gaur AS, Sundaresh, Bandodker SN (1998) Historical period Stone anchors from Vijaydurgh on the west coast of India. Bulletin of the Australian Institute for Maritime Archaeology 22:1-8.

Turekian KK, Wedepohl KH (1961) Distribution of the elements in some major units of the earth's crust. Geological Society of American Bulletin 72:175-192.

U.S. Department of Agriculture (1963) Proceedings of the federal inter-agency sedimentation conference.

Valette-Silver NJ (1993) The use of sediment cores to reconstruct historical trends in contamination of estuarine and coastal sediment. Estuaries 16:577-588.

Venkatramanan S, Ramkumar T, Anithamary I, Vasudevan S (2014) Heavy metal distribution in surface sediments of the Tirumalairajan River estuary and the surrounding coastal area, east coast of India. Arabian Journal of Geosciences 7:123-130. doi:10.1007/s12517-012-0734-z.

Verney R, Brun-Cottan JC, Lafite R, Deloffre J, Taylor JA (2006) Tidally-induced Shear Stress Variability above Intertidal Mudflats in the Macrotidal Seine Estuary. Estuaries and Coasts 29(4):653-664.

Violante A, Krishnamurti GSR, Pigna M (2008) Mobility of trace elements in soil environments. In: Violante A, Huang PM, Gadd GM (eds.), Biophysico-chemical processes of metals and metalloids in soil environments, John Wiley & Sons, Hoboken, NJ, pp. 169-213.

Volvoikar SP (2014) Reconstruction of environment of deposition using mudflat and mangrove sediments along Northern Maharashtra coast, west coast of India. Ph.D. Thesis submitted to Goa University, India.

Volvoikar SP, Nayak GN (2013a) Factors controlling the distribution of metals in intertidal mudflat sediments of Vaitarna estuary, North Maharashtra coast, India. Arabian Journal of Geosciences. doi: 10.1007/s12517-013-1162-4.

Volvoikar SP, Nayak GN (2013b) Depositional environment and geochemical response of mangrove sediments from creeks of northern Maharashtra coast, India. Marine Pollution Bulletine 69:223-227.

Wang B, Fringer OB, Giddings SN, Fong DA (2008) High-resolution simulations of a macrotidal estuary using SUNTANS, Ocean Modelling. doi:10.1016/j.ocemod.2008.08.006.

Wang C, Liu SL, Zhao QH, Deng L, Dong S (2012) Spatial variation and contamination assessment of heavy metals in sediments in the Manwan Reservoir, Lancang River. Ecotoxicology and Environmental Safety 82:32-39.

Weaver CE (1989) Clays, muds, and shales. Developments in sedimentology 44, Elsevier, Amsterdam, pp. 819.

Wensink H (1973) Newer paleomagnetic results of the Deccan Traps, India. Tectonophysics 17:41-59.

Willams TP, Bubb JM, Lester JN (1994) Metal accumulation within saltmarsh environments: a review. Marine Pollution Bulletine 28:277-290.

Wilson RE (1978) Mineralogy, petrology and geochemistry of basalt weathering: B.Sc. Thesis submitted to Latrobe University, pp. 55.

Winterwerp JC (1998) A simple model for turbulence induced flocculation of cohesive sediment. Journal of Hydraulic Research 36(3):309-326.

Winterwerp JC, van Kesteren WGM (2004) Introduction to the physics of cohesive sediment in the marine environment. In: van Loon, T. (ed.), Developments in Sedimentology 56, Elsevier, Amsterdam, pp. 466.

Wotter SET, Niencheski LFH, Milani MR (2011) Chemical speciation and dissolved iron in the pore water of Patos Lagoon Sediments-Brazil. Portugaliae Electrochimica Acta 29(3):155-163.

Wu L, Ma LQ, Martinez GA (2000) Comparison of methods for evaluating stability and maturity of biosolids compost. Journal of Environmental Quality 29:424-429.

Xin P, Robinson C, Li L, Barry DA, Bakhtyar R (2010) Effects of wave forcing on a subterranean estuary. Water Resources Research 46:W12505.

Yuan C, Shi J, He B, Liu J, Liang L, Jiang G (2004) Speciation of heavy metals in marine sediments from the East China Sea by ICP-MS with sequential extraction. Environment International 30:769-783.

Zabetoglou K, Voutsa D, Samara C (2002) Toxicity and heavy metal contamination of surficial sediments from the Bay of Thessaloniki (Northwestern Aegean Sea) Greece. Chemosphere 49:17-26.

Zakir HM, Shikazono N (2011) Environmental mobility and geochemical partitioning of Fe, Mn, Co, Ni and Mo in sediments of an urban river. Journal of Environmental Chemistry and Ecotoxicology 3:116-126.

Zhang BL, Liu M, Hou LJ, Ou DN, Liu QM (2002) The temporal and spatial variation of nitrogen in sediments and waters from Shanghai coastal zone. Resources and Environment in the Yangtze Basin 11:250-254.

Zhang J, Huang WW, Martin JM (1988) Trace metals distribution in Huanghe (Yellow River) estuarine sediments. Estuarine Coastal and Shelf Sciences 26:499-526. doi:10.1016/0272-7714(88)90003-0.

Zhang W, Yu L, Lu M, Hutchinson SM, Feng H (2007) Magnetic approach to normalizing heavy metal concentrations for particle size effects in intertidal sediments in the Yangtze Estuary, China. Environmental Pollution 147:238-244.

Zhuang W, Gao X (2014) Assessment of heavy metal impact on sediment quality of the Xiaoqinghe estuary in the coastal Laizhou Bay, Bohai Sea: inconsistency between two commonly used criteria. Marine Pollution Bulletin 83(1):352-357.

Zingde MD, Ram A, Sharma P, Abidi SAH (1995) Seawater intrusion and behaviour of dissolved boron, fluoride, calcium, magnesium and nutrients in Vashisti estuary. In: Agarwal VP, Sharma CB, Abidi SAH and Zingde MD (eds.), Complex carbohydrates & advances in biosciences, pp. 563-580.

Zong Y, Lloyd JD, Leng MJ, Yim WWS, Huang GQ (2006) Reconstruction of the Holocene monsoon history from the Pearl River Estuary, southern China, using diatoms and organic carbon isotope ratios. Holocene 16:251-263.

Zourarah B, Maanan M, Robin M, Carruesco C (2009) Sedimentary records of anthropogenic contribution to heavy metal content in Oum Er Bia estuary (Morocco). Environmental Chemistry Letters 7:67-78. doi:10.1007/s10311-008-0138-1.

Zwolsman JJG, Berger GW, van Eck GTM (1993) Sediment accumulation rates, historical input, post-depositional mobility and retention of major elements and trace metals in salt marsh sediments of the Scheldt estuary, SW Netherlands. Marine Chemistry 44:73-94.

Arab J Geosci (2015) 8:9389–9405
DOI 10.1007/s12517-015-1823-6

ORIGINAL PAPER

Processes and factors regulating the distribution of metals in mudflat sedimentary environment within tropical estuaries, India

Maheshwar R. Nasnodkar · G. N. Nayak

Received: 25 June 2014 / Accepted: 23 January 2015 / Published online: 25 March 2015

Abstract The present study investigates processes and factors which determine the distribution of grain size, organic carbon and metals in mudflat sediment cores collected from lower regions of three tropical estuaries, viz., Mandovi, Sharavathi and Gurupur. The three rivers are similar in terms of monsoonal characteristics and discharge pattern, but are different in tidal range, catchment area geology and anthropogenic activities. The data revealed increase in finer sediments, organic carbon and metals in the recent years in Mandovi and Sharavathi estuaries, while the data revealed decrease in the Gurupur estuary. The increase in finer sediments in Mandovi and Sharavathi estuaries was attributed to catchment area activities, rainfall and runoff and mixing behaviour within estuaries. The change in the morphology of the Mangalore spit led to an increase in coarser sediments in the recent years in the Gurupur estuary. The similarity in distribution pattern of metals to that of finer sediments and organic carbon in three estuaries indicated the role of finer sediments and organic carbon in distribution of metals. In addition, correlation, factor and cluster analyses suggested the role of Fe and/or Mn oxide in adsorption of metals onto sediments. However, the factors regulating distribution of metals varied among the three estuaries, which are attributed to variations in rock types in their basins, in addition to changes in response to natural forces and human activities.

M. R. Nasnodkar · G. N. Nayak (✉)
Department of Marine Sciences, Goa University,
Taleigao 403206, Goa, India
e-mail: nayak1006@rediffmail.com

G. N. Nayak
e-mail: gnnayak@unigoa.ac.in

Keywords Mudflats · Mandovi · Sharavathi · Gurupur · Finer sediments · Coarser sediments

Introduction

Estuaries are proved to be accumulation sites of sediments and contaminants (Madkour et al. 2011). Trace metals are introduced into the estuarine environment as a result of natural processes as well as from pollutants released by human activities (Jordao et al. 2002). Metals in the dissolved phase get adsorbed onto suspended matter, gradually sink to the bottom and later incorporate into cohesive sediments of mudflats within estuaries due to their high mud content. Higher concentrations of metals are found in finer sediments of mudflats (Tam and Wong 2000) due to a synergetic action of physical (surface area) and chemical (mineralogy) characteristics of the particles. In addition, metal distribution also depends upon organic matter content (Emam and Saad-Eldin 2013) and depositional environment of sediments (Willams et al. 1994). Over the last decade, the study of estuarine mudflat sediment cores has proved to be an excellent tool for understanding of natural processes regulating metal distribution in coastal depositional environments (Vinodhini and Narayanan 2008). The understanding of processes and factors affecting metals concentration helps in determining metal behaviour within coastal environments. As a result, an increasing demand for understanding of processes and factors regulating metal distribution has emerged in the recent years (Jingchun et al. 2010; Volvoikar and Nayak 2013). The present study involves grain size, organic carbon and metal analysis of sediment cores collected from the three tropical estuaries along central west coast of India. All the three rivers, namely Mandovi,

Sharavathi and Gurupur, originate in the Western Ghats and drain into the Arabian Sea. The three rivers are largely similar with respect to period of rainfall they receive and runoff, but are different from each other in terms of tidal energy, rocks present in their basins, geomorphology and human activities.

Study area

The Mandovi river forms an important estuarine system on the central west coast of India. The river is 84 km long and has a catchment area of 1150 km^2 (Pathak et al. 1988). It drains through the Western Ghats. The river receives an annual average rainfall of 2932 mm. It has a tidal range of 2.3 and 1.5 m during spring and neap tide, respectively (Rao et al. 2011). During monsoon, a salt wedge is formed at the mouth region due to strong tidal action and large riverine flow. There are about 27 active large mines in the basin area of Mandovi that generate 1500–6000 tons of rejects per day per mine, a substantial portion of which is expected to ultimately end up in the river (Fernandes and Nayak 2009). The estuarine channel of the Mandovi river is widely used for the transport of iron and ferromanganese ores to the Marmugao harbour throughout the year. The Sharavathi river originates near Ambuthirtha and joins the Arabian Sea at Honnavar. It has a total length of 130 km and a catchment area of 3600 km^2 (Ramachandra et al. 2004). The annual average rainfall near Honnavar is 3521 mm (Avinash et al. 2008), and Sharavathi has a tidal range of 1.41 and 0.66 m during spring and neap tide, respectively (Kumar et al. 2011). In 1964, a dam was constructed near Linganamakki on Sharavathi, which is used for the generation of hydroelectric power. There were well-established open cast mining activities in the catchment area of this river; however, they have been halted since the last few years. The extensive urbanisation, especially near Honnavar, has exposed estuary to increasing stress from domestic wastes in addition to activities like agriculture and sand mining. The Gurupur river is also known as Phalguni/Kulur river. It has a total length of 87 km and a catchment area of 540.62 km^2. The Gurupur estuary receives an annual average rainfall of 3900 mm (Kumar et al. 2010). The highest tide is 1.54 m near Mangalore and decreases to 0.25 m during neap tide (Radheshyam et al. 2010). The Kudremukh mine of Karnataka is one of the largest iron ore mine within the catchment area of Gurupur. The iron ore concentrate from Kudremukh mine was transported to Kudremukh Iron Ore Company Limited (KIOCL) located at Mangalore through pipelines; the ore was pelletised and then exported to different countries. The mine has not been in working conditions for the past few years. The Baikampady industrial zone accommodates various chemical and pharmaceutical industries and is located on the bank of the Gurupur river.

In the present study, an attempt has been made to understand the processes and factors determining the distribution of metals in the sediments of estuaries facing dissimilar natural and anthropogenic pressure.

Materials and methods

Sample collection

Three mudflat sediment cores were collected from the lower estuarine regions of Mandovi (latitude, 15°30′22.67″ N, and longitude, 73°49′26.36″ E), Sharavathi (latitude, 14°15′52.94″ N, and longitude 74°26′18.92″ E) and Gurupur river (latitude, 12°52′20.54″ N, and longitude, 74°49′28.35″ E) (Fig. 1).The three cores were collected during the field survey conducted from 6th to 11th of May 2011. The cores were sampled by inserting the hand-held PVC corer (150 cm length and 6.5 cm diameter) into the intertidal mudflat sediments. The length of the cores collected from Mandovi (MD-1), Sharavathi (S-1) and Gurupur (GP-1) estuaries were 58, 68 and 60 cm, respectively. All the three cores were sub-sampled at 2-cm interval using the plastic knife in order to avoid metal contamination. The sub-samples were carefully transferred to pre-labelled polyethylene bags and then brought to the laboratory in ice boxes. The sampling station locations were obtained by a hand-held global positioning system (GPS).

Laboratory analysis

In the laboratory, sub-samples were oven dried at 60 °C. The sediment component analysis was carried out following pipette technique (Folk 1974), after dissociation of clay particles and oxidation of organic matter with 10 % sodium hexametaphosphate and 30 % H_2O_2, respectively. For the geochemical analysis, a portion of the dried sediment samples was finely powdered using mortar and pestle. Part of the powdered and homogenised samples was used for the estimation of organic carbon. Total organic carbon (TOC) was determined by exothermic heating and oxidation with potassium dichromate and silver sulphate, followed by titration of excess dichromate with 0.5 N ferrous ammonium sulphate (Walkley and Black 1934; Gaudette et al. 1974). The remaining part of powdered and homogenised samples was used for elemental analysis, in which samples were completely dissolved in HF/HNO_3/$HClO_4$ (7:3:1) and dried on a hot plate using total dissolution technique (Jarvis and Jarvis 1985). The digested samples were then aspirated for Fe, Mn, Pb, Ni, Co, Cu, Zn and Cr with the help of Varian AA 240 FS flame atomic absorption spectrometry (AAS) with an air/acetylene flame at specific wavelengths. The accuracy of the analytical method was tested by digesting standard reference material 2702 obtained from National Institute of Standards and Technology (NIST)

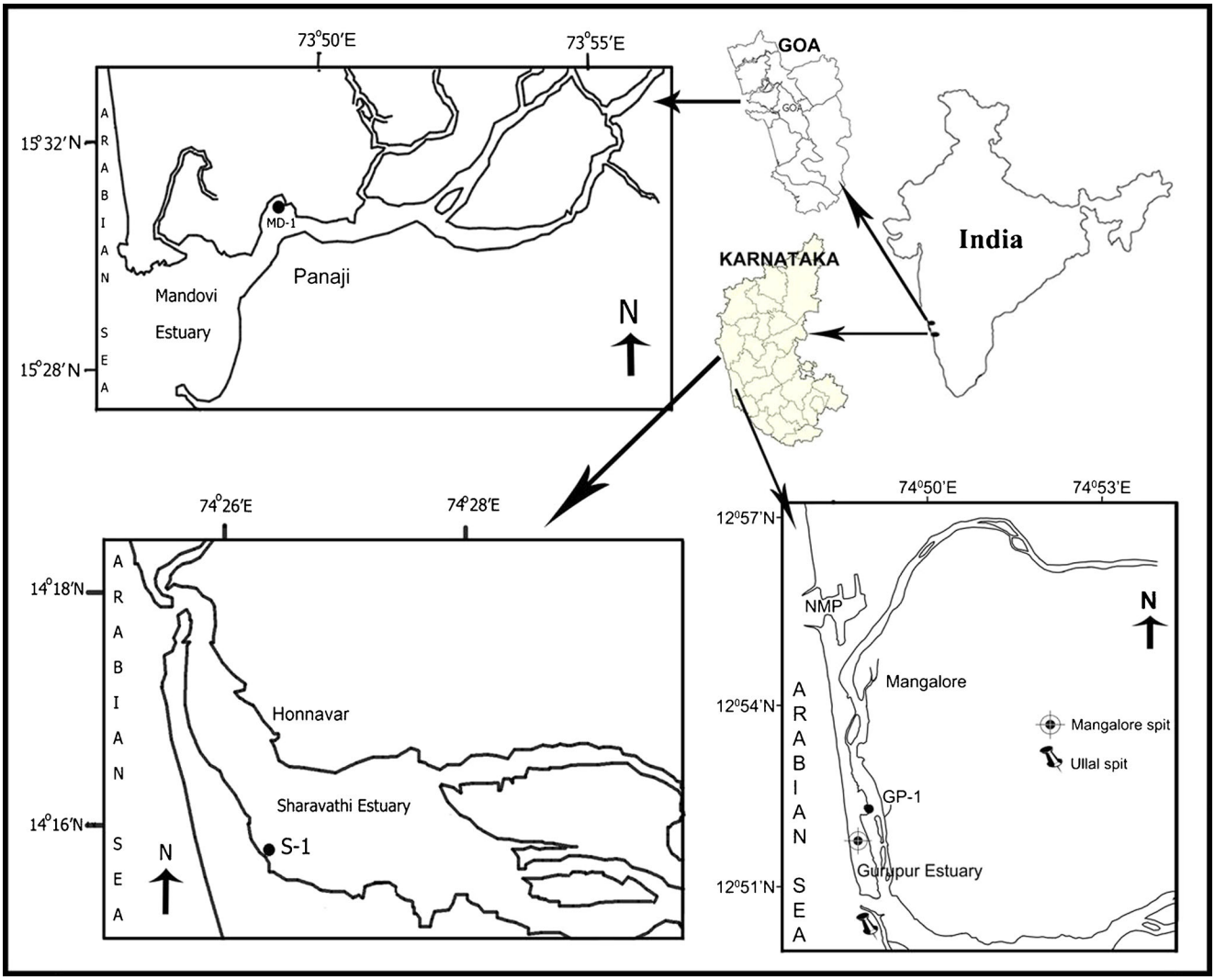

Fig. 1 Map showing sampling locations

and was aspirated into the AAS. The recoveries of all the metals were good, which lie between 89 and 97 %. The instrument was also checked for its reproducibility by repeating standard after every ten samples.

Statistical analysis

The correlation analysis between sand, silt, clay, organic carbon and metals of cores MD-1, S-1 and GP-1 were performed. Additionally, principal component analysis (PCA) involving factor and cluster analyses were attempted to understand source and association by using the software Statistica 7.

Results

The cores MD-1, S-1 and GP-1 could be divided into two vertical sections based on the differences in sediment colour:

1. Brown colour with grey patches from 0 to 44 cm in core MD-1, from 0 to 40 cm in core S-1 and from 0 to 30 cm in core GP-1
2. Light and dark grey colour from 44 to 58, 40 to 68 and 30 to 60 cm in cores MD-1, S-1 and GP-1 respectively.

Sediment components

The range and average percentage of sand–silt–clay in sections I and II of cores MD-1, S-1 and GP-1 are given in Table 1. As can be seen from Table 1, in section II, which represents the recent sediments, there is an increase in finer sediments in cores MD-1 and S-1, while core GP-1 shows enrichment of coarser sediments. The down core variations of sand–silt–clay of cores MD-1, S-1 and GP-1 are shown in the Fig. 2a, b and c respectively. The cores MD-1, S-1 and GP-1 divided into sections I and II based on the variations in sediment parameters agrees with sections divided based on

Table 1 Range and average of sediment components and organic carbon in sediments of cores MD-1, S-1 and GP-1

Sample location		Sand (%)		Silt (%)		Clay (%)		Org. C (%)	
		Range	Average	Range	Average	Range	Average	Range	Average
MD-1	Section II	3.15–52.15	25.07	28.89–54.36	43.44	14.48–45.36	31.49	1.66–3.33	2.67
	Section I	62.90–72.29	67.59	10.11–15.14	12.82	17.60–22.92	19.59	0.48–0.86	0.68
S-1	Section II	21.75–86.39	55.91	0.78–35.08	17.88	0.12–50.32	26.21	0.18–2.05	1.02
	Section I	42.39–94.28	86.53	0.36–16.49	5.62	0.64–41.12	7.85	0.12–1.31	0.30
GP-1	Section II	37.82–91.55	73.36	5.29–34.18	17.46	1.00–28.00	9.18	0.2–1.67	0.66
	Section I	27.17–93.49	53.66	1.80–52.67	26.07	2.64–33.52	20.27	0.09–1.87	1.20

colour variations. In core MD-1, sand percentage is more than the average line in section I and is lesser than the average line in section II. In section I of core MD-1, sand dominates over silt and clay with an average value of 67.59 %. The distribution pattern of coarser as well as finer sediments does not show much variation in section I. In section II, the average sand percentage (25.07 %) reduces to less than half of section I and shows sudden decrease up to 40-cm depth, followed by gentle decrease towards the surface. The decreasing trend of sand is very well compensated by increasing trend of silt and clay. Like core MD-1, sand percentage in core S-1 is more than the average line and less than the average line in sections I and II, respectively. In section I of core S-1, sand shows sharp increase from bottom to 66-cm depth and further remains nearly constant throughout the section. The silt shows a corresponding opposite trend to that of sand profile. The clay percentage decreases sharply from bottom to 66-cm depth, from where gradual decrease is seen. In section II of core S-1, a decreasing pattern of sand is observed, which is compensated by increasing pattern of silt and clay. In core GP-1, distinct different behaviour of sand is observed from other two cores. In section I of core GP-1, sand shows overall decreasing trend with its percentage less than the average line. The distribution patterns of silt and clay is opposite to that of sand. In section II of core GP-1, percentage of sand is more than the average line and that of clay is less than the average line and does not show much variation up to 12-cm depth. Further above, sand percentage decreases while clay percentage increases. The silt shows increasing trend up to the surface.

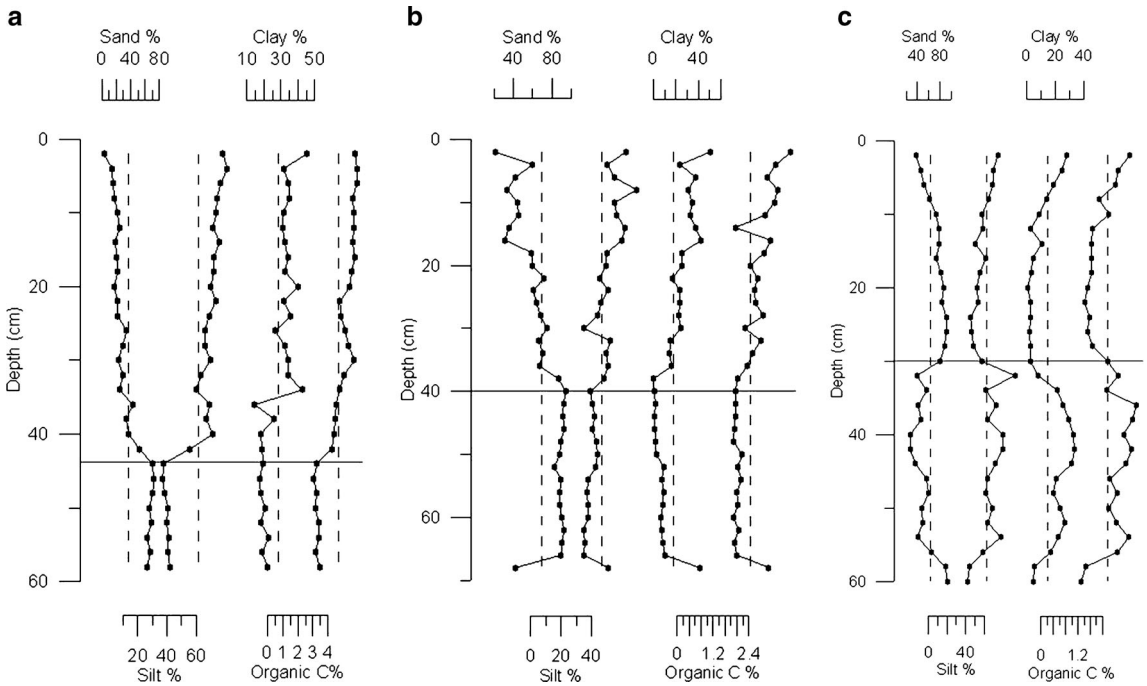

Fig. 2 **a** Down core variation of sediment components and organic carbon with vertical lines of average values in core MD-1. **b** Down core variation of sediment components and organic carbon with vertical lines of average values in core S-1. **c** Down core variation of sediment components and organic carbon with vertical lines of average values in core GP-1

Organic carbon

The range and average concentration of organic carbon in sections I and II for cores MD-1, S-1 and GP-1 are given in Table 1. The average organic carbon percentage has increased in the recent years in cores MD-1 and S-1, while it has decreased in core GP-1. As can be seen from the Fig. 2a, organic carbon percentage remains constant in section I, while in section II, overall increasing trend is observed up to the surface of core MD-1. In section I of core S-1 (Fig. 2b), organic carbon shows sudden decrease from bottom to 66-cm depth, from where its concentration remains nearly constant throughout the section. In section II (Fig. 2b), increasing distribution pattern of organic carbon is observed up to the surface, with prominent decrease seen at 14-cm depth. In section I of core GP-1 (Fig. 2c), the concentration of organic carbon increases with erratic trends from bottom to 36-cm depth and further shows a decrease. In section II (Fig. 2c), organic carbon shows overall increasing trend up to the surface with increase being more prominently observed in the top 12 cm of the core GP-1.

Metal geochemistry

The range and average concentration of metals (Fe, Mn, Pb, Ni, Co, Cu, Zn and Cr) in sections I and II for cores MD-1, S-1 and GP-1 are given in the Table 2. In cores MD-1 and S-1, all the metals (except Fe and Zn in core S-1) show higher average concentration in section II than in section I, whereas in core GP-1, average metal concentration (except Pb and Zn) is higher in section I than in section II.

The vertical profile of metal concentration for cores MD-1, S-1 and GP-1 are shown in the Fig. 3a, b and c, respectively. In core MD-1, Mn, Pb, Ni, Co and Zn do not show much variation throughout section I. Cu and Cr exhibit increasing distribution pattern, while Fe percentage decreases in section I with a sharp increase observed at 54-cm depth. In section II, Fe shows overall increasing distribution pattern up to the surface with prominent decrease observed from 18 to 6-cm depth. Cu and Mn exhibit similar distribution pattern with increasing trend up to the surface. Pb, Zn and Cr show gentle decrease up to the surface with sharp increase observed in case of Pb and Zn at 26- and 40-cm depth, respectively. Ni exhibit increasing pattern up to 30-cm depth, from where its concentration gradually decreases towards the surface. Co shows gentle increase up to 22-cm depth, followed by sudden increase up to 20-cm depth. The upper 20 cm of the section II shows nearly constant concentration of Co. In section I of core S-1, Fe, Pb, Co and Cr show decreasing trend with wide fluctuations. Mn and Zn exhibit overall increasing distribution pattern up to 52-cm depth, which is followed by fluctuating trend. Cu and Ni show increasing trend. In section II, Mn, Pb, Ni, Co and Cu show increasing distribution pattern, while Fe shows overall decreasing trend up to the surface. Zn exhibits wide fluctuations

Table 2 Range and average of Fe, Mn, Pb, Ni, Co, Cu, Zn and Cr in sediments of cores MD-1, S-1 and GP-1

Sample location		Fe (%)		Mn (ppm)		Pb (ppm)		Ni (ppm)		Co (ppm)		Cu (ppm)		Zn (ppm)		Cr (ppm)	
		Range	Average	Range	Average	Range	Average	Range	Average	Range	Average	Range	Average	Range	Average	Range	Average
MD-1	Section II	0.78–5.64	3.28	417–1366	744	27–180	52	36–58	45	13–23	18	20–31	23	35–1531	223	53–121	77
	Section I	0.31–4.77	1.68	336–494	403	30–116	48	27–36	33	8–13	9	10–18	15	141–304	209	23–174	74
S-1	Section II	0.37–3.57	1.80	36–181	115	31–95	61	26–51	39	3–15	9	5–43	21	85–2293	497	18–61	42
	Section I	0.31–6.02	2.79	16–192	115	28–64	46	11–39	23	3–11	5	2–14	7	33–2165	1026	5–96	39
GP-1	Section II	1.58–4.38	2.64	60–155	101	24–37	31	16–49	35	4–10	7	4–22	11	359–1919	925	29–125	76
	Section I	1.08–5.91	4.28	43–156	115	22–38	31	13–59	44	3–12	9	2–38	20	278–463	397	16–127	85

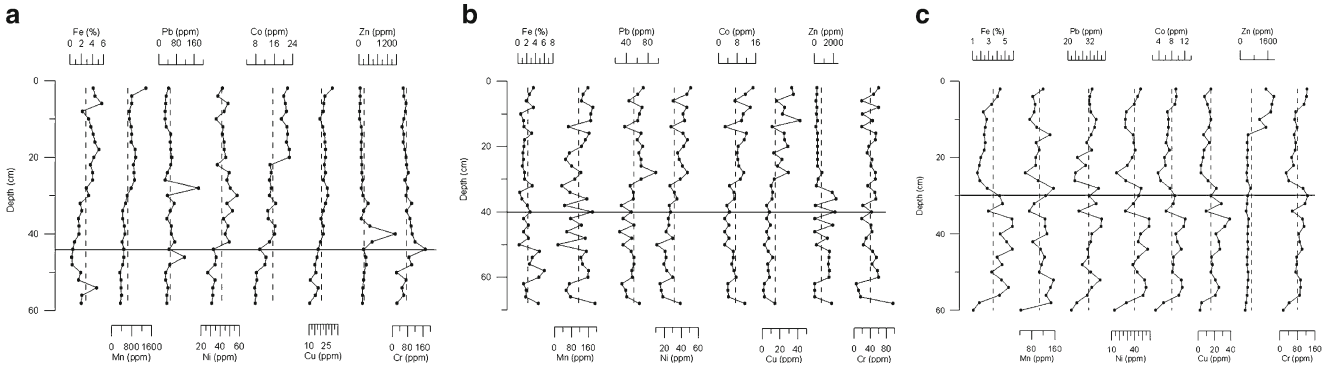

Fig. 3 **a** Down core variation of Fe, Mn, Pb, Ni, Co, Cu, Zn and Cr with vertical lines of average values in core MD-1. **b** Down core variation of Fe, Mn, Pb, Ni, Co, Cu, Zn and Cr with vertical lines of average values in core S-1. **c** Down core variation of Fe, Mn, Pb, Ni, Co, Cu, Zn and Cr with vertical lines of average values in core GP-1

up to 32-cm depth, followed by gentle decrease towards the surface. The concentration of Cr increases up to 16-cm depth which is followed by fluctuating trend up to the surface. In core GP-1, all the metals (except Zn) show overall increasing trend in section I. The concentration of Zn remains nearly constant throughout section I. In section II, Mn and Cu concentration decreases up to the surface. Fe, Ni, Co and Cr show overall decreasing pattern up to 8-cm depth. Further above, their concentration increases towards the surface. Pb concentration decreases up to 20-cm depth and further shows increase towards the surface. Zn exhibits nearly constant concentration up to 14-cm depth, which is followed by an increase.

Discussion

Sediment components

When the distribution of sediment components in section I of Mandovi, Sharavathi and Gurupur estuaries is compared, it is observed that, in section I of cores MD-1 and S-1, coarser sediments are higher with an average sand percentage of 86.53 % in core S-1 and 67.59 % in core MD-1. The core GP-1 is enriched with finer sediments in section I along with organic carbon. In section II of cores MD-1 and S-1, the percentage of finer sediments and organic carbon is higher, while in core GP-1, average sand percentage is much higher than finer sediments. The grain size of sediment reflects prevailing hydrodynamic energy conditions (Dolch and Hass 2008). Therefore, the variation in the percentage of sand between sections I and II of cores MD-1 and S-2 indicates transition from a relatively higher-energy depositional environment to lower-energy environment, whereas it also suggests transition from lower-energy depositional environment to higher-energy environment (Fox et al. 1999) in core GP-1. Further, large variation in sand, silt and clay in section II of cores MD-1 and S-1 compared to section I indicates fluctuation in hydrodynamic conditions. Highest freshwater discharge occurs during the south-west monsoon (Kessarkar et al. 2010) along the west coast of India, and the runoff of the rivers for the remaining period of the year is almost negligible and estuary increasingly becomes an extension of sea (Shetye et al. 2007). A major dam constructed on the Sharavathi river in the mid-1960s and smaller dams on tributaries of Mandovi, for diversion of river water for drinking and irrigational purposes in the recent years, are responsible for the decrease in fresh water runoff. This in turn enhances tidal surge regulating changed mixing processes leading to deposition of fine-grained sediments in the recent years. Additionally, the contribution of finer sediments due to the anthropogenic activities like mining, industrial discharge, agricultural practices, and domestic wastes along with natural processes (Wallbrink and Olley 2004) within their catchment area cannot be ignored. The geological formations within catchment area of Mandovi estuary include Western Dharwar Craton (WDC) of meso-archaean age. The WDC is characterised by high-Mg basalts and komatites with meta-volcanic and meta-sedimentary rocks (Naqvi 2005). The geological formations within Sharavathi catchment area include pre-Cambrian rocks. The Dharwar system and peninsular gneiss are the two major groups of rocks found in the Sharavathi river basin. The Dharwar system contains metamorphic rocks and is rich in iron and manganese. The peninsular gneisses are crystalline rocks and are made up of granite, granodiorite, granito-gneiss, migmatite, etc. The rate and intensity of weathering of these rocks vary with respect to properties of minerals and their resistance (Mukherjee 2013). The rock types present in the catchment area, therefore, might also contribute for the variation in percentage of silt and clay between Mandovi and Sharavathi estuaries, in the recent years. In mudflat sediments of Gurupur estuary, however, coarser sediments are dominant in the recent years. Gurupur and adjacent Netravathi rivers join the Arabian Sea near Mangalore and give rise to two spits, the northern sand spit at the Gurupur river known as “Mangalore spit” and the southern sand spit

"Ullal spit" at the Netravati river. The supply of sediment for the growth of these spits is reported as from longshore drift and river discharge (Kunte and Wagle 1991). The estuarine mouths of Gurupur and Netravathi rivers have been reportedly migrating towards the north since long (Bannur et al. 1991; Gangadhar 1995), forcing the two spits to change the shape, size and orientation (Hegde and Raveendra 2000). The alignment of the shoal near the estuarine mouth of the Netravathi river has altered the flow direction towards the Gurupur estuary (Hegde and Raveendra 2000). This might have resulted in the erosion of the Mangalore spit, directing coarser sediments into the Gurupur estuary. Raghavan et al. (2001) stated that the Mangalore spit, which consists of coarse to fine sand, has reduced by 750 m from its distal end in length, and its width has increased by 155 m from 1910 to 1993. Therefore, it may be construed that erosion of the Mangalore spit may have led to the increase in coarser sediments observed in the recent years in the Gurupur estuary as corroborated from the present analysis.

When the sediment components are plotted on a triangular diagram proposed by Pejrup (1988) to understand hydrodynamic conditions prevailed during deposition of sediments, it is observed that sediments of section I of core MD-1 (Fig. 4a) containing coarser sediments with sand percentage between 50 to 90 % fall within group BII and sediments from section II of the same core (Fig. 4a) fall largely in group CIII indicating change in depositional environment with time. In section I of core S-1 (Fig. 4b) with coarser sediments, the points fall in group A indicating deposition under more dynamic conditions as they vary from hydrodynamic I (calm conditions) to IV (extremely violent conditions). Sediments of section II (Fig. 4b) with comparatively finer sediments fall within group BII and CII, indicating their deposition under less violent conditions. Finer sediments from section I of core GP-1 (Fig. 4c) falls largely in group C indicating their deposition under less violent (II) to relatively violent conditions (III). In the recent years, coarser sediments from section II of core GP-1 (Fig. 4c) fall largely in group B, indicating deposition under relatively violent (III) to extremely violent conditions (IV).

The distribution pattern of organic carbon is largely similar to that of silt and clay in all three cores, suggesting higher affinity of finer sediments towards organic carbon (Kumar and Sheela 2013) due to the higher surface area/volume ratio of finer sediment grain (Zhou et al. 2007) and similarity in settling velocity (Raj et al. 2013). The increase in organic carbon concentration in the top few centimetres of the three cores suggests the increasing discharge of organic matter associated with industrial, agricultural, mining and domestic wastes into the estuaries in the recent years. Organic matter concentration is highest near the sediment surface and further down decreases. The decrease in organic carbon concentration with depth in section II of cores MD-1 and S-1 reflects the

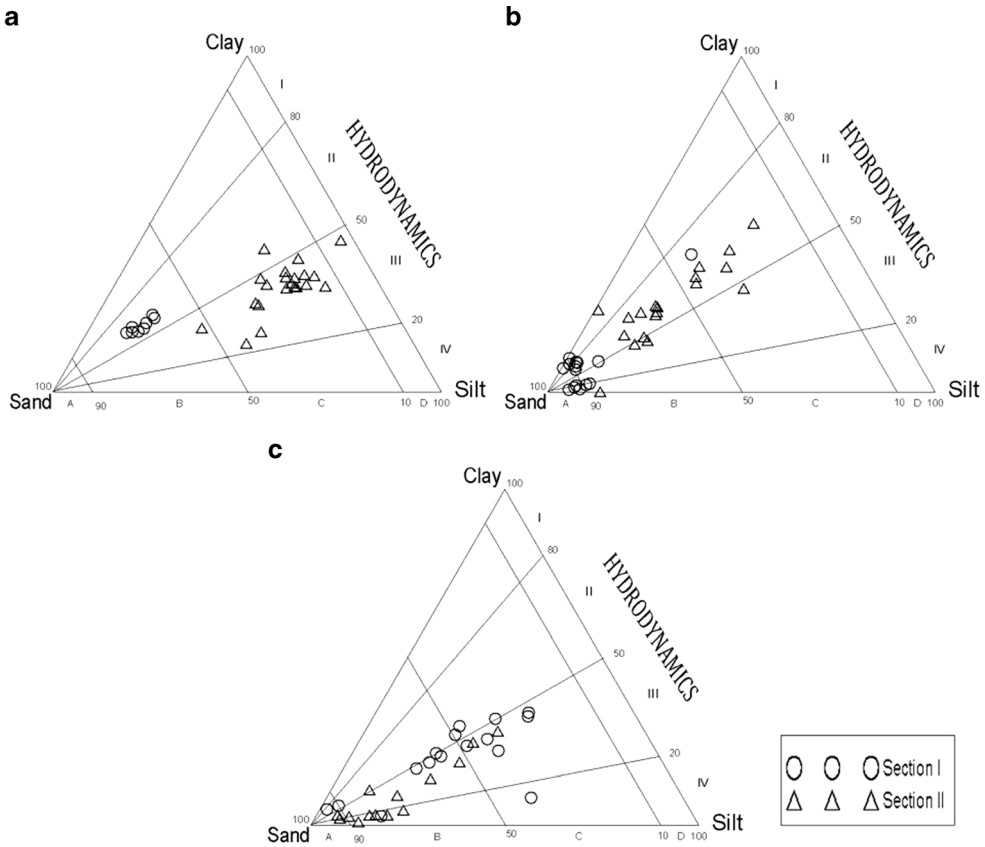

Fig. 4 Triangular diagram for the classification of hydrodynamics of cores MD-1 (**a**), S-1 (**b**) and GP-1 (**c**) (Pejrup 1988)

degradation of organic matter due to the microbial activity (Singh and Nayak 2009). Further, the lower concentration of organic carbon observed in section II of core GP-1 than in section I and in section I of cores MD-1 and S-1 than in section II suggests dilution by the influx of coarse-grained sediments (Pichaimani et al. 2008) in these sections.

Metal geochemistry

The higher average concentration of most of the metals observed in section II than in section I of cores MD-1 and S-1 can be related to their association with finer sediments (Abílio et al. 2006) and organic matter. The anthropogenic activities in the recent times (Harikumar et al. 2009) must have contributed additional metal input. The finer sediments provide active surfaces for the adsorption of metals. Furthermore, the complexing nature of organic carbon plays important role in binding of the metals (Chatterjee et al. 2007). In cores MD-1 and S-1, most of the metals and organic carbon decreases with depth indicating that metals are significantly redistributed by the degradation of organic carbon. During initial deposition, trace metals associated with organic matter (Salomons and Forstner 1984) may be getting redistributed by early aerobic degradation of organic matter, resulting in a gradual decrease in metal concentration with depth (Valette-Silver 1993). The higher percentage of Mn (in sections I and II) and Fe (in section II) in core MD-1 than cores S-1 and GP-1 reflects the greater input of Fe and Mn from mining activities in the catchment area of the Mandovi river. This was also reported earlier by Bukhari (1994). Upon reaching sediments, Fe and Mn oxides are readily reduced into anoxic sediments either as electron acceptors in microbial mediated respiratory oxidation of organic carbon (Thamdrup 2000) or reduced chemically by hydrogen sulphide (Kappler and Straub 2005). Reduced Fe and Mn may remobilise and precipitate as carbonates, adsorb onto clay minerals, carbonates, and metal oxide (Kristiansen et al. 2002) in relatively oxic conditions. The enrichment of Fe and Mn in section II of core MD-1, therefore, indicates that they are precipitated as insoluble oxy-hydroxide in sediments when brought across a redox gradient into an oxidising environment (Brown et al. 2000), while their lower concentration in section I suggests their dissolution under reducing diagenetic conditions (Dulaiova et al. 2008; Ram et al. 2009). Further, the similar distribution pattern of Mn and Cu in section II of core MD-1 indicates that distribution of Cu is regulated by Mn in the redox boundaries and is precipitated onto Mn oxide (Kumar and Edward 2009). Distribution of Ni and Co seems to be regulated by Fe. Likewise, while considering the distribution of metals in the Sharavathi estuary, it is observed that most of the metals in section I of core S-1 exhibit wide fluctuations, which suggest their mobilisation from the sediments. As seen from the triangular diagram, section I of core S-1 is enriched in coarser sediments (Fig. 4b) with sand percentage between 90 and 100 %. In coarser sediments, the porosity is much higher compared to finer sediments, and there is enough opportunity for the metals to get mobilised from the coarser sediments (Clark 1992). This is supported from the increasing distribution pattern of Mn, Pb, Ni, Co and Cu observed in finer sediments enriched section II of core S-1 compared to section I. Cr distribution, however, seems to be regulated by Fe. The distribution pattern of metals in core GP-1 reveals decrease in metal concentration in section II than in section I, which can be attributed to dilution of concentration by input of coarser sediments in section II in recent years as discussed earlier. According to German and Svensson (2002), the change in particle size distribution results in a variation in distribution pattern of metals in the sediments, with higher proportion of metals associated with finer fractions than coarser. Further, the similarity between the profiles of Fe, Ni, Co and Cr seen in section II of core GP-1 indicates that either these elements have undergone similar early-diagenetic remobilisation and re-precipitation around the redox boundary or that these elements are derived from the similar source. The variations in metal distribution is associated with the extent to which the precipitation or dissolution of Fe and Mn oxide/hydroxide act as specific "sink" or source of metal (Lacuraj and Maria 2006). The lack of coincident peaks between the redox sensitive elements (Fe and Mn) and Ni, Co and Cr in the present study point out that early-diagenetic remobilisation has not significantly affected the vertical distributions of these trace metals. Grain size is one of the important factors that regulate the distribution of metals in the coastal area (Venkatramanan et al. 2013). The distribution pattern of all the studied elements (except Zn) agrees with the distribution pattern of grain size and organic carbon in both the sections of core GP-1, which suggests that sediment grain size exerts a significant control on the vertical distribution of metals. The enrichment of Zn in the top 14 cm of the section II of core GP-1 indicates different source, probably originating from the anthropogenic activities (Liu et al. 2011) in the Gurupur river. In the present study, it is seen that the distribution of metals in all three estuaries is regulated by sediment grain size. Tidal range is one of the factors that affect the sediment grain size, and its amplitude varies from high to low along west coast of India from north to south, respectively (Mukhopadhyay and Karisiddaiah 2014). Hence, tidal range may also be a factor regulating metals distribution in these tropical estuaries.

According to Bowen (1979), concentration of Fe, Mn, Pb, Ni, Co, Cu Zn and Cr in world sediments is 4.1 %, 770 ppm, 16 ppm, 52 ppm, 8 ppm, 32 ppm, 127 ppm and 71 ppm, respectively. On comparison of average metals concentration of three estuaries with the world sediments, only Pb and Zn are found to be higher in all three estuaries. The three estuaries being reservoirs of the mining-related activities, as well as agricultural and domestic wastes, the input of Pb and Zn from automobile exhaust and domestic waste may be the major source of their enrichment in sediments.

Section wise comparison of cores MD-1, S-1 and GP-1

Pearson's correlation

To understand the influence of sediment components on metal distribution in the sediment, Pearson's correlation analysis among the grain size, organic carbon and metals were performed. In section I of core MD-1 (Table 3), most of the metals (except Mn, Co and Zn) show independent behaviour. Mn, Co and Zn, however, show significant positive correlation with sand. In addition, significant correlation of Mn with Co is noted. This suggested adsorption of Co and Zn onto the Mn oxide coatings on the sand grains (Badr et al. 2008). The coarser sediments stay in place for a longer period of time (Tesssier and Campbell 1982) and therefore sometimes develop oxide coatings and, hence, adsorb more trace metals. Further, the Mandovi estuary receives mining wastes from its catchment area, and the presence of heavy minerals or coarser fractions of mine and industrial wastes may also increase metal concentration in the coarser fractions. The results of correlation analysis for section II of core MD-1(Table 4) show difference in metal associations, revealing that there is no single decisive factor governing the distribution of metals. It is the coarser as well as finer sediments along with organic carbon and Fe–Mn oxide, which are regulating the distribution of metals. Input from large-scale open cast mining of ferromanganese is very much expected at this site. However, distribution pattern and association of metals indicate post depositional mobilisation and concentration of metals.

In section I of core S-1 (Table 5), all the trace metals (except Ni) show significant correlation with Fe and Mn. Ni shows good correlation only with Mn. Fe–Mn are known to scavenge metals from the water column (Venkatramanan et al. 2014) and therefore suggests important role of Fe and Mn oxy-hydroxide in the adsorption of metals. Furthermore, these trace metals show significant correlation among themselves, suggesting that they are derived from the common source. The finer sediments and organic carbon show good correlation with some of the metals. The coatings of organic matter are prevalent in fine-grained sediments (Basaham 2009), and these coatings bind a variety of trace elements (Wangersky 1986). Like section I, a good correlation of metals with clay and organic carbon is also noticeable in section II of core S-1 (Table 6). However, it is only Mn oxide that seems to play an important role in the adsorption of metals as significant correlation of Mn with Ni, Co and Cu is observed. According to Zabetoglou et al. (2002), Fe and Mn oxide/hydroxide have high affinity towards most trace metals, and Fe often correlates well with concentrations of other metals in aquatic environments. However, in case of section II of core S-1, only Mn is found to correlate well with most of the studied elements as compared to Fe, indicating that Mn is the major carrier for metals.

In both the sections of core GP-1 (Tables 7 and 8), most of the trace metals show significant correlation with Fe along with finer sediments and organic carbon, suggesting that their distribution is strongly controlled by Fe cycling than Mn cycling. The basin area of the Gurupur river is overlaid by the Pliocene to recent laterite capped plateaus and alluvium over the gneisses and continental type of sedimentary deposits with dolerite and norite dikes (Radhakrishna and Vaidyanadhan 1994) containing iron-bearing minerals. The natural weathering of these rocks may be the source of Fe in the Gurupur river sediments. Further, as mentioned earlier, the Kudremukh iron ore mine is located in the catchment area of the Gurupur river and the heavy rainfall in this region must be bringing large amount of Fe-rich material from the catchment area into the river, which may have favoured the adsorption of trace metals. The inter-relationships observed among Pb, Ni, Co, Cu, Zn and Cr in section I of core GP-1 suggest similar

Table 3 Correlation between sand, silt, clay, organic carbon and metals in section I of core MD-1 (n=8)

MD-1 (I)	sand %	silt %	clay %	ORG.C %	Fe (%)	Mn (ppm)	Pb (ppm)	Ni (ppm)	Co (ppm)	Cu (ppm)	Zn (ppm)	Cr (ppm)
Sand (%)	1.00											
Silt (%)	−0.92	1.00										
clay %	−0.94	0.72	1.00									
Org. C %	−0.65	0.56	0.64	1.00								
Fe (%)	−0.83	0.72	0.81[a]	0.53	1.00							
Mn (ppm)	0.83[a]	−0.93	−0.62	−0.51	−0.65	1.00						
Pb (ppm)	0.60	−0.72	−0.41	−0.56	−0.42	0.71	1.00					
Ni (ppm)	0.64	−0.61	−0.59	−0.03	−0.38	0.65	0.51	1.00				
Co (ppm)	0.86[a]	−0.89	−0.71	−0.57	−0.76	0.82[a]	0.77[b]	0.60	1.00			
Cu (ppm)	0.23	−0.48	0.02	−0.46	0.09	0.54	0.38	−0.04	0.28	1.00		
Zn (ppm)	0.80[a]	−0.81	−0.69	−0.59	−0.68	0.65	0.66	0.44	0.95[a]	0.27	1.00	
Cr (ppm)	0.68	−0.79	−0.50	−0.17	−0.55	0.84[a]	0.25	0.54	0.53	0.43	0.38	1.00

[a] Correlation is significant at 0.01 level

[b] Correlation is significant at 0.02 level

Table 4 Correlation between sand, silt, clay, organic carbon and metals in section II of core MD-1 (n=21)

MD-1 (II)	Sand (%)	Silt (%)	Clay (%)	Org. C (%)	Fe (%)	Mn (ppm)	Pb (ppm)	Ni (ppm)	Co (ppm)	Cu (ppm)	Zn (ppm)	Cr (ppm)
Sand (%)	1.00											
Silt (%)	−0.74	1.00										
Clay (%)	−0.84	0.25	1.00									
Org. C (%)	−0.80	0.68[a]	0.59[a]	1.00								
Fe (%)	−0.73	0.65[a]	0.52[b]	0.76[a]	1.00							
Mn (ppm)	−0.74	0.59[a]	0.58[a]	0.59[a]	0.75[a]	1.00						
Pb (ppm)	0.23	−0.37	−0.03	−0.18	−0.23	−0.08	1.00					
Ni (ppm)	0.29	−0.61	0.07	−0.24	−0.26	−0.35	0.29	1.00				
Co (ppm)	−0.66	0.65[a]	0.42	0.72[a]	0.60[a]	0.55[a]	−0.24	−0.45	1.00			
Cu (ppm)	−0.60	0.31	0.62[a]	0.40	0.40	0.68[a]	0.25	0.20	0.22	1.00		
Zn (ppm)	0.53[a]	−0.28	−0.53	−0.62	−0.55	−0.44	0.13	0.16	−0.30	−0.20	1.00	
Cr (ppm)	0.78[a]	−0.67	−0.58	−0.84	−0.76	−0.64	0.32	0.40	−0.61	−0.28	0.65[a]	1.00

[a] Correlation is significant at 0.01 level

[b] Correlation is significant at 0.02 level

source or a similar enrichment mechanism of these trace metals in the Gurupur river sediments.

From Pearson's correlation analysis, it is clear that there is difference in behaviour of the metals in the three estuaries and also within two sections of the cores MD-1and S-1. The dominance of Fe cycling in GP-1 and Mn cycling in S-1 may be the result of variations in source rock in their basins and factors affecting the source rock. The geological factors differ among the three estuaries and can affect the weathering of source rocks (Nesbitt and Young 1996), which in turn affect the chemical composition of the sediments. In addition, human activities may be the factor responsible for the observed metal variations within two sections of the cores MD-1 and S-1.

Principal component analysis (PCA)

PCA has been used in the evaluation of environmental data to explore associations and origins of trace elements (Kulahcl and Şen 2008), obtaining interesting conclusions that are not immediately obvious (Zeng and Wu 2013).

Factor analysis

In present study, factor analysis was performed on data set of cores MD-1, S-1 and GP-1 in order to identify the major factors that determine the distribution of metals in sediment. The numbers of factors are selected on the basis of criteria given by Kaiser (1960), with eigenvalues >1. Tables 9, 10 and 11

Table 5 Correlation between sand, silt, clay, organic carbon and metals in section I of core S-1 (n=15)

S-1 (I)	Sand (%)	Silt (%)	Clay (%)	Org. C (%)	Fe (%)	Mn (ppm)	Pb (ppm)	Ni (ppm)	Co (ppm)	Cu (ppm)	Zn (ppm)	Cr (ppm)
Sand (%)	1.00											
Silt (%)	−0.73	1.00										
Clay (%)	−0.96	0.50	1.00									
Org. C (%)	−0.95	0.68[a]	0.92[a]	1.00								
Fe (%)	−0.41	0.17	0.45	0.28	1.00							
Mn (ppm)	−0.43	0.32	0.41	0.30	0.82[a]	1.00						
Pb (ppm)	−0.55	0.39	0.53	0.46	0.72[a]	0.85[a]	1.00					
Ni (ppm)	−0.59	0.58[b]	0.50	0.44	0.55	0.79[a]	0.66[a]	1.00				
Co (ppm)	−0.79	0.42	0.83[a]	0.70[a]	0.80[a]	0.78[a]	0.84[a]	0.68[a]	1.00			
Cu (ppm)	−0.60	0.58[b]	0.52	0.57[b]	0.61[a]	0.79[a]	0.83[a]	0.81[a]	0.77[a]	1.00		
Zn (ppm)	−0.29	0.37	0.22	0.22	0.70[a]	0.90[a]	0.88[a]	0.64[a]	0.65[a]	0.80[a]	1.00	
Cr (ppm)	−0.69	0.59[b]	0.63[a]	0.63[a]	0.73[a]	0.75[a]	0.75[a]	0.74[a]	0.84[a]	0.89[a]	0.72[a]	1.00

[a] Correlation is significant at 0.01 level

[b] Correlation is significant at 0.02 level

Table 6 Correlation between sand, silt, clay, organic carbon and metals in section II of core S-1 (n=19)

S-1 (II)	Sand (%)	Silt (%)	Clay (%)	Org. C (%)	Fe (%)	Mn (ppm)	Pb (ppm)	Ni (ppm)	Co (ppm)	Cu (ppm)	Zn (ppm)	Cr (ppm)
Sand (%)	1.00											
Silt (%)	−0.84	1.00										
Clay (%)	−0.93	0.59[a]	1.00									
Org. C (%)	−0.62	0.48	0.60[a]	1.00								
Fe (%)	−0.44	0.50	0.32	0.54[b]	1.00							
Mn (ppm)	−0.60	0.44	0.60[a]	0.66[a]	0.19	1.00						
Pb (ppm)	−0.14	−0.14	0.30	0.48	0.03	0.44	1.00					
Ni (ppm)	−0.39	0.14	0.49	0.69[a]	0.20	0.73[a]	0.82[a]	1.00				
Co (ppm)	−0.50	0.27	0.56[a]	0.84[a]	0.39	0.76[a]	0.75[a]	0.93[a]	1.00			
Cu (ppm)	−0.49	0.28	0.54[b]	0.67[a]	0.22	0.68[a]	0.62[a]	0.84[a]	0.75[a]	1.00		
Zn (ppm)	0.29	−0.18	−0.32	−0.23	−0.43	0.06	0.03	−0.11	−0.14	−0.24	1.00	
Cr (ppm)	−0.13	0.05	0.15	0.41	0.29	0.43	0.60[a]	0.67[a]	0.69[a]	0.44	0.38	1.00

[a] Correlation is significant at 0.01 level

[b] Correlation is significant at 0.02 level

represent the number of factors in cores MD-1, S-1 and GP-1, respectively.

Three factors identified in section I of core MD-1 constitutes 86 % of the total variance. The first factor, contributing 63.79 % of the total variance shows significant loading on sand, Co and Zn and good loading on Mn and Pb. This association indicates the role of Mn oxide coatings on coarser sediments in the binding of metals and, hence, can be called as coarser sediment controlled factor. Factor 2 with 12.27 % of the total variance has significant loadings on Cu, and good loadings on Mn and Pb can be referred to as Mn oxide controlled factor (I). In factor 3 with 10.33 % of the total variance, significant loadings on Mn, Ni and Cr and good loadings on sand and Co are observed. It can be termed as Mn oxide controlled factor (II). Within this section, two groups of metals are distinguished to be associated with Mn. Mn oxide have long been recognised as important adsorbing phase governing the cycling of trace metals in aquatic environments (Murray 1987). In section II of core MD-1, two factors are evident, accounting for 69 % of the total variance. Factor 1 has significant loadings on clay, organic carbon, Mn, Fe and Cu and good loadings on silt and Co. This factor accounts for 54.07 % of the total variance and suggests association of these metals with finer fractions. This factor can be called as clay controlled factor, assuming the elements are enriched in the clay fraction. Factor 2 with 15.78 % of the total variance shows significant loadings for Ni and good loadings for Pb, Cr and Cu. This factor reveals good association of these trace metals, suggesting that they are derived from a common source, which may be anthropogenic. Therefore, in section I of the core collected

Table 7 Correlation between sand, silt, clay, organic carbon and metals in section I of core GP-1 (n=16)

GP-1 (I)	Sand (%)	Silt (%)	Clay (%)	Org. C (%)	Fe (%)	Mn (ppm)	Pb (ppm)	Ni (ppm)	Co (ppm)	Cu (ppm)	Zn (ppm)	Cr (ppm)
Sand (%)	1.00											
Silt (%)	−0.90	1.00										
Clay (%)	−0.83	0.50	1.00									
Org. C (%)	−0.86	0.75[a]	0.75[a]	1.00								
Fe (%)	−0.76	0.68[a]	0.63[a]	0.96[a]	1.00							
Mn (ppm)	−0.14	0.07	0.19	0.33	0.41	1.00						
Pb (ppm)	−0.68	0.65[a]	0.52	0.80[a]	0.80[a]	0.50	1.00					
Ni (ppm)	−0.64	0.51	0.62[a]	0.86[a]	0.90[a]	0.67[a]	0.84[a]	1.00				
Co (ppm)	−0.69	0.57[b]	0.63[a]	0.92[a]	0.95[a]	0.61[b]	0.87[a]	0.98[a]	1.00			
Cu (ppm)	−0.76	0.72[a]	0.58[a]	0.94[a]	0.93[a]	0.32	0.88[a]	0.85[a]	0.90[a]	1.00		
Zn (ppm)	−0.71	0.60[b]	0.64[a]	0.85[a]	0.88[a]	0.53	0.88[a]	0.93[a]	0.93[a]	0.85[a]	1.00	
Cr (ppm)	−0.55	0.63[a]	0.28	0.76[a]	0.86[a]	0.46	0.81[a]	0.80[a]	0.83[a]	0.79[a]	0.82[a]	1.00

[a] Correlation is significant at 0.01 level

[b] Correlation is significant at 0.02 level

Table 8 Correlation between sand, silt, clay, organic carbon and metals in section II of core GP-1 (n=14)

GP-1 (II)	Sand (%)	Silt (%)	Clay (%)	Org. C (%)	Fe (%)	Mn (ppm)	Pb (ppm)	Ni (ppm)	Co (ppm)	Cu (ppm)	Zn (ppm)	Cr (ppm)
Sand (%)	1.00											
Silt (%)	−0.96	1.00										
Clay (%)	−0.96	0.85[a]	1.00									
Org. C (%)	−0.93	0.86[a]	0.93[a]	1.00								
Fe (%)	−0.89	0.84[a]	0.88[a]	0.92[a]	1.00							
Mn (ppm)	0.05	−0.12	0.02	−0.05	0.22	1.00						
Pb (ppm)	−0.39	0.42	0.33	0.42	0.55	0.45	1.00					
Ni (ppm)	−0.47	0.46	0.45	0.45	0.71[a]	0.68[b]	0.50	1.00				
Co (ppm)	−0.84	0.82[a]	0.79[a]	0.81[a]	0.92[a]	0.29	0.71[a]	0.75[a]	1.00			
Cu (ppm)	−0.21	0.24	0.15	0.33	0.40	0.43	0.59[b]	0.39	0.35	1.00		
Zn (ppm)	−0.83	0.82[a]	0.77[a]	0.77[a]	0.70[a]	−0.19	0.45	0.19	0.73[a]	0.30	1.00	
Cr (ppm)	−0.81	0.79[a]	0.76[a]	0.79[a]	0.93[a]	0.36	0.67[a]	0.79[a]	0.96[a]	0.47	0.70[a]	1.00

[a] Correlation is significant at 0.01 level

[b] Correlation is significant at 0.02 level

from the Mandovi estuary, sand and Mn oxide seem to be major factors, while in section II, clay played a major role in the distribution of metals.

Section I of core S-1 has two factors contributing 83 % of the total variance. Factor 1 with 66.64 % of the total variance has significant positive loading for sand while significant negative loadings for finer sediments, organic carbon and metals. The results, therefore, indicate difference in geochemical behaviour of coarser and finer sediments and suggest that the metals in this section are associated with finer sediments and organic carbon. Factor 2 with 17.07 % of the total variance has good loadings for Zn, Mn, Fe and Pb, indicating the role of Fe–Mn oxide in adsorption of metals and, hence, can be termed as Fe–Mn oxide controlled factor. Section II of core S-1 has three factors accounting for 80 % of the total variance. Factor 1 with 51.31 % of the total variance has significant loadings for Pb, Ni, Co, Cu and Cr and good loadings for organic carbon and Mn. This factor can be called as Mn oxide controlled factor. Factor 2 has significant loadings on silt and clay and good loadings on organic carbon, Fe and Mn. This factor can be called as finer sediments controlled factor. Factor 3 shows good loadings on Fe, organic carbon and Cu. This factor can be termed as organic carbon controlled factor. Thus, in section I of the core collected from the Sharavathi river, finer sediments, organic carbon and Fe–Mn oxide are the major factors, while in section II, it is the Mn oxide along with finer sediments and organic carbon are regulating the distribution of metals. The elements readily get sorbed or co-precipitated onto the Fe–Mn hydroxide or oxide (Lee 1975) in finer sediments due to their larger surface area. Fe and Mn exhibit similar behaviour in aquatic environment. They get reduced in anoxic conditions and are oxidised under oxic conditions (Lin et al. 2011). However, the nature, crystallinity, size of the crystals, surface charge of metal oxide and mixed metal oxide (e.g. Fe–Al oxide) also play an important role in the sorption selectivity of trace elements in cationic form (Violante et al. 2008). This may have caused difference in behaviour of Fe/Mn oxide in section II.

Table 9 Factor analysis matrix after varimax rotation for core MD-1

	MD-1 (section I)			MD-1 (section II)	
	Factor 1	Factor 2	Factor 3	Factor 1	Factor2
Variance (%)	63.79	12.27	10.33	54.07	15.78
Sand (%)	*0.792*	0.096	0.566	*−0.916*	0.242
Silt (%)	*−0.645*	−0.377	−0.643	0.571	−0.661
Clay (%)	*−0.816*	0.169	−0.420	*0.854*	0.182
Org. C (%)	*−0.824*	−0.421	0.162	*0.823*	−0.341
Fe (%)	−0.793	0.172	−0.399	*0.789*	−0.340
Mn (ppm)	0.502	0.450	*0.713*	*0.825*	−0.166
Pb (ppm)	0.613	0.427	0.260	−0.008	0.671
Ni (ppm)	0.267	−0.135	*0.822*	−0.089	*0.812*
Co (ppm)	*0.795*	0.212	0.464	0.597	−0.521
Cu (ppm)	0.052	*0.973*	0.123	*0.756*	0.425
Zn (ppm)	*0.831*	0.193	0.277	−0.627	0.153
Cr (ppm)	0.163	0.291	*0.861*	*−0.763*	0.474

The italicised values represent significant positive/negative correlation among the variables in each factor

Sections I and II of core GP-1 have two factors each with 85 and 83 % of the total variance, respectively. In section I, factor 1 with 74.29 % of the total variance has significant loadings for silt, clay, organic carbon and Cu and good loadings for Fe, Zn, Pb, Co, Ni and Cr. This factor can be called as finer sediments controlled factor. Factor 2 with 11.70 % of the total variance shows significant loadings on Mn, Ni, Pb, Co,

Table 10 Factor analysis matrix after varimax rotation for core S-1

	S-1 (section I)		S-1 (section II)		
	Factor 1	Factor 2	Factor 1	Factor 2	Factor 3
Variance (%)	66.64	17.07	51.31	19.91	9.48
Sand (%)	*0.808*	0.577	−0.204	*−0.934*	−0.157
Silt (%)	−0.631	−0.422	−0.054	*0.934*	0.041
Clay (%)	*−0.757*	−0.553	0.340	*0.772*	0.207
Org. C (%)	*−0.721*	−0.655	0.645	0.544	0.237
Fe (%)	*−0.751*	0.393	0.155	0.477	0.462
Mn (ppm)	*−0.844*	0.470	0.643	0.567	−0.165
Pb (ppm)	*−0.877*	0.293	*0.898*	−0.124	0.023
Ni (ppm)	*−0.820*	0.116	*0.952*	0.189	0.081
Co (ppm)	*−0.938*	−0.024	*0.907*	0.335	0.116
Cu (ppm)	*−0.903*	0.151	*0.778*	0.312	0.207
Zn (ppm)	*−0.768*	0.552	0.025	−0.141	*−0.967*
Cr (ppm)	*−0.922*	0.045	*0.752*	0.066	−0.366

The italicised values represent significant positive/negative correlation among the variables in each factor

Zn and Cr and good loadings on Fe, Cu and organic carbon. This factor can be called as Fe–Mn oxide controlled factor. In section II, factor 1 with 65.02 % of the total variance has significant loadings for silt, clay, organic carbon, Fe, Co, Zn and Cr, suggesting the role of finer sediments and organic carbon in the adsorption of metals. This factor can be called as finer sediments controlled factor. Factor 2 with18.23 % of the total variance shows significant loadings for Mn, Pb and Ni and good loadings for Cu, Cr, Co and Fe. This factor can be called as Fe–Mn oxide controlled factor. The factor analysis

Table 11 Factor analysis matrix after varimax rotation for core GP-1

	GP-1 (I)		GP-1 (II)	
	Factor 1	Factor 2	Factor 1	Factor 2
Variance (%)	74.29	11.7	65.02	18.23
Sand (%)	*−0.948*	-0.207	*−0.975*	−0.135
Silt (%)	*0.866*	0.165	*0.944*	0.128
Clay (%)	*0.769*	0.198	*0.933*	0.132
Org. C (%)	*0.814*	0.535	*0.934*	0.183
Fe (%)	0.697	0.661	*0.856*	0.457
Mn (ppm)	−0.150	*0.871*	−0.222	*0.891*
Pb (ppm)	0.571	*0.710*	0.343	*0.719*
Ni (ppm)	0.490	*0.846*	0.345	*0.808*
Co (ppm)	0.563	*0.810*	*0.802*	0.538
Cu (ppm)	*0.735*	0.593	0.147	0.675
Zn (ppm)	0.588	*0.745*	*0.881*	0.039
Cr (ppm)	0.457	*0.746*	*0.759*	0.608

The italicised values represent significant positive/negative correlation among the variables in each factor

suggests that finer sediments and Fe–Mn oxide are the major factors influencing the distribution of metals in both the sections of core GP-1. The affinity between finer fractions and trace elements is attributed to their larger surface area (El-Kashouty and El-Sabbagh 2011) and higher cation exchange capacity (Nair and Ramachandran 2002). It is important to note here that though the concentrations of trace metals are drastically decreased in section II due to larger input of coarser sediments in core GP-1, the factors regulating trace metals within sediments were not affected.

Cluster analysis

Cluster analysis is a multivariate technique, whose primary purpose is to classify the objects of the system into categories or clusters based on their similarities. The results of a hierarchical clustering procedure are displayed graphically using a tree diagram (Fig. 5a–f), also known as a dendrogram, which shows all the steps in the hierarchical procedure (Richard and Dean 2002). Cluster analysis was applied to the different parameters analysed in sediment, employing a complete linkage method with Euclidean distance.

The dendrogram plot consists of two clusters in section I of core MD-1. The first cluster shows association of finer sediments and organic carbon forming group with Fe. The larger surface area of finer sediments and organic coatings must have facilitated adsorption of Fe (Lu et al. 2005). The second cluster comprises of sand, Mn, Pb, Ni, Co, Cu, Zn and Cr. The presence of Mn oxide coating over the coarser sediments may have caused adsorption of these metals. In section II of core MD-1, three clusters are observed. The first cluster comprises of Fe and Cr indicating the role of Fe in the distribution of Cr. The second cluster consists of finer sediments, organic carbon, Cu and Mn. This cluster suggests association of Cu and Mn with finer sediments and organic matter. The association of Co, Ni, Zn and Pb with sand is evident from the third cluster. Tam and Wong (2000) reported that the difference in trace metal concentrations between fine-grained and sand-sized fractions became less significant when the site is more contaminated. Mining waste may increase metals concentration in the sediments of the Mandovi estuary.

In section I of core S-1, three clusters are observed. The first cluster consists of Cr, Cu, Zn, Pb, Mn, Co and Fe. The metals in this cluster may be associated with Fe–Mn oxide. The second cluster shows association of finest fraction clay with organic carbon, while association of Ni with silt and sand is seen from the third cluster. Three clusters are evident from section II of core S-1. The first cluster consists of Cr, Pb, Cu, Co, Ni, Mn and organic carbon. Similar to results of correlation analysis, cluster analysis also shows the role of Mn oxide in distribution of metals in the recent years in the Sharavathi estuary. The second cluster shows the association of Fe with finer sediments, whereas the association of Zn with

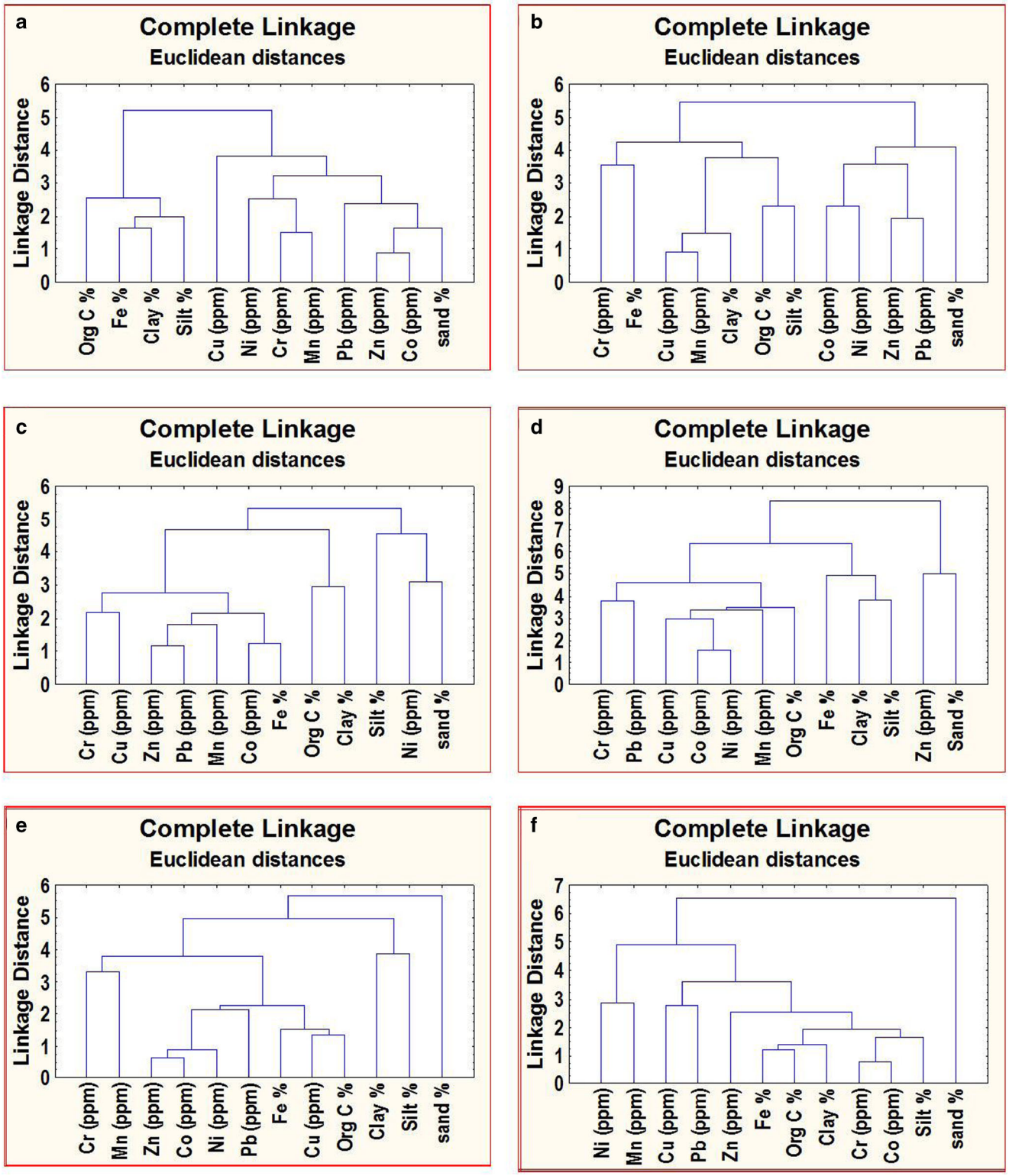

Fig. 5 Cluster analysis of cores MD-1 [section I (**a**), section II (**b**)], S-1 [section I (**c**), section II (**d**)] and GP-1 [section I (**e**), section II (**f**)]

coarser sediments is seen from the third cluster. The distribution pattern of Zn in section II of the core S-1 is different from the rest of the metals, and its association with coarser sediments suggests non-natural source of Zn in the recent years.

In both the sections of core GP-1, three clusters are observed. In section I, Cr and Mn form the first cluster, which suggests the role of Mn oxide in distribution of Cr. The second cluster consists of Zn, Co, Ni, Pb, Fe, Cu and organic carbon. Second cluster, therefore, indicates association of these metals with Fe oxide.

The third cluster comprises of silt and clay. In section II, distribution of Ni seems to be regulated by Mn as they form first cluster. The second cluster consists of Cu and Pb, indicating their similar source or enrichment mechanism in the recent sediments. The third cluster comprises of finer sediments, organic carbon, Zn, Fe, Cr, Co. The metals in the third cluster may be associated with finer sediments, organic carbon and Fe oxide. Cluster analysis strongly supports the results obtained through factor analysis and helps in delineating the factors regulating the metals distribution.

Conclusion

The sediment cores analysed from the lower estuarine regions of the three tropical estuaries revealed increase in finer sediments in the Mandovi and Sharavathi estuaries in the recent years, while they revealed increase in coarser sediments in the Gurupur estuary. In Mandovi and Sharavathi estuaries, the catchment area activities, rainfall, runoff and mixing behaviour led to the increase in the concentration of finer sediments in the recent years. The association of metals with finer sediments and organic carbon facilitated increased metal concentration in the recent years in these estuaries. However, in Gurupur estuary, dilution of metal concentration is observed by input of coarser sediments in the recent years. The correlation, factor and cluster analyses showed difference in metals behaviour in the three estuaries. In Mandovi estuary, there is no single decisive factor governing the distribution of metals. Sediment components along with Fe and/or Mn oxide regulated distribution of metals. In Sharavathi estuary, Mn oxide governed the distribution of metals, while in Gurupur estuary, the distribution of metals is largely regulated by Fe oxide. In addition, metals showed difference in their associations with Fe and/or Mn oxide within cores collected from Mandovi and Sharavathi estuaries. This difference in metal behaviour is attributed to variations in rock types in their basins, in addition to changes in response to natural forces and human activities, with time, as well as variation in tidal range.

Acknowledgement One of the authors (Maheshwar R. Nasnodkar) wishes to thank the Department of Science and Technology (DST) for granting fellowship under "Innovation in Science Pursuit for Inspired Research" (INSPIRE) programme

References

Abílio G, Cupelo ACG, Rezende CE (2006) Heavy metal distribution in sediments of an offshore exploration area, Santos basin, Brazil. Geochim Bras 20(1):71–86

Avinash KG, Diwakar PG, Joshi NV, Ramachandra TV (2008) Landslide susceptibility mapping in the downstream region of Sharavathi river basin, Central Western Ghats. In: Proceedings of the 24th annual symposium on space and technology ISROI ISc technology cell, Indian Institute of Science, Bangalore

Badr NBE, El-Fiky AA, Mostafa AR, Al-Mur BA (2008) Metal pollution records in core sediments of some Red Sea coastal areas, Kingdom of Saudi Arabia. Environ Monit and Assess 155:509–526

Bannur CR, Sherieff AN, Basappa RM, Shreedhara V (1991) Application of remote sensing technique in detection of morphological changes in the vicinity of estuarine mouths—a case study pertaining to D.K. district. Workshop on Indian remote sensing satellite mission and its application

Basaham AS (2009) Geochemistry of Jizan shelf sediments, southern Red Sea coast of Saudi Arabia. Arab J Geosci 2:301–310

Bowen HJM (1979) The environmental chemistry of the elements. Academic Press, London, New York

Brown ET, Callonnec LL, German CR (2000) Geochemical cycling of redox-sensitive metals in sediments from Lake Malawi: a diagnostic paleotracer for episodic changes in mixing depth. Geochim Cosmochim Acta 64(20):3515–3523

Bukhari SS (1994) Studies on mineralogy and geochemistry of bed and suspended sediment of Mandovi river and its tributaries in Goa, west coast of India. Thesis, Goa University

Chatterjee M, Filho EVS, Sarkar SK, Sella SM, Bhattacharya A, Satpathy KK, Prasad MVR, Chakraborty S, Bhattacharya BD (2007) Distribution and possible source of trace elements in the sediment core of a tropical macrotidal estuary and their ecotoxicological significance. Environ Int 33(3):346–356

Clark M (1992) The physical and geochemical controls on heavy metal cycling in Mangal sediments, Wynnum, Brisbane. Thesis, University of Canterbury

Dolch T, Hass HC (2008) Long-term changes of intertidal and subtidal sediment compositions in a tidal basin in the northern Wadden Sea (SE North Sea). Helgol Mar Res 62:3–11

Dulaiova H, Gonneea ME, Henderson PB, Charette MA (2008) Geochemical and physical sources of radon variation in a subterranean estuary—implications for groundwater radon activities in submarine groundwater discharge studies. Mar Chem 110(1–2):120–127

El-Kashouty M, El-Sabbagh A (2011) Distribution and immobilization of heavy metals in Pliocene aquifer sediments in Wadi El Natrun depression, Western Desert. Arab J Geosci 4(5–6):1019–1039

Emam A, Saad-Eldin M (2013) Distribution and environmental geochemistry of some heavy metals in stream sediments of Wadi Allaqi, south eastern desert of Egypt. Arab J Geosci 6(5):1325–1332

Fernandes L, Nayak GN (2009) Distribution of sediment parameters and depositional environment of mudflats of Mandovi estuary, Goa, India. J Coast Res 25(2):273–284

Folk RL (1974) Petrology of sedimentary rocks. Hemphill, Austin

Fox WM, Johnson MS, Jones SR, Leah RT, Copplestone D (1999) The use of sediment cores from stable and developing salt marshes to reconstruct historical contamination profiles in the Mersey Estuary, UK. Mar Environ Res 47:311–329

Gangadhar BH (1995) Long-term shoreline changes of Mulki-Pavanje and Nethravati- Gurpur estuaries, Karnataka. J Indian Soc Remote Sens 23:147–153

Gaudette HE, Flight WR, Toner L (1974) An inexpensive titration method for the determination of organic carbon in recent sediment. J Sediment Petrol 44(1):249–253

German J, Svensson G (2002) Metal content and particle size distribution of street sediments and street sweeping waste. Water Sci Technol 46(6–7):191–198

Harikumar PS, Nasir UP, Mujeebu Rahman MP (2009) Distribution of heavy metals in the core sediments of a tropical wetland system. Int J Environ Sci Technol 6(2):225–232

Hegde AV, Raveendra B (2000) Short-term and long-term geomorphological dynamics of Mangalore spits using IRS-1A/1C data. J Indian Soc Remote Sens 28(4):233–247

Jarvis IJ, Jarvis K (1985) Rare earth element geochemistry of standard sediments: a study using inductively coupled plasma spectrometry. Chem Geol 53:335–344

Jingchun L, Chongling Y, Spencer KL, Ruifeng Z, Haoliang L (2010) The distribution of acid-volatile sulfide and simultaneously extracted metals in sediments from a mangrove forest and adjacent mudflat in Zhangjiang Estuary, China. Mar Pollut Bull 60(8):1209–1216

Jordao CP, Pereira MG, Bellato CR, Pereira JL, Matos AT (2002) Assessment of water systems for contaminants fromdomestic and industrial seweage. Environ Monit Assess 79:55–100

Kaiser HF (1960) The application of electronic computers to factor analysis. Educ Psychol Meas 20:141–151

Kappler A, Straub KL (2005) Geomicrobiological cycling of iron. Rev Mineral Geochem 59:85–105

Kessarkar PM, Rao VP, Shynu R, Mehra P, Viegas BE (2010) The nature and distribution of particulate matter in the Mandovi estuary, central west coast of India. Estuar Coast 33(1):30–44

Kristiansen KD, Kristensen E, Jensen MH (2002) The influence of water column hypoxia on the behaviour of manganese and iron in sandy coastal marine sediment. Estuar Coast Shelf Sci 55:645–654

Kulahcl F, Şen Z (2008) Multivariate statistical analyses of artificial radionuclides and heavy metals contaminations in deep mud of Keban Dam Lake, Turkey. Appl Radiat Isot 66:236–246

Kumar SP, Edward JKP (2009) Assessment of metal concentration in the sediment cores of Manakudy estuary, south west coast of India. Indian J Mar Sci 38(2):235–248

Kumar SP, Sheela MS (2013) Studies on the sediment characteristics of Manakudy estuary, south west coast of India. Int Res J Environ Sci 2(11):78–83

Kumar A, Jayappa KS, Deepika B, Dinesh AC (2010) Hydrological-drainage analysis for evaluation of groundwater potential in a watershed basin of southern Karnataka, India: a remote sensing and GIS approach. In: Proceedings of the 1st international applied geological congress, Department of Geology, Islamic Azad University—Mashad Branch, Iran

Kumar VS, Dora GU, Philip S, Pednekar P, Singh J (2011) Variations in tidal constituents along the nearshore waters of Karnataka, west coast of India. J Coast Res 27(5):824–829

Kunte PD, Wagle BG (1991) Spit evolution and shore drift direction along south Karnataka coast, India. Giorn Geol 53:71–80

Lacuraj C, Maria S (2006) Geochemical index of trace metals in the surficial sediments from the western continental shelf of India, Arabian Sea. Environ Geochem Health 28:509–518

Lee GF (1975) Role of hydrous metal oxides in the transport of heavy metals in the environment. In: Krenkel PA (ed) Heavy metals in the aquatic environment. Pergamon press, Oxford, pp 137–153

Lin CY, Abdullah MH, Musta B, Praveena MS, Aris AZ (2011) Stability behaviour and thermodynamic states of iron and manganese in sandy soil aquifier Manukan island, Malaysia. Nat Resour Res 20(1). doi: 10.1007/s11053-011-9136-2

Liu B, Hu K, Jiang Z, Yang J, Luo X, Liu A (2011) Distribution and enrichment of heavy metals in a sediment core from the Pearl River Estuary. Environ Earth Sci 62:265–275

Lu XQ, Werner I, Young TM (2005) Geochemistry and bioavailability of metals in sediments from northern San Francisco Bay. Environ Int 31:593–602

Madkour HA, Obirikorang KA, Amisah S, Otchere FA, Adjei-Boateng D (2011) Relationship between heavy metal concentrations in bottom sediments and the clam, Galatea Paradoxa (Born 1778) from the Volta estuary, Ghana. J Environ Prot 2:720–728

Mukherjee S (2013) Clays as neutralizers against environmental protection. In: Mukherjee S (ed) The science of clays: applications in industry, engineering and environment. Springer, Netherlands, p 252

Mukhopadhyay R, Karisiddaiah SM (2014) The Indian coastlines: processes and landforms. In: Kale VS (ed) Landscapes and landforms of India. Springer, Dordrecht, pp 91–105

Murray JW (1987) Mechanisms controlling the distribution of trace elements in oceans and lakes. Sources and fate of aquatic pollutants. Am Chem Soc, In, pp 91–130

Nair MNM, Ramachandran KK (2002) Textural and trace elemental distribution in sediments of the Beypore estuary (SW coast of India) and adjoining inner shelf. Indian J Mar Sci 31(4):295–304

Naqvi SM (2005) Geology and evolution of the Indian Plate (from Hadean to Holocene—4 Ga to 4 Ka). Capital Publishing Company, New Delhi, p 450

Nesbitt HW, Young GM (1996) Petrogenesis of sediments in absence of chemical weathering: effects of abrasion and sorting on bulk composition and mineralogy. Sedimentology 43:341–358

Pathak MC, Kotnala KL, Prabaharan N (1988) Effects of bridge piers on a tropical estuary in Goa, India. J Coast Res 4(3):475–481

Pejrup M (1988) The triangular diagram for classification of estuarine sediments: a new approach. In: de Boer PL, van Gelder A and Nios SD (eds) Tide influenced sedimentary environments and facies, pp 289–300

Pichaimani SV, Jonathan MP, Srinivasalu S, Rajeshwara-Rao N, Mohan SP (2008) Enrichment of trace metals in surface sediments from the northern part of Point Calimere, SE coast of India. Environ Geol 55: 1811–1819

Radhakrishna BP, Vaidyanadhan R (1994) Geology of Karnataka. Geol Soc India, Bangalore, pp 9–17

Radheshyam B, Rao S, Shirlal KG (2010) On numerical modelling of waves, currents and sediment movement around Gurupur–Netravathi river mouth. Int J Earth Sci Eng 3(4):538–552

Raghavan BR, Vinod BT, Dimple KA, Prabhu HV, Udayashankar HN, Murthy TRS (2001) Evaluation of the Nethravathi spit complex, west coast of India: Integrated change detection study using topographic and remotely sensed data. Indian J Mar Sci 30(4):268–270

Raj S, Jee PK, Panda CR (2013) Textural and heavy metal distribution in sediments of Mahanadi estuary, east coast of India. India J GeoMar Sci 42(3):370–374

Ram A, Borole DV, Rokade MA, Zingde MD (2009) Diagenesis and bioavailability of mercury in the contaminated sediments of Ulhas Estuary, India. Mar Pollut Bull 58(11):1685–1693

Ramachandra TV, Subhashchandran MD, Sreekantha DM, Rao GR, Ali S (2004) Cumulative impact assessment in the Sharavathi river basin. Int J Environ Dev 1(1):113–135

Rao VP, Shynu R, Kessarkar PM, Sundar D, Michael GS, Narvekar T, Blossom V, Mehra P (2011) Suspended sediment dynamics on a seasonal scale in the Mandovi and Zuari estuaries, central west coast of India. Estuar Coast Shelf Sci 91:78–86

Richard AJ, Dean WW (2002) Applied multivariate statistical analysis. Prenticee Hall, London, p 265

Salomons W, Forstner U (1984) Metals in the hydrocycle. Springer, Berlin, p 349

Shetye SR, Kumar MD, Shankar D (2007) The Mandovi and Zuari estuaries. National Institute of Oceanography, Goa, p 145

Singh KT, Nayak GN (2009) Sedimentary and geochemical signatures of depositional environment of sediments in mudflats from a microtidal Kalinadi estuary, central west coast of India. J Coast Res 25(3):641–650

Tam NFY, Wong YS (2000) Spatial variation of heavy metals in surface sediments of Hong Kong mangrove swamps. Environ Pollut 110(2): 195–205

Tessier A, Campbell PGC (1982) Particulate trace metal speciation in stream sediments and relationship with grain size: implications for geochemical exploration. J Geochem Explor 6:77–104

Thamdrup B (2000) Bacterial manganese and iron reduction in aquatic sediments. Adv Microb Ecol 16:41–84

Valette-Silver NJ (1993) The use of sediment cores to reconstruct historical trends in contamination of estuarine and coastal sediment. Estuaries 16:577–588

Venkatramanan S, Ramkumar T, Anithamary I (2013) Distribution of grain size, clay mineralogy and organic matter of surface sediments from Tirumalairajan estuary, Tamilnadu, east coast of India. Arab J Geosci 6:1371–1380

Venkatramanan S, Ramkumar T, Anithamary I, Vasudevan S (2014) Heavy metal distribution in surface sediments of the Tirumalairajan River estuary and the surrounding coastal area, east coast of India. Arab J Geosci 7:123–130. doi:10.1007/s12517-012-0734-z

Vinodhini R, Narayanan M (2008) Bioaccumulation of heavy metals in organs of fresh water fish *Cyprinus carpio* (Common carp). Int J Environ Sci Technol 5(2):179–182

Violante A, Krishnamurti GSR, Pigna M (2008) Mobility of trace elements in soil environments. In: Violante A, Huang PM, Gadd GM (eds) Biophysico-chemical processes of metals and metalloids in soil environments. Wiley, Hoboken, pp 169–213

Volvoikar SP, Nayak GN (2013) Factors controlling the distribution of metals in intertidal mudflat sediments of Vaitarna estuary, North Maharashtra coast, India. Arab J Geosci. doi:10.1007/s12517-013-1162-4

Walkley A, Black JA (1934) The determination of organic carbon by rapid titration method. Soil Sci 37:29–38

Wallbrink P, Olley J (2004) Sources of fine grained sediment in incised and un-incised channels, Jugiong Creek, NSW, Australia. In Golosov V, Belyaez V, Walling DE (ed) Sediment transfer through the fluvial system, vol 288. IAHS, Pub., Oxfordshire, pp 165–169

Wangersky PJ (1986) Biological control of trace metal residence time and speciation: a review and synthesis. Mar Chem 18:269–297

Willams TP, Bubb JM, Lester JN (1994) Metal accumulation within saltmarsh environments: a review. Mar Pollut Bull 28:277–290

Zabetoglou K, Voutsa D, Samara C (2002) Toxicity and heavy metal contamination of surficial sediments from the Bay of Thessaloniki (Northwestern Aegean Sea) Greece. Chemosphere 49:17–26

Zeng H, Wu J (2013) Heavy metal pollution of lakes along the mid-lower reaches of the Yangtze river in China: intensity, sources and spatial patterns. Int J Environ Res Public Health 10(3):793–807

Zhou G, Zhang M, Ji D, Zhu Q (2007) Tree-kernel based relation extraction with context-sensitive structured parse tree in formation. In EMNLP/CoNLL